Understanding the role of green infrastructure in climate change resiliency of transportation infrastructure

by

Victoria Saunders Thomas

A THESIS

submitted in partial fulfillment of the requirements for the degree

MASTER OF SCIENCE

Department of Biological and Agricultural Engineering
Carl R. Ice College of Engineering

KANSAS STATE UNIVERSITY
Manhattan, Kansas

2020

Approved by:

Major Professor
Dr. Stacy Hutchinson

Copyright

Abstract

The Earth's climate is currently changing faster than at any point in the history of modern civilization, primarily as a result of human activities (Reidmiller et al., 2018). In addition to increases in very hot days and heat waves, more frequent and intense extreme weather events are expected (Herring et al., 2019; Reidmiller et al., 2018; Transportation Research Board, 2008) Trenberth, 2011). The increased flooding caused by the intensification of the hydrologic cycle heightens the risk to America's aging transportation infrastructure. The intent of this research is to understand if and to what extent green infrastructure can increase the climate change resiliency of transportation infrastructure across a watershed. To meet this objective, a Personal Computer Storm Water Management Model (PCSWMM) of the Blue River Watershed (BRW) in the greater Kansas City Metropolitan Area created by Kelsey McDonough (2018) was adapted and updated. Twelve different low impact development scenarios with varying levels of green infrastructure were evaluated across a range of design storm events in both one and two-dimensional models. The percent reduction in peak flow, total volume of flow, and flood extent between each scenario and the current conditions were evaluated. Results demonstrate that increasing the percentage of "disconnectedness" i.e. water flows from impervious surfaces onto vegetated surfaces before reaching streams, and adding a 150 foot riparian buffer significantly decreased the simulated peak inflow and total volume of water near important transportation infrastructure. The reductions were greatest for the water quality event (>90% reduction) and decreased to an approximately 10% reduction for the 100 year, 24 hour storm event for the maximum green infrastructure scenario. Increasing disconnectedness to at least 25% with the riparian buffer reduced flood extent approximately 8% for the 1, 5, and 10-year design storms. Minimal flood extent reductions were seen for the 100-year design storm. These results indicate

that increasing green infrastructure does increase the climate change resiliency of transportation infrastructure, however additional structural flood control is needed to reduce flood extent greater than 10% and for flood control of design storms of 100+ years.

Table of Contents

List of Figures

List of Tables

List of Abbreviations

AIMS	Automated Information Mapping System
ANOVA	Analysis of Variance
APWA	American Public Works Association
ASCE	American Society of Civil Engineers
BRW	Blue River Watershed
CDC	Centers for Disease Control and Prevention
CHI	Computational Hydraulics Int.
CMIP	Coupled Model Intercomparison Project
CSO	Combined Sewer Overflow
DEM	Digital Elevation Model
DSIMPERV	Depression Storage for Impervious Cover
DSPERV	Depression Storage for Pervious Cover
EURV	Excess Urban Runoff Volume
FEMA	Federal Emergency Management Agency
GHG	Greenhouse Gases
GI	Green Infrastructure
GIS	Geographic Information System
HUC	Hydrologic Unit Code
KC	Kansas City
KDOT	Kansas Department of Transportation
LID	Low Impact Development
LiDAR	Light Detection and Ranging
MARC	Mid-America Regional Council
MEA	Millenium Ecosystem Assessment
NFIP	National Flood Insurance Program
NIMPERV	Manning's Roughness for Impervious Cover
NLCD	National Land Cover Database
NOAA	National Oceanic and Atmospheric Administration
NPDES	National Pollutant Discharge Elimination System
NPERV	Manning's Roughness for Pervious Cover
NPV	Net Present Value
NRCS	National Resources Conservation Service
NSE	Nash Sutcliffe Efficiency
PCSWM	Personal Computer Storm Water Management Model
RCP	Representative Concentration Pathway
SCM	Stormwater Control Measure
SCS	Soil Conservation Surface
SWMM	Storm Water Management Model
TCW	Tomahawk Creek Watershed

TIGER	Transportation Investment Generating Economic Recovery
U.S. EPA	United States Environmental Protection Agency
UN	United Nations
USD	United States Dollars
USDA	United States Department of Agriculture
USGS	United States Geological Survey
WQv	Water Quality Volume

Acknowledgements

Thank you to the members of my committee for their support, guidance, and knowledge transfer throughout my undergraduate and graduate studies at K-State. Dr. Stacy Hutchinson, thank you for all your patience throughout modeling ups and downs, always being willing to find time to meet, and encouraging me to pursue graduate school. Dr. Shawn Hutchinson, thank you for all of your GIS- related assistance that has been integral to model development progress. Dr. Trisha Moore thank you for introducing me to green infrastructure and your corgi.

A large thank you goes out to Dr. Kelsey McDonough for going above and beyond to answer questions, provide guidance, make edits, and overcome 16-hour time differences. This thesis would not exist without your foundation of work and continued help!

I would also like to thank my office mates: Jessica, Laura, and Ali for keeping things fun down in 007 and always indulging my chat breaks. Thank you to all of the wonderful friends I made at K-State through Blue Key, K-State Proud, SGA, AXiD, and more for forever impacting me for the better!

Another large thank you to Kirk and Kelly Horner is due for offering their house as my new office space post covid-19 induced campus shutdowns. Thanks for the food, space, and lack of judgement with my nocturnal work schedule. A special thank you to Kellan for keeping me sane with daily phone calls and Corgi Kane pictures.

Thank you to Diane Patrick for the mentorship, delicious brunches, and always stimulating conversations.

Thank you to all of the wonderful public school teachers I have had throughout the past 17 years, who inspired my love of learning that led me to graduate school.

Lastly, I could not have reached this point without all of the support from my family: humans and pets. Thank you Betty for providing mutual grad school commiserating, Grandma for all the phone calls on my walks home from campus, Mom for starting and nurturing my love of learning and reminders that I have it easy compared to how research was done in your day ☺ , and Dad for all the reminders of how much I am loved. Thanks Callie, Aggie, Kane, Ernie, Little Lion, and Sally for being outstanding pets.

Dedication

I dedicate this thesis to my Mom for her courage and positive attitude in all challenges.

Chapter 1 - Introduction

1.1 Problem Statement

The Earth's climate is currently changing faster than at any point in the history of modern civilization, primarily as a result of human activities (Reidmiller et al., 2018). One side effect of climate change is more frequent and intense extreme weather events (Herring et al., 2019; Reidmiller et al., 2018; Trenberth, 2011). It has been predicted by many climate scientists that the wet places will get wetter, and the dry places get drier (Güneralp et al., 2015; Held and Soden, 2006; Liu and Allan, 2013; Putnam and Broecker, 2017). Knowledge of the intensity of precipitation is just as vital as the precipitation volume in order to forecast the impacts on soil moisture, stream flow, and flooding. It can seem counterintuitive that there may be increased droughts along with increased precipitation. However, if the precipitation occurs in concentrated, intense events that create a substantial volume of runoff, infiltration of runoff into the soil profile will decrease and reduce water availability for plants and stream base flow (Trenberth, 2011).

The intensification and acceleration of the hydrologic cycle is also expected to increase the frequency and hazard of flood events (Hirabayashi et al., 2013). The intensification of the hydrologic cycle is represented by the Clausius-Clapyeron equation, which implies that relative humidity will increase exponentially with temperature, leading to increased moisture for precipitation (Huntington, 2006; Trenberth, 2011). Precipitation is usually the strongest predictor of flooding, with larger rainfall amounts resulting in increased flooding and property loss (Brody et al., 2012). Observational records from 1962-2011 of 774 USGS stream gages in the central United States presented strong evidence for the increasing frequency of flooding (Mallakpour and Villarini, 2015). By 2030, 40% of global urban land is expected to be located in high-frequency flood zones, increasing from 30% in 2000 (Güneralp et al., 2015). Flooding is a

deadly and expensive natural hazard, and many cities are worried about increased flooding in the future (Abdelrahman et al., 2018; Klenzendorf et al., 2015; Pestana et al., 2013; Peters and Studley, 2014; Pinos and Timbe, 2019; Rangari et al., 2018). After studying the International Disaster Database developed by the United States Office for Foreign Disaster Assistance and Centre for Research on the Epidemiology of Disasters, Jonkman (2005) found that 1,816 freshwater floods killed over 175,000 people and affected over 2.27 billion people globally from January 1975-June 2002. Additionally, the National Flood Insurance Program (NFIP) has paid out over $65 billion in flood damages since 1978, with costs not adjusted for inflation (FEMA, 2019).

The 2018 US Fourth National Climate Assessment noted that transportation, which is the "backbone of economic activity", is threatened by a changing climate (Global Change Research Program, p. 481). Furthermore, the American Society of Civil Engineers rated America's infrastructure at a D+ in 2017, showing that much of America's infrastructure is deteriorating and at increased risk, which includes flood risk. Floods can cause lasting damage to infrastructure due to the force of floodwater, debris, and sediment (Güneralp et al., 2015). Even temporarily impassable roads due to standing water can affect the economy and well-being of citizens. The primary cause of flood-related mortality in developed countries is drowning while in a motor vehicle (Doocy et al., 2013). Additionally, typical infrastructure design, operation, financing principles, and regulatory standards do not account for climate change nor the risk of cascading infrastructure failure (Reidmiller et al., 2018). Not only is transportation vulnerable to climate change, but in 2016 the transportation sector became the top contributor of U.S. greenhouse gas emissions (U.S. Energy Information Administration, 2017).

Climate change is not the only factor driving increased risk to transportation infrastructure due to flooding. As of 2018, 82% of North Americans lived in urban areas and by 2050, that number is expected to increase to 90% (UN, 2019). Urbanization leads to increased peak discharge, volume and frequency of floods due to the increase in impervious land cover (Konrad, 2003). The effects of climate change exacerbate the already increased flood risk due to urbanization.

Management decisions that direct development away from flood-prone zones and adopt green infrastructure on a large-scale can safeguard urban infrastructure from these increasing flood risks (Güneralp et al., 2015). A literature review over 250 publications on low impact development and found that bioretention systems reduced peak flow rates and runoff volumes by 40-97% depending on magnitude of the storm event (Ahiablame et al., 2012). In addition to flood reduction, green infrastructure provides ecosystem services such as mitigation of the urban heat island effect, improving air quality, providing habitat, and providing aesthetic and recreational services (Ahiablame and Shakya, 2016; Demuzere et al., 2014; Gómez-Baggethun and Barton, 2013; Larsen, 2015; McDonough, 2015; U.S. EPA, 2012). The Mid-America Regional Council (MARC) defines resiliency in their 2017 *Climate Resiliency Strategy* as "the ability of a system or community to survive disruption and to anticipate, adapt, and flourish in the face of change." The benefits of green infrastructure listed above help cities to not only survive flooding events, but also increase their resiliency in the face of change.

City officials often rely on models to inform their management decisions because models help minimize expensive field studies and "predict the future," (Baffaut et al., 2015; Blöschl et al., 2007; Noori et al., 2016). There is a gap in existing literature of studies utilizing semi-lumped hydrologic models of a large watershed to evaluate the effectiveness of low impact development

at mitigating increased urban runoff volume and flow peak due to climate change (Ahiablame et al., 2012; Ahiablame and Shakya, 2016; Qin et al., 2013; Zahmatkesh et al., 2015). The findings of this research add not only to the base of knowledge of the flood reduction potential of green infrastructure, but also to the challenges and benefits of large-scale hydrologic modeling.

1.2 Objectives

The primary goal of this research is to understand if and to what extent green infrastructure can increase the climate change resiliency of transportation infrastructure across a watershed. This research will answer the following questions:

1. To what extent can the adoption of green infrastructure increase the climate change resiliency of transportation infrastructure across a watershed?
2. What modeling challenges are associated with answering questions 1?

To accomplish these goals, a Personal Computer Storm Water Management Model (PCSWMM) of the Blue River Watershed (BRW) in the greater Kansas City Metropolitan Area created by Kelsey McDonough (2018) was adapted and updated to meet these objectives. In order to provide a more detailed evaluation of the research questions, a smaller model of the Tomahawk Creek subwatershed of the BRW was created.

1.3 Significance of Work

The Kansas City Region has suffered fourteen deaths, $49 million in crop damages, and $111.6 million in property damage due to flooding since 1993 (Mid-America Regional Council, 2015). Substantial rainfall increases for seasonal spring and fall rain in addition to extreme events are projected (Anderson and Walker, 2015). Annual precipitation is predicted to increase roughly 1.5” by midcentury (2021-2060) even if emissions are curbed to the A1B lower emission scenario described in the National Climate Assessment (2014). If greenhouse gas emissions

continue at their current rate, scenario A1F1, annual average precipitation is projected to increase 5.8 inches to 44.6 inches for 2061-2100 (Anderson and Walker, 2015). This rainfall will be seen in more extreme, concentrated events, as the number of consecutive dry days is also expected to increase from 30.9 days/year to 39.5 days/ year (Anderson and Walker, 2015). This amplification of existing climate-related risks is of grave concern to managers and citizens of an already flood-prone Kansas City metro region.

The Mid-America Regional Council (MARC) is a nonprofit association of city and county governments and the metropolitan planning organization for all nine counties of the bistate Kansas City Region. In 2017, they released a Climate Resilience Strategy in which their second action goal is increasing trees and green infrastructure. Their report also notes a lack of analysis of risks and vulnerabilities associated with climate change effects on transportation. This research helps inform their goal of creating and implementing a Regional Transportation Climate Resiliency Action Plan. This research also aligns with their goal of utilizing increased green infrastructure. The Tomahawk Watershed is of particular significance because it contains the most congested four-lane highway in the state: U.S. Highway 69 (Ritter, 2020). Around 80,000 vehicles travel on US-69 in Johnson County each day, and the Kansas Department of Transportation (KDOT) estimates traffic will double by 2045 (KDOT, 2018). Vulnerability of stormwater systems to climate change varies according to regional climate patterns and natural and engineered site-specific factors (Heidrich et al., 2013). A site-specific study is required to better estimate the climate change effects on stormwater under varying development scenarios.

Chapter 2 - Literature Review

2.1 Climate Change Impacts on Flooding

Nine of the 10 warmest years on record have occurred since 2005, with 2019 being the second-warmest year on record (NOAA, 2020). Greenhouse gases such as carbon dioxide (CO_2), methane, ozone, halocarbons/ chlorofluorocarbons, and nitrous oxide, as well as water vapor and visible particulates trap outgoing infrared radiation and warm the planet – an effect understood since the late nineteenth century (Klein and Bauman, 2014). Model-based simulations of the increasing atmospheric CO_2 content predict that the Northern Hemisphere is expected to warm faster than the Southern Hemisphere (Putnam and Broecker, 2017). Increases in the frequency and intensity of heavy precipitation events in most parts of the United States have been observed and are expected to continue (Reidmiller et al., 2018; Transportation Research Board, 2008). In addition to observed trends, there is a direct and scientifically explainable influence of a warming climate on precipitation. The water holding capacity of air increases by about 7% per 1°C warming, which leads to increased water vapor in the atmosphere as explained by the Clausius-Clapyeron relation (Trenberth, 2011). The increased water vapor supplies increased moisture to storms, driving individual thunderstorms, extratropical rain or snow storms, or tropical cyclones to have more intense precipitation events (Trenberth, 2011). Additionally, rising temperatures cause more precipitation to occur as rain instead of snow and earlier snow melt, leading to increased runoff and risk of flooding in early spring along with increased risk of summer drought in continental areas (Trenberth, 2011). A literature review by Huntington (2006) found that despite of uncertainties due to spatial and temporal data limitations, the observed trends in most variables are consistent with an intensification of the water cycle during part or all

of the 20th century at regional to continental scales, and that this trend is expected to continue (Huntington, 2006).

Higher intensity rain events can quickly saturate soils and lead to flooding. A modeling study that examined two watersheds in Iowa found that the future 100-year flood event could have runoff increased between 47-52% in the larger Cedar River catchment and 25-34% in the smaller South Skunk catchment (Quintero et al., 2018). The authors used precipitation from the High-Resolution National Climate Change Dataset climate projections and the Hillslope-Link model to transform the rainfall into discharge simulations. Another study in the central United States used observation records from 774 USGS gages to determine that, while there is limited evidence of significant changes in the magnitude of flood peaks, strong evidence points to an increasing frequency of flooding from 1962-2011 (Mallakpour and Villarini, 2015). Milly et al. (2002) investigated the changes in risk of floods with discharges exceeding the 100-year levels from basins larger than 200,000 km^2 using both streamflow measurements and numerical simulations of climate change. They found that the frequency of these "great floods" increased substantially during the twentieth century, and the model suggests that the trend will continue (Milly et al., 2002).

Flooding is among the most expensive and deadly climate-related disasters, with recent losses from flooding reaching tens of billions of US dollars and thousands of deaths annually (Hirabayashi et al., 2013). One notable example was the extreme flooding associated with Hurricane Harvey's record doubling rainfall accumulations (Vano et al., 2019). Historic flooding of the Missouri river in 2019 caused widespread damage to roads, bridges, and levees, with the total event leading to three deaths and $10.8 billion in damages (Smith, 2020). Hirabayshi (2013) used outputs of 11 atmosphere-ocean general circulation models to compute a global projection

of climate change induced changes in flooding. He found that for the period 2071-2100, the current 100-year flood event is projected to occur about every 10-50 years in many of the world's largest river basins. This large change in return period is caused by a ~10-30% increase in flood discharge. These results align with the results from previously mentioned studies and reports (Milly et al., 2002; Quintero et al., 2018; Reidmiller et al., 2018; Transportation Research Board, 2008)

Flash floods are the most lethal, while river floods affect the largest number of people (Jonkman, 2005). Flash floods are defined by unpredictable and high intensity rainfall events, whereas river floods can be caused by high precipitation levels over an extended period of time snow melt, or flow blockage. NOAA defines flash floods as excessive rainfall occurring in a short period of time, typically less than 6 hours. Additionally, flashiness is directly inversely proportional to the contributing catchment size (McDonough et al., In review). Streams characterized as "flashy" are identified by high rates of change in streamflow, while more stable streams have slower rates of change (Baker et al., 2004; Jayakaran et al., 2016; McDonough, 2018). River flooding, in contrast, is influenced by upstream precipitation, generally lasts longer than flash flooding, and typically can be predicted in advance. The 2019 Missouri River flooding mentioned earlier is a classic example of river flooding caused by above-normal snowpack, saturated soil conditions, deeply frozen soils, and above-average precipitation (NOAA, 2019).

The power of flash flooding can be devastating to infrastructure and life. In 2003, flash flooding in Emporia, Kansas turned "a little creek we never paid attention to" into a six to seven foot wall of water that swept over the Kansas Turnpike, sweeping cars 1.5 miles off the road and causing six fatalities (Emporia Gazette, 2003). A reverend from Kansas City observed "the concrete barriers (between lanes) were being tossed around like feathers," (Hanna, 2003).

Twelve years later and two miles north on the Kansas Turnpike, tragedy struck again. All it took was six to ten inches of water covering the turnpike for another car to be swept into the flooded ditch. The flash flooding off the Flint Hills "jammed up against the culvert," formed a whirlpool, and sucked 21-year old Zachary Clark and his mustang down as Good Samaritans watched helplessly (Potter, 2015). The expected effects of climate change, both increasing average annual precipitation and extreme precipitation events, can increase both flash and river flooding.

2.2 Urbanization Impacts on Flooding

As of 2018, 82% of North Americans are living in urban areas and by 2050 it is expected to be 90% (UN, 2019). Global urbanization has occurred rapidly since 1950, having increased from 751 million to 4.2 billion in 2018 (UN, 2019). The associated landcover modification from natural areas to impervious, such as streets, roofs, and parking lots associated with urban landscapes, negatively influences the hydrologic regime (Charlton, 2008; Driscoll et al., 2010; Glascoe and Christy, 2004; McDonough et al., In review; Noori et al., 2016; Rosgen, 1996; U.S. EPA, 2000). The removal of permeable land cover and natural depression storage leads to decreased groundwater recharge and increased surface runoff (Konrad, 2003; National Research Council, 2002). Urban streams tend to have both a higher peak discharge and a larger total volume of discharge than rural streams (Konrad, 2003). The decreased infiltration and groundwater recharge also leads to lower baseflow during dry conditions. A study in Alabama looking at the spatial impacts of urbanization confirmed previous research that urbanization modifies downstream evapotranspiration rates, flood peaks, sediment transport rates, concentration of water quality constituents; that small flood events are more sensitive to urbanization than large flood events; and that land use-land cover changes have a larger impact on peak flows than runoff volumes (Noori et al., 2016). A study looking at the spatial

configuration of landcover changes found that the removal of natural ecosystem function is more detrimental than the increase in impervious cover (McDonough et al., In review). These hydrologic changes can be observed visually in the adjustment of the hydrograph's rising limb and baseflow (Figure 2.1).

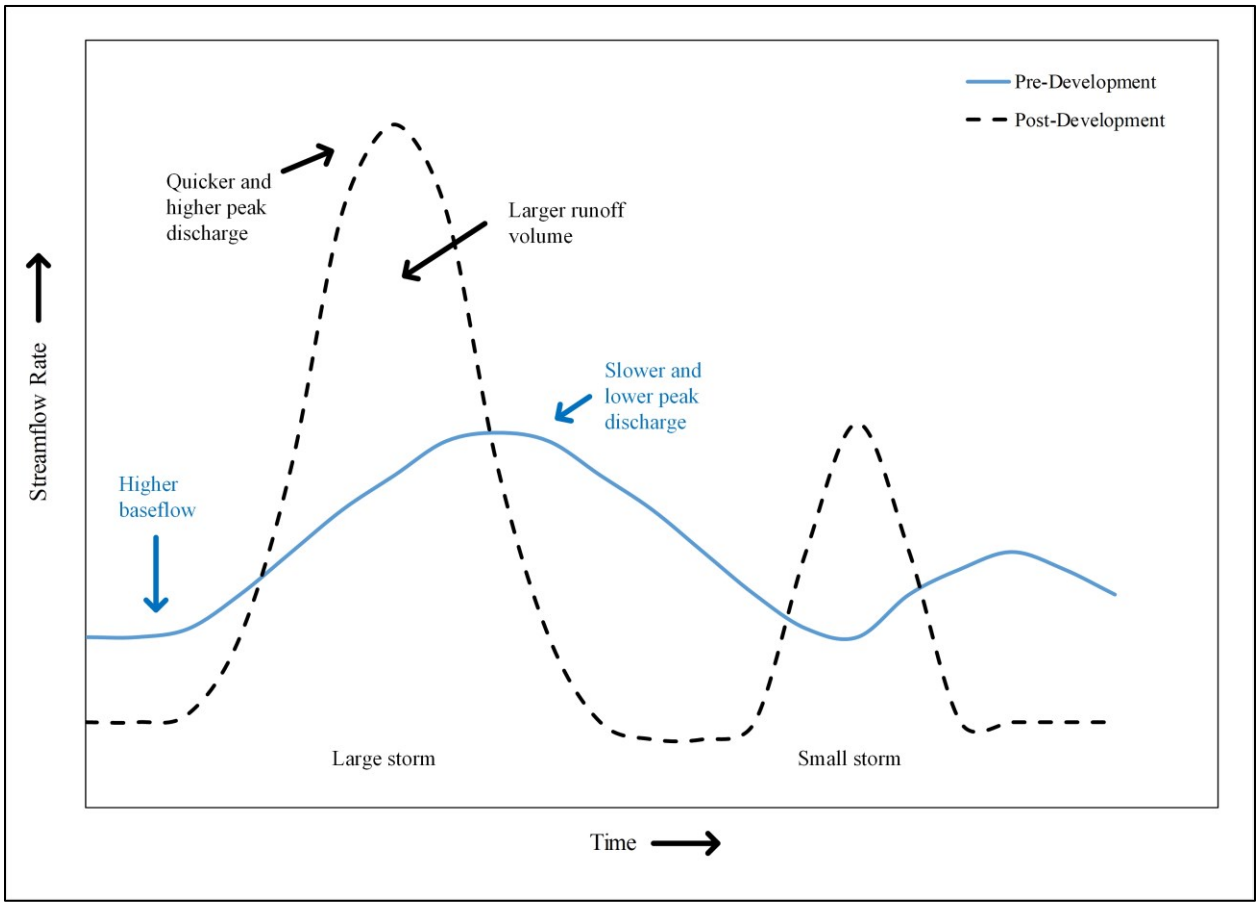

Figure 2.1. Urbanization alters the hydrograph to have higher peak discharge and total discharge volume (Adapted from Glascoe and Christy, 2004).

Increased runoff in developed areas carries sediment and pollutants, while simultaneously contributing to streambank erosion, leading to increased sediment loads in rivers, which can decrease the amount of available flood storage in rivers and reservoirs (Charlton, 2008; Kaplan and Ayers, 2000). The U.S. EPA lists sediment as the most common freshwater pollutant. Once an area reaches approximately 10-20% imperviousness, urban stream quality is consistently

classified as poor (National Research Council, 2002). Watersheds with impervious surfaces greater than 25% will likely result in a change in hydrologic regime where stream function is reduced to that of a stormwater conduit (Kaplan and Ayers, 2000). The most concentrated sediment releases come from even relatively minor construction activities, which are prevalent in urban areas (MARC, n.d.). Lane's proportion (1955) describes the relationship between sediment discharge, stream discharge, particle size, and slope (Equation 1.1).

$$Sediment\ LOAD\ x\ \ Sediment\ Size\ \propto Stream\ SLOPE\ x\ Stream\ Discharge \quad 1.1)$$

A change in any of the four variables will set up a series of mutual adjustments resulting in direct, physical changes in river characteristics to restore equilibrium (Rosgen, 1996). For example, an increase in sediment load can result in increasing stream slope and discharge.

Natural river channels are not built large enough to carry flood flow, which is meant to spread out over a connected floodplain. Rivers have been "straightened, leveed (severed from their floodplain), deepened, over-widened, lined with foreign materials, steepened, diverted, and altered" for well-meaning flood control causing unintended continuing maintenance problems and risk of failure (Rosgen, 1996, p. 1-2). Channelization compresses the period of water conveyance, making streams flashier, increasing erosion rates, and indirectly reducing survivability of riparian vegetation by lowering the water table and reducing the frequency of overbank flow (National Research Council, 2002). The downstream effects include higher flood peaks and greater loading of sediment, nutrients, and contaminants that can silt in reservoirs, channels, and culverts (Keane, 2019; National Research Council, 2002). Increased sedimentation also increases the cost of treating drinking water, negatively impacts biodiversity, and acts as a carrier for nutrients that cause eutrophication (MARC, n.d.).

Bankfull flow occurs when the channel is just at the point of overflowing onto the floodplain and typically occurs every 1.5 years in rural streams (Rosgen, 1996). In urban

streams, bankfull flow occurs closer to every 1.1 years due to the increased runoff from impervious surfaces(Rosgen, 1996). The bankfull stage "corresponds to the discharge at which channel maintenance is the most effective, that is, the discharge at which moving sediment, forming or removing bars, forming or changing bends and meanders, and generally doing work that results in the average morphologic characteristics of channels", (Dunne and Leopold, 1978). In other words, the most geomorphic work (i.e. erosion) is done on the river at bankfull flow and increased occurrences of bankfull in urban areas lead to more erosion.

Additionally, global population growth leads to more intensive urbanization in flood prone areas (Jonkman, 2005). The effects of urbanization and climate change can be seen in the upward trend of flood claims paid by the NFIP in the 21st century (FEMA, 2019). There were no years with over 2 billion loss dollars paid from 1978-2003. However, from 2003-2018 the average loss dollars paid was 3.7 billion, a substantial increase correlated with urbanization.

The energy consumption per unit area for cities is orders of magnitude higher than the same for rural, vegetated, or less developed areas (Velasco and Roth, 2010). Even though urban areas only comprise ~2% of global land area, they released 71% of the total CO_2 emissions of anthropogenic origin as of 2009 (Canadell et al., 2009). This shows the magnitude of cities' role in climate change, as carbon dioxide is responsible for more than 60% of the 2.6 Watts/ m^2 warming that has occurred from the increase in anthropogenic, long-lived GHGs (Canadell et al., 2009). This presents a positive feedback loop for climate change and increased flooding, as urbanization increases GHG emissions and flooding, and climate change further increases flooding as demonstrated in Section 2.1.

2.3 Green Infrastructure

To combat urbanization's negative hydrological and water quality effects, stormwater management practices developed in the early 1990s aimed to recreate the predevelopment hydrology including infiltration, storage, and evaporation (U.S. EPA, 2000). These practices seek to capture and infiltrate precipitation, increasing groundwater recharge and reducing the volume and frequency of runoff that would otherwise contribute to flooding and pollution problems (U.S. EPA, 2012). These practices have different names across the globe, including Low Impact Development (LID) (U.S. EPA, 2000), Storm Water Controls (SCMs), Best Management Practices (BMPs) or Green Infrastructure (GI) in the United States; Water Sensitive Urban Design (WSUD) in Australia (Roy et al., 2008); and Sustainable Urban Drainage Systems (SUDS) in the United Kingdom (Roshni et al., 2015). The terms LID and GI are used interchangeably in this thesis. It is important to note that green infrastructure developed as an alternative to traditional gray infrastructure. Conventional gray infrastructure has dominated the history of stormwater management, and has the main goal of moving water offsite as quickly as possible, typically through concrete pipes and channels (U.S. EPA, 2000). While this technique does adequately avoid ponded water, quickly moving large volumes of water, including the sediments and pollutants picked up along the way, only moves the flooding, erosion, and pollution problems to downstream communities (Nordman et al., 2018). In addition to environmental benefits, LID can often provide economic benefits. For example, replacing the "gray" stormwater control mechanisms such as curbs and gutters with strategically located bioretention areas, compact weir outfalls, depressions, grass channels, wetland swales, and basins saved a developer in North Carolina 72% or $175,000 of the stormwater construction costs (U.S. EPA, 2000).

2.3.1 Green Infrastructure Practices

Examples of common green infrastructure practices include bioretention cells/ rain gardens, constructed stormwater wetlands, green roofs, permeable pavement, and grass swales. Due to the large scale and coarse resolution of the model used in this study, lot scale practices such as those listed above were not examined. Instead, common, non-structural GI practices such as disconnection of impervious surfaces and conservation of riparian buffers were examined and will be further explained below.

Non-structural BMPs aim to retain or restore existing natural soil, vegetative, and hydrologic conditions to reduce stormwater runoff and improve water quality (APWA, 2012). They differ from structural BMPs in that they are not engineered specifically to collect, convey, and/ or store a specific amount of stormwater runoff (APWA, 2012). Eliminating direct connections, such as downspouts or sump pumps, that flow directly onto pavement or are piped into stormwater inlets are an easy and cost effective way to move closer to pre-development hydrology.

The Natural Resources Council provided the following definition of riparian areas "Riparian areas are transitional between terrestrial and aquatic ecosystems and are distinguished by gradients in biophysical conditions, ecological processes, and biota. They are areas through which surface and subsurface hydrology connect waterbodies with their adjacent uplands. They include those portions of terrestrial ecosystems that significantly influence exchanges of energy and matter with aquatic ecosystems (i.e., a zone of influence). Riparian areas are adjacent to perennial, intermittent, and ephemeral streams, lakes, and estuarine-marine shorelines" (2002). Their soil and vegetation characteristics are unique and strongly influenced by the presence of water (NRCS, 1996). Riparian areas contain the floodplains developed by rivers depositing

sediment as they have naturally migrated laterally throughout geologic time (Rosgen, 1996). The biological and hydrological benefits of riparian areas are outsized compared to larger upland areas.

The vegetation in riparian buffers decreases flow velocity causing increased infiltration and deposition of sediments, which improves water quality, supports nutrient cycling, increases productivity, and improves fish habitat (NRCS, 1996; U.S. Forest Service, 2017). Additionally, the vegetation stabilizes banks through root strength and takes up nutrients such as nitrogen and phosphorus (National Research Council, 2002; NRCS, 1996). Riparian areas and their connected floodplains are among the most biologically productive and diverse ecosystems on earth (U.S. Forest Service, 2017). River and floodplain restoration has proven to be effective in increasing the abundance and diversity of macrophyte (aquatic plant) populations, which is foundational for sustaining food webs (Lorenz et al., 2012).

Many riparian areas have been significantly altered since European settlement due to the conversion of floodplains to agricultural or developed lands, addition of dams, and construction of thousands of miles of the nation's highways and railroads being constructed along waterways (Rose, 1976; Jensen, 1993; and Lewty, 1995 as cited in National Research Council, 2002). This transportation infrastructure construction led to removal of riparian vegetation, "hardening" of streambanks with concrete and rip rap, realignment of channels, and increased sediment production. Maintaining existing riparian areas or restoring riparian buffers helps reverse these altercations and allows floodplains to be intermittently flooded as intended by nature, without the risk of damaging development built too near stream banks.

Ordinances for required riparian buffer setbacks for proposed development vary according to local laws, but typically range from 20-200 feet (Heraty, 1993). The U.S. EPA

Aquatic Buffer Model Ordinance recommends requiring a minimum of 100 feet for riparian forest buffers, with expansion for the 100-year floodplain, steep slopes, being higher than a third order stream, wetlands, or other critical areas (U.S. EPA, 2002). They suggest a three-zone buffer system with each zone having its own set of allowable uses and vegetative targets. Zone 1, the Streamside Zone, protects the physical and ecological integrity of the stream ecosystem and should extend a minimum of 25 feet from the top of the bank and consist of undisturbed native vegetation. Zone 2, the Middle Zone, provides distance between upland development and the streamside zone and should contain mature native vegetation for a minimum of 50 feet. Zone 3, the Outer Zone, prevents encroachment into the forest buffer and filters runoff from development and should be a minimum of 25 feet between Zone 2 and the nearest permanent structure. Only footpaths, flood control structures, and utility right of ways are allowed in Zone 1; biking paths and stormwater management facilities in Zone 2; and no impervious cover with the exception of paths in Zone 3. The average 100-year floodplain is projected to increase 45% by the year 2100, so it is wise to maximize conservation of riparian areas wherever possible (U.S. EPA, 2015).

2.3.2 Green Infrastructure and Flood and Erosion Reduction

Green infrastructure contributes to flood mitigation by capturing and infiltrating stormwater which reduces the volume of water flowing into streams and slows it down, reducing peak inflow (U.S. EPA, 2015). A study comparing two watersheds in the Minneapolis, MN region found that while grey infrastructure has a fixed conveyance capacity, green infrastructure has a greater capacity to adapt to increased precipitation intensity (Moore et al., 2016). They found that treating as little as 10% of the total watershed area can have appreciable impacts on flooding up to a 80% change in design storm. In highly urbanized areas, redirecting rooftop runoff conveyed in rain gutters from storm sewers and into pervious landscaped areas can

significantly reduce runoff flow to surface waters and reduce the number of combined sewer overflows (U.S. EPA, 2000). Disconnection of rain gutters can effectively be implemented on existing properties with little change to present site designs, making it an easy and affordable form of LID (U.S. EPA, 2000). Roof runoff spilling onto landscaped areas such as lawns reduces input to sewer systems in addition to reducing the amount of potable water needed to irrigate laws. Downsides include that not all lots may have enough storage to infiltrate the additional water, public perception could be negative, and even the small cost to disconnect may discourage some homeowners (Waters et al., 2010). A study in Ontario found that disconnecting only half of the roof gutters in their 23.3 ha (57.6 acre) subcatchment reduced the runoff volume and peak discharge below present values, with a greater reduction for 100% disconnection (Waters et al., 2010). A study in the Bronx, NY found that LID reduced peak flows across different climate change scenarios, although the reduction in peak volume varied by climate change scenario (Zahmatkesh et al., 2015). It is widely recognized that the storage of floodwater on floodplains can reduce flood magnitude downstream (Acreman et al., 2003). A study of 144 counties adjacent to the Gulf of Mexico found that situating development away from floodplains provided less flooding in even high density impervious areas, than low density impervious areas situated within or adjacent to floodplains (Brody et al., 2012). Watson et al. also showed the potential of floodplains to act as green infrastructure that build community resilience to climate change with a study in Vermont (Watson et al., 2016). Mcdonough et al., showed that even slight declines in the percentage of forest cover (-0.0272) leads to an increase in flood flashiness, suggesting that floodplain forest restoration may be effective in providing flood regulation services (In review).

Stormwater best management practices can also improve stormwater quality by mitigating extreme pH values and assisting removal of sediment, petroleum-based materials,

biochemical oxygen demand (BOD), metals, bacteria, nutrients, toxic organic compounds, and other harmful substances (APWA, 2012). BMPs can help communities comply with the U.S. EPA mandated National Pollutant Discharge Elimination System (NPDES) program established under the Clean Water Act in 1972 (APWA, 2012). A study conducted on a 280 km^2 watershed north of Denver, Colorado sought to determine how "infiltration based stormwater practices can be best coordinated with channel restoration projects to improve channel stability and reduce sediment and adsorbed phosphorus loading from channel erosions," (Lammers et al., 2019, p. 2). The modeled the infiltration practices as rain gardens in SWMM, with each rain garden sized to be able to treat the excess urban runoff volume (EURV) from 2002 m^2 (0.5) acres of impervious area. A total of 1.2 km^2 of rain gardens were required to manage the EURV for the study area, or 2.2% of the total modeled area. The streambank restoration practices modeled consisted of sloping banks back to 20°, adding bank armoring, and increasing bank cohesion. Their model results suggest that watershed-scale implementation of stormwater controls that reduce runoff volume across a spectrum of storm size is a more effective approach for reducing channel erosion and pollutant loading than stream restoration. This is an example of how a systems-based solution (watershed wide GI) can be more effective than site-based solutions (stream reach restoration) at managing the cause (stormwater volumes), not just the symptoms (erosion, channel degradation). A study in Wichita, Kansas used PCSWMM and three Logsdon and Chauby (2013) indices: freshwater provisioning index (FWPI), erosion regulation index (ERI), and flood regulation index (FRI) to understand the impact of varying stormwater control measures across an urban watershed (Mcdonough et al., 2017). The three SCMs evaluated were bioretention cells, green roofs, and rain barrels. They found that while bioretention cells reduced erosion immediately downstream of the SCM implementation, they did not significantly reduce

flooding or erosion further downstream in the watershed. Neither the green roofs nor rain barrels demonstrated any freshwater, erosion regulation or flood regulation provisioning services at either location. Furthermore, they found that the extent of ecosystem service provision decreased as the size and magnitude of the storm event increased. This could provide challenges for the efficacy of LID as the frequency of intense storm events increases.

Riparian restoration has the best flood and erosion reduction when started upstream and continuous patches are restored versus disparate patches (Lammers et al., 2019). Additionally, the connectivity of buffers is important for terrestrial wildlife conservation and ecological resilience (Bentrup and Kellerman, 2004; Fremier et al., 2015).

2.3.3 Green Infrastructure and Ecosystem Services

Over the past 50 years, humans have changed ecosystems more rapidly and extensively than in any comparable period of time (Millenum Ecosystem Assessment, 2005). The Millennium Ecosystem Assessment defined ecosystem services as "the benefits people obtain from ecosystems," (2005, p. V). These services include "*provisioning services* such as food, water, timber, and fiber; *regulating services* that affect climate, floods, disease, wastes, and water quality; *cultural services* that provide recreational, aesthetic, and spiritual benefits; and *supporting services* such as soil formation, photosynthesis, and nutrient cycling" (Millennium Ecosystem Assessment, 2005, p. V). Ecosystem services are not synonymous with ecosystem processes; ecosystem services are used by humans while ecosystem processes will occur regardless of humans (McDonough, 2015). Reversing the degradation of ecosystems while meeting increasing demands for their services cannot be met without significant changes in policies, institutions, and practices (Millenum Ecosystem Assessment, 2005).

However, it is challenging to quantify the ecosystem services provided by GI because the benefits are multi-scalar and multi-functional in nature and there is a multiplicity of interactions between the various phenomena (Demuzere et al., 2014). The following paragraphs seek to explain and demonstrate studies that have quantified the benefits of GI beyond the ecosystem service of flood regulation.

Green urban infrastructure contributes to climate change mitigation by directly removing CO_2 from the atmosphere via photosynthetic update during the day, with additional uptake from soils and corresponding below ground activity although a fraction of CO2 is released through night time respiration (Velasco and Roth, 2010). Green urban infrastructure also helps with climate change adaption by providing shading and enhancing evapotranspiration which can reduce air and surface temperature, leading to reduced energy use (Demuzere et al., 2014). This regulating ecosystem service is extremely important as extreme heat was the leading cause of weather-related deaths in the United States from 2000-2009 (CDC, 2013). The urban heat island effect also causes cities to be up to 10°F warmer than surrounding rural areas due to concrete and asphalt absorbing and holding heat, tall building reducing cooling air flows, addition of waste heat from anthropogenic sources, and lack of vegetation (CDC, 2013; Larsen, 2015). Extreme heat also disproportionally harms marginalized groups (Larsen, 2015). A study in Phoenix, Arizona found that wealthier neighborhoods had lower temperatures than lower income neighborhoods due to a higher density of trees and other vegetation (Jenerette et al., 2007). A study using energy exchange and hydrologic models for Greater Manchester, England found that incorporating 10% green cover into highly impervious sites resulted in a 1.7-3.7° decrease in the maximum surface temperature by the 2080s (Gill et al., 2007). The same study found that removing 10% of the green area from the same location increased the projected 2080 surface

temperature by 7-8.2°C. This echoes the theme that it is easier to maintain ecosystem services, rather than recover them once they have been lost. The authors note that drought resistant plants should be used so to maintain evaporative cooling function during the projected increased summer dry spells. They also found that due to projected increases in precipitation is high enough to offset the decreased surface runoff from greenspaces, so it is important to incorporate green infrastructure with additional storage.

The benefits of green infrastructure vary across temporal and spatial scales. For example, benefits noticeable at the site level are not always transferable to a neighborhood or watershed scale. Demuzere et al., synthesized the results from a literature review of green infrastructure benefits across three spatial scales and found that improved water quality, reduced flooding, and cultural services are relevant based on empirical evidence at site, neighborhood, and city scales. There are additional CO2 reduction, reduced energy use, and improved air quality benefits at varying scales (Demuzere et al., 2014).

Given that raising taxes is politically undesirable for many elected officials, and many municipalities face tight budgets, it is important to quantify the economic benefit of green infrastructure. A triple bottom line assessment evaluating economic, environmental, and social benefits is an effective way of understanding the benefits of green infrastructure. Stratus Consulting undertook that challenge for the City of Philadelphia to help them compare the potential benefits of implementing a 50% Low Impact Development scenario versus a 30-foot storage tunnel (2009) to address their combined sewer overflow (CSO) challenges. The 50% Low Impact Development scenario means that 50% of all runoff from impervious areas will be treated with green infrastructure. Table 2.1 demonstrates their findings on just how monetarily beneficial the ecosystem services provided by green infrastructure are.

Table 2.1. City-wide present value benefits of CSO options: cumulative through 2049 (2009 million USD) (Stratus Consulting, 2009)

Benefit Categories	50% LID Option	30' Tunnel option
Increased Recreational Opportunities	$524.5	
Improved aesthetics/ property value (50%)	$574.7	
Reduction in heat stress mortality	$1,057.6	
Water quality/ aquatic habitat enhancement	$336.4	$189.0
Wetland Services	$1.6	
Social costs avoided by green collar jobs	$124.9	
Air quality improvements from trees	$131.0	
Energy savings/ usage	$33.7	-$2.5
Reduced (increased) damage from SO_2 and NO_x emissions	$46.3	-$45.2
Reduced (increased damage from CO_2 emissions	$21.2	-$5.9
Disruption costs from construction and maintenance	-$5.6	-$13.4
Total	**$2,846.4**	**$122.0**

A research team in Grand Rapids, Michigan conducted a similar cost-benefit analysis of multiple green infrastructure practices (Nordman et al., 2018). The authors compared the installation, maintenance, and opportunity costs of GI practices (porous asphalt, rain garden, green roof, infiltration bioretention, conservation of natural areas, and street trees) to the benefits of avoided stormwater runoff costs, pollution reduction, and aesthetic enhancement over the expected life of the system and using net present value. Each GI practice was standardized to treat one inch of rainfall, which is often the design basis for GI. They used a benefit transfer

approach to estimate the net present value (NPV) of capital, operations, and maintenance costs, as well as the direct and indirect benefits. The suite of benefits varied for each GI practice and included flood risk reduction; reductions in stormwater volume, total phosphorus, total suspended solids, and air pollution; scenic amenity value; and CO2 storage. Conserved natural areas had the largest NPV at $109/m3 of water quality volume (WQv) reduced, followed by street trees at $46/m3 WQv, rain gardens at $37/m3 WQv, and porous asphalt at $21/m3 WQv. Infiltrating bioretention basins and green roofs had negative NPVs of $-3.76/m3 WQv and $-47.17/m3 WQv, respectively. The authors note that it is cheaper to avoid generating stormwater runoff rather than treating it later, evidenced by conserving natural areas having the highest NPV.

While green infrastructure provides a host of important ecosystem services, there are some drawbacks. Although green infrastructure has more adaptation potential than conventional infrastructure and often has lower capital costs, it still does require maintenance and resulting operational costs (Larsen, 2015). This maintenance can be costly and not all municipalities have staff dedicated to this maintenance. However, many communities have realized the high return on investment and created stormwater taxes or stormwater utilities. As of 2009, over 800 communities had adopted a stormwater utility to help fund stormwater programs (U.S. EPA, 2009). Furthermore, if native vegetation is used for LID, it requires less maintenance because it has evolved over millennia to thrive in the local climate (APWA, 2012).

The benefits of green infrastructure are more evident for smaller sized storms. GI is often designed only to treat the water quality volume, or the amount of storage needed to capture and treat 90% of the average annual stormwater runoff volume of all 24-hour storms (APWA, 2012).

However, when considering the numerous advantages described above, the low impact development strategy is important for planners to consider.

2.4 Transportation Resiliency

Dwight D. Eisenhower, 34th president of the United States understood the importance of transportation resiliency: "A modern, efficient highway system is essential. …The obsolescence of the nation's highways presents an appalling problem of waste, danger and death. …A network of modern roads is as necessary to defense as it is to our national economy and personal safety." Well-maintained infrastructure is vital to the life of cities, as citizens need to use the roads to drive to work, school, and errands. Transportation systems are designed to accommodate changing weather conditions and a reasonable range of extremes, such as the historic 100 year flood event (Transportation Research Board, 2008). However, there have been observed and predicted changes in weather and climate extremes that push environmental conditions outside the range for which the system was designed, especially increased heat waves and intense precipitation events (Transportation Research Board, 2008). The current 100-year flood event is projected to occur about every 10-50 years in many of the world's largest river basins for the period 2071-2100 (Hirabayashi et al., 2013). Changes in the precipitation distribution upon which infrastructure was designed equates to changes in the risk communities face with respect to flooding, property damage, and human safety (Moore et al., 2016). In Europe, weather stresses represent 30-50% of current road maintenance costs, 10% of which are associated with extreme weather events – mainly extreme heavy rainfalls and floods (Nemry and Demirel, 2012). Historical regional climate patterns may no longer be a reliable guide for transportation planners when the future climate will include different magnitude and frequency of weather and climate extremes as "human-induced changes are superimposed on climate's natural variability"

(Transportation Research Board, 2008, p. 5). Adding to the problem, one out of every five miles of American highway pavement is in poor condition and there is a $836 billion backlog of highway and bridge capital needs (American Society of Civil Engineers, 2020). The United States' aging and deteriorating infrastructure has traditionally been designed for historical climate trends, so it is at heightened risk to increasing flooding, which can cause cascading impacts that threaten the economy, national security, health, and well-being (Reidmiller et al., 2018). In addition to increased inundation from flooding, higher discharge rates can more easily erode road bases and bridge supports, and increased sedimentation can silt in culverts. While coastal flooding is not evaluated in this paper due to the study area being located in the Midwest, it will potentially have the greatest impact on America's transportation infrastructure (Transportation Research Board, 2008). Heat waves pose a risk to transportation infrastructure by the thermal expansion of bridge expansion joints and paved surfaces, softening leading to concerns regarding pavement integrity, traffic-related rutting, and migration of liquid asphalt (Transportation Research Board, 2008). A study in Alaska found that the largest expense and most extensive damage due to projected climate change would be road flooding due to increased precipitation (Melvin 2016). They found that for RCP 8.5, the business as normal emissions scenario, cumulative estimated expenses from climate-related damage to infrastructure were $5.5 billion (2015 dollars) from 2015-2099. However, for RCP 4.5, where emissions begin to decrease around 2040, damages totaled $4.2 billion indicating decreasing GHG emissions could lessen Alaskan infrastructure damages by $1.3 billion this century. Proactive adaptation reduced total projected damages $2.6 billion for RCP 8.5 and $1.9 billion for RCP 4.5. For road flooding, the proactive adaptation provided an annual savings of 80-100%. Adaptation measures included modified binder/sealant application, base-layer strengthening, increased diameter culverts and

drainage systems to protect from increased precipitation and flooding. Melvin also notes that pavements are designed for specific minimum and maximum temperature limits, and temperature fluctuations beyond those limits have the potential to damage pavement surfaces.

A team of researchers set out to quantify the vulnerability of the primary transport infrastructure in Mexico due to climate change (Espinet et al., 2016). They knew that economically quantifying the effects of precipitation and temperature variability was an important step for advancing the rhetoric surround climate change and demonstrating to politicians the importance of proactive, sustainable investment upfront to prevent significant repair costs later. The authors developed the *Infrastructure Planning Support System (IPSS)* to quantify the costs in three steps: 1. determines the projected climate change in the specific region using CMIP 3 or CMIP 5, 2. evaluate climate change impact on the infrastructure using material-specific stress-response equations and materials information. 3. quantify projected damage with construction and maintenance costs. They looked at both kilometers damaged, representing the length of road damaged by rising temperature and precipitation, and opportunity cost, representing the amount of new road that could be built if money was not diverted to repair roads damaged by climate change. The study projected a total fiscal cost of $1.3-$4.8 million USD cumulative cost for 2015-2050 time period. They note that due to the primary road infrastructure typical lifetime of 20-30 years, that any constructed or renovated roads at present day should consider the impact of climate change as it will have serious impact by the mid-point of its lifespan.

The additional increased flooding and erosion effects of urbanization discussed in section 2.1 further exacerbate the problems facing transportation infrastructure. For example, new

developments expose roads constructed in flood-prone areas to increased inundation and erosion hazards (Konrad, 2003).

Chirisa defines resilience as "the ability of a social or ecological system to absorb disturbances while retaining the same basic structure and ways of functioning, the capacity for self-organisation, and the capacity to adapt to stress and change," (2016). The Mid-America Regional Council (MARC) has a more ambitious definition of resiliency in their 2017 *Climate Resiliency Strategy:* "the ability of a system or community to survive disruption and to anticipate, adapt, and flourish in the face of change." The above paragraphs describe the unprecedented risks facing transportation infrastructure and the critical importance of maintaining its function. The challenge is determining proactive, economically effective steps to not only maintain function, but "flourish in the face of change." Benefits of green infrastructure have been noted in section 2.3. The role of this research is to use modeling to determine the extent green infrastructure can increase resiliency of transportation infrastructure, using Kansas City as a case study.

2.5 Hydrologic and Hydraulic Modeling

2.5.1 Model Types

A model is a series of equations that, together, represent some aspect of the physical world and are often compiled for use on a computer (Zeckoski et al., 2015). Hydrologic and water quality models are fundamental scientific tools used to predict, forecast, and explain phenomena at different spatio-temporal scales (Baffaut et al., 2015). City officials often rely on models to inform their management decisions because models help minimize expensive field studies and "predict the future," (Noori et al., 2016). However, there are an abundance of mathematical models utilized for stormwater modeling. It is necessary to determine which model

is appropriate for the desired results and with the available data. Zeckoski et al. sough to determine a single, preferred definition for the various modeling concepts (Table 2.2).

Table 2.2. Definitions of model description terms (Zeckoski et al., 2015)

Term	Definition
Model	
Model	"Model" without further clarification should be used to refer to a series of unparameterized equations representing some aspect of the physical world that have been codified and (where appropriate) compiled for use on a computer.
Model code	The source code of a simulation model.
Model dimensionality	
N-D model	*N* may be 1, 2, or 3; water quality constituents vary over the specified number of dimensions and are averaged over the remaining dimensions.
Analytical vs. numerical models	
Analytical model	"Can be solved mathematically in terms of analytical functions. For example, some models that are based on relatively simple differential equations can be solved analytically by combinations of polynomials, exponential, trigonometric, or other familiar functions" (USEPA, 2009a).
Numerical model	"Approximates a solution of governing partial differential equations which describe a natural process. The approximation uses a numerical discretization of the space and time components of the system or process" (USEPA, 1999).
Deterministic vs. stochastic models	
Deterministic model	Contains no random elements such that a unique set of input variables produces a unique output.
Stochastic model	"Includes variability in model parameters. This variability is a function of (1) changing environmental conditions, (2) spatial and temporal aggregation within the model framework, and (3) random variability" (USEPA, 2009a).
Empirical vs. physically based models	
Empirical model	Structure is derived experimentally from observed data.
Physically based model	Structure is based on the direct mathematical quantification of physical, chemical, and/or biological processes.
Distributed vs. lumped parameter models	
Distributed parameter model	Divides the simulated area into smaller homogeneous subunits or grid cells. Flow in the simulation is routed from one subunit or cell to the next such that model output can be generated at any point in the simulated area (Novotny and Olem, 1994).
Semi-lumped parameter model	Divides a modeled area into subunits within each of which the parameters are considered homogeneous or lumped. The subunits in this case are typically large (e.g., subwatershed scale), larger than the cells used in a fully distributed parameter model.
Lumped parameter model	Relies on one parameter set for an entire simulated area. The parameter set may be the result of an average or weighted average of the characteristics of the entire area, but from the model's point of view the entire area is one homogeneous unit.
Spatial scale	
Field-scale model	Designed to be applied to a small area with a single land use, such as a single paddock or crop field in an agricultural application.
Hillslope-scale model	A special case of a field-scale model that may simulate surface and subsurface flow along a single flow path.
Watershed-scale model	Designed to simulate a larger drainage area including multiple drainage paths, varied land uses, and a distinct channel system. The watershed scale may be applied to areas from a few hectares to as large as hundreds of km^2.
Temporal scale	
Continuous simulation model	Simulates outputs in a sequential basis on (typically) hourly or daily time steps for a period of months or years.
Event-based model	Simulates the runoff and/or pollutant loss from a single storm event.

2.5.2 Modeling Challenges

While some models are useful, all models are ultimately wrong. Every model is a simplified representation of the interconnected physical, chemical, and biological processes that occur within a watershed (National Research Council, 2008). While there are modeling best practices in place, it is impossible to eliminate all uncertainty from modeling.

Due to hydrology being a "context-dependent discipline," questions on how to collect maximum hydrological insight through data collection while minimizing costs are very pertinent

(Blöschl et al., 2007, p. 1241). Hydrological simulations to evaluate LID performance require a highly spatially distributed and explicit modeling approach, however the detailed data is often not available for large urban areas (Krebs et al., 2016). Even with high resolution, one-meter or less LiDAR data, small-scale features such as street curbs that influence urban surface flow are unsatisfactorily represented (Krebs et al., 2016). In order to model discreetly at a high resolution, a 7413-acre subcatchment in Finland was delineated into 56,037 subcatchments (Krebs et al., 2016). The highly discrete Klenzendorf study of decentralized storm water control measures for 368.3 acre watershed took five years to complete (B. Klenzendorf, personal communication, October 21, 2019). Additionally, higher resolution data does not necessarily model results more accurately (Yang et al., 2018). Simpler, lumped models may be preferred in the absence of sufficient data to effectively parameterize a distributed approach, or for simplicity and computational speed (National Research Council, 2002). Mismatches between the scale of the data used to parameterize and calibrate the model, and the objectives of the modeling study can produce misleading conclusions or waste valuable resources (Baffaut et al., 2015). It is an incorrect assumption that relationships found on a small spatial scale can be extrapolated out and remain constant (Blöschl et al., 2007). Different biophysical processes dominate at different spatial scales and it can be difficult at larger scales to identify causality from one change such as land cover change (Blöschl et al., 2007; McDonough et al., In review).

Chapter 3 - Study Area

3.1 Location and Land Use

The Blue River Watershed was the original focus for this study. It compromises 700.8 square kilometers (173,165 acres) in the Central United States (**Error! Reference source not found.**). This watershed is much larger than many of the study areas of modeling projects in existing literature: 99.9%, 82.6%, 99.9%, 99.8%, 90.3%, 99.99% larger respectively (Abdelrahman et al., 2018; Akhter and Hewa, 2016; Broekhuizen et al., 2019; Klenzendorf et al., 2015; Krebs et al., 2016; Rangari et al., 2018; Worthen, 2019). The Blue River Watershed is still 95.7% larger than Kreb's 2016 study addressing the challenges of parameterizing a "large" watershed. This watershed fits into the "river basin" category described in Baffaut et al. (2015), for being larger than 50 km^2 (19.3 mi^2). Their study maintains watershed models are between 50 ha to 50 km^2 (0.2-19.3 mi^2), and models between 100 m^2 to 50 ha (1076 ft^2 - 0.2 mi^2) are "field or small catchment." The watershed is split approximately 60/40 between Kansas and Missouri; 58.23% lies in Johnson County, 37.94% in Jackson, 3.67% in Cass, 0.13% in Wyandotte, and .03% in Miami. The Blue River Watershed (HUC #1030010101) is located within the Lower Missouri-Crooked Watershed (HUC #10300101) in the greater Missouri River Basin. The main branch of the watershed, the Blue River (63.1 km, 39.2 mi.), flows northeast from the headwaters in southern Johnson County to where it joins the Missouri River in eastern Kansas City. The main tributaries to the Blue River are Wolf Creek, Coffee Creek, Indian Creek, Tomahawk Creek, and Brush Creek (Figure 3.1).

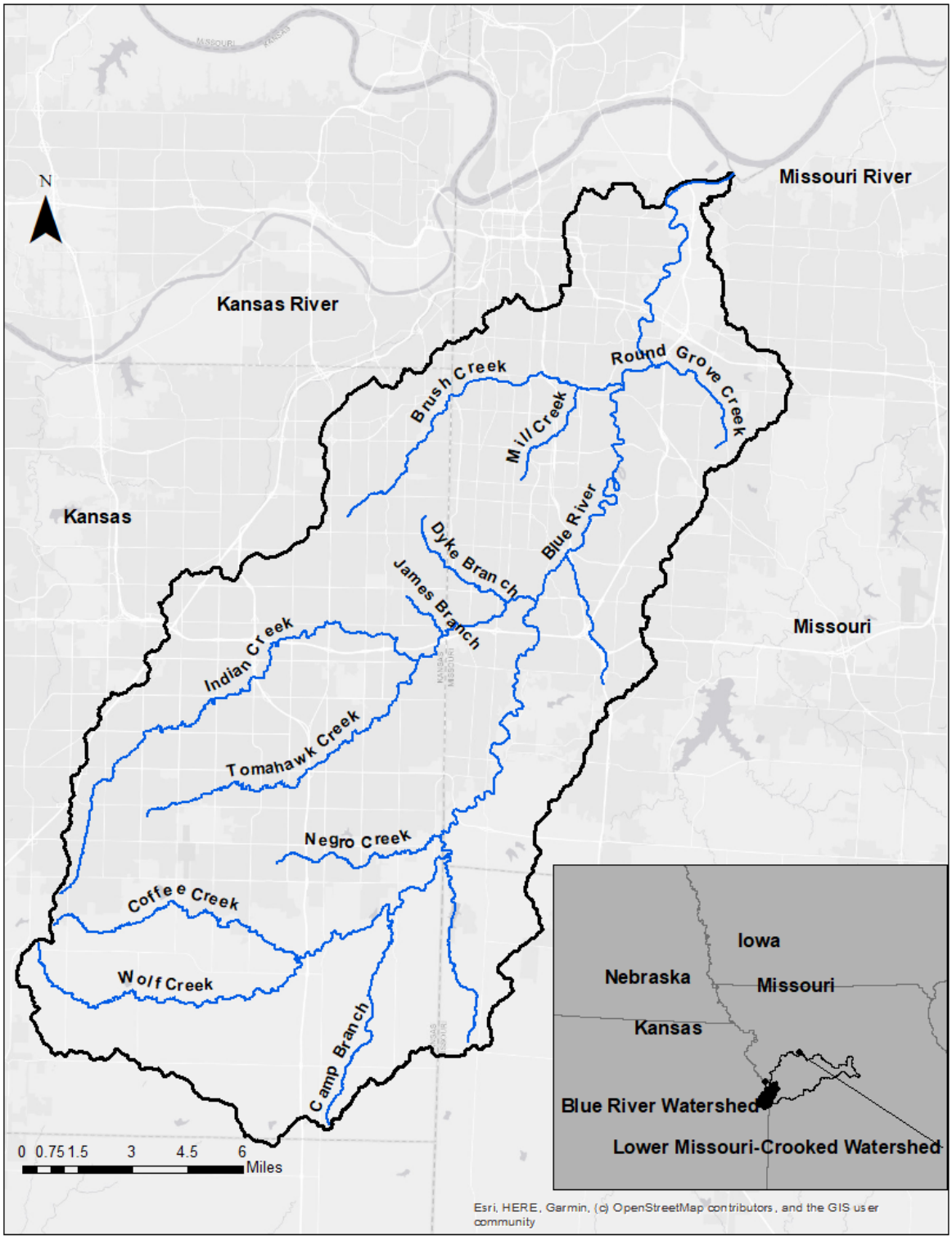

Figure 3.1. The BRW is located at the Kansas-Missouri border and contains 11 main tributaries.

The population of Johnson County has been increasing at a steady pace since World War II, with the United States Census estimating that the population was 597,555 in July 2018. The population of the Kansas City metropolitan area is also growing and was estimated in 2017 to include approximately 2,088,830 people (Open Data Network, 2017). The MARC 2040 forecast predicts a population increase of over 265,000 new residents in Johnson County, over 65,000 new residents in Jackson County, and over 40,000 new residents in Cass County from 2010-2040. This watershed encompasses a large urban-rural gradient, which presents a large opportunity for low impact development in the headwaters as it urbanizes (Figure 3.2).

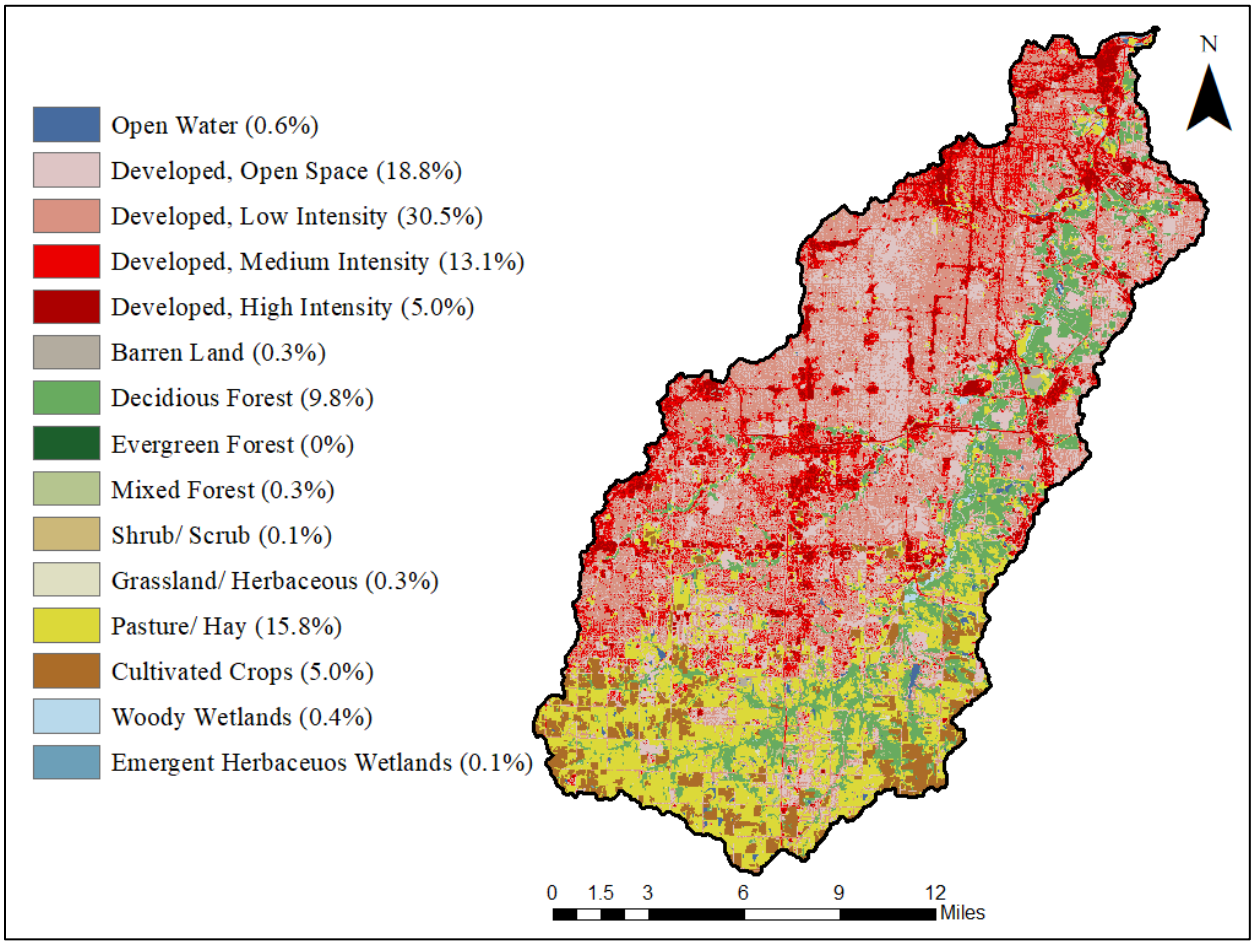

Figure 3.2. The BRW has a notable north-south, urban-rural gradient (Homer et al., 2020).

This watershed intersects two states, five counties, and 21 different cities and unincorporated townships (Figure 3.3). This high level of political fragmentation can lead to adverse water resource management outcomes (Kim et al., 2015).

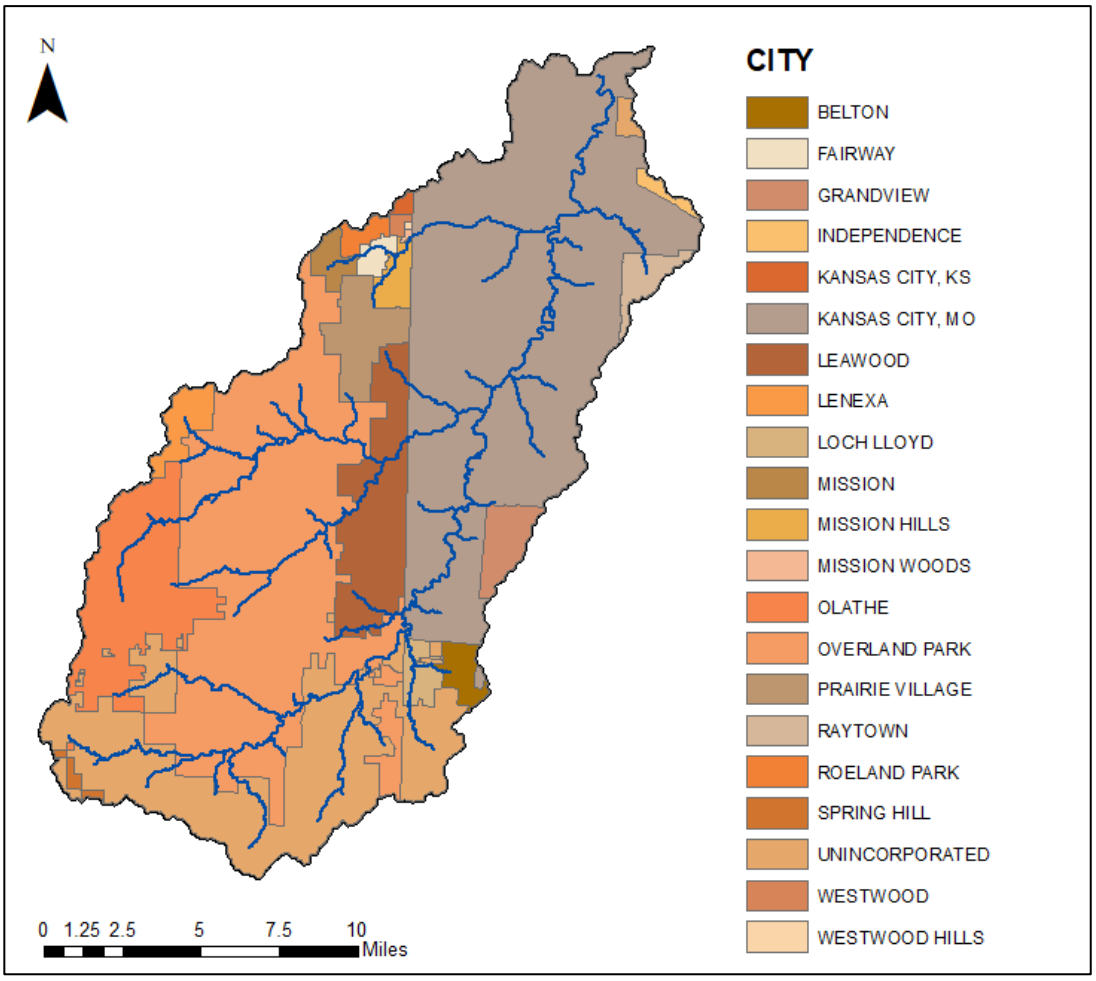

Figure 3.3. The BRW intersects 21 different cities and townships. Political fragmentation in a watershed can lead to adverse water resource outcomes (MARC, 2010).

3.2 Geomorphology

The Blue River Watershed intersects four U.S. EPA Level IV ecoregions: the Osage Cuestas, Wooded Osage Plains, Rolling Loess Plains, and Missouri Alluvial Plain (Figure 3.4) (U.S. EPA, 2013). The physiography of the Osage Cuestas and Wooded Osage Plains are defined by gentle undulating plains and perennial streams, while the Missouri Alluvial Plain is glaciated

level floodplain alluvium with riparian wetlands that have been largely drained (Kansas Native Plant Society, 2019). The Rolling Loess Prairie topography is dominated by irregular plains to low open hills (Iowa Department of Natural Resources, n.d.). Limestone and shale rocks that compose the bedrock geology were formed in sediments deposited in the shallow seas that covered the watershed during the Pennsylvanian subperiod that occurred between 323 to 299 million years ago (Kansas Geological Survey, 1963; O'Connor, 1971). Once the sea levels fell far enough to expose the land, freshwater streams cut deep channels into the limestone and shale that were then filled with sand, silt, and rock fragments from the channel walls (Kansas Geological Survey, 1963). The most prominent soil types in the watershed are Chillicothe silt loam, Oska-Martin silky clay loams, Sharpsburg silt loam, Snead-Urban land complex, and Sibley-Urban land complex, at approximately 19%, 12%, 8%, 6%, and 6% respectively (Soil Survey Staff, 2019).

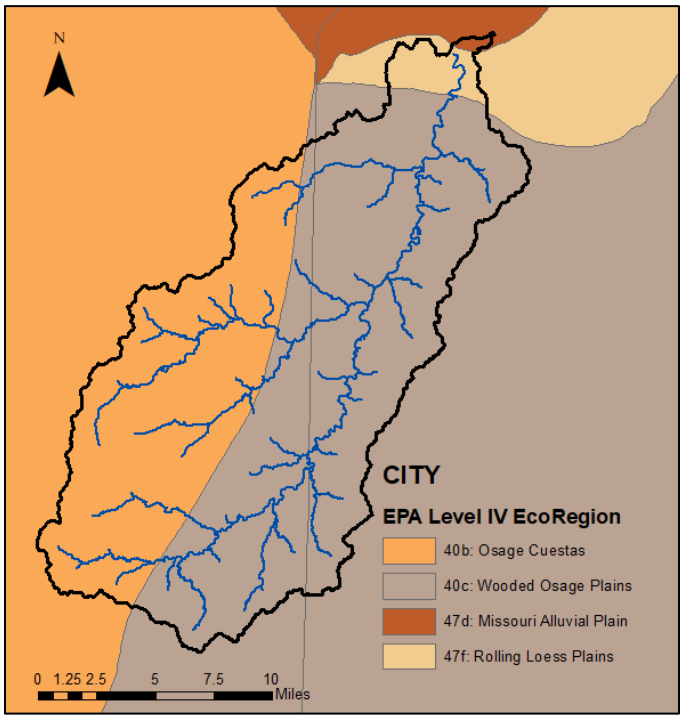

Figure 3.4. The BRW intersects four U.S. EPA Level IV ecoregions (U.S. EPA, 2013).

3.3 Stormwater Control Concerns

Flooding has been a major concern in this watershed since disastrous flooding occurred in 1928 and 1929 (MARC, 2020). A record-setting flood in September 1961 led to a congressional resolution requesting the U.S. Army Corps of Engineers perform a study of the area. After work was authorized in 1970, approximately $250 million has been spent (as of 2003) on channelization and flood control in the lower Blue River (Patti Banks Associates, 2007). Channelization of rivers often leads to instability within the engineered reach, and in the upstream and downstream reaches. For example, enlarging a channel for flood control reduces the velocity, increasing deposition of sediment and need for dredging to maintain capacity (Charlton, 2008). Additionally, engineered channels tend to have less biodiversity than natural streams (Charlton, 2008). An Olsson Associates study found lateral movement of up to 42 feet in Indian Creek from 1998 to 2018 in over 25 locations, 200,000 cubic yards of erosion across 60 miles of stream length (they included Indian Creek tributaries in their study), and that the erosion volume is approximately 3 times the observed in-stream sedimentation volume (Stanton, 2019). While lateral migration can be part of the natural function of a stable stream, it is of major concern to property owners along the edge of Indian Creek. The Ozarks Environmental and Water Resources Institute identified 55 “problem” areas on 5.2 miles of upper Indian Creek that flows between Avalon St. and Pflumm Rd (2013). The problem types include bank erosion and failure, bed erosion undermining a bridge, exposed pipes or cables due to erosion, failed culvert/ inlets due to undermining, hanging culverts due to incision, and sedimentation inside a culvert decreasing flow capacity (Pavlowsky and Owen, 2013). The stream erosion and movement has caused significant public safety and economic concerns, “homes that were once 75 feet from the stream bank are now only 15 feet away; sanitary sewers and gas lines that were once safely 4 feet

below the stream bed are now suspended 3 feet in the air; storm sewers that originally discharged at the edge of the stream are now hanging off the stream bank or entirely broken off; public trails are ready to collapse in the stream in some locations (Olsson Associates, 2014, p. 1). Historic flooding in 2017 led to a strip mall of buildings at Wornall and 103rd being completely inundated and the owners of Coach's sports bar to require a rooftop rescue (Pekarsky, 2017).

While citizens tend to have a short memory in regards to flooding when it comes time to fund flood control projects, the Indian Creek flooding has been so significant that progress is occurring. Concerned voters passed a property tax hike plan that approved $150 million for flood control projects (Canon and Sanderson, 2017). KC Water purchased land near 103rd and Wornall to demolish the flooded buildings from 2017 and replace them with green space (Laflore, 2019). Mayor Pro Tem Kevin McManus acknowledges the importance of planning future development in terms of how it impacts the floodways and wants to encourage residents to increase pervious surfaces on their property to capture water before it flows into Indian Creek (Pepitone, 2019).

3.6 Ecosystem Services

There are numerous parks and trails within the Blue River Watershed including the Overland Park Arboretum, Swope Park, and the 17-mile Indian Creek trail. Upper portions of the Blue River provide recreational sport fishing opportunities for multiple species including largemouth bass, channel catfish, carp, crappie, bluegill and green sunfish (MARC, 2020). Many citizens appreciate the ecosystem services provided and have taken an active desire to protect the watershed. A science teacher founded the Blue River Watershed Association in 1996, and they now operate multiple programs dedicated to educating citizens and protecting the watershed. T.R.U.E Blue (Teaching Rivers in an Urban Environment) educates over 10,000 local students annually in watershed and water quality issues and CPR (Communities Protecting Rivers)

provides funds to repurpose vacant lots into native plantings (Blue River Watershed Association, 2018).

3.7 Tomahawk Creek

The smaller Tomahawk Creek subwatershed of the Blue River Watershed was selected for a more in-depth analysis. The Tomahawk Creek Watershed (TCW) is 59.84 square kilometers (14,788 acres). It comprises 8.5% of the Blue River Watershed (Figure 3.5), and is a nearly fully developed suburban area (Figure 3.6) with an average of 35% imperviousness across the watershed (Figure 3.7). The highest average impervious areas are concentrated around the U.S. Highway 69 corridor in the center of the watershed.

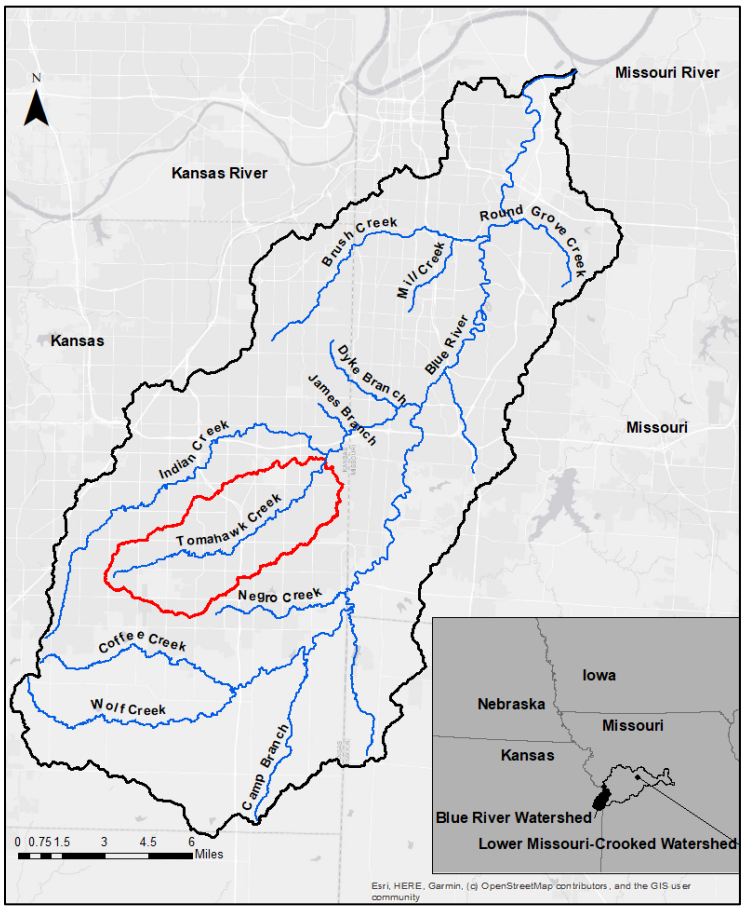

Figure 3.5. Tomahawk creek watershed is located in the center of the BRW.

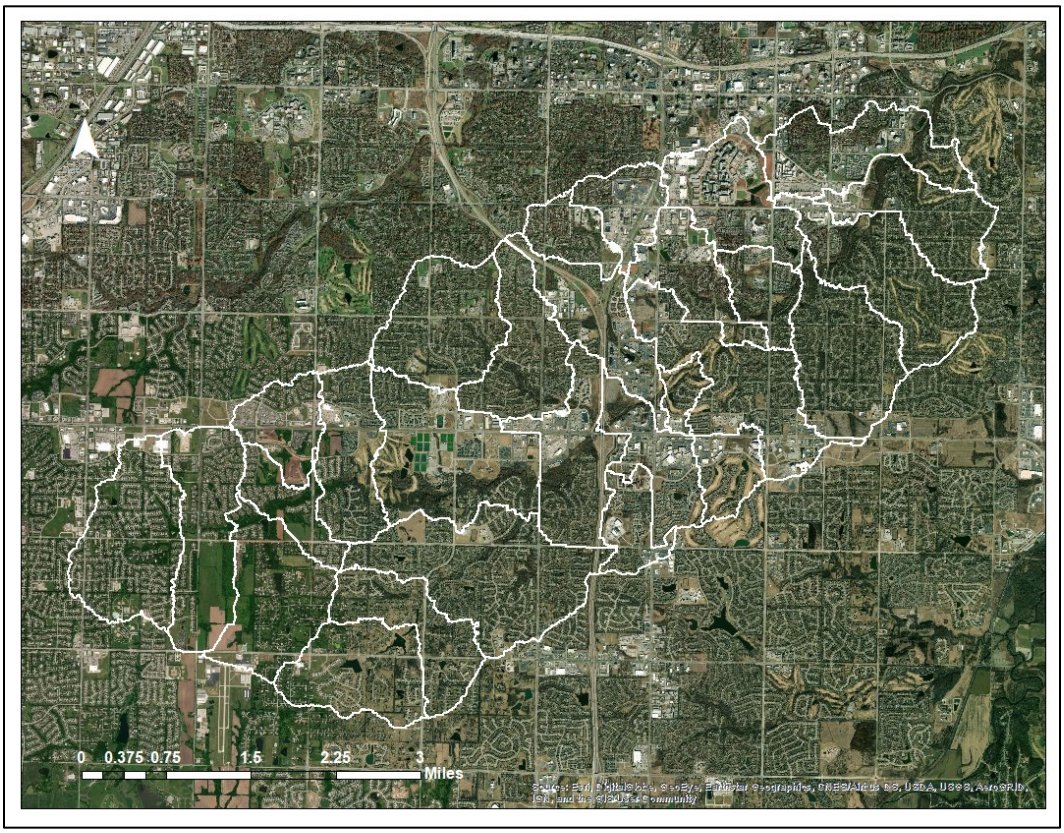

Figure 3.6. Tomahawk Creek Watershed landcover is largely suburban development with golf courses and light industrial mix.

This watershed contains one USGS gage, 06893350, located on the bridge where Tomahawk Creek flows under Roe Avenue. Tomahawk Creek was determined to have a bankfull discharge of 31.15 cms (1,100 cfs) at this location and a bankfull stage of approximately 3 m (9.8 ft) (Peters and Studley, 2014). The flood frequency analysis used to determine bankfull flow can be observed in Appendix A.

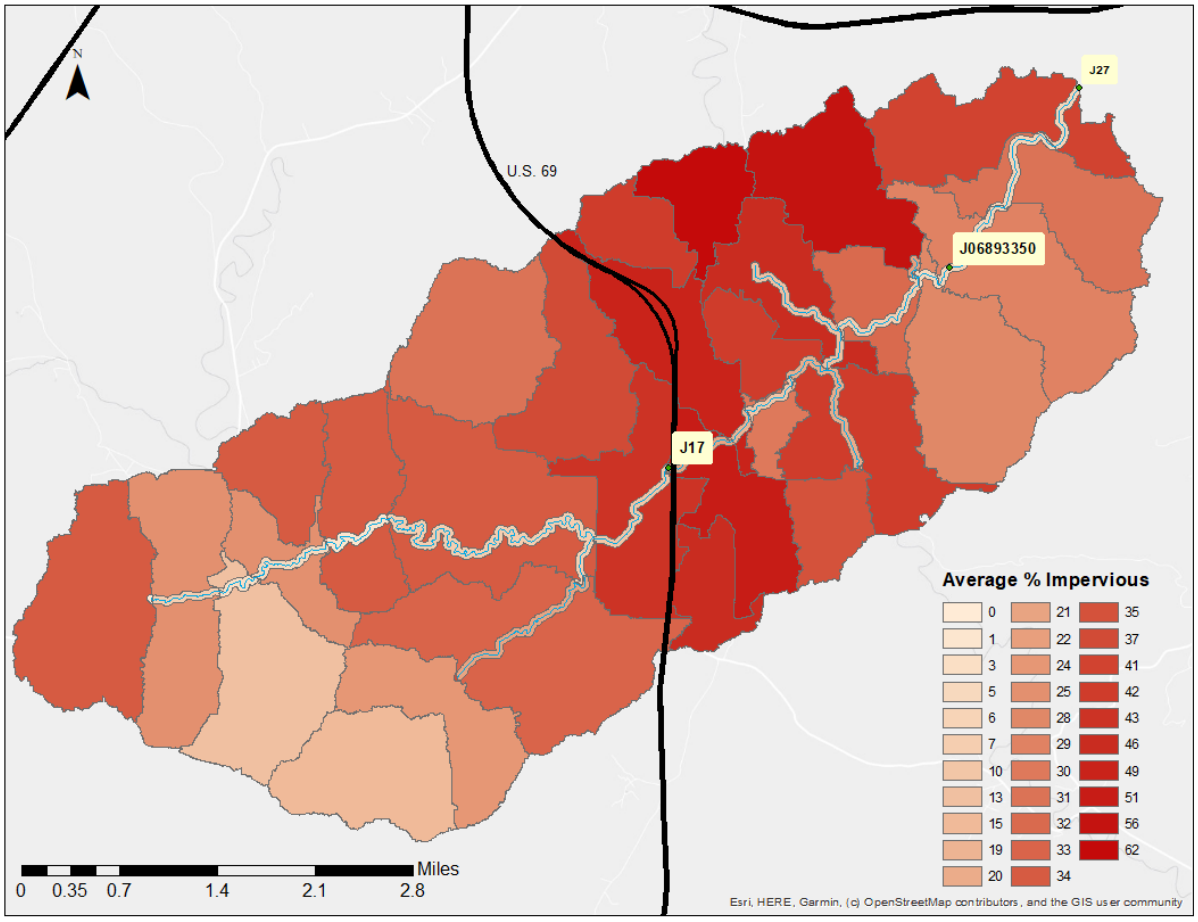

Figure 3.7. Average percent imperviousness in Tomahawk Watershed along with assessment locations

Chapter 4 - Methods

4.1 PCSWMM Theoretical Background

PCSWMM version 7.2.2785 was used for model development and execution. PCSWMM is a commercial version of the current EPA Stormwater Management Model (SWMM5) and is owned by Computational Hydraulics International (CHI). SWMM5 is a dynamic rainfall-runoff simulation model used for single-event and continuous simulation of surface and subsurface hydrology quantity and quality (CHI, 2020). PCSWMM uses the SWMM5 computational engine and extends the capability with support tools and "various techniques to expose the inherent assumptions, uncertainties and errors in the model," including a GIS linkage to provide a spatial interface (James et al., 2010, p. 23). SWMM was one of the first water systems planning computer models, with development beginning in 1969 (James et al., 2010). Today, SWMM5 is one of the most widely used stormwater management models commercially and in academia (Akhter and Hewa, 2016; Broekhuizen et al., 2019; Krebs et al., 2014; McDonough, 2018; Worthen, 2019).

PCSWMM is a physically based, semi-lumped, deterministic model. Physically based models attempt to represent the actual physical processes occurring in the environmental system in contrast to empirical models (Zeckoski et al., 2015). Semi-lumped models are the midway point between distributed and lumped parameter models (Zeckoski et al., 2015). Instead of having simulated areas be small enough to represent uniform characteristics (distributed), or average the characteristics of an entire watershed (lumped), the model is divided at the user's discretion and parameter values are represented by weighted averages for each modeling unit (Zeckoski et al., 2015). Deterministic models contain no random elements, and produce the same outputs each time it is ran with the same inputs (Zeckoski et al., 2015). Deterministic models are

in contrast with stochastic models that reflect the random processes of nature and produce different outputs each time it is ran with the same inputs (Zeckoski et al., 2015).

Surface runoff in SWMM is determined by treating each subcatchment as a nonlinear reservoir. Inflow comes from precipitation and designated upstream subcatchments, and outflows include infiltration, evaporation, and surface runoff. This is essentially a water balance, where inflows minus outflows equals a change in storage. This water balance is solved by SWMM over each time step of a rainfall event. Runoff per unit area, Q, is determined by Manning's equation (Equation 4.1) when the depth of water in the reservoir exceeds the capacity determined by maximum depression storage (James et al., 2010). The equation is calculated with the subcatchment width (W), Manning's roughness coefficient (n), depth of water over the subcatchment (d), depression storage depth (d_s), and slope of the subcatchment (S).

$$Q = \frac{1.49}{n} W (d - d_s)^{5/3} S^{1/2} \tag{4.1}$$

The Green-Ampt method was chosen as the infiltration method (Equation 4.2). This method assumes "that a sharp wetting front exists in the soil column, separating soil with some initial moisture content below from saturated soil above," (James et al., 2010).

$$F = K_e t + S_{avg} M \ln\left[1 + \frac{F}{S_{avg} M}\right] \tag{4.2}$$

The cumulative infiltration depth (F) at time (t) is calculated from the effective hydraulic conductivity (K_e), time (t), average matric suction at the wetting front (S_{avg}), and fillable porosity (M) (Huffman et al., 2013).

SWMM also has capabilities to model snowmelt and groundwater, but those effects were ignored in this analysis. Dynamic wave routing, which produces the most theoretically accurate results by solving the complete one-dimensional Saint-Venant flow equations, was chosen as the routing method for the model (James et al., 2010). The Saint-Venant flow equations calculate the flow within an individual conduit according to the continuity (Equation 4.3) and momentum equations (Equation 4.4);

$$\frac{\partial A}{\partial t} + \frac{\partial Q}{\partial x} = 0 \tag{4.3}$$

$$\frac{\partial Q}{\partial t} + \frac{\partial (\frac{Q^2}{A})}{\partial x} + gA\frac{\partial H}{\partial x} + gAS_f + gAh_l = 0 \tag{4.4}$$

where distance (x), time (t), cross-sectional area (A), flow rate (Q), hydraulic head (H), friction slope (S_f), local energy loss per unit length of the conduit (h_L), and acceleration due to gravity (g) are the input parameters (James et al., 2010). The volume continuity is also calculated at each node.

There is significant equifinality in SWMM, or when many parameter combinations will reproduce the observations equally well with respect to a single error metric (Worthen, 2019). For example, Worthen (2019) found that unreasonable values of K_{sat} were capable of producing an acceptable NSE when varied in tandem with porosity. The most sensitive parameters in the model are Manning's Roughness of overland flow n_0, Depression Storage, D, Manning's roughness in the channel, n_c, and Imperviousness I (Krebs et al., 2014).

PCSWMM software has the capability for two-dimensional modeling by combining the dynamic 1D analysis with a 2D DEM-based overland mesh and layer of any buildings that can obstruct flow. The advantage of the 2D model is that the analysis of the extent and duration of surface water depth, flows, and velocity is enabled throughout the entire 2D mesh. Instead of all

water being routed from each subcatchment into individual conduits, the hydraulic routing within the 2D model occurs from cell to cell within the mesh. The volume of runoff at each cell is calculated from a mass balance analysis of precipitation, net inflow, infiltration and the change in volume (Barnard et al., 2017). The dynamic wave equation, which is based off the St. Venant flow equations, is used for routing between cells and involves backwater effects, or the effect of obstructions such as dams in raising upstream water levels. This model is still based exclusively on overland flow of water and does not model Coriolis, eddy, viscosity, or wind effects.

4.2 1D Model Development

This section describes the development of the baseline existing conditions 1D PCSWMM model of the Tomahawk Creek subwatershed. The Tomahawk Creek model was then modified to incorporate green infrastructure scenarios (Section 4.4) as well as 2D modeling features (Section 4.3). The 2D modeling was also performed on the larger Blue River Watershed. The model development of the Blue River Watershed follows the same steps explained in this section. The model development was done in collaboration with Kelsey McDonough and Jessica Stanton.

ArcGIS was used to pre-process many of the datasets needed to complete the hydrological model. The first step was to delineate the Tomahawk Creek Watershed to determine the flow paths and flow accumulation. One point per meter LiDAR was obtained through the Johnson County Automated Information Mapping System (MJ Harden a GeoEye Company, 2012). The LiDAR data was collected in 2011, and has a vertical accuracy RMSE of .1 m (0.314 ft) and a horizontal accuracy RMSE of 75-centimeter (2.5 ft), which exceeds the National Standard for Spatial Data Accuracy (NSSDA). The National Hydrography Dataset (USGS, 2001) stream network was used alongside PCSWMM's Watershed Delineation Tool (CHI, 2017) to automatically delineate the watershed area and create subcatchments to a target

discretization level of 202 ha (500 acres) (McDonough, 2018). A total of 28 subcatchments, 24 conduits, and 24 junctions were created in this process to represent the natural hydrography of the watershed.

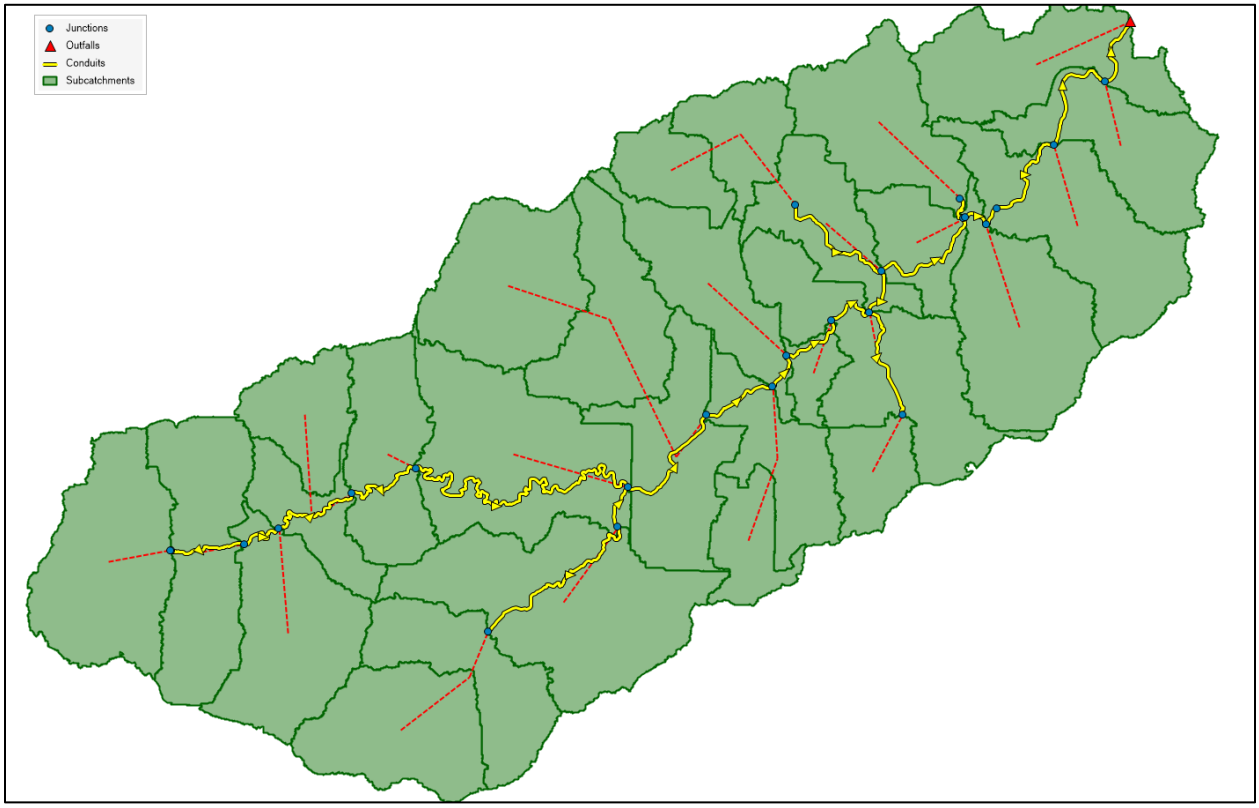

Figure 4.1. 1D PCSWMM Model of Tomahawk Creek Watershed featuring 28 subcatchments, 24 conduits, and 24 junctions. Junction 17 serves as the outfall of the watershed. The red, dashed lines indicated the flow paths of the subcatchments.

Subcatchments are hydrologic units of land that generate surface runoff, infiltrate, or store water for evaporation in response to precipitation (CHI, 2020). The average percent impervious of each subcatchment was determined in ArcGIS from the 2016 National Land Cover Database (NLCD) 2016 Percent Developed Imperviousness (Homer et al., 2020). PCSWMM's Area Weighting Tool (CHI, 2020) was used to assign the Manning's roughness impervious (NIMPERV), Manning's roughness pervious (NPERV), depression storage impervious

(DSIMPERV), and depression storage pervious (DSPERV) from the 2016 NLCD layer (Table 4.1. The depression storage and Manning's roughness parameters were derived from the National Land Cover Database Land Cover types (Adapted from James et al., 2010 & McDonough, 2018)). Soil Survey Geographic Database (SSURGO) data was obtained from the Web Soil Survey for Johnson County, Kansas (Soil Survey Staff, 2019). The Area Weighting Tool was again employed to assign values of conductivity, suction head, and initial deficit for the each subcatchment.

Table 4.1. The depression storage and Manning's roughness parameters were derived from the National Land Cover Database Land Cover types (Adapted from James et al., 2010 & McDonough, 2018).

Land Use/ Land Cover	Gridcode	DSPERV (mm)	DSIMPERV (mm)	NPERV	NIMPERV
Open Water	11	0	0	0	0
Perennial Ice/Snow	12	0	0	0	0
Developed, Open Space	21	2.54	1.27	0.034	0.012
Developed, Low Intensity	22	2.54	1.27	0.034	0.012
Developed, Medium Intensity	23	2.54	1.27	0.034	0
Developed, High Intensity	24	2.54	1.27	0.034	0
Barren Land	31	2.54	0	0.05	0
Deciduous Forest	41	7.62	0	0.40	0
Evergreen Forest	42	7.62	0	0.40	0
Mixed Forest	43	7.62	0	0.40	0
Dwarf Scrub	51	5.08	0	0.24	0

Shrub/Scrub	52	5.08	0	0.24	0
Grassland/ Herbaceous	71	5.08	0	0.24	0
Sedge/ Herbaceous	72	5.08	0	0.24	0
Lichens	73	5.08	0	0.15	0
Moss	74	5.08	0	0.15	0
Pasture/ Hay	81	5.08	0	0.13	0
Cultivated Crops	82	5.08	0	0.17	0
Woody Wetlands	90	7.62	0	0.40	0
Emergent Herbaceous Wetlands	95	7.62	0	0.15	0

Table 4.2. Green Ampt equation parameters were derived from the soil texture (Adapted from James et al., 2010 & McDonough, 2018).

Soil Type	Suction Head (mm)	Conductivity (mm/hr)	Initial Deficit (frac.)
Sand	49.5	120	0.417
Loamy Sand	61.2	30.0	0.401
Loam	88.9	10.9	0.412
Silt Loam	167	3.30	0.434
Sandy Clay Loam	218	1.52	0.486
Clay Loam	209	1.02	0.330
Silty Clay Loam	273	1.02	0.309
Sandy Clay	239	0.508	0.321
Silty Clay	292	0.508	0.432
Clay	316	0.254	0.385

The slope parameter was estimated in ArcGIS by computing the change in elevation between the highest and lowest elevation points in the subcatchment and dividing this change in elevation by the flow length between the elevation points. The overland flow length parameter was assigned to be 30m, a standard length of overland flow. The width was determined by

dividing the subcatchment area by the flow length. The Zero Imperv parameter, or the percent of the impervious area with no depression storage, was set to the PCSWMM recommended value of 25% (CHI, 2020). Subarea routing was set to pervious, and the percent routed parameter was set to 5%. This means that 5% of the percentage of impervious cover will be routed to the pervious area of the subcatchment before flowing to the outlet. All the subcatchment parameters for the 1D Tomahawk Creek Watershed current conditions model can be found in Appendix F.

The two-dimensional cross-section of each conduit, or stream segment, within the model was determined through the Transect Creator tool in PCSWWM (CHI, 2020). First, transect lines were drawn every 200 m based on the 1m LiDAR with elevation measured every 1m along the transect. Then, each transect was examined, and the most representative transect of each stream segment was chosen for the entire conduit. This process was employed instead of averaging all transects within a conduit to avoid the automatic truncation to the shortest length on each side, which is an unavoidable part of the PCSWMM transect creator tool. The bank stations that determine the main channel versus the overbanks was determined visually for each transect (Figure 4.2).

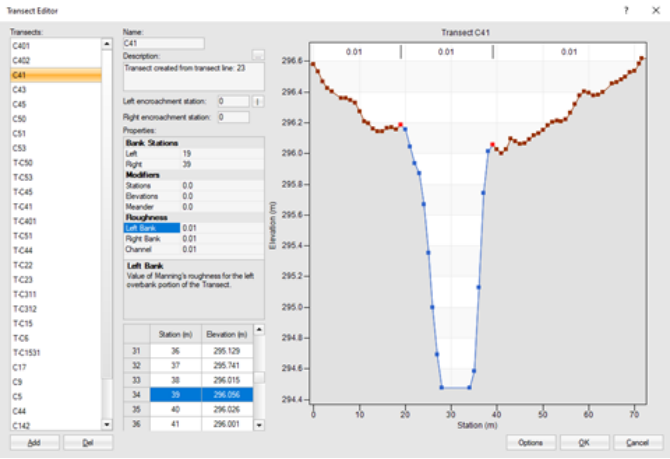

Figure 4.2. Transects were created using 1-meter LiDAR data and the Transect Creator tool in PCSWMM.

A Manning's Roughness value of 0.03 (earth bottom rubble sides) and 0.1 (very weedy reaches of natural streams) were assigned for the channel and overbanks respectively (Huffman et al., 2013). The model could be improved by adding surveyed stream cross sections, but that data was not available. The inlet and outlet offset values were set to 0, and the initial flow was set at 0.

In PCSWMM, junctions are drainage systems nodes where links join together (CHI, 2020). In the Tomahawk Creek model, they represent the confluence of natural channels, where a conduit crosses into a new subcatchment, or represent a location where the hydrological response is of heightened interest. The invert elevation of each junction was determined using the LiDAR dataset. The rim elevation was calculated by adding the depth of the upstream conduit to the invert elevation. The initial depth and surcharge depth were set to 0. Junction ponding was enabled in order to keep excess volume overflows from leaving the system. Allowing ponding keeps excess water at the junction until the conduit has enough capacity for the water to rejoin the system. The Tomahawk model only contains one outfall, which is located at the outlet of the watershed, and its attributes were determined following the same steps as all model junctions. Additionally, the stormwater network is not included due to the size of the model, complexity of the network, and availability of quality data. Therefore, this model only evaluates overland flow.

The average, monthly pan evaporation for the Kansas City area (Table II, NOAA, 1982a) was multiplied by a coefficient of 74% (Map4; NOAA, 1984b) to convert Class A pan

evaporation to free water surface evaporation (McDonough, 2018). Evaporation from the free water surface was used as the average, monthly evaporation rate in the model.

Table 4.3. Average monthly evaporation for Kansas City, Missouri (Adapted from McDonough, 2018)

	Jan	Feb	Mar	Apr	May	Jun	Jul	Aug	Sep	Oct	Nov	Dec
Average pan evaporation (mm/month)	38	47	88	138	186	202	225	205	145	114	61	40
Average free water surface evaporation (mm/month)	26	34	65	102	136	149	166	152	107	84	45	29

4.3 2D Model Development

The 1D Tomahawk Creek model, described in Section 4.2, serves as the base of the Tomahawk Creek 2D model. Additionally, a 2D model was created for the entire Blue River Watershed. There were a few changes in the base Blue River Watershed model development from the process described in Section 4.2. A USGS 3-meter DEM was used for the elevation dataset because a 1-m LiDAR dataset was not available for the entire BRW. The 2011 NLCD was used to determine the % impervious, Manning's roughness, and depression storage for the subcatchments. Additionally, the slope was determined by utilizing the Set DEM slope tool in PCSWMM that averaged the surface slope along the National Hydrography streams dataset to determine the slope parameter for each subcatchment. This was done to reduce the model build time for a larger watershed, and resulted in slightly higher slopes than the method used for the Tomahawk watershed. The subcatchment parameters for the Blue River Watershed current conditions model can be found in Appendix H.

The PCSWMM software has the potential for two dimensional modeling of free surface flow by combining the dynamic 1D analysis with a 2D overland mesh and obstructions layer (CHI, 2020). The advantage of the 2D model is enabling analysis of the extent and duration of surface water depth, flows, and velocity throughout the entire 2D mesh. The 1D model, and processes described earlier, determines the amount of water in the conduits. Then, the flood extent of the water is able to be modeled through the connection with the 2D cells (Figure 4.4). The volume of runoff at each cell is calculated from a mass balance analysis of precipitation, net inflow, infiltration and the change in volume (Barnard et al., 2017). The dynamic wave equation, which is based off of the St. Venant flow equations, is used for routing between cells and involves backwater effects, or the effect of obstructions in raising upstream water levels. This model is still based exclusively on overland flow of water and does not model Coriolis, eddy, viscosity, or wind effects.

The addition of 2D modeling capabilities requires the addition of new layers not used in the 1D model. Of the 11 possible layers to add for 2D modeling, only the bounding, 2D nodes, obstruction, centerline, and DEM layers – each of which are explained in the following sections – were used in the construction of the 2D models. The same model creation process was utilized for both the Tomahawk and Blue River Watershed models. Two dimensional modeling requires high amounts of computational time as the area to be model increases (CHI, 2020; Klenzendorf et al., 2015; Pinos and Timbe, 2019), so 2D modeling was only conducted around areas where the streams and important highway systems intersected.

The 2015 TIGER primary and secondary roads were obtained from the Geospatial Data Gateway to determine the areas of importance (U.S. Department of Commerce, 2015). Secondary roads are main arteries, usually in the U.S. Highway, State Highway and/or County

Highway system (U.S. Department of Commerce, 2015). Two types of 2D mesh were used in the models: hexagonal and directional. Directional mesh can be used to represent flow along a specified path such as a stream channel (CHI, 2020). The boundary layer for the directional mesh was drawn manually in PCSWMM using the LiDAR/DEM as a guide to coincide with the natural channel (Figure 4.2). A centerline layer was also drawn manually in PCSWMM to coincide with the center of the natural channel. The centerline layer is used for the 2D directional mesh generation to define the predominant direction of flow. A 150-meter buffer was created around the centerlines in ArcGIS 2D to serve as the boundary layer for the hexagonal mesh. The hexagonal mesh is the default mesh type in PCSWMM and can be used to represent large, open areas such as floodplains (CHI, 2020). The hexagonal mesh was assigned a 30-meter resolution and Manning's roughness of 0.1 and the directional mesh was assigned a 10-meter resolution and Manning's roughness of 0.03. The 2D Nodes layer that defines the approximate locations of the 2D cells in the 2D network was generated using the Generate Points tool in PCSWM, which optimizes the size and shape of the resulting 2D cells, based on the obstruction and boundary layers (CHI, 2020). The obstructions layer represents all the physical buildings that could obstruct flood flows. A 2018 buildings footprint layer was obtained from Johnson County AIMS and the city of Kansas City, Missouri (AIMS, 2018). The 2D cells layer was created using the Create Mesh tool in PCSWMM, the invert elevation was determined using the DEM/ LiDAR (Figure 4.3) (CHI, 2020). The resulting 2D models included 20,369 nodes and 18,291 cells in the Blue River Watershed and 5,177 nodes and 5,182 cells in the Tomahawk Creek watershed. The 2D model uses lumped subcatchments with subcatchment runoff draining to specific 1D nodes that are connected directly to the 2D mesh. This is appropriate for integrated 1D-2D modeling where the cause of flooding is due to stream bank overtopping (CHI, 2020).

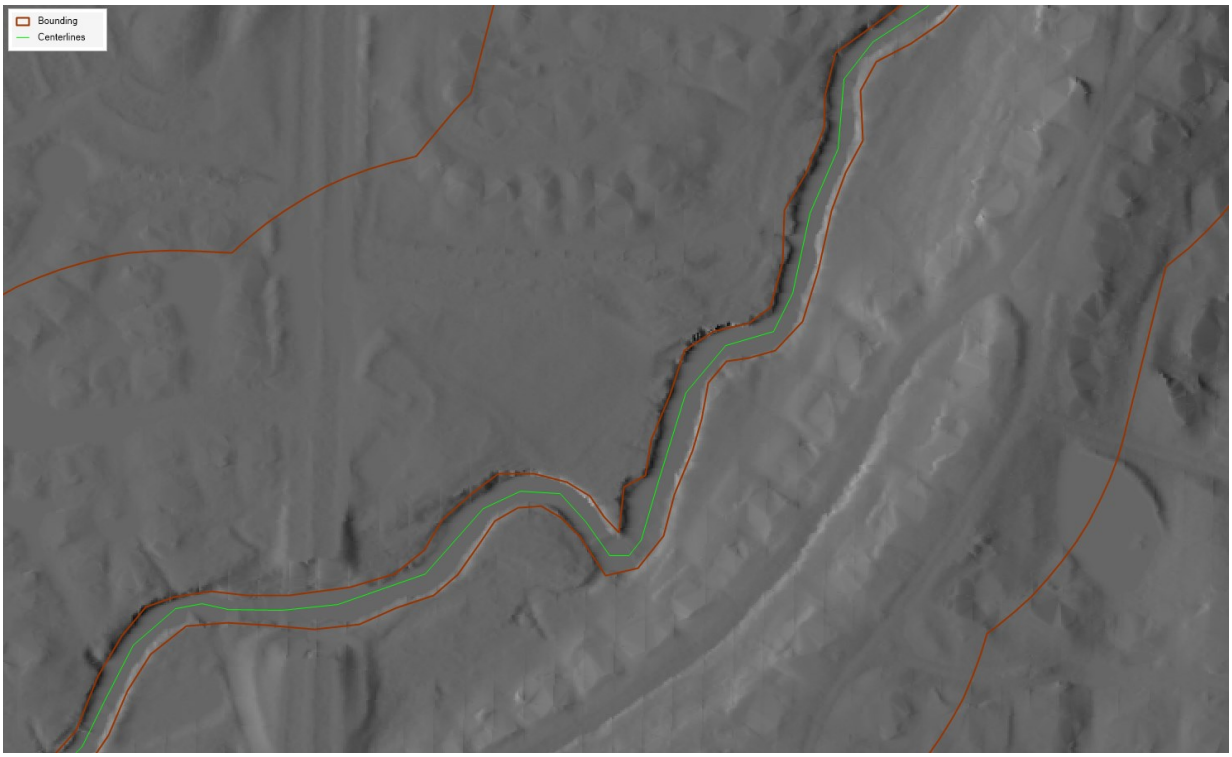

Figure 4.3. Example of directional (interior) and hexagonal (exterior) boundary layer.

Figure 4.4. The 2D mesh creation includes a boundary, 2D nodes, 2D cells, LiDAR, and obstructions layer.

4.4 Scenario Development

Twelve different scenarios with varying levels of green infrastructure were created to understand linkages between green infrastructure and possible reductions in peak inflow, total inflow volume, and flood extent (Table 4.6). The percent routed subcatchment parameter was adjusted to simulate changing percentages of green infrastructure. This function does not change the amount of impervious cover, which can be hard to do in an almost entirely built-out environment. Instead, it changes the percentage of runoff from the impervious areas that is directed onto pervious area before reaching the subcatchment outlet or stream conduit. This is an example of increasing the disconnectedness of impervious surfaces, such as disconnecting storm drains, or adding bioretention cells in parking lots. This approach for simulating disconnection was also used to model decentralized green stormwater controls for the city of Austin Texas Watershed Protection Department (Geosyntec Consultants, 2017).

Table 4.4. Description of scenario conditions

Scenario	Description
0	0% routed to pervious, no deciduous forest riparian buffer
5	5% routed to pervious, no deciduous forest riparian buffer, "current conditions or baseline"
25	25% routed to pervious, no deciduous forest riparian buffer
50	50% routed to pervious, no deciduous forest riparian buffer
75	75% routed to pervious, no deciduous forest riparian buffer
100	100% routed to pervious, no deciduous forest riparian buffer
0R	0% routed to pervious, with deciduous forest riparian buffer
5R	0% routed to pervious, with deciduous forest riparian buffer
25R	0% routed to pervious, with deciduous forest riparian buffer
50R	0% routed to pervious, with deciduous forest riparian buffer
75R	0% routed to pervious, with deciduous forest riparian buffer
100R	0% routed to pervious, with deciduous forest riparian buffer, "maximum GI"

Half of the scenarios also include the full restoration of the floodplain with a deciduous forest riparian buffer. Following the EPA model ordinance described in Section 2.3.1, 150 feet was chosen as the buffer width. Using the landcover from the 2016 NLCD, all developed

(including impervious cover), agricultural, and barren lands within the 150 ft buffer were converted to deciduous forest (Table 4.6) (Figure 4.5). Any pre-existing water, forest, shrubland, or herbaceous land cover was not converted.

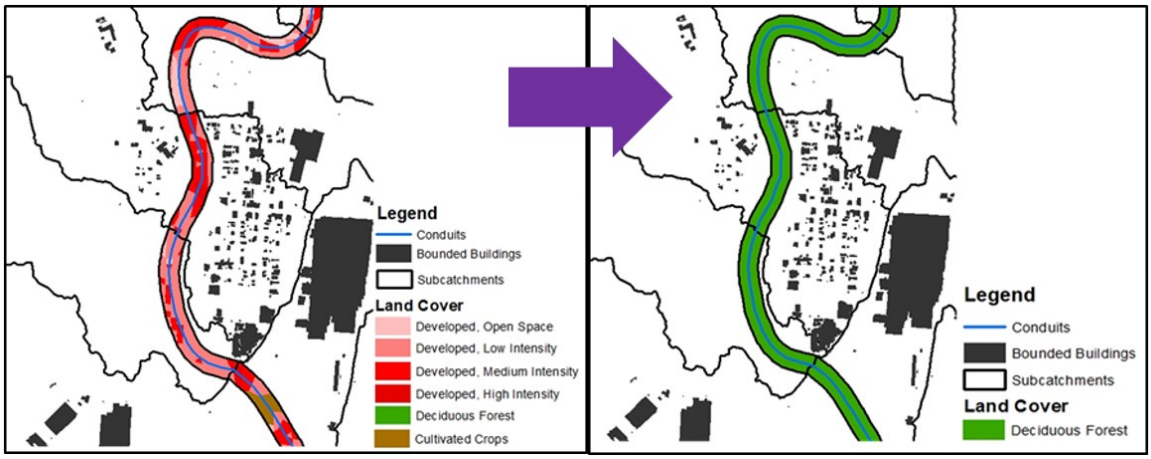

Figure 4.5. Landcover change within the 150 ft. riparian buffer

This was accomplished by creating a CSV file with the existing gridcodes, and a second column with the land cover codes that each pre-existing code was being converted to. The tables were then joined in GIS using the pre-existing GRIDCODE as the shared field for both. The new buffer layer was joined to the existing subcatchments layer using the union tool in GIS. Then the routing was updated so that all subcatchment surface runoff was routed through a riparian buffer before entering the stream (Figure 4.6). The percent impervious attribute was updated to 0 within every riparian buffer subcatchment. The Area Weighting tool was employed again to update the depression storage and Manning's roughness coefficient for the new buffers (Table 4.1). In the Tomahawk Creek Watershed, 1.36 km^2 (0.53 mi^2), or 61%, of the land within the buffer was converted to deciduous forest. In the BRW, 7.18 km^2 (2.77 mi^2), or 51% of the land within the buffer was converted to deciduous forest. The subcatchment parameters with the addition of the deciduous forest riparian buffer (Scenario 5R) can be found in Appendix G for the TCW, and Appendix I for the BRW.

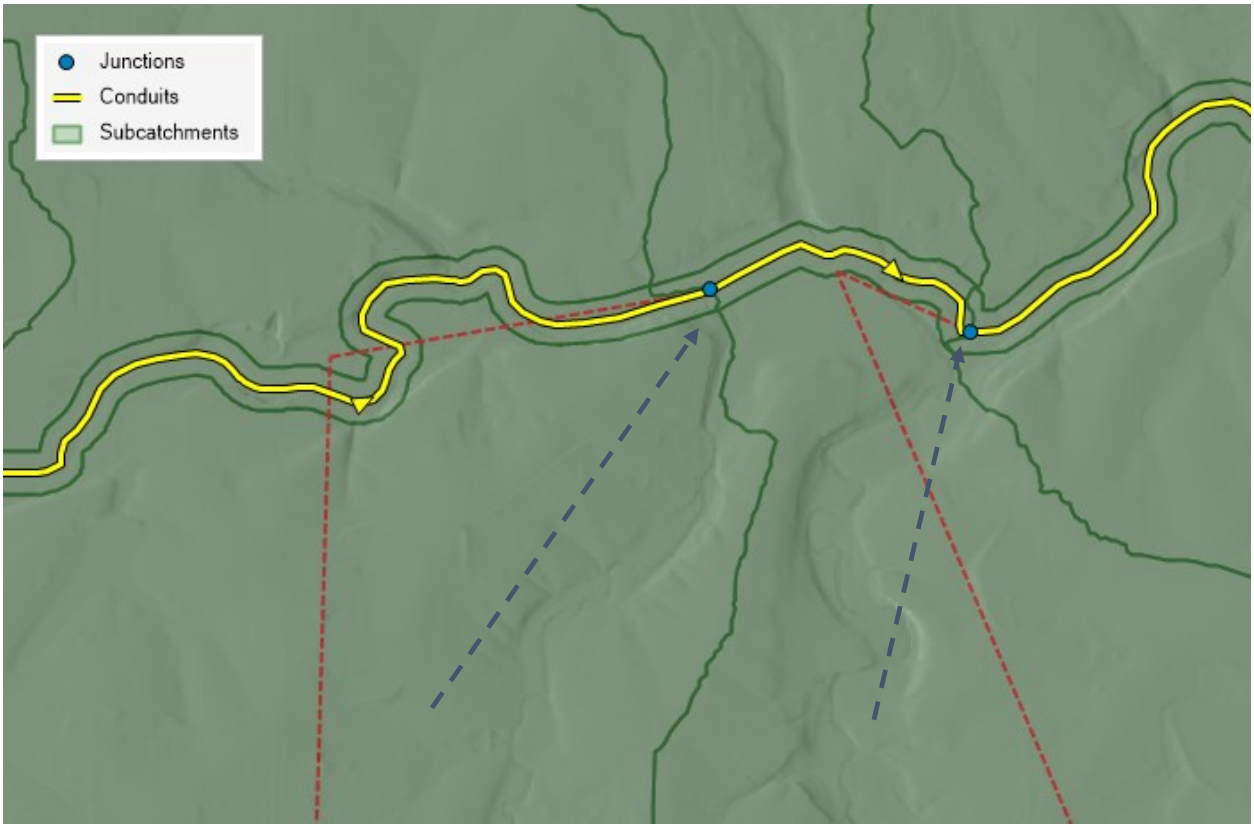

Figure 4.6. The routing was updated so that the subcatchment runoff would be routed through the riparian buffer before being routed to the outlet (red arrow). The blue arrow shows the routing without the addition of riparian buffers.

4.5 Design Storms

Rainfall data from NOAA's Atlas 14 Point Precipitation Frequency Estimates Shawnee 2S rain gauge was used to model various design storm events (Table 4.5). The precipitation depths for the 1, 5, 10, 25, and 100 year, 24 hour storms were used to model a range of storms that can impact the Kansas City area over the next 100 years. These design storms are based off years of precipitation data for the region. A design storm represents the probability a storm of a given magnitude will occur in a given year. Dividing 100 by the storm year shows you the percent probability that it will occur in any given year. For example, the 2-year storm has a 50% probability of occurring any given year, while the 100 year storm has a 1% chance of occurring any given year.

Table 4.5. NOAA Atlas 14 precipitation-frequency estimates with 90% confidence intervals. The numbers in parenthesis are at the lower and upper bounds of the 90% confidence interval (Sanja et al., 2013).

1-year, 24-hour storm	5-year, 24-hour storm	10-year, 24-hour storm	25-year, 24-hour storm	100-year, 24-hour storm
3.08 in (2.53-3.79)in	4.63 in (3.78-5.69)in	5.48 in (4.45-6.76)in	6.71 in (5.32-8.49)in	8.76 in (6.57-11.3)in
78.2 mm (64.3-96.3)mm	118 mm (96-145)mm	139 mm (113-172)mm	170 mm (135-216)mm	223 mm (170-287)mm

Section 2.1 discussed how utilizing past precipitation data may not sufficiently predict future precipitation events as the frequency and intensity of storms increase with climate change. It is reasonable to assume that the high numbers in parenthesis represent what the design storms might shift to during climate change. This is because that number represents the upper bound of the 90% confidence interval for each design storm. As climate change shifts events towards more extreme, shifting the number towards the tail of the of the distribution is appropriate.

The water quality volume storm (1.37-inch, 24hour), which green infrastructure is designed to treat, along with the 1-inch, 24-hour storm were also evaluated. Because climate change is predicted to increase the intensity of precipitation events, the 1-inch and 1.37-inch precipitation events were also test over a 6-hour period. The precipitation events are modeled using the Soil Conservation Service (SCS), Type II rainfall distribution with a 15-minute rainfall interval, which is appropriate for the region (Figure 4.7). This models the maximum rainfall as occurring at noon of the first simulated day if it is a 24-hour storm. In order to account for any lag in streamflow, the simulation period is five days.

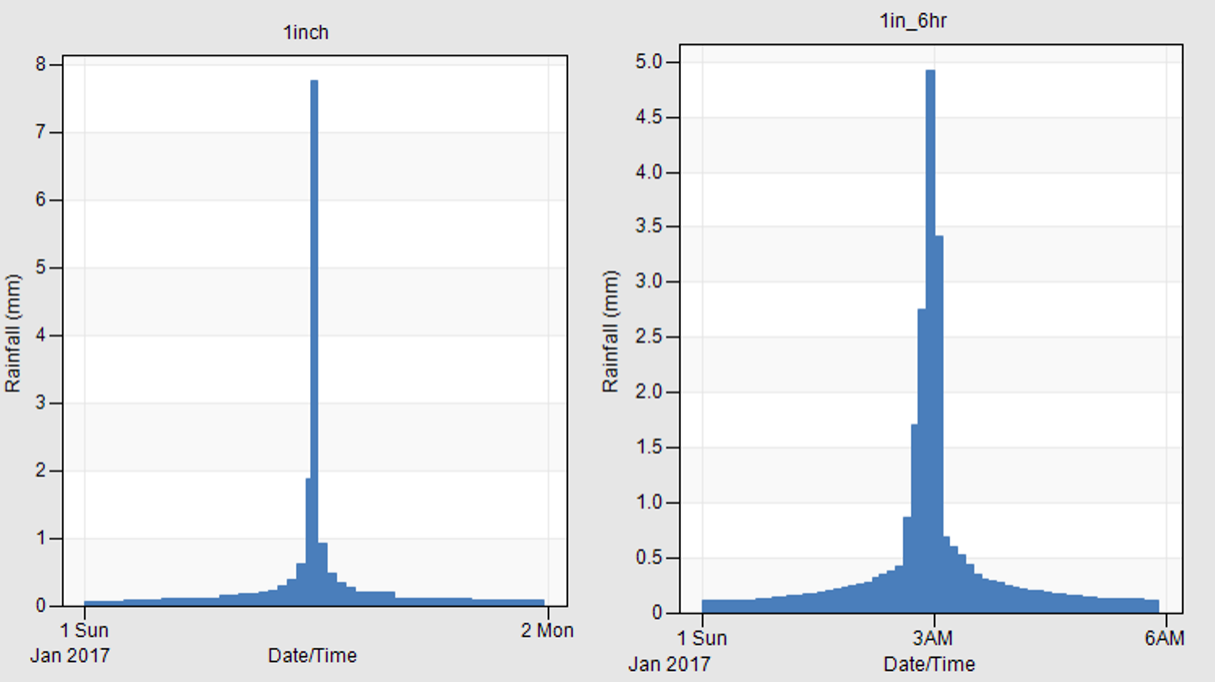

Figure 4.7. 1-inch storm with an SCS, Type II rainfall distribution with 24-hour (left) and 6-hour (right) intensity.

4.6 Calibration and Validation

Observed, 15-minute precipitation from a Roe Avenue @ Tomahawk Creek rain gauge (Latitude 38°54'22", Longitude 94°38'24" NAD83) was obtained from Ybairy Duin with StormWatch.Com, a flood warning system that monitors stream flow and precipitation in real-time throughout a network of remote weather stations located throughout the Kansas City Metropolitan Area (Duin, 2020). This precipitation was used alongside 15-minute streamflow from USGS gage 06893500 to calibrate and validate the model. Utilizing precipitation data on the same temporal scale and from the same location as the USGS greatly improved the calibration and validation from earlier attempts with hourly precipitation data from a rainfall gauge near the beginning of Tomahawk Creek.

The Nash-Sutcliffe Efficiency (NSE) is a normalized statistic that determines the relative magnitude of the residual variance (“noise”) compared to the measured data variance

("information") (Nash and Sutcliffe, 1970; Zeckoski et al., 2015) This statistical measure compares the observed versus simulated data, in this case the hydrograph (Mcdonough et al., 2017; Worthen, 2019; Zeckoski et al., 2015). NSE values range between -∞ and 1, with NSE=1 being a perfect match, NSE = 0 indicating the model predictions are as accurate as the mean of the observed data, and negative values indicating that the mean observed value is a better predictor than the simulated value (CHI, 2020; Moriasi et al., 2007). Equation 4.5 shows how NSE is computed, where Y_i^{obs} is the observed hydrograph at time *i*, Y_i^{sim} is the simulated hydrograph at time *i*, Y^{mean} is the mean of observed values, and *n* is the total number of observed hydrograph values (Moriasi et al., 2007; Shamsi and Koran, 2017). A NSE value of 0.4-1.0 is considered acceptable for all model applications (Table 4.6) (Shamsi and Koran, 2017).Table 4.6. NSE goodness-of-fit ratings for model calibration, adapted from (Shamsi and Koran, 2017)

$$NSE = 1 - \frac{\sum_{i=1}^{n}(Y_i^{obs} - Y_i^{sim})^2}{\sum_{i=1}^{n}(Y_i^{obs} - Y^{mean})^2} \quad 4.5)$$

Table 4.6. NSE goodness-of-fit ratings for model calibration, adapted from (Shamsi and Koran, 2017)

NSE Range	Calibration Rating	Model Application
0.5 to 0.1	Excellent	Planning, Preliminary Design, Final Design
0.4 to 0.49	Very good	Planning, Preliminary Design, Final Design
0.3 to 0.39	Good	Planning, Preliminary Design
0.2 to 0.29	Fair	Planning
-∞ < 0.2	Poor	Screening

The coefficient of determination (R^2) is a key output of regression analysis (CHI, 2020). This coefficient describes the degree of collinearity between simulated and measured data (Moriasi et al., 2007). An R^2 of 1 indicates that the observed values have a perfect, positive linear correlation with the modeled values (Shamsi and Koran, 2017). Typically, values greater

than 0.5 are considered acceptable (Santhi et al., 2001 and Van Liew et al. 2003, as cited in Moriasi, 2007).

A model is considered successfully calibrated when it reproduces observations within "some subjectively acceptable level of precision (Daggupati et al., 2015; Konikow and Bredehoeft, 1992; Zeckoski et al., 2015, p. 1625). The model was calibrated from January 1, 2017 – December 21, 2017 and validated from January 1, 2018 – December 31, 2018. The model was calibrated to optimize the NSE for total streamflow on a continuous basis. However, due to the NSE rating falling in the "excellent" range and the R^2 being substantially higher than 0.5 or "acceptable," the original 1D Tomahawk model was considered successfully calibrated without changing any input parameters. The validation run also received an "excellent" rating, showing that this choice was acceptable. These results show that the original conditions Tomahawk Creek 1D model accurately simulates the surface hydrology of the watershed and is suitable for associated planning, preliminary design, and final design purposes (Table 4.6).

Table 4.7. Continuous streamflow (cms) calibration and validation results for the original TCW at USGS Tomahawk Creek gage J06892500

	Calibration (1/1/2017 – 12/31/2017))	Validation (1/1/2018 – 12/31/2018)
Nash Sutcliffe Efficiency (NSE)	0.850	0.723
Coefficient of Determination (R^2)	0.868	0.838

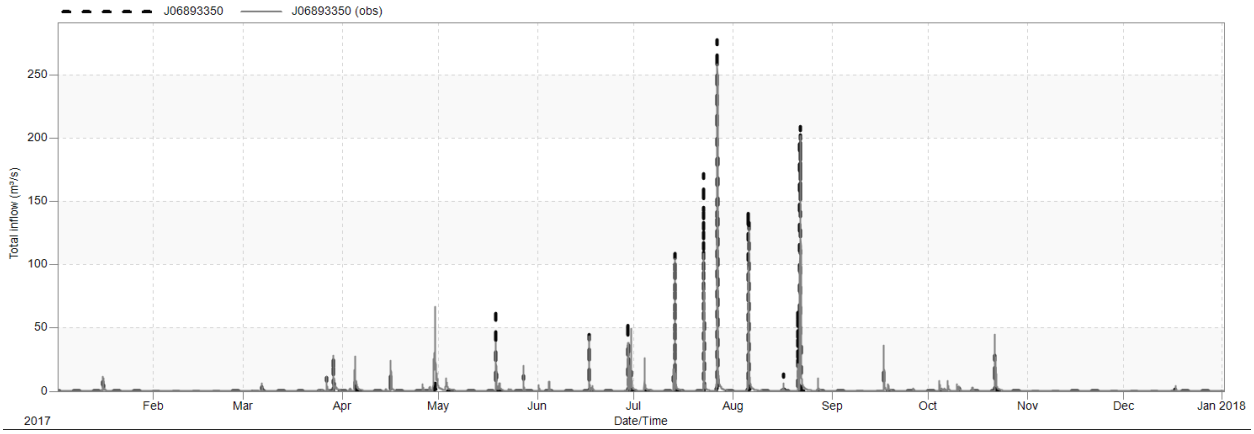

Figure 4.8. Continuous streamflow (cms) calibration results for the TCW at USGS Tomahawk Creek gage J06892500 from 1/1/2017-12/31/2017.

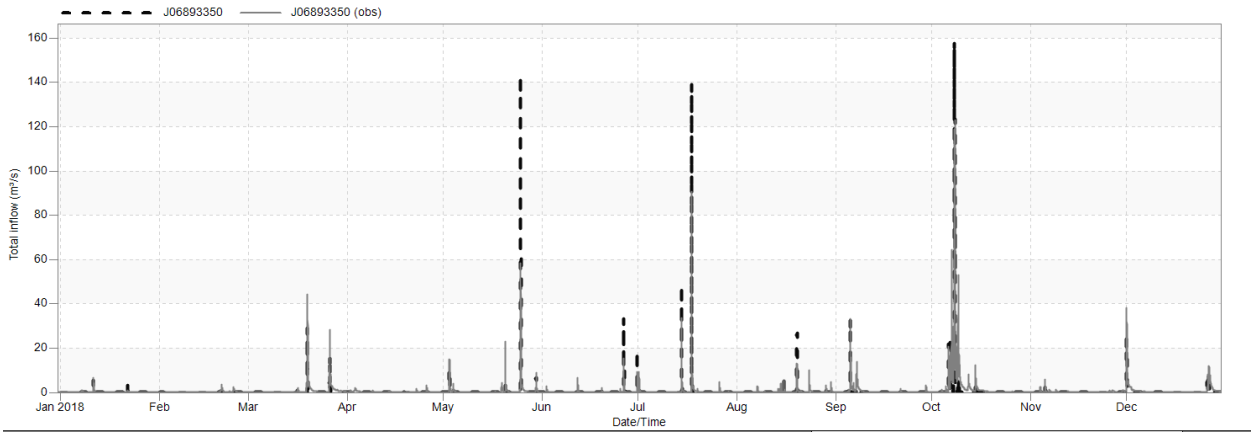

Figure 4.9. Continuous streamflow (cms) validation results for USGS Tomahawk Creek gage J06892500 from 1/1/2018-12/31/2018.

In order to ensure it was an "apples to apples, not apples to oranges" comparison, a model including the new riparian buffer subcatchments and routing, but with the original conditions within the riparian buffer was utilized as the base model for Scenarios 0-100. This base model was also calibrated and validated. Again, the NSE values were high enough that no input parameters needed to be changed for the model to be suitable for associated planning, preliminary design, and final design purposes (Table 4.8).

Table 4.8. Continuous streamflow (cms) calibration and validation results for the TCW riparian buffer base model at USGS Tomahawk Creek gage J06893350.

	Calibration (1/1/2017 – 12/31/2017))	Validation (1/1/2018 – 12/31/2018)
Nash Sutcliffe Efficiency (NSE)	0.753	0.691
Coefficient of Determination (R^2)	0.785	0.711

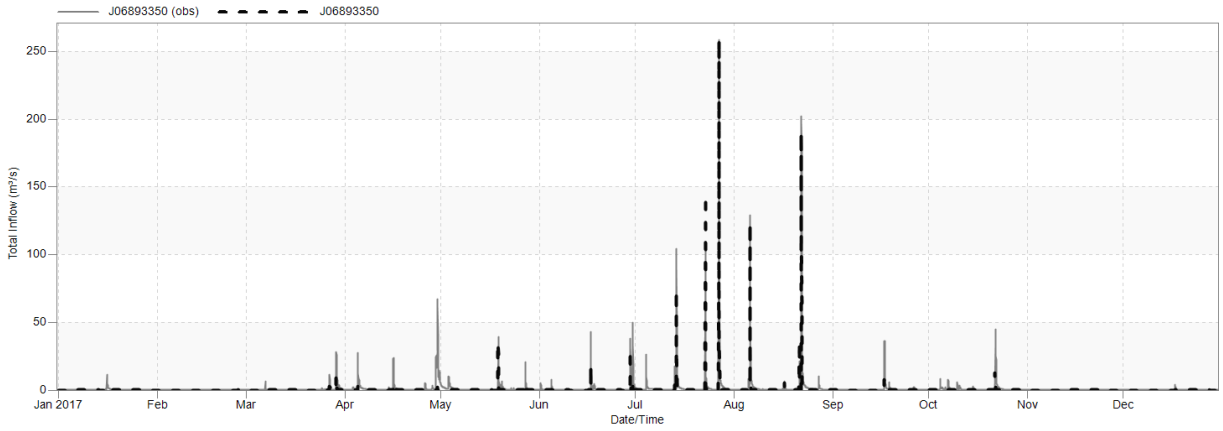

Figure 4.10. Continuous streamflow (cms) calibration results for the TCW riparian buffer base model at USGS Tomahawk Creek gage J06893350 from 1/1/2017-12/31/2017.

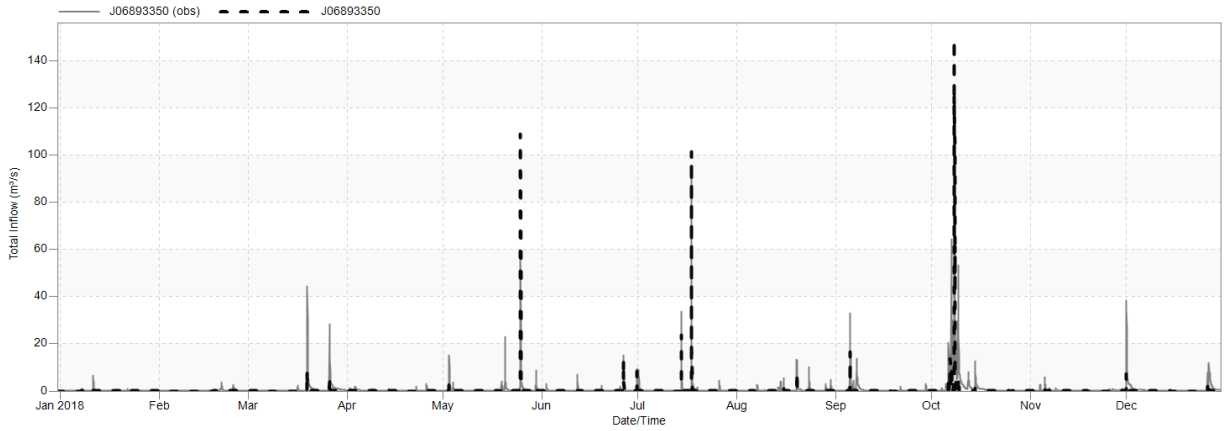

Figure 4.11. Continuous streamflow (cms) calibration results for the TCW riparian buffer base model at USGS Tomahawk Creek gage J06893350 from 1/1/2018-12/31/2018.

The BRW model was calibrated to one location, the USGS gage at the BRW outlet (06893578). Three parameters were changed during the calibration process: subcatchment length (50% uncertainty), channel roughness (10% uncertainty), and zero imperv (50% uncertainty).

The model parameter calibration uncertainty ranges were recommended by James (2010). The model was calibrated from 1/1/2016-12/31/2016 and achieved an NSE of 0.534 (Figure 4.12). The model was validated from 1/1/2017-12/31/2017 and achieved an NSE of 0.66 (Figure 4.13). These results demonstrate that the BRW model is suitable for associated planning, preliminary design, and final design purposes (Table 4.6).

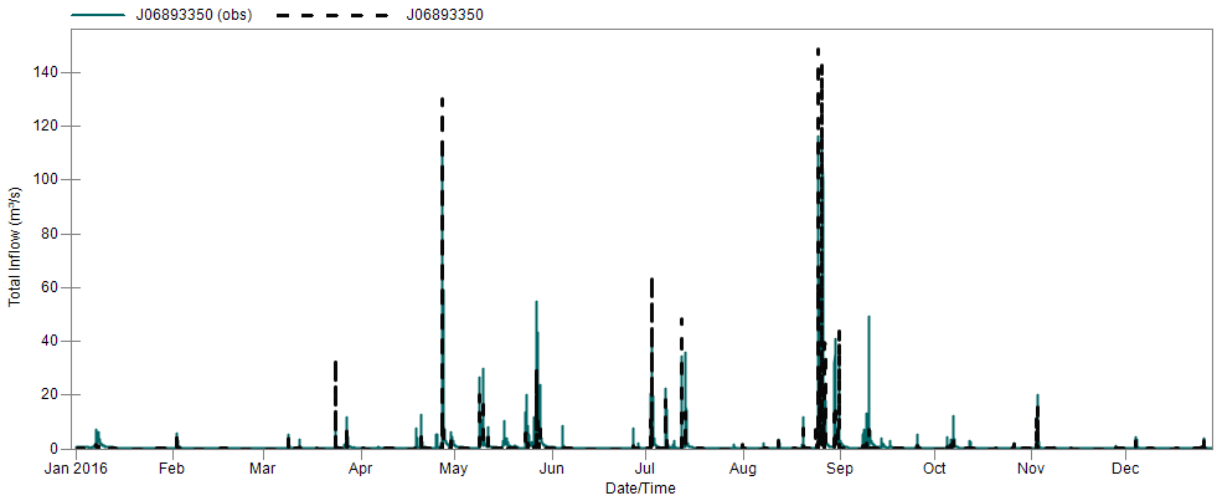

Figure 4.12. Continuous streamflow (cms) calibration results for the original BRW model at USGS Tomahawk Creek gage J06893350 from 1/1/2016-12/31/2016.

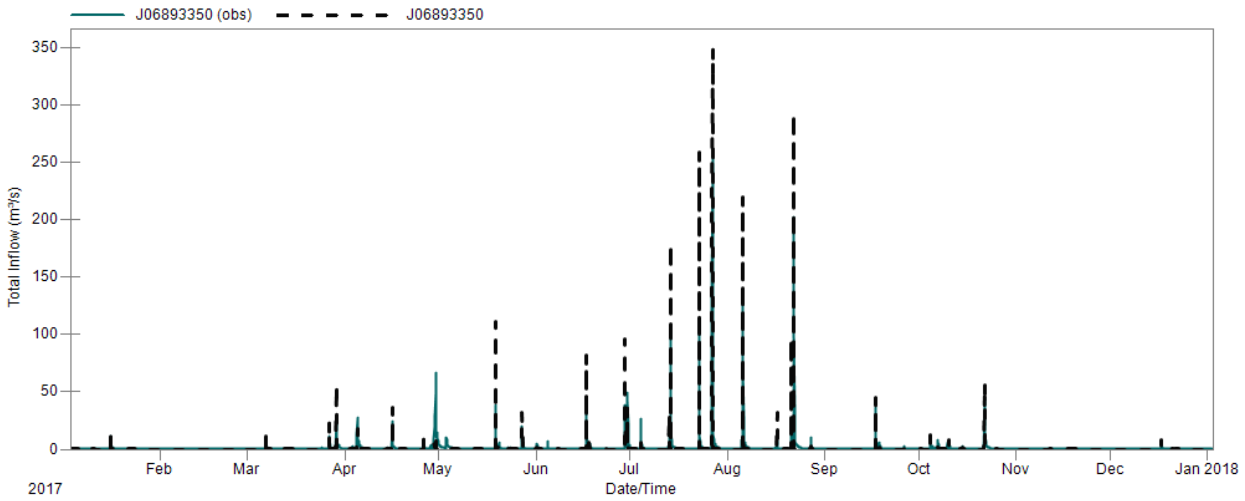

Figure 4.13. Continuous streamflow (cms) validation results for the original BRW model at USGS Tomahawk Creek gage J06893350 from 1/1/2017-12/31/2017.

A riparian buffer layer with the original landcover was added to the calibrated BRW model, and calibrated (Figure 4.14) and validated (Figure 4.15) to allow for the "apples to apples" comparison. The base model with the riparian buffer layer, with and without the land cover change, was the base of the 2D mesh creation outlines in Section 4.3. The NSE and R^2 values were high enough (Table 4.9) that no additional input parameters needed to be changed for the model to be suitable for associated planning, preliminary design, and final design purposes (Table 4.6).

Table 4.9. Continuous streamflow (cms) calibration and validation results for the BRW riparian buffer base model at USGS Tomahawk Creek gage J06893350.

	Calibration (1/1/2016 – 12/31/2016)	Validation (1/1/2017 – 12/31/2017)
Nash Sutcliffe Efficiency (NSE)	0.721	0.794
Coefficient of Determination (R^2)	0.746	0.804

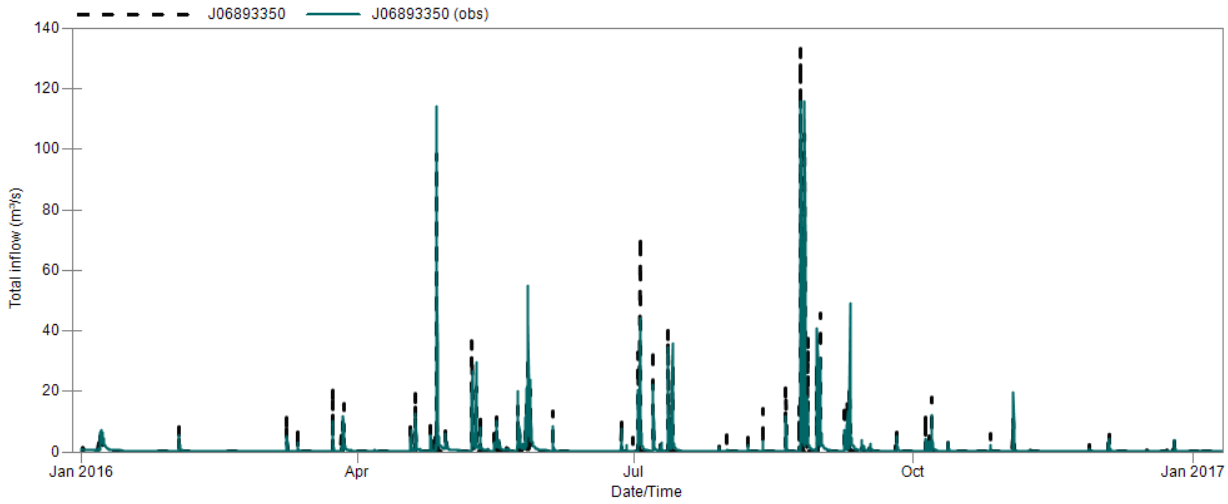

Figure 4.14. Continuous streamflow (cms) calibration results for the base riparian buffer BRW model at USGS Tomahawk Creek gage J06893350 from 1/1/2016-12/31/2016.

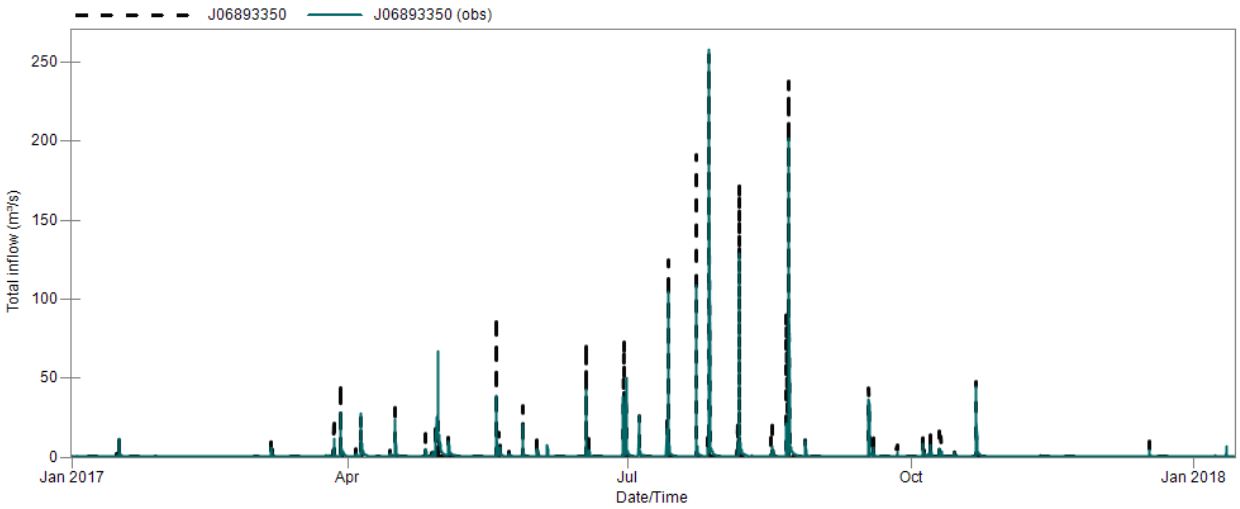

Figure 4.15. Continuous streamflow (cms) validation results for the base riparian buffer BRW model at USGS Tomahawk Creek gage J06893350 from 1/1/2017-12/31/2017.

4.7 Statistical Analysis

SWMM operates as a deterministic model with no variability in output under the same treatment condition (Zeckoski et al., 2015). In order to allow for variability among results to be statistically analyzed, a complete block design (CBD) using a generalized linear model was

applied to the data. The CBD method is a restricted design in which experimental units are first selected into homogenous blocks, and the treatments are applied to each block (Mendenhall and Sincich, 2012). The blocks were the various precipitation events and each green infrastructure scenario was the treatment applied to each block. The linear regression model has each Scenario as the x value, and either peak inflow or volume as the y value for the 1D results. In the 2D results, the x-value was the Scenario while the flood extent was the y value.

R is a free, open-source, and widely-used software environment for statistical computing and graphics. One of the most widely used statistical methods of analysis of variance or simply ANOVA. The ANOVA procedure was applied in R and evaluated using the Tukey-Kramer Honest Significant Difference test for all pairwise combinations of scenario to scenario and precipitation event to precipitation event. Each pairwise comparison was analyzed at a Type I family-wise error rate of 5%, with the null hypothesis $H_{0)}$ $\mu_1 = \mu_2$ and the alternative hypothesis, H_a) $\mu_1 \neq \mu_2$. The null hypothesis for each pairwise comparison was that the two scenarios are not significantly different as factors within the linear model. If the error (p) is < 0.05, then the null hypothesis is rejected and the difference between scenarios is significant. If the error is (p) > 0.05 is failed to be rejected. The Tukey-Kramer method must be used to analyze all sets of pairwise comparisons, and it assumes normal distribution, homogeneity of variance, and independent observations within and among blocks (McDonough, 2015). The code used in R can be found in Appendix B.

Chapter 5 - Results and Discussion

The results discussed in this chapter indicate that implementation of a 150 ft. riparian buffer and increasing the percent of water that flows through green spaces before reaching the stream to at least 25% reduces peak inflow, total volume of inflow, and flood extent. These reductions are most prominent for the water quality and smaller storms. However, significant peak inflow and total inflow volume reductions were still seen for the 100-year design storm. The flood extent was reduced approximately 8% for the 1, 5, and 10-year design storms with implementation of Scenario 25R. Minimal flood extent reductions were seen for the 100-year design storm. These results indicate that increasing green infrastructure does increase the climate change resiliency of transportation infrastructure, however additional structural flood control is needed to reduce flood extent greater than 10% and for flood control of design storms of 100+ years.

While water quality was not explicitly evaluated by the BRW and TCW models, the increase in infiltration observed by reduced inflow volumes indicate that more water is treated by percolating through the soil and water quality improvements could be expected. No scenarios decreased the peak discharge rate below bankfull flow, indicating the substantial erosion control will not be observed by the GI implementation.

5.1 1D Statistical Analysis Results

The Tukey Honest Significant Difference test was conducted to statistically examine differences in peak and total inflow between scenarios (see Section 4.7 for more information on statistical analysis). The varying levels of green infrastructure for each scenario are described in Table 4.6. Comparisons which returned a p-value of less than 0.05 indicated a significant difference in peak and/or total inflow between scenarios (Table 5.1). It is not surprising that the

difference between 0% and 5% routing failed to be proven significant for all pairwise scenario comparisons. Only adding a riparian buffer, and not increasing the percent routed over 5% failed to yield a significant difference for all results, except for the peak inflow at J06893500. Adding a riparian buffer and increasing the percent routed to at least 25% reduced peak inflow and volume significantly when compared to the baseline conditions, except for the peak inflow at J17. This could be due to J17 having a smaller contributing area, so the peak inflow values are lower than at the following junctions.

Table 5.1. Results of the Tukey Honest Significant Difference test. Comparisons with a p-value of less than 0.05 indicate a significant difference between the results, and are shaded in gray.

	J06893500		J17		J27	
	Peak Inflow	Volume	Peak Inflow	Volume	Peak Inflow	Volume
5N-0N	Fail to Reject	Fail to Reject	Fail to Reject	Fail to Reject	Fail to Reject	Fail to Reject
5N-25N	Fail to Reject	Fail to Reject	Fail to Reject	Fail to Reject	Significant	Fail to Reject
5N-50N	Significant	Fail to Reject	Significant	Fail to Reject	Significant	Significant
5N-75N	Significant	Significant	Significant	Significant	Significant	Significant
5N-100N	Significant	Significant	Significant	Significant	Significant	Significant
5N-0R	Fail to Reject	Fail to Reject	Fail to Reject	Fail to Reject	Fail to Reject	Fail to Reject
5N-5R	Significant	Fail to Reject	Fail to Reject	Fail to Reject	Fail to Reject	Fail to Reject
5N-25R	Significant	Significant	Fail to Reject	Significant	Significant	Significant
5N-50R	Significant	Significant	Significant	Significant	Significant	Significant
5N-75R	Significant	Significant	Significant	Significant	Significant	Significant
5N-100R	Significant	Significant	Significant	Significant	Significant	Significant

Each rainfall event was also compared to one another to evaluate statistical significance. Every rainfall event was significantly different from one another, except three pairwise comparisons. The comparison of the 1-inch, 6 hour storm and 1.37-inch, 24 hour storm failed to

be proven significant for any results. This shows the importance of the rainfall intensity. A smaller volume of rainfall occurring over a shorter period of time can cause the same or greater amount of peak and total inflow than a larger volume of rainfall over a longer time. RStudio Tukey Honest Significance Test results for scenario-scenario and storm-storm comparisons for peak inflow and volume at each station can be found in Appendix D.

5.2 1D Model Results

Each GI scenario was compared against the baseline (Scenario 5; Table 4.4) to quantitatively assess the impact of increased LID on climate change resilience for transportation infrastructure. The change in peak inflow and total inflow were evaluated at three different locations (17, J06893350, and J27) in the 1D Tomahawk Creek Watershed (Figure 5.1). Junction 17 is located adjacent to U.S. Highway 69 and has 3270.2 hectares of contributing area. Junction 06893350 is the USGS gage that the model was calibrated to and has 59.8% more contributing area than J17. J27 is the outfall of the model and has 83% more contributing area than J17.

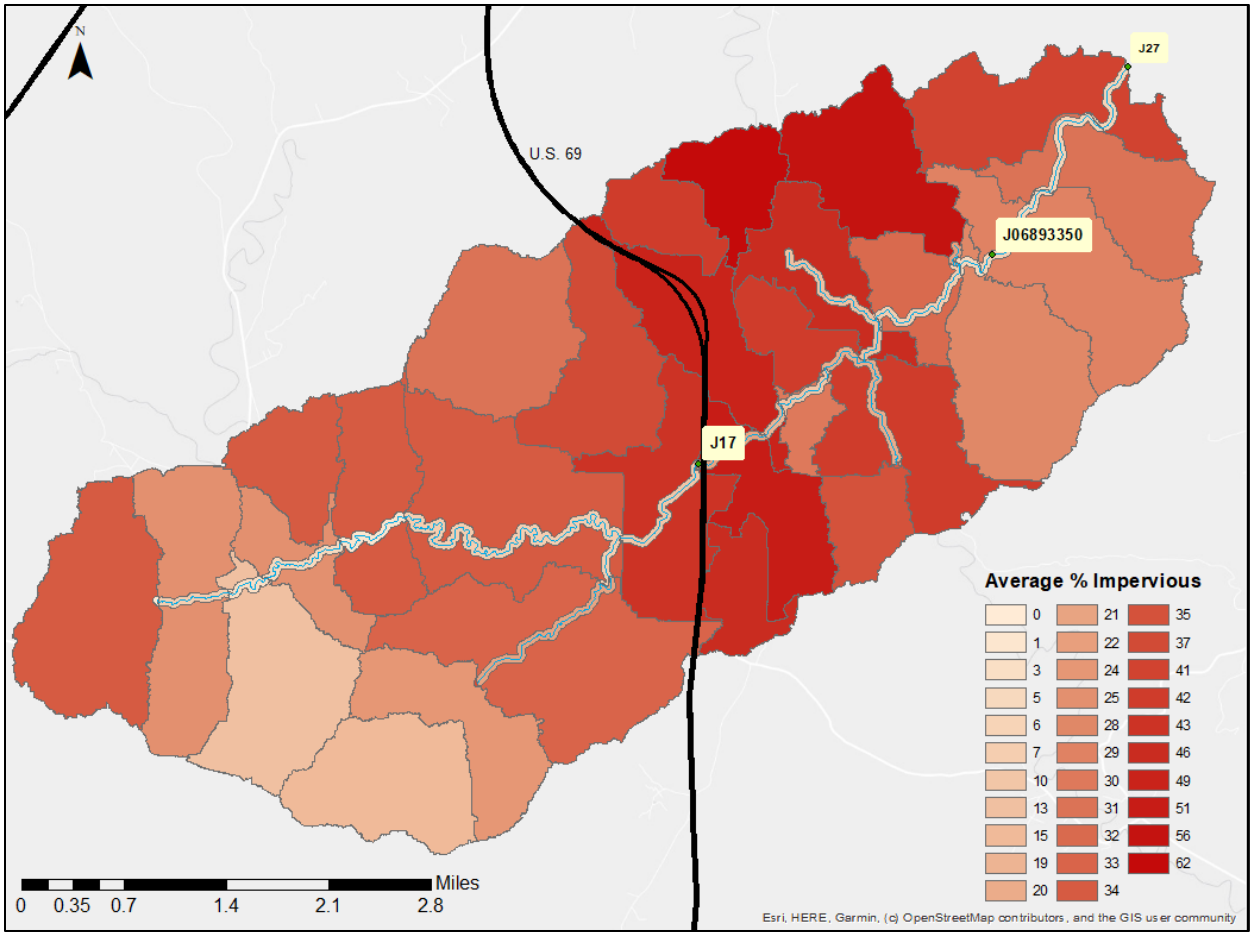

Figure 5.1. Peak and total inflow are monitored at three locations (J17, J06893350, and J27) in the Tomahawk Creek Watershed.

The hydrographs and tables showing the percent reduction in peak inflow and volume for each scenario comparison to the baseline for each design storm at each of the monitoring locations are located in Appendix D. The percent change for each scenario was determined by Equation 5.1.

$$\frac{current\ conditions\ value - scenario\ x\ value}{current\ conditions\ value}\ x\ 100 \qquad 5.1)$$

The scenarios varied the percentage of runoff routed to pervious (indicated by the scenario number) and the inclusion of a riparian buffer (indicated by R) (Table 4.4). Substantial reductions in peak inflow and total volume were observed for the 1-inch, 24-hour event (Table

5.2) (Figure 5.2). Scenario 100R, the maximum GI scenario, resulted in the infiltration of all the precipitation before reaching J17, and J06893350 and J27 saw 96% and 98% reductions in total inflow. Scenario 100R also resulted in 95% reductions in peak inflow and total volume for the water quality storm (1.37-inch, 24-hour) at J17 (

Table 5.3). However, the reductions were less prominent at J27 and J17, likely due to the higher contributing drainage area (

Table 5.3). These results show that green infrastructure is highly effective at reducing both peak inflow and total volume of discharge for 1.37-inch and lower, 24-hour storms, which in Kansas City represents 90% of all stormwater runoff volume on an annual basis (APWA, 2012). These results are consistent with other studies that found implementing green infrastructure successfully treated small storms. Akhter and Hewa (2016) found that implementing bioretention to treat 100% of the impervious area effectively reduced the peak inflow and total volume of 2-20 year floods.

The geospatially varying discharge reduction benefits of GI can be observed by comparing the hydrographs shown in Figure 5.3, 5.4, and 5.5. The hydrograph is reduced to almost a straight line for Scenario 50R, 75R, and 100R at the “headwaters”, J17, (Figure 5.3), while the middle of the watershed, J06893350, has higher discharge values and less flattening of the curve (Figure 5.4). The hydrograph at the outlet of the watershed, J27, closely resembles idealized hydrographs showing the flattening of the hydrograph from post-development to pre-development conditions (Figure 5.5). These results indicate that the increased climate resilience benefits received from GI depend on the location of the transportation infrastructure. For smaller storms, the GI peak inflow and volume reduction benefits were most prominent in the

headwaters. For larger storms, the peak inflow reduction for all GI benefits from all increase GI scenarios tended to be highest from

Table 5.2. Percent reduction in peak inflow and total volume of inflow from current conditions for the 1-inch, 24-hour precipitation event. Shading indicates statistically significant results.

1-inch, 24-hour						
	Peak Inflow (cms)			Total Volume (m^3)		
Scenario	J17	J06893350	J27	J17	J06893350	J27
0	-22.21	-11.08	-6.27	-11.32	-9.75	-9.85
25	71.59	39.37	25.09	37.09	34.80	35.17
50	92.79	77.58	56.76	67.96	67.87	69.27
75	97.97	91.07	87.56	92.36	89.31	91.13
100	100.00	95.62	98.78	100.00	94.13	96.39
0R	41.77	21.22	4.75	30.78	25.77	25.03
5R	57.51	29.22	11.07	37.81	32.65	32.06
25R	90.31	58.90	36.10	59.29	56.42	56.60
50R	96.39	86.52	66.45	78.81	79.76	81.23
75R	99.78	94.83	93.14	96.01	92.74	94.66
100R	100.00	97.86	99.32	100.00	95.63	97.70

Table 5.3. Percent reduction in peak inflow and total volume of inflow from current conditions for the 1.37-inch, 24-hour precipitation event. Shading indicates statistically significant results.

1.37-inch, 24-hour						
	Peak Inflow (cms)			Total Volume (m^3)		
Scenario	J17	J06893350	J27	J17	J06893350	J27
0	-6.44	-9.36	-10.87	-8.60	-7.72	-7.97
25	25.07	27.85	29.48	31.58	27.40	27.93
50	51.25	44.57	27.66	61.13	50.42	50.76
75	62.17	48.44	28.52	77.57	62.45	62.75
100	89.20	52.82	30.13	93.36	73.19	72.87
0R	23.61	18.49	16.43	22.92	19.68	18.87
5R	30.12	25.39	21.23	29.78	26.03	25.48
25R	51.93	45.46	35.46	53.77	47.66	47.64
50R	69.55	57.28	38.27	74.48	64.51	64.44
75R	80.46	59.47	43.33	86.60	73.51	73.48
100R	94.95	61.93	46.57	95.34	78.52	77.85

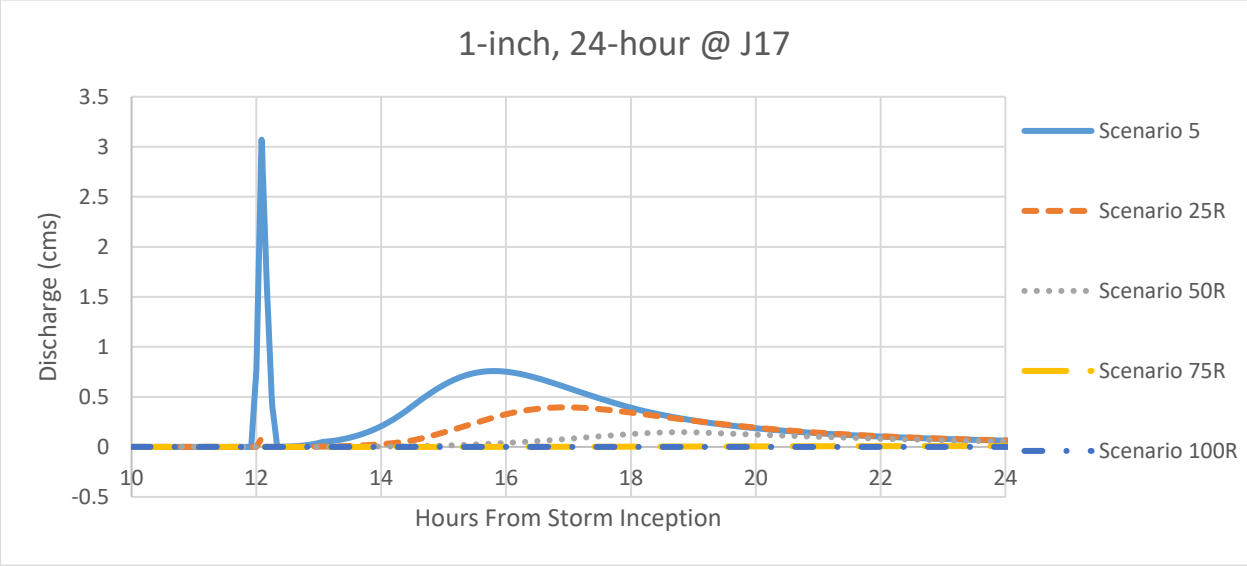

Figure 5.2. Hydrograph displaying changes between baseline conditions (scenario 5) and varying levels of GI implementation for the 1-inch, 24-hour storm at J17.

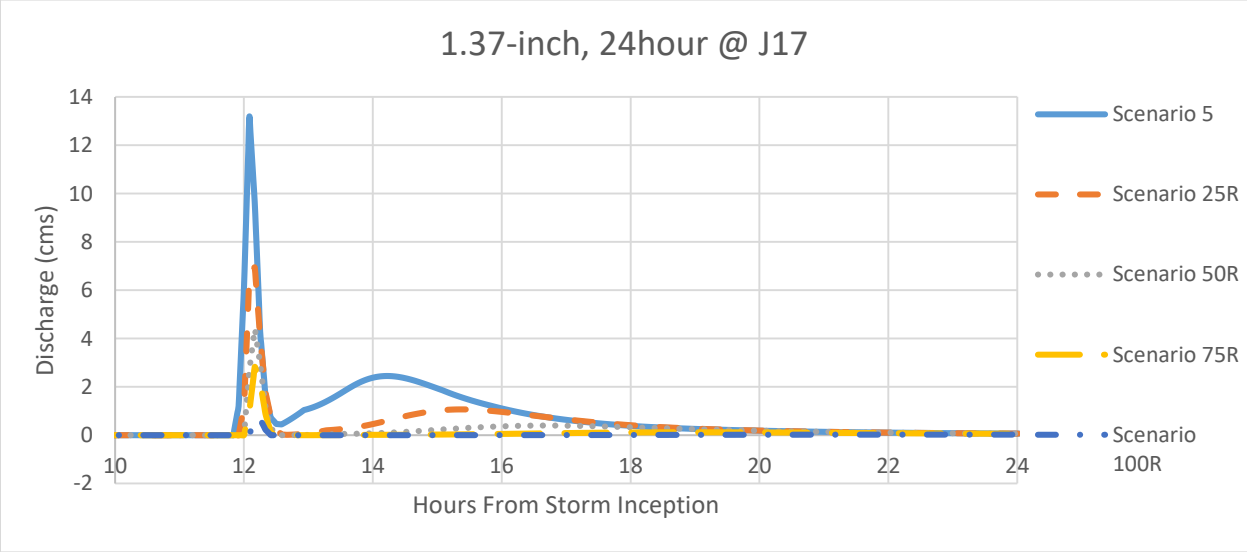

Figure 5.3. Hydrograph displaying changes between baseline conditions (scenario 5) and varying levels of GI implementation for the 1.37-inch, 24-hour storm at J17.

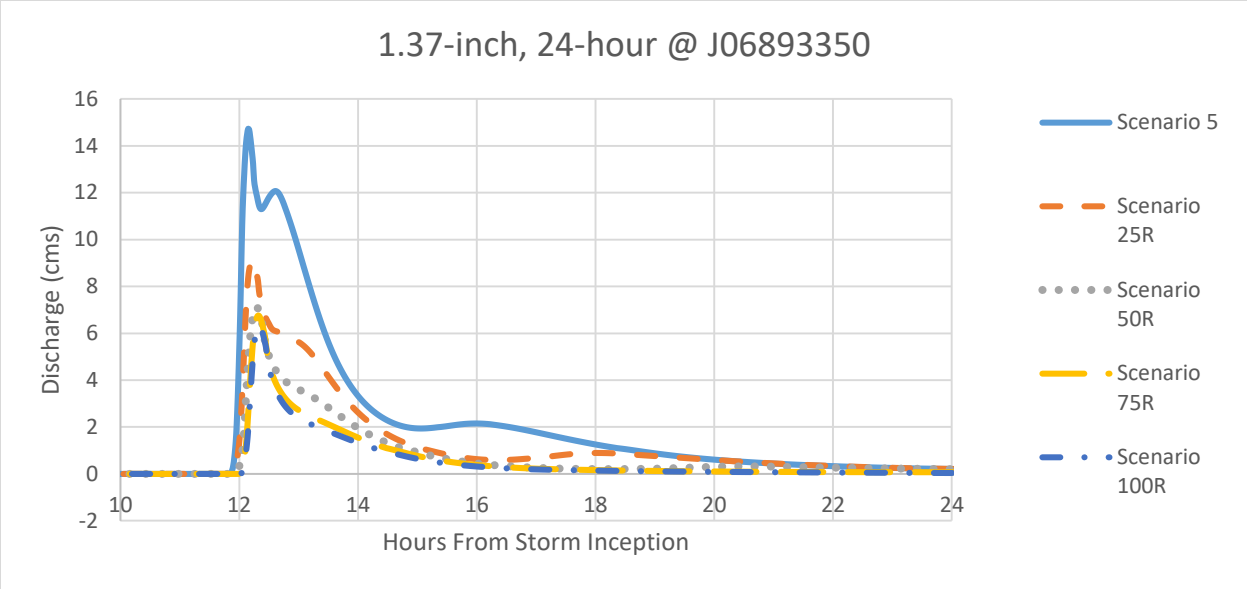

Figure 5.4. Hydrograph displaying changes between baseline conditions (scenario 5) and varying levels of GI implementation for the 1.37-inch, 24-hour storm at J06893350.

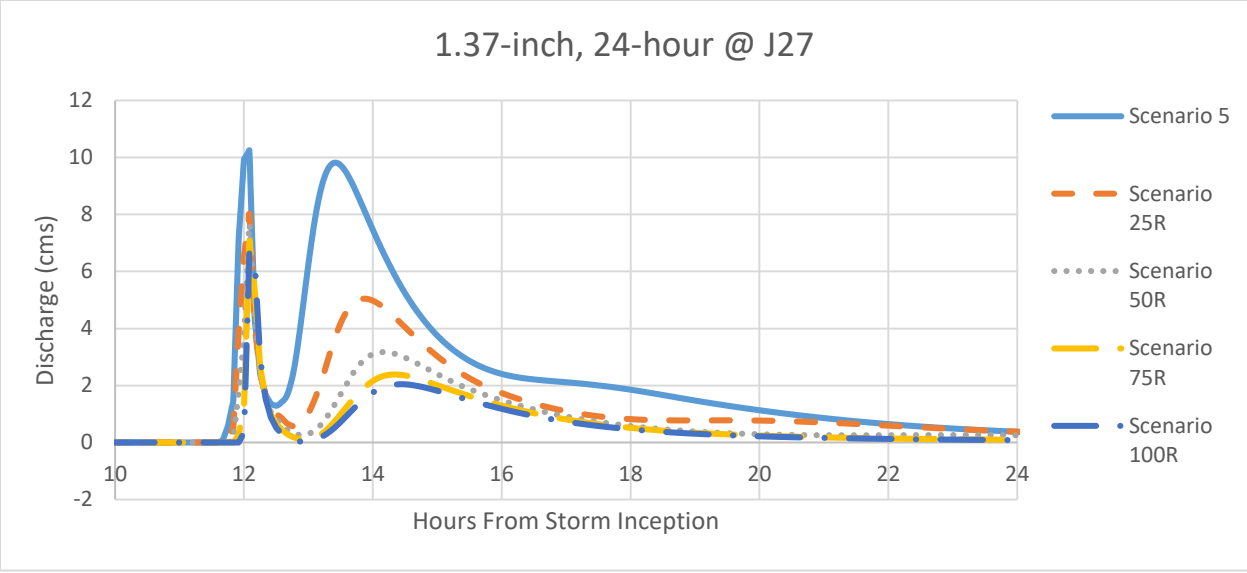

Figure 5.5. Hydrograph displaying changes between baseline conditions (scenario 5) and varying levels of GI implementation for the 1.37-inch, 24-hour storm at J27.

The similarity between the 1.37-inch, 24-hour storm and 1-inch, 6-hour storm can be observed by comparing their nearly indistinguishable hydrographs (Figure 5.5 and 5.6). This

shows how increasing intensity of storms due to climate change is comparable to increasing the volume of precipitation at the same intensity. It is also important to note that the hydrographs displayed from the event-based storm events are not taking into account base flow and antecedent moisture conditions. The initial and final discharge is in addition to whatever baseflow there would be in the channel at the storm inception.

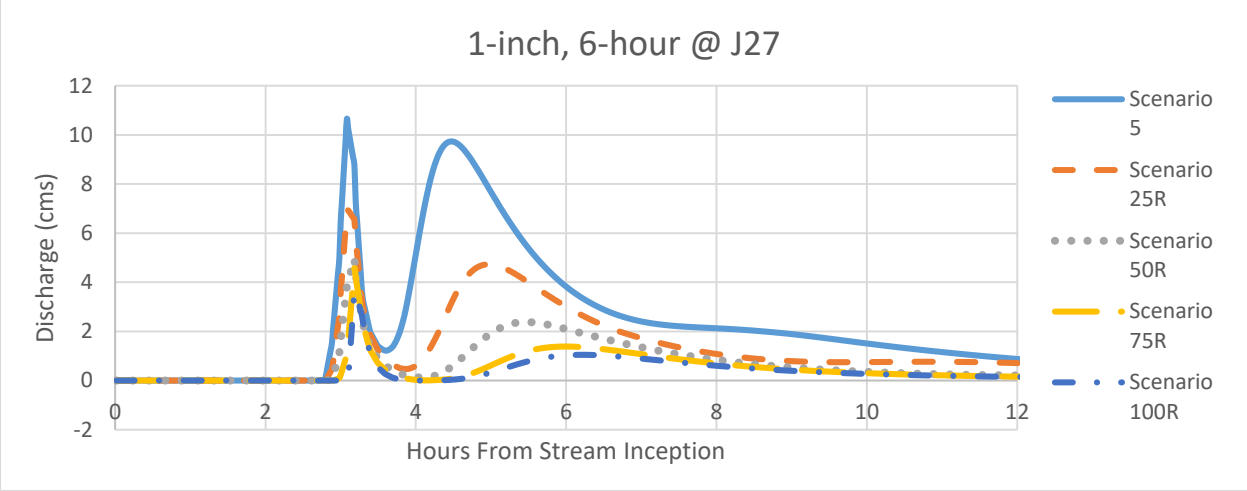

Figure 5.6. Hydrograph displaying changes between baseline conditions (scenario 5) and varying levels of GI implementation for the 1-inch, 6-hour storm at J27.

The peak flow and total inflow reductions from LID decline with an increase in design storm magnitude, which is understandable because GI is typically designed to treat the water quality volume storm (1.37-inches, 24-hour) in Kansas City. This aligns with the research from McDonough (2017) that the extent of flood and erosion regulating services decreases as the size and magnitude of storm even increases. It is likely that the soils in pervious areas become fully saturated during the larger storm-events and are unable to infiltrate more water. However, after the large drop in reduction from the 1.37-inch storm to the 1-year storm, similar reductions in peak inflow and total volume were observed for both the 1-year, 24-hour storm (Figure 5.7) to the 100-year, 24-hour storm (Figure 5.8) comparing scenario to scenario. These results show that

there is still a significant peak inflow and total inflow reduction observed by adding a riparian buffer and increasing the percent routed to pervious above 25% even for the 100-year, 24-hour design storm (Table 5.4). As the 100-year flood event is predicted to occur every 10-15 years in the future due to climate change (Hirabayashi et al., 2013), these significant reductions become especially promising. Additionally, these results are consistent with other studies of green infrastructure.

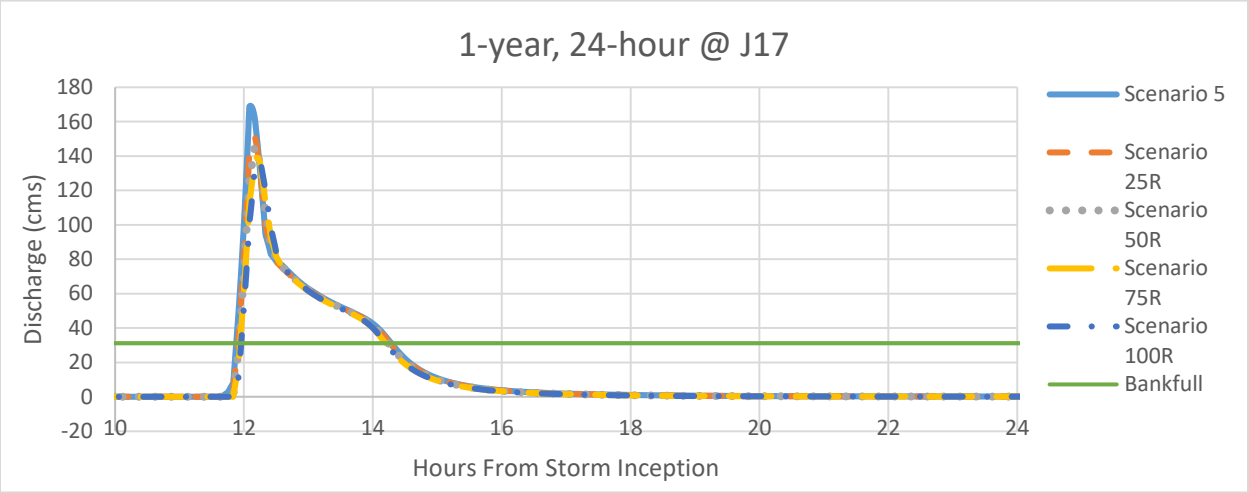

Figure 5.7. Hydrograph displaying changes between baseline conditions (scenario 5) and varying levels of GI implementation for the 1-year, 24-hour storm at J17.

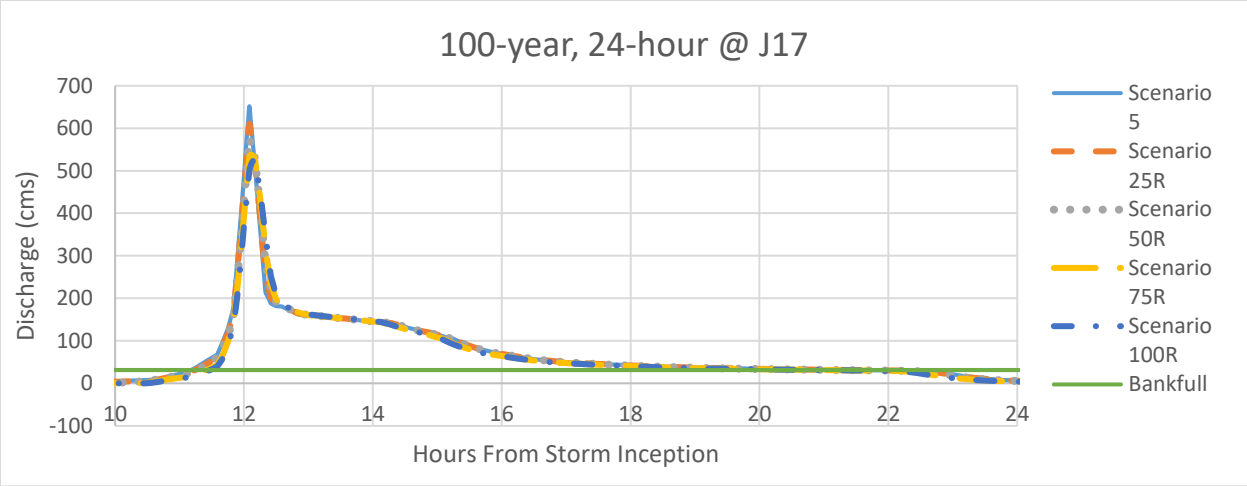

Figure 5.8. Hydrograph displaying changes between baseline conditions (scenario 5) and varying levels of GI implementation for the 100-year, 24-hour storm at J17.

Table 5.4. Percent reduction in peak inflow and total volume with addition of 150 ft. riparian buffer and 25% "disconnectedness". Shading indicates statistically significant results.

	Scenario 25R					
	Peak Inflow (cms)			Total Volume (m^3)		
Storm	J17	J06893350	J27	J17	J06893350	J27
1in, 24-hour	90.31	58.90	36.10	59.29	56.42	56.60
1in, 6-hour	51.36	49.53	44.41	55.85	49.74	49.93
1.37in, 24-hour	51.93	45.46	35.46	53.77	47.66	47.64
1.37in, 6-hour	20.06	29.63	28.97	28.27	26.13	25.34
1-year, 24-hour	13.94	12.87	14.59	7.43	8.18	7.51
5-year, 24-hour	10.60	5.01	3.97	4.18	4.98	3.55
10-year, 24-hour	9.80	4.90	0.70	3.66	4.52	3.86
25-year, 24-hour	8.88	2.85	0.52	3.24	4.06	3.85
100-year, 24-hour	6.51	2.20	0.47	2.78	3.56	4.39

The peak inflow and total inflow reductions increase as the percent routed to impervious increases, reaching a maximum reduction with 100% of runoff from impervious areas being routed to a pervious surface. Different junctions see the highest reductions in peak inflow or total volume depending on the storm, indicating that different processes dominate varying with precipitation level and location within the watershed. For example, the highest reduction in peak

inflow and total volume from the baseline (Scenario 5) to Scenario 100R occurs at J06893350 for the 1-year, 24-hour storm (Table 5.5). This could be because J06983350 has the highest concentration of impervious cover in its contributing area (Figure 5.1). Meanwhile, the peak inflow reductions from the baseline to Scenario 100R are highest at J17 for the 1-inch, 24-hour; 1-inch, 6-hour; 5-year, 24-hour; 10-year, 24-hour; 25-year, 24-hour; and 100-year, 24-hour storms. This could be due to smaller watersheds tending to be "flashier" than larger watersheds (Baker et al., 2004; Mogollón et al., 2016). J17 has the smallest contributing area, so it would be consistent with previous studies for the largest changes in peak inflow to be seen at the junction closest to the headwaters of the TCW (Baker et al., 2004; Mcdonough et al., 2017; Mogollón et al., 2016).

Table 5.5. Percent reduction in peak inflow and total volume with addition of 150 ft. riparian buffer and 100% "disconnectedness". Shading indicates statistically significant results.

	Scenario 100R, "Maximum GI Implementation"					
	Peak Inflow (cms)			Total Volume (m^3)		
Storm	J17	J06893350	J27	J17	J06893350	J27
1in, 24-hour	100.0	97.9	99.3	100.0	95.6	97.7
1in, 6-hour	100.0	77.3	71.1	99.9	86.4	86.9
1.37in, 24-hour	95.0	61.9	46.6	95.3	78.5	77.8
1.37in, 6-hour	42.5	43.6	39.5	50.7	44.8	43.3
1-year, 24-hour	22.0	24.6	22.6	13.0	15.1	14.2
5-year, 24-hour	20.9	11.3	10.8	8.1	9.9	7.4
10-year, 24-hour	20.1	10.7	4.3	7.1	8.8	7.6
25-year, 24-hour	19.2	7.3	5.8	6.4	7.9	7.4
100-year, 24-hour	19.2	7.5	1.6	8.3	11.4	12.1

With an average of 33.6% impervious cover, Tomahawk Creek Watershed is well above the threshold (>25% impervious) that will likely result in stream reduction being reduced to that of a stormwater conduit (Kaplan and Ayers, 2000). It is also well above the threshold of impervious cover (>10-20%) where urban stream quality is consistently classified as poor

(National Research Council, 2002). Akhter and Hewa (2016) also observed significant increases in Flow Duration Curves, mean discharge, and Flood Frequency Curves once impervious cover exceeded 10%. It can be challenging to change the percent of impervious cover in an almost entirely built-out environment. The above results indicate that significant peak inflow and total volume reductions can be seen from the 1-inch to 100-year storm without decreasing the percent impervious cover throughout the watershed. Instead, the percentage of runoff from impervious areas that is directed onto pervious area before reaching the subcatchment outlet or stream conduit can be increased. This is an example of increasing the disconnectedness of impervious surfaces, such as disconnecting roof gutters. Increasing the percent routed to at least 75% showed significant reductions in peak inflow and total volume for every design storm, even without riparian buffer implementation (Table 5.1). Increasing the percent routed to at least 50% resulted in significant reductions in peak inflow at all junctions across all design storms without implementation of a riparian buffer (Table 5.1). These results are consistent with the results from Waters et al. (2010) that found 50% disconnection of roof gutters reduced runoff volume and peak discharge below present values, with greater reduction seen with 100% disconnection.

Implementing only a riparian buffer, and maintaining percent routed at 5% did not achieve significant peak inflow and volume reduction benefits (Table 5.1). However, once a riparian buffer was added and percent routed increased to at least 25%, significant peak inflow and total volume reductions were observed across all storms at all junctions. Except significant peak inflow reductions were not observed at J17 until percent routed reached 50%. These results show that coupling the riparian buffer and increased disconnectedness is more effective than either of the practices individually.

While rivers are often only thought of in terms of conveying water, equally important to their form and processes is the sediment load they carry. Bankfull flow occurs when the channel is just at the point of overflowing onto the floodplain and typically occurs every 1.1 years in urban streams (Rosgen, 1996). The bankfull stage "corresponds to the discharge at which channel maintenance is the most effective, that is, the discharge at which moving sediment, forming or removing bars, forming or changing bends and meanders, and generally doing work that results in the average morphologic characteristics of channels", (Dunne and Leopold, 1978). No scenarios decreased the peak discharge rate below bankfull flow, indicating the substantial erosion control will not be observed by the GI implementation. Additionally, the largest reduction in the duration of time the discharge was above bankfull, was only 15 minutes for the maximum GI scenario for the 1-year, 24-hour storm.

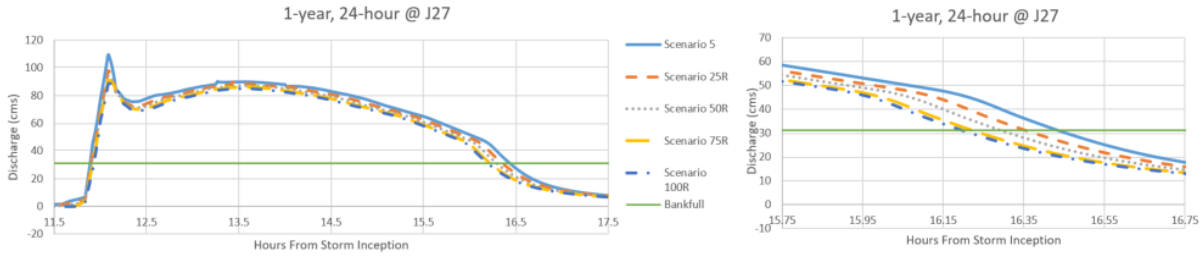

Figure 5.9. Green Infrastructure failed to decrease the peak discharge below bankfull flow or substantially decrease the duration of time the discharge was above bankfull flow.

However, the critical shear stress of the bank and bed soil also influences the approximate erosion threshold and should be analyzed to improve erosion threshold estimates (Lammers et al., 2019). For example, a stream with fine loam bed material will be more susceptible to erosion at the same discharge rate that a stream with coarse bed material would not see erosion (Pomeroy et al., 2008). While erosion rates were not explicitly modeled, there are many examples of GI reducing stream erosion in literature. Lammers et al. (2019) looked at

increasing bioretention across a watershed along with channel restoration ad found that implementing rain gardens to treat the excess urban runoff volume (EURV) reduced pollutant loading 70%. Pomeroy et al. conducted a study of how stormwater management design criteria can maintain geomorphic stability in Kansas City Metropolitan Area Streams and found that reducing runoff volume is essential for controlling channel erosion. Although a runoff volume of 30-65% was necessary to restore pre-development hydraulic conditions in urban streams in Australia (Anim et al., 2019). Reducing the magnitude and duration of peak flows also helps minimize channel erosion (Lammers et al., 2019). While all of these results point to the erosion-reducing potential of the significant peak flow and volume reductions from GI implementation, a study focusing on erosion should be conducted to conclusively determine the erosion benefits.

5.3 2D Model Results

The Tukey Honest Significant Difference test was conducted to statistically examine differences in flood extent between scenarios 5N, 25R, and 100R (see Section 4.7 for more information on statistical analysis). Comparisons which returned a p-value of less than 0.05 indicated a significant difference in flood extent (Table 5.1). The null hypothesis was rejected for all flood extent comparisons, indicating they were not proven to be significantly different. This could be due to all of the flood areas being hundreds of thousands of square meters. Each of the rainstorm comparisons were significant, except the 5 and 10-year storms were not proven to be statistically different.

5.3.1 Tomahawk Creek Watershed

Scenario 100R, the maximum GI scenario resulted in 14.4 – 9.9% of the flood extent being reduced for the 1, 5, and 10-year storms (Table 4.6) (Figure 5.10-11). Additionally, the flood extent reduction was larger than the total inflow volume reduction observed at J17 for the 1, 5,

and 10 year-storms. The difference in flood reduction between Scenario 25R and Scenario 100R are not significantly different nor very large, indicating increasing percent routed to at least 25% will achieve most of the benefits an increase to 100% would achieve, with substantially higher return on investment. The flood reduction benefits were substantially smaller for the 100-year storm (Table 5.6). Scenario 25R did not result in any flood reduction, and Scenario 100R only resulted in a 2.7% reduction in flood extent (Table 5.6). These results indicate that implementing green infrastructure and a riparian buffer will reduce flood extent approximately 10% for 10-year and under storms, but will have minimal results for large (100-year+) storm events. Geosyntec consultants modeled a 82% reduction in the number of inundated structures for the 25-year, 24-hour event and 29% reduction in the number of inundated structures for the 100-year, 24-hour event for their maximum GI scenario (2017). However, their large percent reductions can be accounted for in the extensiveness of their maximum GI scenario, in which increasing the percent routing accounted for only 10% of the GI measures implemented. Additionally, the substantial reduction in flood extent between the 25-year and 10-year event is consistent with the flood extent results presented here.

Table 5.6. The percent reduction from current conditions of 2D flood extent and 1D total inflow volume at J17 for Scenarios 25R and 100R. All 1D results are significant, 2D results were not tested for statistical significance.

		1-year, 24-hour	5-year, 24-hour	10-year, 24-hour	100-year, 24-hour
2D Flood Extent Reduction	Scenario 25R	8.0	7.9	7.8	-1.2
	Scenario 100R	14.4	9.9	11.3	3.7
1D Total Inflow Volume Reduction at J17	Scenario 25R	7.4	4.2	3.7	2.8
	Scenario 100R	13	8.1	7.1	8.3

If the magnitude of flood peaks does not increase substantially due to climate change, but instead the frequency of storms increases as Mallakpour and Vallarnini (2015) found, green infrastructure can help increase climate change resiliency of transportation frequency. This is

evidenced by the reduction in flood extent for 10-year and smaller storms. Additionally, green infrastructure has greater capacity to adapt to increased precipitation than grey infrastructure (Moore et al., 2016). However, Milly et al. (2002) found that the frequency of floods above the 100-year level increased substantially during the 20th century and is predicted to increase. If the 100-year flood occurs every 10-50 years as Hirabayashi (2013) predicts, these results show that the flood extent will not be greatly reduced. However, one benefit of the riparian buffer implementation is that flooding extent within the buffer would not result in any property damage

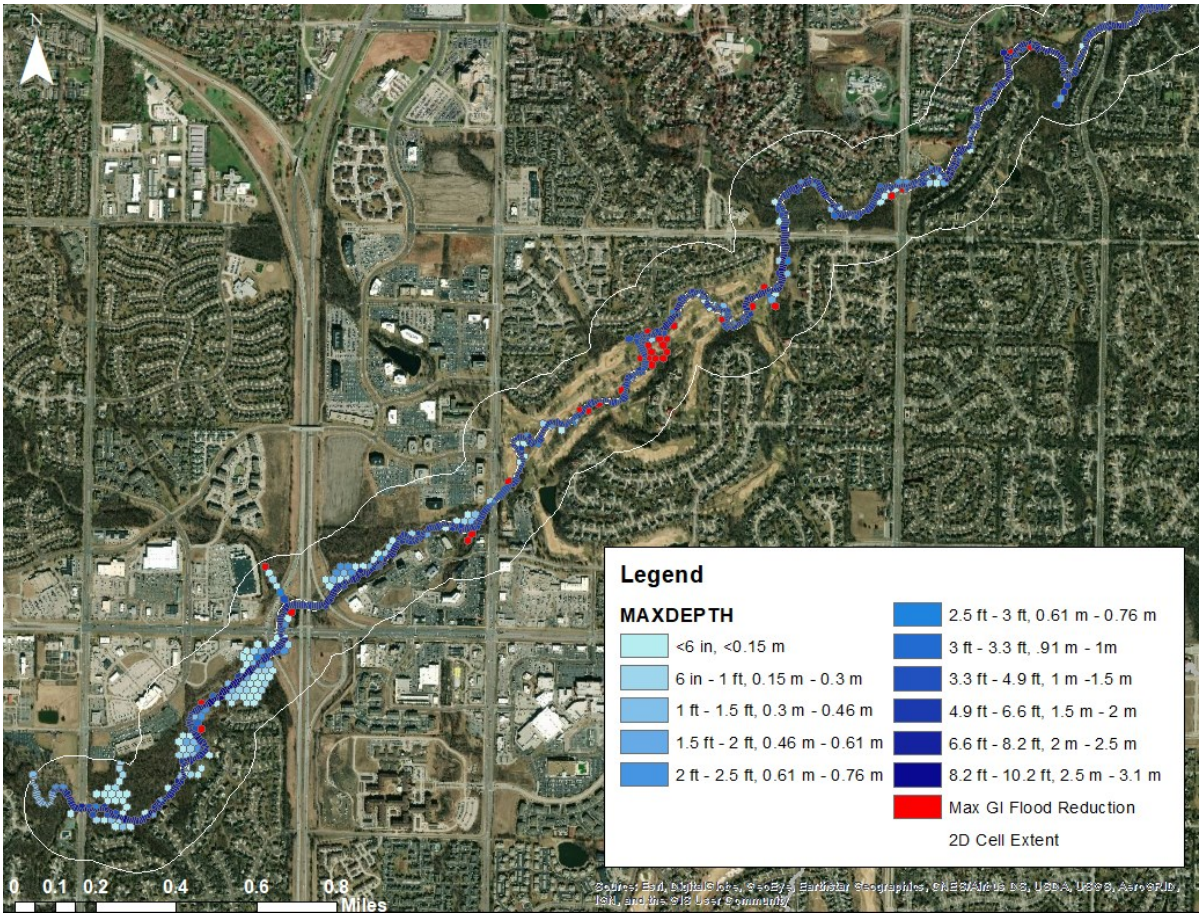

Figure 5.10. There was a 14.4% flood extent reduction for the 1-year, 24-hour storm in the Tomahawk Creek Watershed with maximum GI measures (Scenario 100R) implemented.

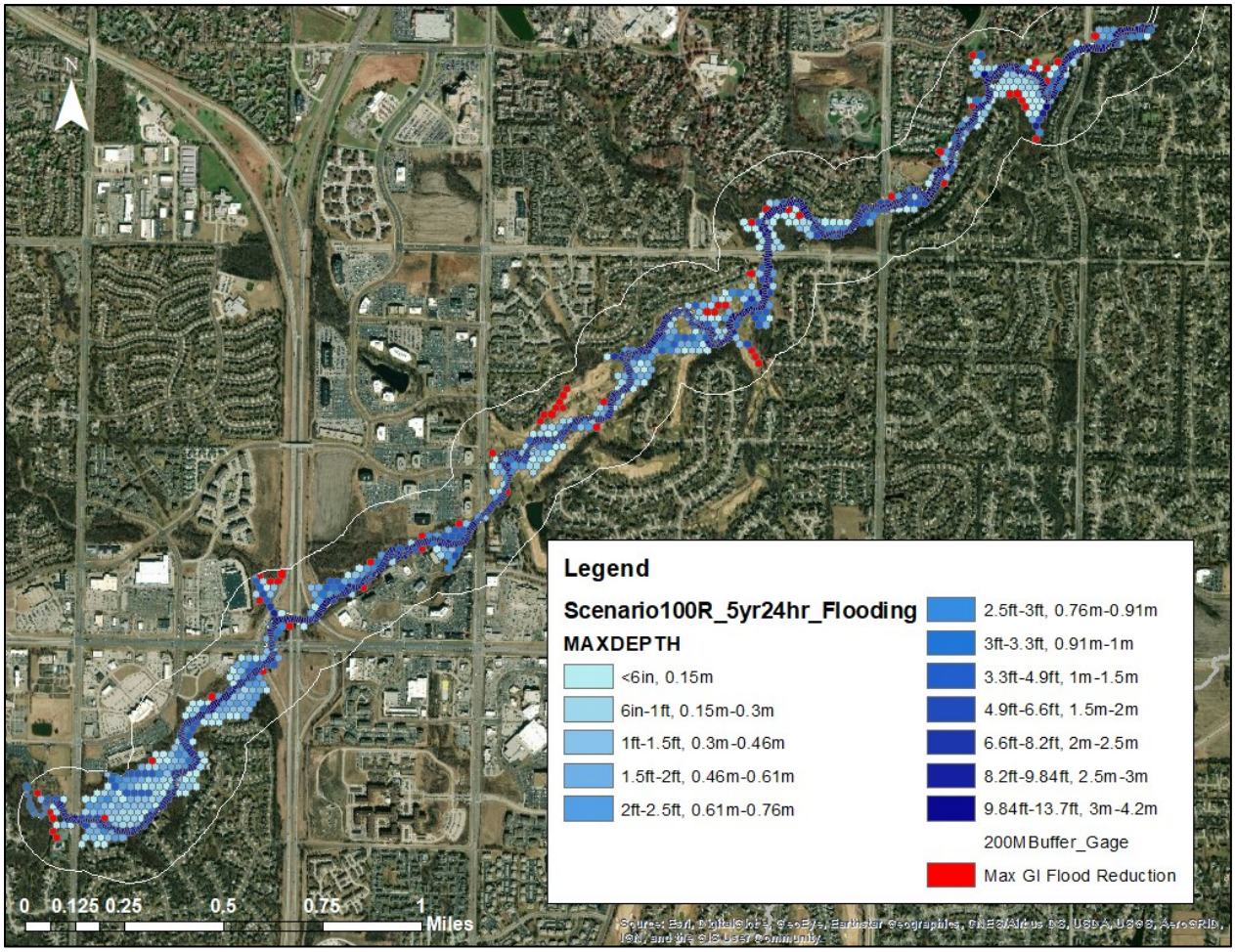

Figure 5.11. There was a 9.9% flood extent reduction for the 5-year, 24-hour storm in the Tomahawk Creek Watershed with maximum GI measures (Scenario 100R) implemented.

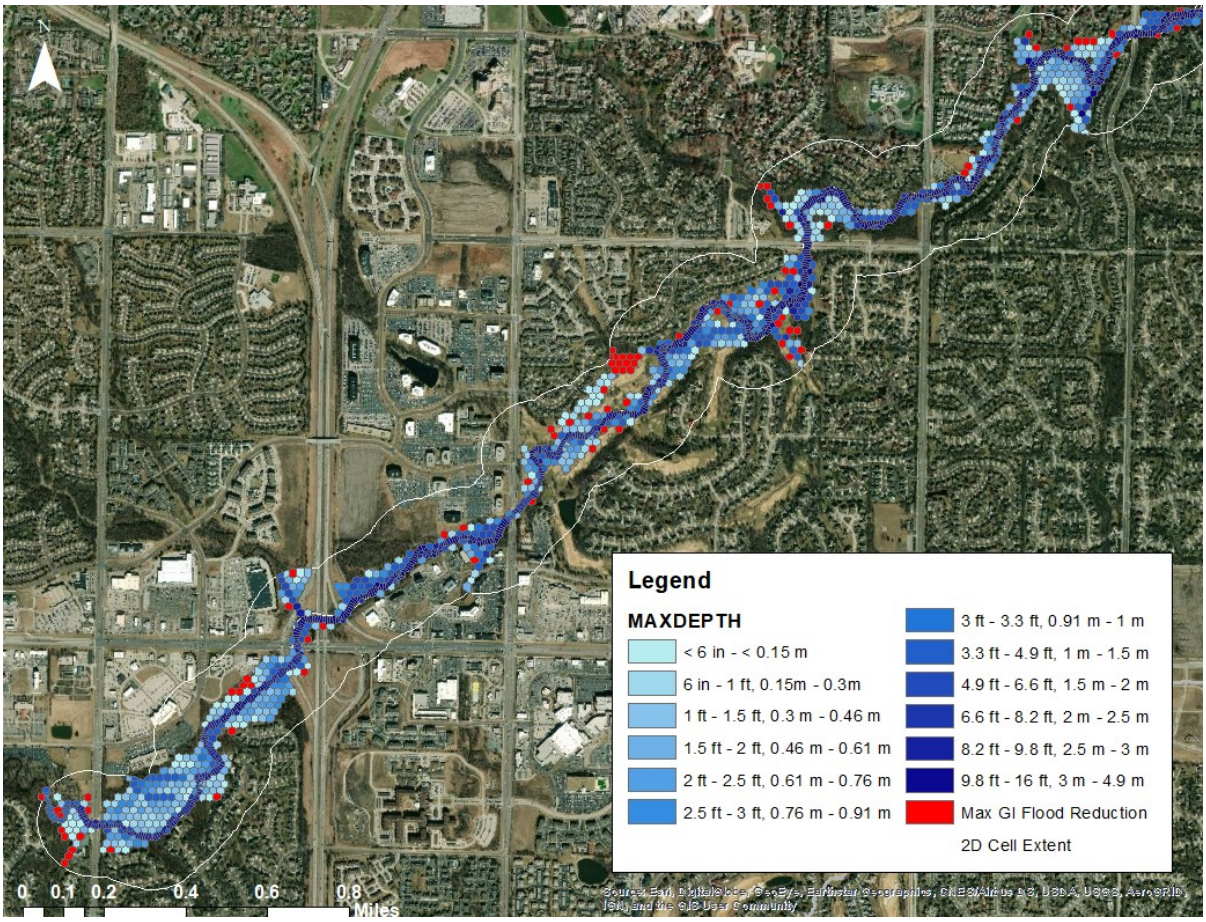

Figure 5.12. There was a 11.3% flood extent reduction for the 10-year, 24-hour storm in the Tomahawk Creek Watershed with maximum GI measures (Scenario 100R) implemented.

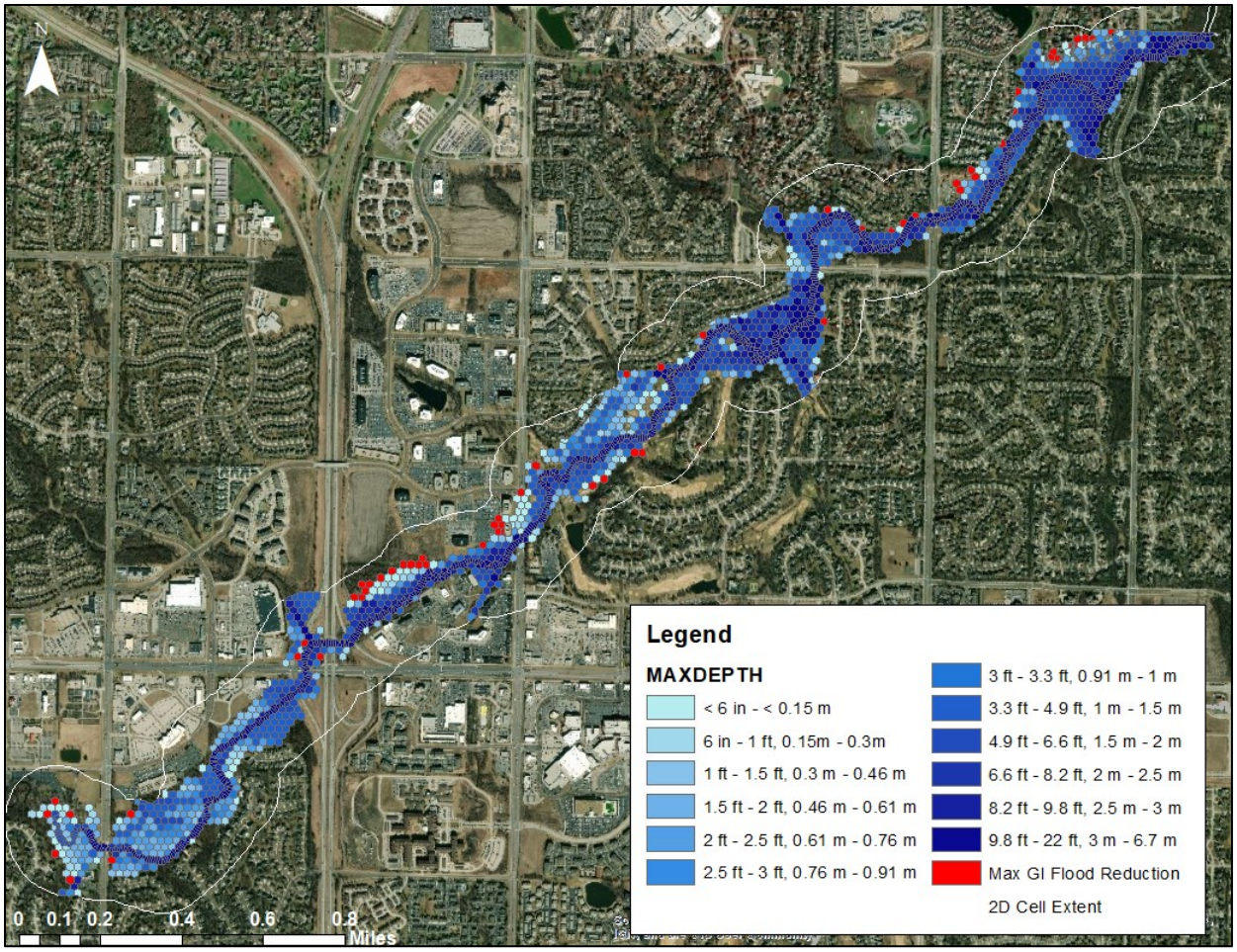

Figure 5.13. There was a 3.7% flood extent reduction for the 100-year, 24-hour storm in the Tomahawk Creek Watershed with maximum GI measures (Scenario 100R) implemented.

5.3.2 Blue River Watershed

The flood reduction extent was observed to be 0.3% for Scenario 25R and 1.8% for Scenario 100R for the 5-year, 24-hour design storm. A potential cause for this problem is the boundary layer of the 2D mesh not being large enough for the larger volumes of water consistent with larger contributing watershed area. This can cause floodwaters to pool and backup against the boundaries. Results more consistent with the results presented in 5.3.1 are expected if the 2D mesh layer is extended. However, the modeling time will increase with the increased number of 2D cells.

5.3 Discussion

These results indicate that increasing green infrastructure does increase the climate change resiliency of transportation infrastructure, however additional structural flood control is needed to reduce flood extent greater than 10% and for flood control of design storms of 100+ years. These results are consistent with the body of work on LID and increased climate change resiliency. Zahmatkesh (2015) found that LID reduced peak flows across a range of climate change future precipitation scenarios. Watson et al. (2016) showed the potential of floodplain restoration to build resilience to climate change. This research does provide new insights, by showing that increasing disconnectedness at least 25% and adding a riparian buffer provides similar flood reduction benefits as the maximum GI scenario of 100% disconnectedness with the riparian buffer.

Approximately 61% of the land within the 150 foot riparian buffer in the TCW is developed/agricultural and would need to be converted to riparian forest to match the study. This comes out to 135.5 hectares (335 acres), or 2.6% of the entire watershed cover. Jarran Tindle of the Kansas Forest Service offered a rough cost estimate via email for the planting and maintenance costs of a riparian forest buffer. The standard projects using bare-root tree and shrub seedlings cost $2000 per acre for planting and $2000 per acre for the mowing, weed control, and replacement plantings it takes to establish a healthy buffer in the first few years. Without accounting for the property prices and imminent domain problems, to implement a standard riparian buffer would require $670,000 in capital planting costs and an additional $670,000 in operational costs the first few years. A more progressive planting using tree and shrub seeds instead of bare-root seedlings would cost $1,000 to plant and $1,000 in maintenance for the first few years. Again ignoring the property prices and imminent domain problems,

implementing a standard riparian buffer would require $335,000 in capital planting costs and an additional $335,000 in operational costs the first few years. The conditions of the planting site, weather, methods of planting, and maintenance can alter the cost of a riparian buffer. As such, his estimates are accurate within $500 per acre and depend on the aforementioned conditions (Tindle, 2018).

The Lenexa, Overland Park, Olathe, and Prairie Village municipal codes contain a stream setback ordinance limiting development in stream corridors (Lenexa, Kansas, 2019; Olathe, Kansas, 2019; Overland Park, Kansas, 2019; Prairie Village, Kansas, 2019). Unfortunately, these codes only apply to new development and much of the development of Indian Creek occurred before these codes were enacted.

These findings are not only relevant for the Kansas City Metro Area. These findings should be transferable to any locations with similar climate, soils, and impervious cover. Valuation of broader societal benefits, or ecosystem services, provided by structural and non-structural green infrastructure was beyond the scope of this study, though quantification of such benefits as generated by bioinfiltration and other green infrastructure systems is an area of active research and many benefits of GI were discussed in Chapter 2.

Chapter 6 - Conclusions

The primary goal of this research was to understand if and to what extent green infrastructure can increase the climate change resiliency of transportation infrastructure across a watershed. To meet this objective, a Personal Computer Storm Water Management Model (PCSWMM) of the Blue River Watershed (BRW) in the greater Kansas City Metropolitan Area created by Kelsey McDonough (2018) was adapted and updated.

Twelve different low impact development scenarios with varying levels of green infrastructure were evaluated across a range of design storm events in both one and two dimensional models. Green infrastructure was represented through implementation of a 150-foot deciduous forest riparian buffer and increasing the percent routed subcatchment parameter in PCSWMM. This function does not change the amount of impervious cover, which can be hard to do in an almost entirely built-out environment. Instead, it changes the percentage of runoff from the impervious areas that is directed onto pervious area before reaching the subcatchment outlet or stream conduit. This is an example of increasing the disconnectedness of impervious surfaces, such as disconnecting storm drains, or adding bioretention cells in parking lots.

The percent reduction in peak flow, total volume of flow, and flood extent between each scenario and the current conditions were evaluated. Results demonstrate that increasing the percentage of disconnectedness to at least 25%, and adding a 150-foot riparian buffer significantly decreased the simulated peak inflow and total volume of water near important transportation features. The reductions were greatest for the water quality event (>90% reduction) and decreased to an approximately 10% reduction for the 100 year, 24 hour storm event for the maximum green infrastructure scenario. This indicated that green infrastructure works best for water quality storms and smaller. The largest peak inflow and total inflow

reductions were seen for Scenario 100R, the maximum GI scenario. This indicates that extent of GI benefits have a direct, positive correlation with the extent of GI implemented. Implementing only a riparian buffer, and maintaining percent routed at 5% did not achieve significant peak inflow and volume reduction benefits. Adding a riparian buffer and increasing percent routed to at least 25% achieved significant peak inflow and total volume reductions across all storm events. This indicated that coupling the riparian buffer with increased disconnectedness is more effective than either of the practices individually. The TCW flood extent was reduced approximately 8% for the 1, 5, and 10-year design storms with implementation of Scenario 25R. Minimal flood extent reductions were seen for the 100-year design storm. These results indicate that increasing green infrastructure does increase the climate change resiliency of transportation infrastructure, however additional structural flood control is needed to reduce flood extent greater than 10% and for flood control of design storms of 100+ years.

It can be challenging to change the percent of impervious cover in an almost entirely built-out environment. The above results indicate that significant peak inflow and total volume reductions can be seen from the 1-inch to 100-year storm without decreasing the percent impervious cover throughout the watershed. Instead, the percentage of runoff from impervious areas that is directed onto pervious area before reaching the subcatchment outlet or stream conduit can be increased along with targeted riparian buffer restoration. This increased disconnectedness can be accomplished through disconnecting roof gutters, implementing bioswales adjacent to parking lots, and disconnecting outfalls from streams. The scenario with the highest return on investment is Scenario 25R. This scenario allows for the lowest percent increase in disconnectedness, yet still achieves significant and comparable results to Scenario

50R, 75R and 100R. These findings are not only relevant for the Kansas City Metro Area. These findings should be transferable to any locations with similar climate, soils, and impervious cover.

While water quality was not explicitly evaluated by the BRW and TCW models, the increase in infiltration observed by reduced inflow volumes indicate that more water is treated by percolating through the soil and water quality improvements could be expected. No scenarios decreased the peak discharge rate below bankfull flow or substantially reduced the duration of time the discharge was above bankfull flow, indicating the substantial erosion control will not be observed by the GI implementation. In addition to the peak discharge, total volume, and flood extent reductions, additional benefits can be expected from increased GI. The increased infiltration can help cities, such as Kansas City, Missouri, who are under EPA decree for combined sewer overflows reduce the amount of water getting into sewers.

References

Abdelrahman, Y. T., El Moustafa, A. M., Elfawy, M. (2018). Simulating flood urban drainage networks through 1D/2D model analysis. *Journal of Water Management Modeling*, *2018*. https://doi.org/10.14796/JWMM.C454

Acreman, M., Riddington, R., Booker, D. J. (2003). Hydrological Impacts of Floodplain Restoration: A Case Study of the River Cherwell, UK. *Hydrology and Earth System Sciences*. https://doi.org/DOI: 10.5194/hess-7-75-2003

Ahiablame, L., Engel, B., Chaubey, I. (2012). Effectiveness of Low Impact Development Practices: Literature Review and Suggestions for Future Research. *Water, Air, & Soil Pollution*, *223*(7), 4253–4274. https://doi.org/10.1007/s11270-012-1189-2

Ahiablame, L., Shakya, R. (2016). Modeling flood reduction effects of low impact development at a watershed scale. *Journal of Environmental Management*, *171*, 81–92. https://doi.org/10.1016/j.jenvman.2016.01.036

AIMS. (2018). Building_PL. Johson County - AIMS (Automated Information Mapping System).

Akhter, M. S., Hewa, G. A. (2016). The Use of PCSWMM for Assessing the Impacts of Land Use Changes on Hydrological Responses and Performance of WSUD in Managing the Impacts at Myponga Catchment, South Australia. *Water*, *8*(11), 511. https://doi.org/10.3390/w8110511

Anderson, C., Walker, D. (2015). *Understanding Long-Term Climate Changes for Kansas City, Missouri*. ClimateLOOK. Retrieved from https://www.kcwaterservices.org/wp-content/uploads/2016/05/ClimateLOOK-for-Kansas-City-Missouri-033116.pdf

Anim, D. O., Fletcher, T. D., Pasternack, G. B., Vietz, G. J., Duncan, H. P., Burns, M. J. (2019). Can catchment-scale urban stormwater management measures benefit the stream

hydraulic environment? *Journal of Environmental Management*, *233*, 1–11. https://doi.org/10.1016/j.jenvman.2018.12.023

APWA. (2012). *Manual of Best Management Practices for Stormwater Quality*. Mid-American Regional Council, American Public Works Association. Retrieved from http://kcmetro.apwa.net/content/chapters/kcmetro.apwa.net/file/Specifications/BMPManual_Oct2012.pdf

ASCE. (2020). 2017 American Infrastructure Report Card. Retrieved March 9, 2020, from https://www.infrastructurereportcard.org

Baffaut, C., Dabney, S. M., Smolen, M. D., Youssef, M. A., Bonta, J. V., Chu, M. L., … Arnold, J. G. (2015). Hydrologic and Water Quality Modeling: Spatial and Temporal Considerations. *Transactions of the ASABE*, *58*(6), 1661–1680. https://doi.org/10.13031/trans.58.10714

Baker, D. B., Richards, R. P., Loftus, T. T., Kramer, J. W. (2004). A New Flashiness Index: Characteristics and Applications to Midwestern Rivers and Streams1. *JAWRA Journal of the American Water Resources Association*, *40*(2), 503–522. https://doi.org/10.1111/j.1752-1688.2004.tb01046.x

Barnard, T., Agnaou, M., Barbis. (2017). Two Dimensional Modeling to Simulate Stormwater FLows at Photovoltaic Solar Energy Sites. *Chi Journal*. https://doi.org/DOI: 10.14796/JWMM.C428

Bentrup, G., Kellerman, T. (2004). Where should buffers go? Modeling riparian habitat connectivity in northeast Kansas. *Journal of Soil and Water Conservation*, *59*(5), 209–215.

Blöschl, G., Ardoin-Bardin, S., Bonell, M., Dorninger, M., Goodrich, D., Gutknecht, D., … Szolgay, J. (2007). At what scales do climate variability and land cover change impact on flooding and low flows? *Hydrological Processes*, *21*(9), 1241–1248. https://doi.org/10.1002/hyp.6669

Blue River Watershed Association. (2018). *2018 Annual Report*. Retrieved from https://www.brwa.net/file_download/inline/6c9c5865-62db-4c58-8889-8e121c159fd1

Brody, S., Kim, H., Gunn, J. (2012). Examining the Impacts of Development Patterns on Flooding on the Gulf of Mexico Coast: *Urban Studies*. https://doi.org/10.1177/0042098012448551

Broekhuizen, I., Leonhardt, G., Marsalek, J., Viklander, M. (2019). Calibration event selection for green urban drainage modelling. *Hydrology and Earth System Sciences Discussions*, 1–29. https://doi.org/10.5194/hess-2019-67

Canadell, J. G., Ciais, P., Dhakal, S., Le Quere, C., Patwardhan, A., Raupach, M. R. (2009). *The Human perturbation of the carbon cycle: the global carbon cycle II* (UNESCO-Score_UNEP Policy Brief No. 10). UNESCO: Division of Ecological and Earth Sciences. Retrieved from https://unesdoc.unesco.org/ark:/48223/pf0000186137

Canon, S., Sanderson, S. (2017, July 27). When will Indian Creek's flooding be fixed? *Kansas City Star*. Retrieved from https://www.kansascity.com/news/local/article164032392.html

CDC. (2013). *Climate Change and Extreme Heat Events*. Centers for Disease Control and Prevention. Retrieved from https://www.cdc.gov/climateandhealth/pubs/ClimateChangeandExtremeHeatEvents.pdf

Charlton, R. (2008). *Fundamentals of Fluvial Geomorphology*. New York, NY: Routledge.

CHI. (2020). *PCSWMM Support Articles*. Guelph, Ontario, Canada: Computational Hydraulics Int. Retrieved from https://support.chiwater.com/77608/getting-started

Chirisa, I., Bandauko, E., Mazhindu, E., Kwangwama, N. A., Chikowore, G. (2016). Building resilient infrastructure in the face of climate change in African cities: Scope, potentiality and challenges. *Development Southern Africa*, *33*(1), 113–128. https://doi.org/10.1080/0376835X.2015.1113122

Daggupati, P., Pai, N., Ale, S., Douglas-Mankin, K. R., Zeckoski, R. W., Jeong, J., … Youssef, M. A. (2015). A Recommended Calibration and Validation Strategy for Hydrologic and Water Quality Models. *Transactions of the ASABE*, *58*(6), 1705–1719. https://doi.org/10.13031/trans.58.10712

Demuzere, M., Orru, K., Heidrich, O., Olazabal, E., Geneletti, H., Orru, H., … Faehnle, M. (2014). Mitigating and adapting to climate change: Multi-functional and multi-scale assessment of green urban infrastructure. *Journal of Environmental Management*, *146*, 107–115. https://doi.org/10.1016/j.jenvman.2014.07.025

Doocy, S., Daniels, A., Murray, S., Kirsch, T. D. (2013). The human impact of floods: a historical review of events 1980-2009 and systematic literature review. *PLoS Currents*, *5*(2013). https://doi.org/10.1371/currents.dis.f4deb457904936b07c09daa98ee8171a

Driscoll, M., Clinton, S., Jefferson, A., Manda, A., McMillan, S. (2010). Urbanization Effects on Watershed Hydrology and In-Stream Processes in the Southern United States. *Water*, 605–649. https://doi.org/doi:10.3390/w2030605

Duin, Y. (2020). StormWatch. Retrieved April 1, 2020, from https://www.stormwatch.com/home.php

Dunne, T., Leopold, L. B. (1978). *Water in Environmental Planning*. New York: W.H. Freeman and Co.

Emporia Gazette. (2003, September). 2003 FLOOD KILLS SIX. Retrieved March 8, 2020, from http://www.emporiagazette.com/news/article_91c4a3b7-981f-562c-b89f-fcbf6fbd2310.html

Espinet, X., Schweikert, A., van den Heever, N., Chinowsky, P. (2016). Planning resilient roads for the future environment and climate change: Quantifying the vulnerability of the primary transport infrastructure system in Mexico. *Transport Policy*, *50*, 78–87. https://doi.org/10.1016/j.tranpol.2016.06.003

FEMA. (2019). Loss Dollars Paid by Calendar Year. Retrieved March 9, 2020, from https://www.fema.gov/loss-dollars-paid-calendar-year

Fremier, A. K., Kiparsky, M., Gmur, S., Aycrigg, J., Craig, R. K., Svancara, L. K., … Scott, J. M. (2015). A riparian conservation network for ecological resilience. *Biological Conservation*, *191*, 29–37. https://doi.org/10.1016/j.biocon.2015.06.029

Geosyntec Consultants. (2017). *Impact of Decentralized Green Stormwater Controls: Modeling Results Summary*. Austin, Texas: City of Austin Watershed Protection Department.

Gill, S. E., Handley, J. F., Ennos, A. R., Pauleit, S. (2007). Adapting Cities for Climate Change: The Role of the Green Infrastructure. *Built Environment (1978-)*, *33*(1), 115–133. https://doi.org/10.2148/benv.33.1.115

Glascoe, S., Christy, A. (2004). *Literature Review and Analysis: Coastal Urbanization and Microbial Contamination of Shellfish Growing Areas* (No. PSAT04- 09). Olympia, Washington: Puget Sound Action Team. Retrieved from

https://www.researchgate.net/publication/301283177_Literature_Review_and_Analysis_Coastal_Urbanization_and_Microbial_Contamination_of_Shellfish_Growing_Areras

Gómez-Baggethun, E., Barton, D. N. (2013). Classifying and valuing ecosystem services for urban planning. *Ecological Economics*, *86*, 235–246. https://doi.org/10.1016/j.ecolecon.2012.08.019

Güneralp, B., Güneralp, İ., Liu, Y. (2015). Changing global patterns of urban exposure to flood and drought hazards. *Global Environmental Change*, *31*, 217–225. https://doi.org/10.1016/j.gloenvcha.2015.01.002

Hanna, J. (2003, September 1). I-35 flood sweeps away family. Retrieved March 8, 2020, from https://www2.ljworld.com/news/2003/sep/01/i35_flood_sweeps/

Heidrich, O., Dawson, R. J., Reckien, D., Walsh, C. L. (2013). Assessment of the climate preparedness of 30 urban areas in the UK. *Climatic Change*. https://doi.org/10.1007/s10584-013-0846-9

Held, I., Soden, B. (2006). Robust Responses of the Hydrological Cycle to Global Warming. *Journal of Climate*, *19*, 5686–5699.

Heraty, M. (1993). *Riparian buffer programs: a guide to developing and implementing a riparian buffer program as an urban best management practice*. Washington D.C.: Metropolital Washington Council of Governments, USEPA OFfice of Wetlands, Oceans and Watersheds.

Herring, S. C., Christidis, N., Hoell, A., Hoerling, M. P., Scott, P. A. (2019). Explaining Extreme Events in 2017 from a Climate Perspective, *100*(1), S1–S117. https://doi.org/10.1175/BAMS-ExplainingExtremeEvents2017.1.

Hirabayashi, Y., Mahendran, R., Koirala, S., Konoshima, L., Yamazaki, D., Satoshi Watanabe, … Shinjiro Kanae. (2013). Global flood risk under climate change. *Nature Climate Change*, *3*(9), 816–821. https://doi.org/10.1038/nclimate1911

Homer, C., Dewitz, J., Jin, S., Xian, G., Costello, C., Danielson, P., … Riitters, K. (2020). Conterminous United States land cover change patterns 2001–2016 from the 2016 National Land Cover Database. *ISPRS Journal of Photogrammetry and Remote Sensing*, *162*, 184–199. https://doi.org/10.1016/j.isprsjprs.2020.02.019

Huffman, R. L., Fangmeier, D. D., Elliot, W. J., Workman, S. R. (2013). *Soil and Water Conservation Engineering* (Seventh). St. Joseph, MI: ASABE.

Huntington, T. G. (2006). Evidence for intensification of the global water cycle: Review and synthesis. *Hydrology*, *319*(1), 83–95. https://doi.org/DOI: 10.1016/j.jhydrol.2005.07.003

Iowa Department of Natural Resources. (n.d.). Ecoregion 47f: Rolling Loess Prairie. Retrieved January 23, 2020, from https://programs.iowadnr.gov/bionet/Docs/Ecoregions/47f

James, W., Rossman, L., James, R. (2010). *User's Guide to SWMM5*. Guelph, Ontario, Canada: CHI.

Jayakaran, A. D., Smoot, Z. T., Park, D. M., Hitchcock, D. R. (2016). Relating stream function and land cover in the Middle Pee Dee River Basin, SC. *Journal of Hydrology: Regional Studies*, *5*, 261–275. https://doi.org/10.1016/j.ejrh.2015.12.064

Jenerette, G. D., Harlan, S. L., Brazel, A., Jones, N., Larsen, L., Stefanov, W. L. (2007). Regional relationships between surface temperature, vegetation, and human settlement in a rapidly urbanizing ecosystem. *Landscape Ecology*, *22*(3), 353–365. https://doi.org/10.1007/s10980-006-9032-z

Jonkman, S. N. (2005). Global Perspectives on Loss of Human Life Caused by Floods. *Natural Hazards*, *34*(2), 151–175. https://doi.org/10.1007/s11069-004-8891-3

Kansas Geological Survey. (1963, December). Geologic History of Kansas. Retrieved January 23, 2020, from http://www.kgs.ku.edu/Publications/Bulletins/162/03_strat_c.html

Kansas Native Plant Society. (2019, February 7). Ecoregions of Kansas. Retrieved January 23, 2020, from http://www.kansasnativeplantsociety.org/ecoregions.php

Kaplan, M., Ayers, M. (2000). *Impervious Surface Cover Concepts and Thresholds: Supporting documentation for water quality and watershed management planning rules*. Trenton, NJ: New Jersey Dept. of Environmental Protection, Division of Watershed Management. Retrieved from https://rucore.libraries.rutgers.edu/rutgers-lib/37001/pdf/1

KDOT. (2018, January). Traffic Cound Map of Kansas City Metro Area Johnson and Wyandotte County Kansas. Retrieved from https://www.ksdot.org/Assets/wwwksdotorg/bureaus/burTransPlan/maps/CountMaps/Cities/kcmetro2016.pdf

Keane, T. (2019). *LAR734: Rivers-Processes and Forms*. Kansas State University.

Kim, J. H., Keane, T. D., Bernard, E. A. (2015). Fragmented local governance and water resource management outcomes. *Journal of Environmental Management*, *150*, 378–386. https://doi.org/10.1016/j.jenvman.2014.12.002

Klein, G., Bauman, Y. (2014). *The Cartoon Introduction to Climate Change*. Washington D.C.: Island Press.

Klenzendorf, B., Poresky, A., Kelly, M., Christman, M. (2015). 1D/2D Modeling of Decentralized Stormwater Control Measures for Flood Mitigation in Austin, Texas.

World Environmental and Water Resources Congress 2015, 204–213. https://doi.org/10.1061/9780784479162.019

Konikow, L. F., Bredehoeft, J. D. (1992). Ground-water models cannot be validated. *Advances in Water Resources*, *15*(1), 75–83. https://doi.org/10.1016/0309-1708(92)90033-X

Konrad, C. P. (2003). *Effects of Urban Development on Floods* (No. Fact Sheet 076-03). U.S. Geological Survey. Retrieved from https://pubs.usgs.gov/fs/fs07603/

Krebs, G., Kokkonen, T., Setälä, H., Koivusalo, H. (2016). Parameterization of a Hydrological Model for a Large, Ungauged Urban Catchment. *Water*, *8*(10), 443. https://doi.org/10.3390/w8100443

Krebs, G., Kokkonen, T., Valtanen, M., Setälä, H., Koivusalo, H. (2014). Spatial resolution considerations for urban hydrological modelling. *Journal of Hydrology*, *512*, 482–497. https://doi.org/10.1016/j.jhydrol.2014.03.013

Laflore, A. (2019, May 21). With another day of heavy rain, experts keep working to prevent flooding near Indian Creek. Retrieved January 27, 2020, from https://fox4kc.com/2019/05/21/with-another-day-of-heavy-rain-experts-keep-working-to-prevent-flooding-near-indian-creek/

Lammers, R. W., Dell, T. A., Bledsoe, B. P. (2019). Integrating Stormwater Management and Stream Restoration Strategies for Greater Water Quality Benefits. *Journal of Environmental Quality*, *0*(0). https://doi.org/10.2134/jeq2019.02.0084

Larsen, L. (2015). Urban climate and adaptation strategies. In *Frontiers in ecology and the environment.* (Vol. 13, pp. 486–492). https://doi.org/10.1890/150103

Lenexa, Kansas. Municipal Code Article 4-1-0 (2019). Retrieved from http://online.encodeplus.com/regs/lenexa-ks/doc-viewer.aspx?secid=2363#secid-2363

Liu, C., Allan, R. P. (2013). Observed and simulated precipitation responses in wet and dry regions 1850–2100. *Environmental Research Letters*, *8*(3), 034002. https://doi.org/10.1088/1748-9326/8/3/034002

Lorenz, A., Korte, T., Sundermann, A., Januschke, K., Haase, P. (2012). Macrophytes respond to reach-scale river restorations. *Journal of Applied Ecology*, *49*, 202–212. https://doi.org/10.2307/41433340

Mallakpour, I., Villarini, G. (2015). The changing nature of flooding across the central United States. *Nature Climate Change*, *5*(3), 250–254. https://doi.org/10.1038/nclimate2516

MARC. (n.d.). *What is Sediment Pollution?* Kansas City, Missouri. Retrieved from https://cfpub.epa.gov/npstbx/files/ksmo_sediment.pdf

MARC. (2010, November). Cities. Retrieved from https://www.marc.org/Data-Economy/Maps-and-GIS/GIS-Data/GIS-Datasets

MARC. (2020). Watersheds of the Kansas City Region: Blue River. Retrieved January 26, 2020, from http://www.marc2.org/Watershed/watershed.asp?ID=3

McDonough, K. (2015). *Understanding the relationship between urban best management practices and ecosystem services*. Kansas State University, Manhattan, Kansas. Retrieved from https://krex.k-state.edu/dspace/handle/2097/20508

McDonough, K. (2018). *A multiscale perspective of water resources and ecosystem services*. Kansas State University, Manhattan, Kansas.

McDonough, K., Hutchinson, S., Liang, J., Hefley, T., Hutchinson, S. (In review). Spatial configurations of land cover influence flood regulation ecosystem services. *Journal of Water Resources, Planning & Management*.

Mcdonough, K., Moore, T., Hutchinson, S. (2017). Understanding the relationship between stormwater control measures and ecosystem services in an urban watershed. *Journal of Water Resources Planning and Management*, *143*(5), 04017008–4017006. https://doi.org/10.1061/(ASCE)WR.1943-5452.0000751

Mendenhall, W., Sincich, T. (2012). *A Second Course in Statistics: Regression Analysis* (7th ed.). Boston, MA: Pearson Education Inc.

Millenum Ecosystem Assessment. (2005). *Ecosystems and Human Well-being: Synthesis*. Washington D.C.: Island Press. Retrieved from https://www.millenniumassessment.org/documents/document.356.aspx.pdf

Milly, P. C. D., Wetherald, R. T., Dunne, K. A., Delworth, T. L. (2002). Increasing risk of great floods in a changing climate. *Nature*, *415*(6871), 514–517. https://doi.org/10.1038/415514a

MJ Harden a GeoEye Company. (2012). LidarBreakline_PL. Retrieved from https://aims.jocogov.org/AIMSData/DataInfo.aspx#what.1

Mogollón, B., Villamagna, A. M., Frimpong, E. A., Angermeier, P. L. (2016). Mapping technological and biophysical capacities of watersheds to regulate floods. *Ecological Indicators*, *61*, 483–500. https://doi.org/10.1016/j.ecolind.2015.09.049

Moore, T., Gulliver, J., Stack, L., Simpson, M. (2016). Stormwater management and climate change: vulnerability and capacity for adaptation in urban and suburban contexts. *Climatic Change*, *138*(3–4), 491–504. https://doi.org/10.1007/s10584-016-1766-2

Moriasi, D. N., Arnold, J. G., Van Liew, M. W., Bingner, R. L., Harmel, R. D., T. L. Veith. (2007). Model Evaluation Guidelines for Systematic Quantification of Accuracy in

Watershed Simulations. *Transactions of the ASABE*, *50*(3), 885–900. https://doi.org/10.13031/2013.23153

Nash, J. E., Sutcliffe, J. V. (1970). River flow forecasting through conceptual models part I — A discussion of principles. *Journal of Hydrology*, *10*(3), 282–290. https://doi.org/10.1016/0022-1694(70)90255-6

National Research Council. (2002). *Riparian Areas: Functions and Strategies for Management*. Washington D.C.: The National Academies Press.

National Research Council. (2008). *Urban Stormwater Management in the United States*. Washington, D.C.: The National Academies Press. Retrieved from https://www.wef.org/globalassets/assets-wef/3---resources/topics/o-z/stormwater/stormwater-resources/nrc_stormwaterreport.pdf

Nemry, F., Demirel, H. (2012). Impacts of Climate Change on transport: a focus on road and rail transport infrastructures. *IDEAS Working Paper Series from RePEc*. Retrieved from http://search.proquest.com/docview/1698612494/?pq-origsite=primo

NOAA. (2019, March 21). 2019 National Hydrologic Assessment. Retrieved March 8, 2020, from https://www.nws.noaa.gov/oh/2019NHA.html

NOAA. (2020). Climate. Retrieved February 23, 2020, from https://www.noaa.gov/climate

Noori, N., Kalin, L., Sen, S., Srivastava, P., Lebleu, C. (2016). Identifying areas sensitive to land use/land cover change for downstream flooding in a coastal Alabama watershed. *Regional Environmental Change*, *16*(6), 1833–1846. https://doi.org/10.1007/s10113-016-0931-5

Nordman, E. E., Isely, E., Isely, P., Denning, R. (2018). Benefit-cost analysis of stormwater green infrastructure practices for Grand Rapids, Michigan, USA. *Journal of Cleaner Production*, *200*, 501–510. https://doi.org/10.1016/j.jclepro.2018.07.152

NRCS. (1996). *Ripairan Areas Environmental Uniqueness, Functions, and Values* (No. 11). United States Department of Agriculture Natural Resources Conservation Service. Retrieved from https://www.nrcs.usda.gov/wps/portal/nrcs/detail/national/technical/?cid=nrcs143_014199

O'Connor, H. (1971). Geology and Ground-Water Resources of Johnson County. Retrieved January 23, 2020, from http://www.kgs.ku.edu/General/Geology/Johnson/index.html

Olathe, Kansas. Municipal Code Chapter 17.06 Stream Corridor Requirements (2019). Retrieved from https://olathe.municipal.codes/Code/17.06

Olsson Associates. (2014). *Indian Creek Watershed Fluvial Geomorphology for City of Olathe*. Retrieved from https://www.olatheks.org/home/showdocument?id=2203

Open Data Network. (2017). Population Count Data for Kansas City Metro Area (MO-KS). Retrieved March 16, 2020, from https://www.opendatanetwork.com/entity/310M200US28140/Kansas_City_Metro_Area_MO_KS/demographics.population.count?year=2017

Overland Park, Kansas. Municipal Code Ordinance 18.365 Stream Corridor Requirements (2019). Retrieved from http://online.encodeplus.com/regs/overlandpark-ks/export2doc.aspx?pdf=1&tocid=018.

Patti Banks Associates. (2007). *Upper Blue River Watershed: A shared vision and commitment to water quality and watershed health.* Kansas City, MO: EPA Region 7.

Pavlowsky, R. T., Owen, M. R. (2013). *Indian Creek Fluvial Geomorphology Study*. Olathe, KS. Retrieved from https://oewri.missouristate.edu/assets/OEWRI/IndianCreek_OEWRI_11_26_2013_Final_1.pdf

Pekarsky, M. (2017, July 27). 'Embarrassed and thankful'- Owners of Coach's Bar recount 4+ hours trapped in flooded restaurant. Retrieved January 27, 2020, from https://fox4kc.com/2017/07/27/embarrassed-and-thankful-owners-of-coachs-bar-recount-4-hours-trapped-in-flooded-restaurant/

Pepitone, J. (2019, September 30). KCMO tears down buildings damaged by record flooding along Indian Creek. *Fox4KC*. Retrieved from https://fox4kc.com/2019/09/30/kcmo-tears-down-building-damaged-by-record-flooding-along-indian-creek/

Pestana, R., Matias, M., Canelas, R., Araujo, A., Roque, D., Van Zeller, E., … Heleno, S. (2013). Calibration of 2D hydraulic inundation models in the floodplain region of the Lower Tagus River. Presented at the ESA Living Planet Symposium, Edinburgh, United Kingdom. Retrieved from https://www.researchgate.net/publication/259781829_Calibration_of_2D_hydraulic_inundation_models_in_the_floodplain_region_of_the_Lower_Tagus_River

Peters, A. J., Studley, S. E. (2014). *Flood-Inundation Maps for Indian Creek and Tomahawk Creek, Johnson County, Kansas, 2014 (ver. 1.1, January 2016)* (U.S. Geological Survey Scientific Investigations Report 2014-5202). United States Geological Survey. Retrieved from http://dx.doi.org/10.3133/sir20145202.

Pinos, J., Timbe, L. (2019). Performance assessment of two-dimensional hydraulic models for generation of flood inundation maps in mountain river basins. *Water Science and Engineering*, *12*(1), 11–18. https://doi.org/10.1016/j.wse.2019.03.001

Pomeroy, C. A., Postel, N. A., O'Neill, P. A., Roesner, L. A. (2008). Development of Storm-Water Management Design Criteria to Maintain Geomorphic Stability in Kansas City Metropolitan Area Streams. *Journal of Irrigation and Drainage Engineering*, *134*(5), 562–566. https://doi.org/10.1061/(ASCE)0733-9437(2008)134:5(562)

Potter, T. (2015). Kansas Turnpike motorists helpless as flood swallowed car, driver. Retrieved March 12, 2020, from https://www.kansas.com/news/local/article27402568.html

Prairie Village, Kansas. Municipal Code Chapter XIV. Stormwater. Article 7. Stream Setback Requirements and Controls (2019).

Putnam, A. E., Broecker, W. S. (2017). Human-induced changes in the distribution of rainfall. *Science Advances*, *3*(5), e1600871. https://doi.org/10.1126/sciadv.1600871

Qin, H., Li, Z., Fu, G. (2013). The effects of low impact development on urban flooding under different rainfall characteristics. *Journal of Environmental Management*, *129*, 577–585. https://doi.org/10.1016/j.jenvman.2013.08.026

Quintero, F., Mantilla, R., Anderson, C., Claman, D., Krajewski, W. (2018). Assessment of Changes in Flood Frequency Due to the Effects of Climate Change: Implications for Engineering Design. *Hydrology; Basel*, *5*(1). http://dx.doi.org/10.3390/hydrology5010019

Rangari, V. A., Gonugunta, R., Umamahesh, N. V., Patel, A. K., Bhatt, C. M. (2018). 1D-2D modeling of urban floods and risk map generation for the part of Hyderabad city. *ISPRS* -

International Archives of the Photogrammetry, Remote Sensing and Spatial Information Sciences, *XLII–5*, 445–450. https://doi.org/10.5194/isprs-archives-XLII-5-445-2018

Reidmiller, D. R., Avery, C. W., Easterling, D. R., Kunkel, K. E., Lewis, K. L. M., Maycock, T. K., Stewart, B. C. (2018). *Fourth National Climate Assessment: Volume II Impacts, Risks, and Adaptation in the United States* (p. 1515). Washington, DC, USA: U.S. Global Change Research Program (USGRP). Retrieved from https://nca2018.globalchange.gov/downloads/NCA4_2018_FullReport.pdf

Ritter, S. (2020, February 13). The most congested highway in Johnson County could get $300M expansion — with tolls. Retrieved March 7, 2020, from https://www.kansascity.com/news/local/article240272946.html

Rosgen, D. (1996). *Applied River Morphology*. Pagosa Springs: Wildland Hydrology.

Roshni, J., Wade, R., Jefferies, C. (2015). Smart SUDS: recognising the multiple-benefit potential of sustainable surface water management systems. *Water Science and Technology*, *71*(2), 242–251. https://doi.org/10.2166/wst.2014.484

Roy, A., Wenger, S., Fletcher, T., Walsch, C., Ladson, A., Shuster, W., … Brown RR. (2008). Impediments and solutions to sustainable, watershed-scale urban stormwater management: lessons from Australia and the United States. *Environmental Management*, *42*(2), 344–59. https://doi.org/10.1007/s00267-008-9119-1

Sanja, P., Martin, D., Pavlovic, S., Roy, I., St. Laurent, M., Trypaluk, C., … Bonnin, G. (2013). *NOAA Atlas 14 Volume 8 Version 2, Precipitation-Frequency Atlas of the United States, Midwestern States*. Silver Spring, MD: NOAA, National Weather Service.

Shamsi, U. M. (Sam), Koran, J. (2017). Continuous Calibration. *Journal of Water Management Modeling*. https://doi.org/10.14796/JWMM.C414

Smith, A. B. (2020, January 8). 2010-2019: A landmark decade of U.S. billion-dollar weather and climate disasters | NOAA Climate.gov. Retrieved February 23, 2020, from https://www.climate.gov/news-features/blogs/beyond-data/2010-2019-landmark-decade-us-billion-dollar-weather-and-climate

Soil Survey Staff. (2019). *Web Soil Survey*. Natural Resources Conservation Service, United States Department of Agriculture. Retrieved from https://websoilsurvey.sc.egov.usda.gov/App/WebSoilSurvey.aspx

Stanton, T. (2019, February). *Measuring Actual Stream Erosion in the Indian Creek Watershed: LiDAR-Based Fluvial Geomorphic Evaluation*. Powerpoint Slides. Retrieved from http://www.marc2.org/Assets/Environment/WQEC/2019/1-C_Measuring-Actual-Stream-Erosion-in-Indian-Creek-Watershed-opt.pdf

Stratus Consulting. (2009). *A Triple Bottom Line Assessment of Traditional and Green Infrastructure Options for Controlling CSO Events in Philadelphia's Watersheds*. Retrieved from https://www.epa.gov/sites/production/files/2015-10/documents/gi_philadelphia_bottomline.pdf

Tindle, J. (2018, November 28). Blue River Watershed Riparian Buffer.

Transportation Research Board. (2008). *Potential Impacts of Climate Change on U.S. Transportation* (No. Transportation Research Board Special Report 290). Washington D.C.: National Research Council of the National Academies. Retrieved from http://onlinepubs.trb.org/onlinepubs/sr/sr290.pdf

Trenberth, K. E. (2011). Changes in precipitation with climate change. *Climate Research*, *47*(1–2), 123–138. https://doi.org/10.3354/cr00953

UN. (2019). *World Urbanization Prospects 2018: Highlights*. New York: United Nations Department of Economic and Social Affairs. Retrieved from https://population.un.org/wup/Publications/Files/WUP2018-Highlights.pdf

U.S. Department of Commerce. (2015, Juy). TIGER 2015 Roads. Retrieved from https://gdg.sc.egov.usda.gov/Catalog/ProductDescription/TGRROAD.html

U.S. Energy Information Administration. (2017). *May 2017 Monthly Energy Review* (p. 243). U.S. Department of Energy. Retrieved from https://www.eia.gov/totalenergy/data/monthly/archive/00351705.pdf

U.S. EPA. (2000). *Low Impact Development (LID) - A Literature Review*. Washington, DC, USA: US EPA Office of Water.

U.S. EPA. (2002). Aquatic Buffer Model Ordinance [Collections and Lists]. Retrieved March 10, 2020, from https://www.epa.gov/sites/production/files/2015-12/documents/2002_09_19_nps_ordinanceuments_buffer_model_ordinance1.pdf

U.S. EPA. (2009). *Funding Stormwater Programs* (No. EPA 901-F-09-004). Retrieved from https://www3.epa.gov/region1/npdes/stormwater/assets/pdfs/FundingStormwater.pdf

U.S. EPA. (2012). *Benefits of Low Impact Development: How LID Can Protect Your Community's Resources* (p. 2). Washington, DC, USA: Office of Wetlands, Oceans, and Watersheds.

U.S. EPA. (2013). Level III and IV Ecoregions of the Counterminous United Stated. Corvallis, Oregon: U.S. EPA National Health and Environmental Effects Research Library. Retrieved from https://www.epa.gov/eco-research/level-iii-and-iv-ecoregions-continental-united-states.

U.S. EPA, O. (2015, October 1). Manage Flood Risk [Overviews and Factsheets]. Retrieved March 12, 2020, from https://www.epa.gov/green-infrastructure/manage-flood-risk

U.S. Forest Service. (2017). *Appendix F: Ecosystem Services Provided by Floodplains*. United States Department of Agriculture. Retrieved from https://www.fs.usda.gov/nfs/11558/www/nepa/98306_FSPLT3_4130975.pdf

Vano, J. A., Dettinger, M. D., Cifelli, R., Curtis, D., Dufour, A., Miller, K., … Wilson, A. M. (2019). Hydroclimatic Extremes as Challenges for the Water Management Community: Lessons from Oroville Dam and Hurricane Harvey. In *Explaining Extremes of 2017 from a Climate Perspective*. Bull. Amer. Metero. Soc.

Velasco, E., Roth, M. (2010). Cities as Net Sources of CO2: Review of Atmospheric CO2 Exchange in Urban Environments Measured by Eddy Covariance Technique. *Geography Compass*, : 1238–1259. https://doi.org/DOI: 10.1111/j.1749-8198.2010.00384.x

Waters, D., Watt, E. W., Marsalek, J., Anderson, B. (2010). Adaptation of a Storm Drainage System to Accomodate Increased Rainfall Resulting from Climate Change. *Journal of Environmental Planning and Management*, *46*(5), 755–770. https://doi.org/: http://dx.doi.org/10.1080/0964056032000138472

Watson, K. B., Ricketts, T., Galford, G., Polasky, S., O'Niel-Dunne, J. (2016). Quantifying flood mitigation services: The economic value of Otter Creek wetlands and floodplains to Middlebury, VT. *Ecological Economics*, *130*, 16–24. https://doi.org/10.1016/j.ecolecon.2016.05.015

Worthen, L. L. (2019, May). *A Diagnostic Analysis of SWMM to Simulate Hydrologic Behavior within LID Systems*. Syracuse University. Retrieved from https://surface.syr.edu/thesis/321

Yang, Q., Dai, Q., Han, D., Zhu, X., Zhang, S. (2018). Impact of the Storm Sewer Network Complexity on Flood Simulations According to the Stroke Scaling Method. *Water*, *10*(5), 645. https://doi.org/10.3390/w10050645

Zahmatkesh, Z., Burian, Steven J., Karamouz, Mohammad, Tavakol-Davani, Hassan, Goharian, Erfan. (2015). Low-Impact Development Practices to Mitigate Climate Change Effects on Urban Stormwater Runoff: Case Study of New York City. *Journal of Irrigation and Drainage Engineering*, *141*(1), 04014043. https://doi.org/10.1061/(ASCE)IR.1943-4774.0000770

Zeckoski, R. W., Smolen, M. D., Moriasi, D. N., Frankenberger, J. R., Feyereisen. (2015). Hydrologic and Water Quality Terminology as Applied to Modeling. *Transactions of the ASABE*, *58*(6), 1619–1635. https://doi.org/10.13031/trans.58.10713

Appendix A - Appendix A -Flood Frequency Analysis for Tomahawk Creek USGS Gage J06893350

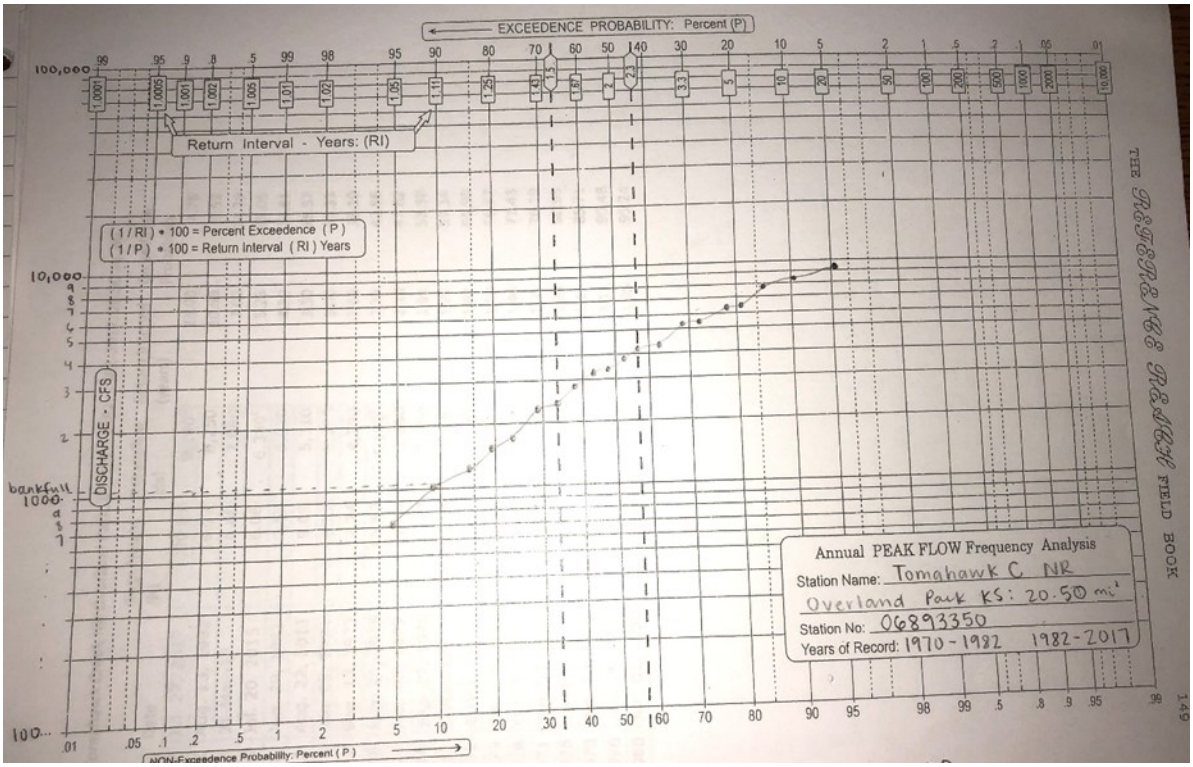

Figure A.1. Flood frequency analysis of USGS Gage 06893350 at Tomahawk Creek. Bankfull flow occurs every 1.1 years in urban streams and was determined to be 1,100 cfs (31.15 cms).

Appendix B - R Code Used for Statistical Analysis

```
#####Install & load the packages that you need to run this script

install.packages("multcompView")

library(multcompView)
#For more info, see package: https://cran.r-
project.org/web/packages/multcompView/multcompView.pdf

#####Set your working directory
setwd("C:/Users/tori21/Desktop/Stats") #Change your working directory to whatever directory
you are in

getwd() #Check to see that your working directory was changed correctly

#####Load your file into R Studio
file <-"Volume_J06893500.csv" #Change name of file you are loading
data<-read.table(file, header=TRUE, sep = ",", dec = ".") #Load your file into R Studio
data1 <- data.frame(data) #Convert your file to a dataframe
View(data1) #View your file - it should look like it does in the CSV!

#####Run ANOVA & a Tukey test on your dataset
#Here, we will start with 'Scenario' as the x-value and 'Peak Inflow' as the y-value

model1 <- lm(data1$Volume ~ data1$Scenario + data1$Precip) #Create a linear regression
model for your dataset
summary(model1) #See the results of your linear regression model. Remember p<0.05 is
significant!
anova(model1) #Run an ANOVA on your linear regression model.

aov1 <- aov(data1$Volume ~ data1$Scenario + data1$Precip) #Fit the analysis of variance
model
Tukey1 <- TukeyHSD(aov1, conf.level = 0.95) #Run the Tukey method; adjust confidence level
as necessary

Tukey1[["data1$Scenario"]] #View your results. The far left column shows the two scenarios
that have been compared. The adjusted p-value indicates whether the difference is significant.
Tukey1[["data1$Precip"]] #View your results. The far left column shows the two scenarios that
have been compared. The adjusted p-value indicates whether the difference is significant.

plot(aov1) #You can plot the results of your AOV. Use the arrows in the plot window to cycle
through the graphs - there are 4 in total.
plot(Tukey1, las=1) #You can plot the results of your Tukey test. Use the arrows to cycle
through the plots - there are two in total.
```

```
#Create a boxplot of your results >> Let's start w/ Scenario as the factor
generate_label_df <- function(Tukey1, variable){
  Tukey.levels <- Tukey1[[variable]][,4]
  Tukey.labels <- data.frame(multcompLetters(Tukey.levels)['Letters'])
  Tukey.labels$treatment=rownames(Tukey.labels)
  Tukey.labels=Tukey.labels[order(Tukey.labels$treatment) , ]
  return(Tukey.labels)
}

LABELS <- generate_label_df(Tukey1 , "data1$Scenario")

my_colors <- c(
  rgb(143,199,74,maxColorValue = 255),
  rgb(242,104,34,maxColorValue = 255),
  rgb(111,145,202,maxColorValue = 255)
)

a1 <- boxplot(data1$Volume ~ data1$Scenario , ylim=c(min(data1$Volume) ,
1.1*max(data1$Volume)) , col=my_colors[as.numeric(LABELS[,1])] , ylab="Volume" ,
main="")
over <- 0.1*max( a1$stats[nrow(a1$stats),] )
text( c(1:nlevels(data1$Scenario)) , a1$stats[nrow(a1$stats),]+over , LABELS[,1]  ,
col=my_colors[as.numeric(LABELS[,1])] )

#Create a boxplot of your results >> Now use Precip as the factor
generate_label_df <- function(Tukey1, variable){
  Tukey.levels <- Tukey1[[variable]][,4]
  Tukey.labels <- data.frame(multcompLetters(Tukey.levels)['Letters'])
  Tukey.labels$treatment=rownames(Tukey.labels)
  Tukey.labels=Tukey.labels[order(Tukey.labels$treatment) , ]
  return(Tukey.labels)
}

LABELS <- generate_label_df(Tukey1 , "data1$Precip")

my_colors <- c(
  rgb(143,199,74,maxColorValue = 255),
  rgb(242,104,34,maxColorValue = 255),
  rgb(111,145,202,maxColorValue = 255)
)

a2 <- boxplot(data1$Volume ~ data1$Precip , ylim=c(min(data1$Volume) ,
1.1*max(data1$Volume)) , col=my_colors[as.numeric(LABELS[,1])] , ylab="Volume" ,
main="")
over <- 0.1*max( a2$stats[nrow(a2$stats),] )
```

```
text( c(1:nlevels(data1$Precip)) , a2$stats[nrow(a2$stats),]+over , LABELS[,1]  ,
col=my_colors[as.numeric(LABELS[,1])] )
```

Appendix C - All Tomahawk 1D Hydrographs & Results Tables

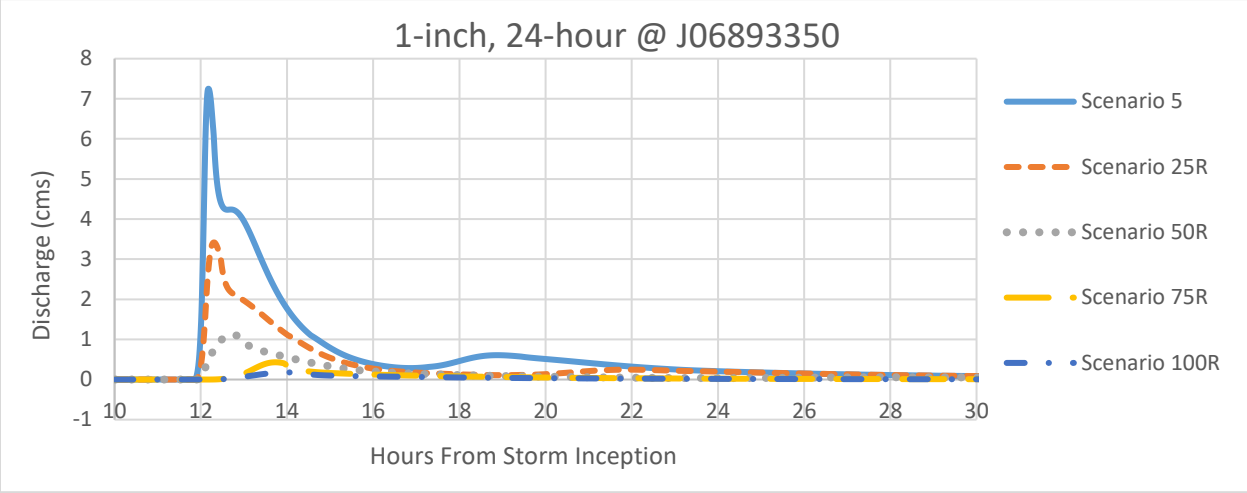

Figure C.1. Hydrograph displaying changes between baseline conditions (scenario 5) and varying levels of GI implementation for the 1-inch, 24-hour storm at J06893359.

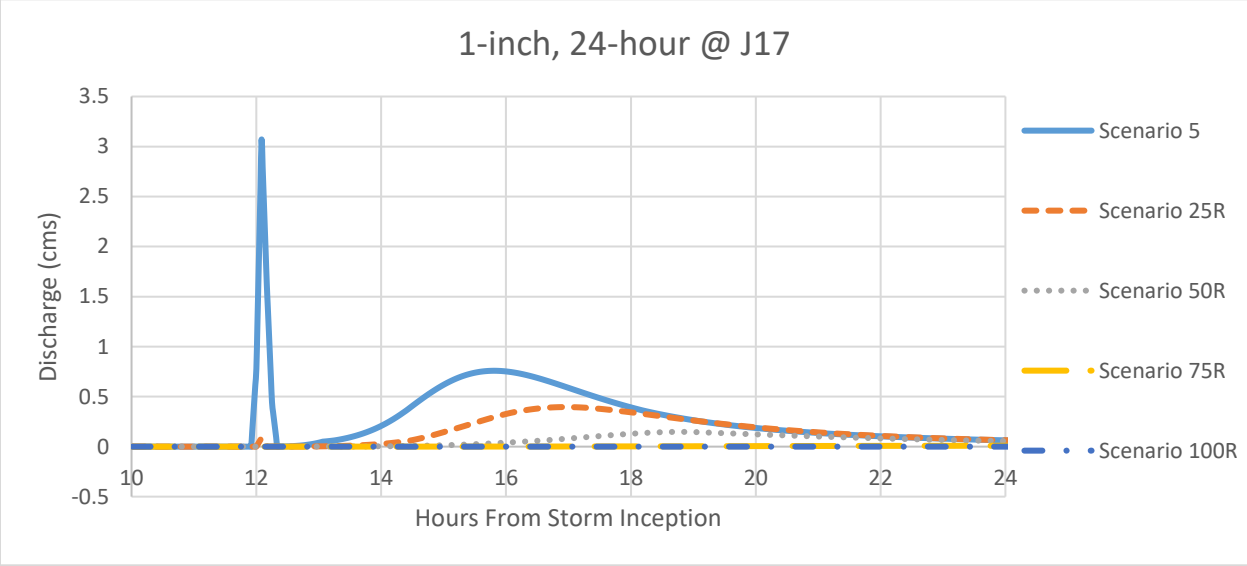

Figure C.2. Hydrograph displaying changes between baseline conditions (scenario 5) and varying levels of GI implementation for the 1-inch, 24-hour storm at J17.

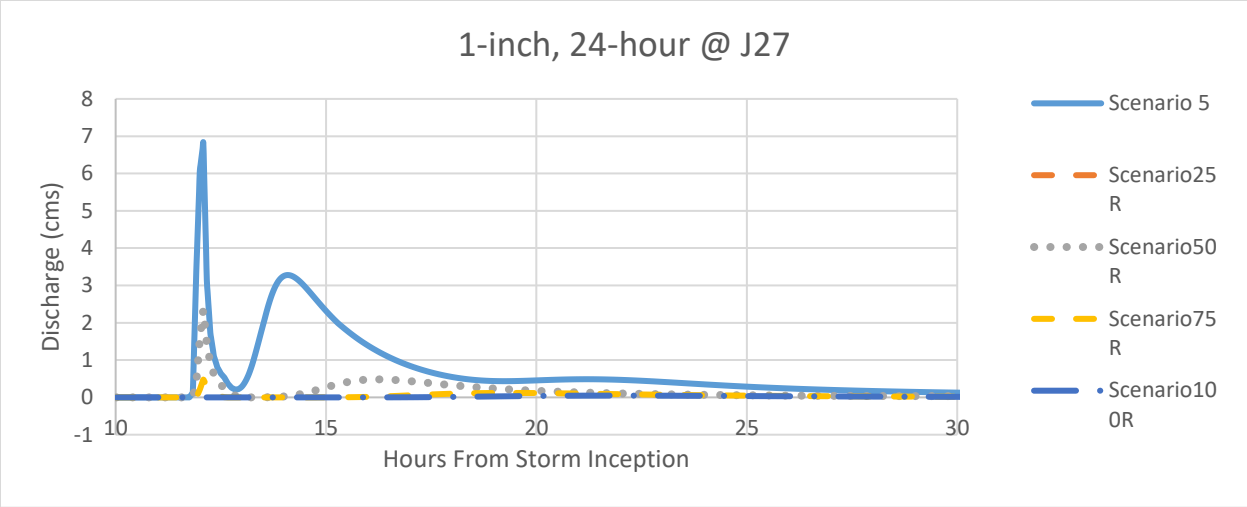

Figure C.3. Hydrograph displaying changes between baseline conditions (scenario 5) and varying levels of GI implementation for the 1-inch, 24-hour storm at J27.

Table C.1. Percent reduction in peak inflow and total volume of inflow from current conditions for the 1-inch, 24-hour precipitation event. Shading indicates statistically significant results.

1-inch, 24-hour						
	Peak Inflow (cms)			Total Volume (m^3)		
Scenario	J17	J06893350	J27	J17	J06893350	J27
0	-22.21	-11.08	-6.27	-11.32	-9.75	-9.85
5	0.00	0.00	0.00	0.00	0.00	0.00
25	71.59	39.37	25.09	37.09	34.80	35.17
50	92.79	77.58	56.76	67.96	67.87	69.27
75	97.97	91.07	87.56	92.36	89.31	91.13
100	100.00	95.62	98.78	100.00	94.13	96.39
0R	41.77	21.22	4.75	30.78	25.77	25.03
5R	57.51	29.22	11.07	37.81	32.65	32.06
25R	90.31	58.90	36.10	59.29	56.42	56.60
50R	96.39	86.52	66.45	78.81	79.76	81.23
75R	99.78	94.83	93.14	96.01	92.74	94.66
100R	100.00	97.86	99.32	100.00	95.63	97.70

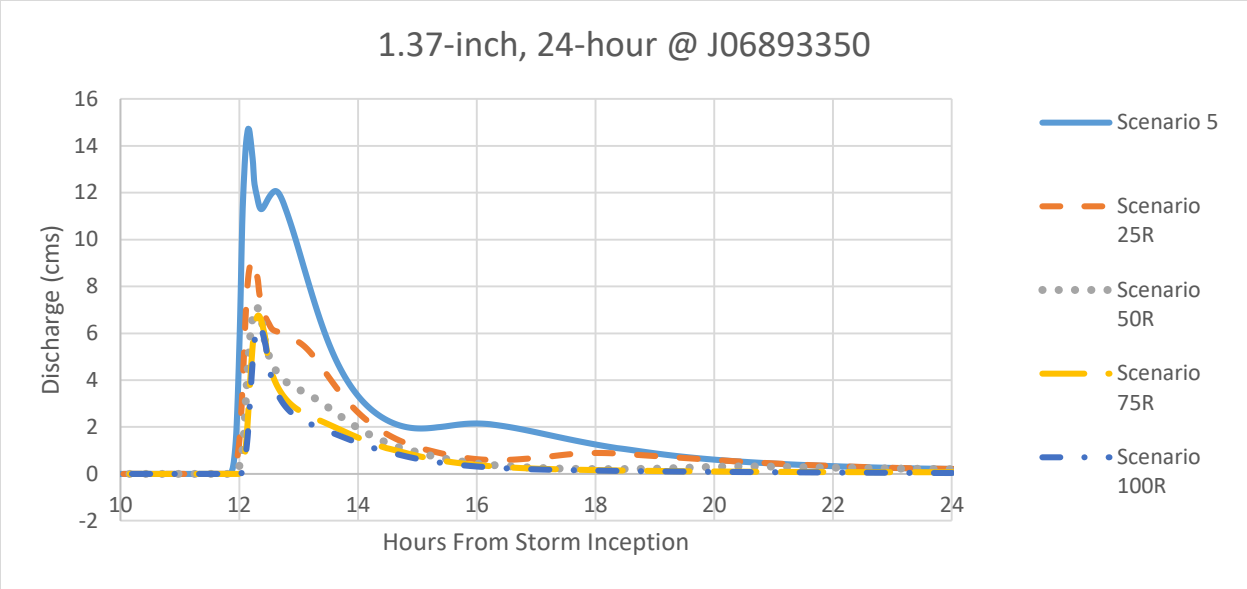

Figure C.4. Hydrograph displaying changes between baseline conditions (scenario 5) and varying levels of GI implementation for the 1.37-inch, 24-hour storm at J06893350.

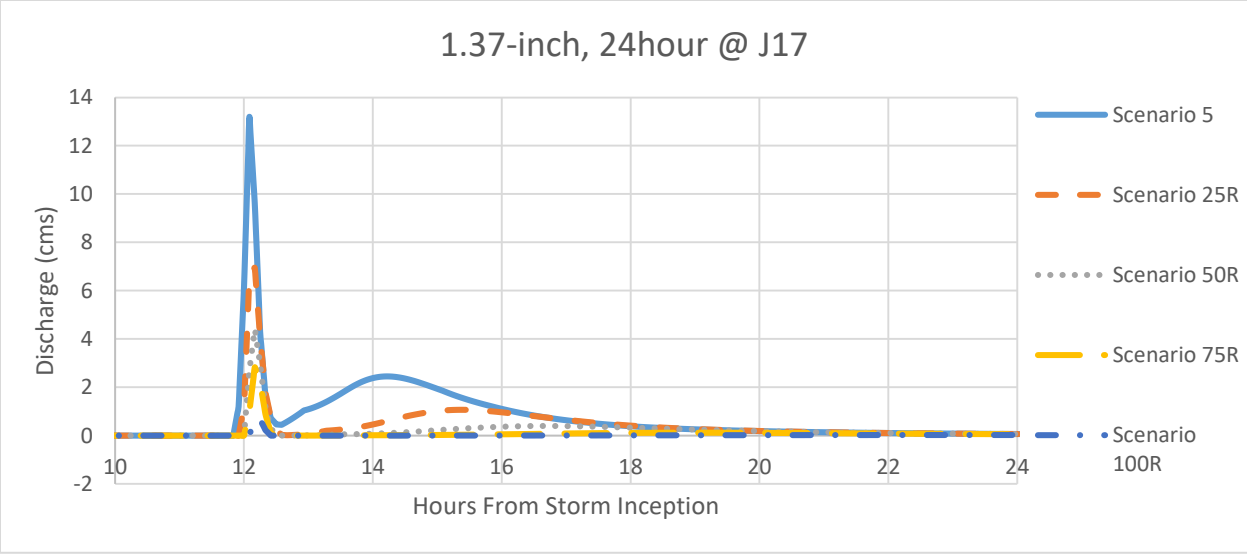

Figure C.5. Hydrograph displaying changes between baseline conditions (scenario 5) and varying levels of GI implementation for the 1.37-inch, 24-hour storm at J17.

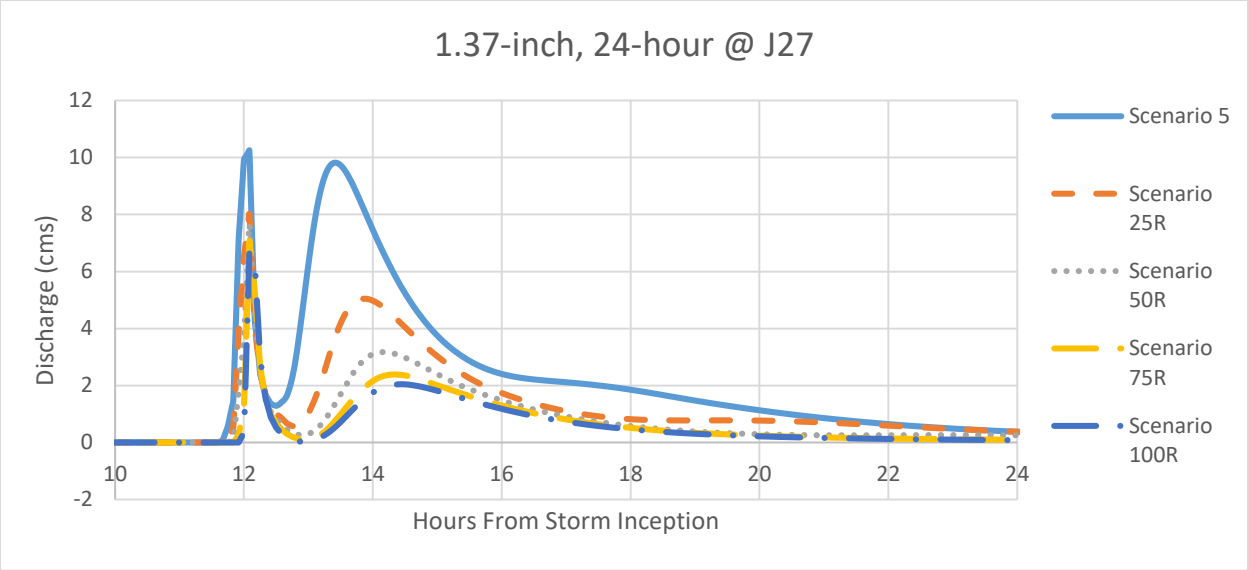

Figure C.6. Hydrograph displaying changes between baseline conditions (scenario 5) and varying levels of GI implementation for the 1.37-inch, 24-hour storm at J27.

Table C.2. Percent reduction in peak inflow and total volume of inflow from current conditions for the 1.37-inch, 24-hour precipitation event. Shading indicates statistically significant results.

	1.37-inch, 24-hour					
	Peak Inflow (cms)			Total Volume (m^3)		
Scenario	J17	J06893350	J27	J17	J06893350	J27
0	-6.44	-9.36	-10.87	-8.60	-7.72	-7.97
5	0.00	0.00	0.00	0.00	0.00	0.00
25	25.07	27.85	29.48	31.58	27.40	27.93
50	51.25	44.57	27.66	61.13	50.42	50.76
75	62.17	48.44	28.52	77.57	62.45	62.75
100	89.20	52.82	30.13	93.36	73.19	72.87
0R	23.61	18.49	16.43	22.92	19.68	18.87
5R	30.12	25.39	21.23	29.78	26.03	25.48
25R	51.93	45.46	35.46	53.77	47.66	47.64
50R	69.55	57.28	38.27	74.48	64.51	64.44
75R	80.46	59.47	43.33	86.60	73.51	73.48
100R	94.95	61.93	46.57	95.34	78.52	77.85

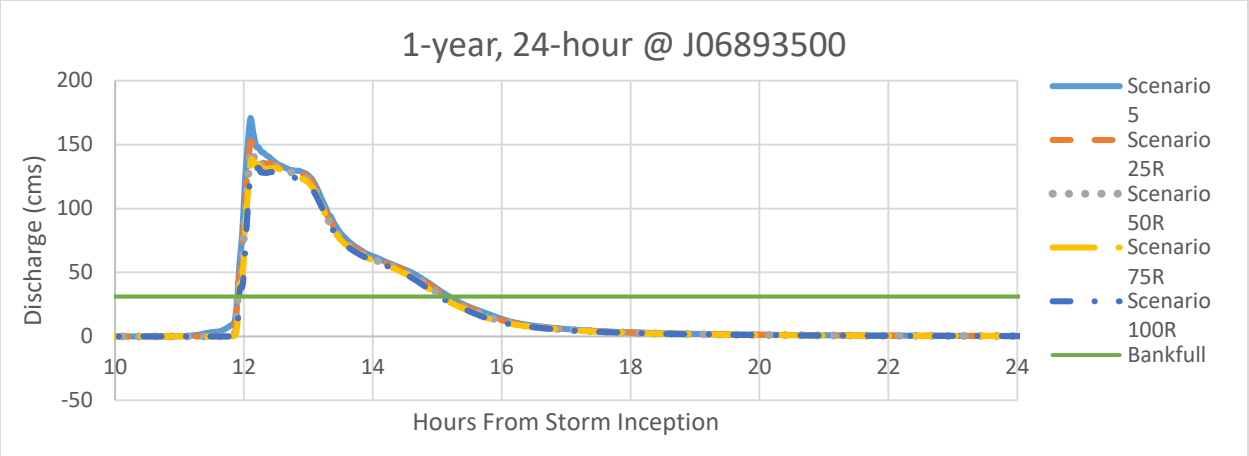

Figure C.7. Hydrograph displaying changes between baseline conditions (scenario 5) and varying levels of GI implementation for the 1-year, 24-hour storm at J06893350.

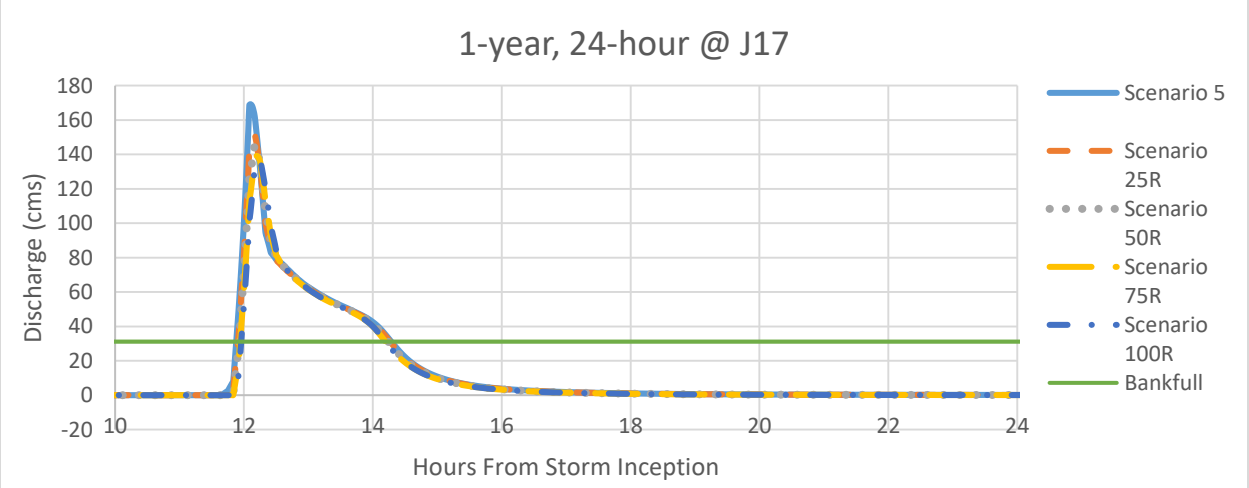

Figure C.8. Hydrograph displaying changes between baseline conditions (scenario 5) and varying levels of GI implementation for the 1-year, 24-hour storm at J17.

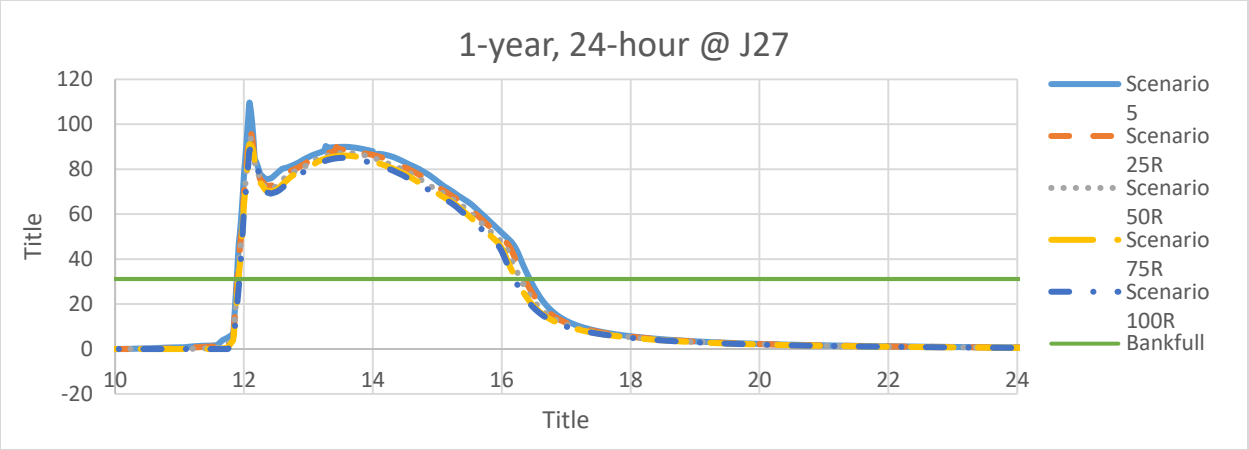

Figure C.9. Hydrograph displaying changes between baseline conditions (scenario 5) and varying levels of GI implementation for the 1-year, 24-hour storm at J27.

Table C.3. Percent reduction in peak inflow and total volume of inflow from current conditions for the 1-year, 24-hour precipitation event. Shading indicates statistically significant results.

1-year, 24-hour						
	Peak Inflow (cms)			Total Volume (m^3)		
Scenario	J17	J06893350	J27	J17	J06893350	J27
0	-1.54	-1.09	-1.22	-0.26	-0.72	-0.70
5	0.00	0.00	0.00	0.00	0.00	0.00
25	5.69	3.26	6.20	2.26	2.73	2.67
50	9.27	8.01	11.26	5.01	5.85	5.82
75	12.86	13.39	15.20	7.60	8.82	8.56
100	16.10	17.51	17.65	8.64	10.59	10.11
0R	11.32	9.04	9.25	5.52	5.37	4.77
5R	11.89	10.13	10.03	5.65	6.01	5.26
25R	13.94	12.87	14.59	7.43	8.18	7.51
50R	17.24	16.48	17.59	9.36	10.59	10.04
75R	20.88	20.82	20.57	12.18	13.39	12.77
100R	21.96	24.60	22.56	13.00	15.08	14.18

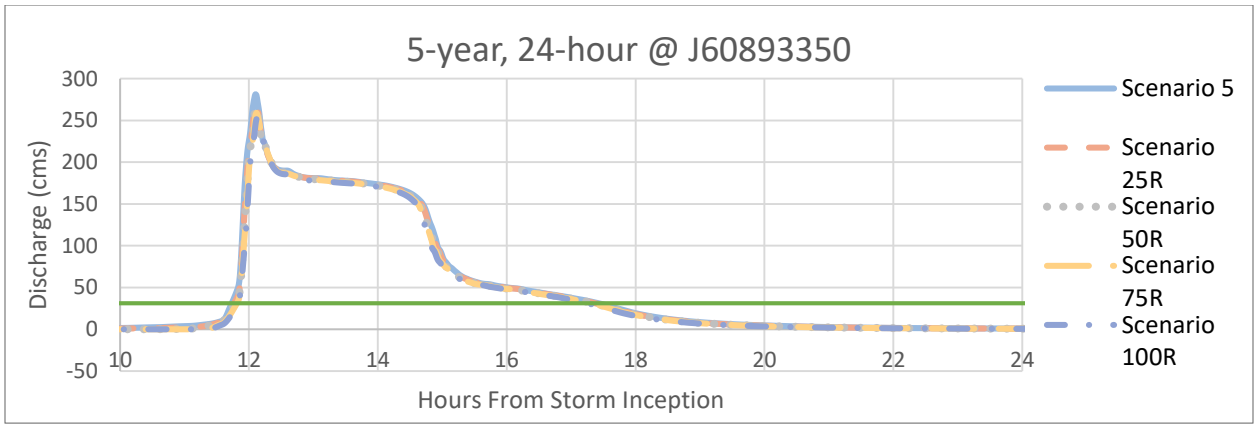

Figure C.10. Hydrograph displaying changes between baseline conditions (scenario 5) and varying levels of GI implementation for the 5-year, 24-hour storm at J06893350.

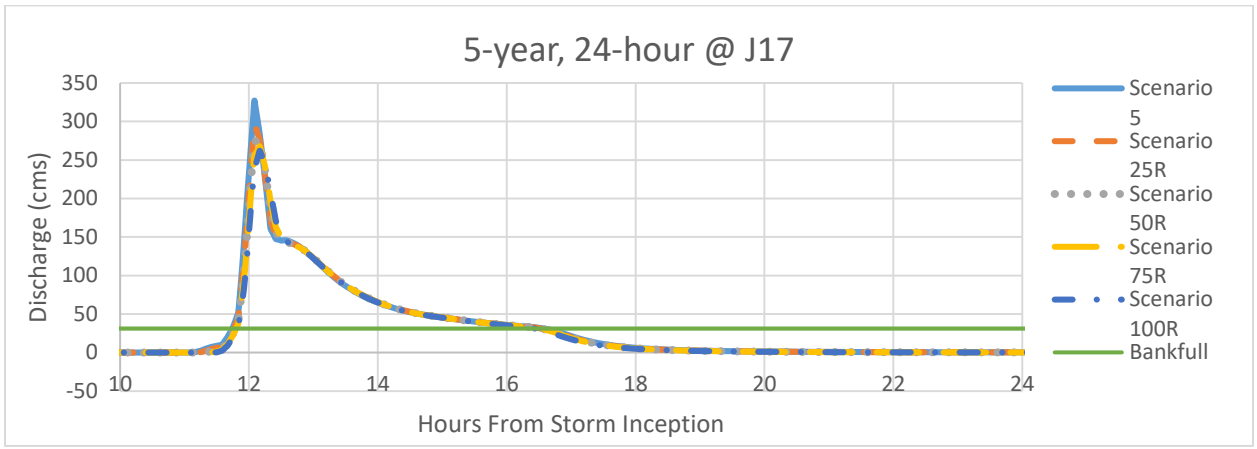

Figure C.11. Hydrograph displaying changes between baseline conditions (scenario 5) and varying levels of GI implementation for the 5-year, 24-hour storm at J06893350.

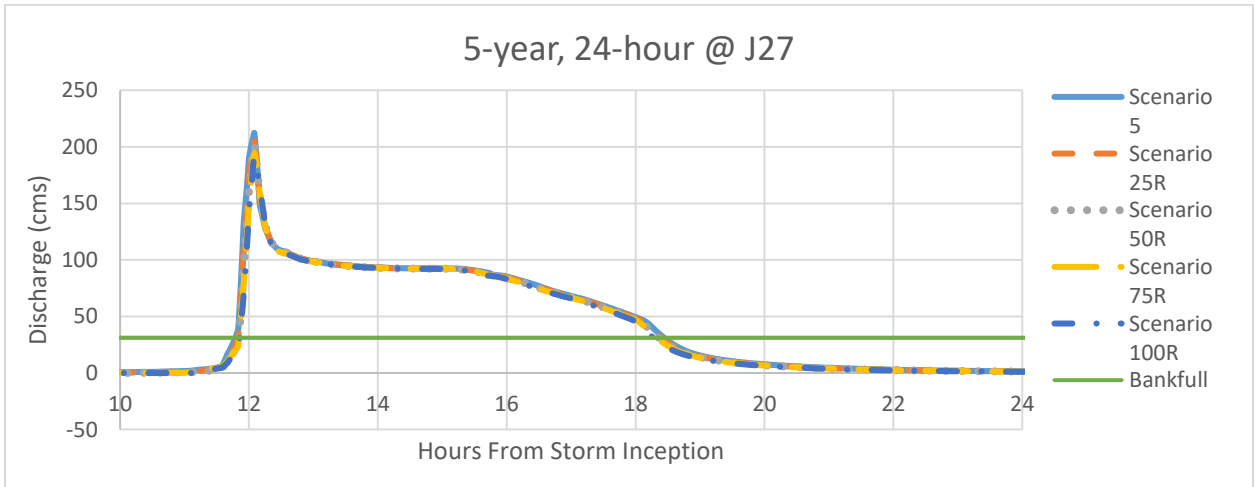

Figure C.12. Hydrograph displaying changes between baseline conditions (scenario 5) and varying levels of GI implementation for the 5-year, 24-hour storm at J27.

Table C.4. Percent reduction in peak inflow and total volume of inflow from current conditions for the 5-year, 24-hour precipitation event. Shading indicates statistically significant results.

5-year, 24-hour						
	Peak Inflow (cms)			Total Volume (m^3)		
Scenario	J17	J06893350	J27	J17	J06893350	J27
0	-1.51	-0.39	-0.33	-0.12	-0.33	-0.35
5	0.00	0.00	0.00	0.00	0.00	0.00
25	5.98	1.55	1.40	1.21	1.68	1.78
50	13.07	3.81	3.50	2.67	3.74	3.81
75	15.43	6.03	6.68	4.06	5.68	5.20
100	17.78	8.50	8.50	5.70	7.44	6.41
0R	3.80	3.35	2.33	3.15	3.33	1.95
5R	5.16	3.74	2.61	3.15	3.59	2.17
25R	10.60	5.01	3.97	4.18	4.98	3.55
50R	17.09	6.77	6.21	5.45	6.70	5.16
75R	19.08	8.64	9.10	6.61	8.39	6.28
100R	20.86	11.32	10.83	8.06	9.93	7.37

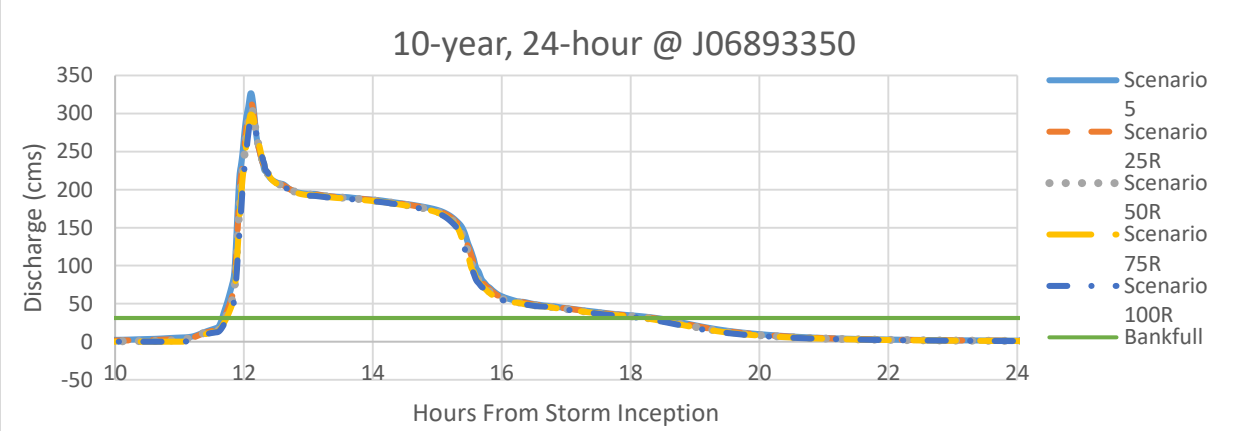

Figure C.13. Hydrograph displaying changes between baseline conditions (scenario 5) and varying levels of GI implementation for the 10-year, 24-hour storm at J06893350.

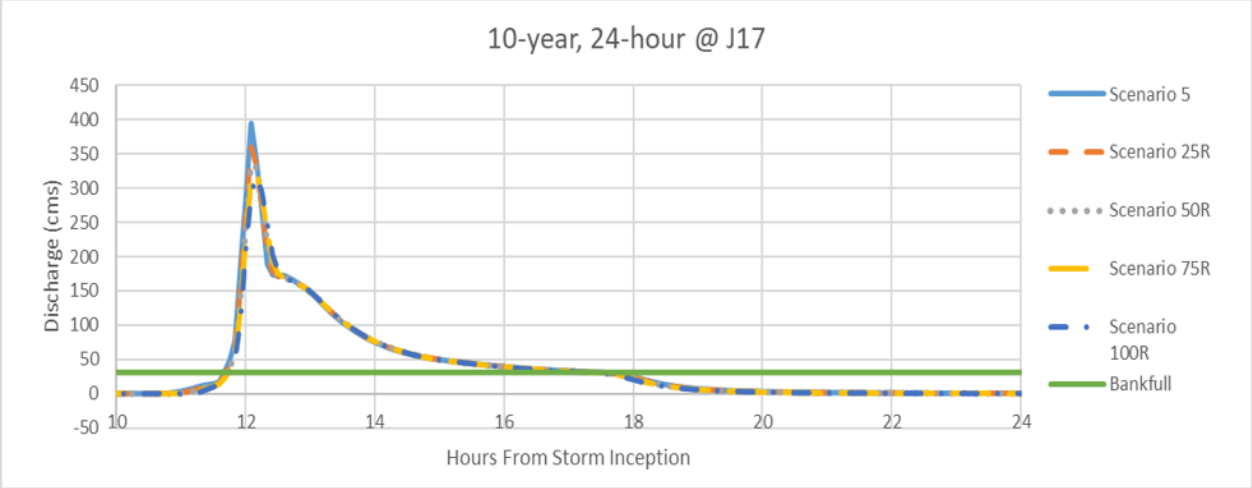

Figure C.14. Hydrograph displaying changes between baseline conditions (scenario 5) and varying levels of GI implementation for the 10-year, 24-hour storm at J17.

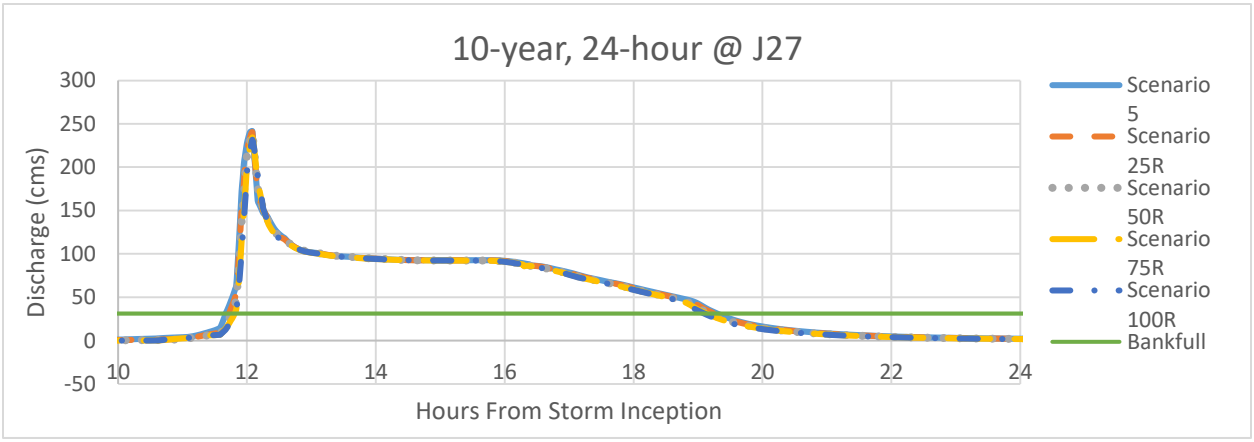

Figure C.15. Hydrograph displaying changes between baseline conditions (scenario 5) and varying levels of GI implementation for the 10-year, 24-hour storm at J27.

Table C.5. Percent reduction in peak inflow and total volume of inflow from current conditions for the 10-year, 24-hour precipitation event. Shading indicates statistically significant results.

10-year, 24-hour						
	Peak Inflow (cms)			Total Volume (m^3)		
Scenario	J17	J06893350	J27	J17	J06893350	J27
0	-1.58	-0.46	-0.04	-0.34	-0.50	-0.56
5	0.00	0.00	0.00	0.00	0.00	0.00
25	5.80	1.67	0.25	1.16	1.78	2.04
50	12.74	3.98	0.50	2.70	3.74	4.00
75	15.20	6.90	1.28	3.95	5.55	5.90
100	17.14	9.58	2.52	4.97	6.63	6.60
0R	3.02	2.86	0.37	2.46	2.60	1.85
5R	4.40	3.25	0.45	2.75	3.04	2.26
25R	9.80	4.90	0.70	3.66	4.52	3.86
50R	16.21	7.02	1.16	5.06	6.25	5.41
75R	18.54	9.27	3.14	6.17	7.82	6.97
100R	20.10	10.73	4.26	7.09	8.81	7.56

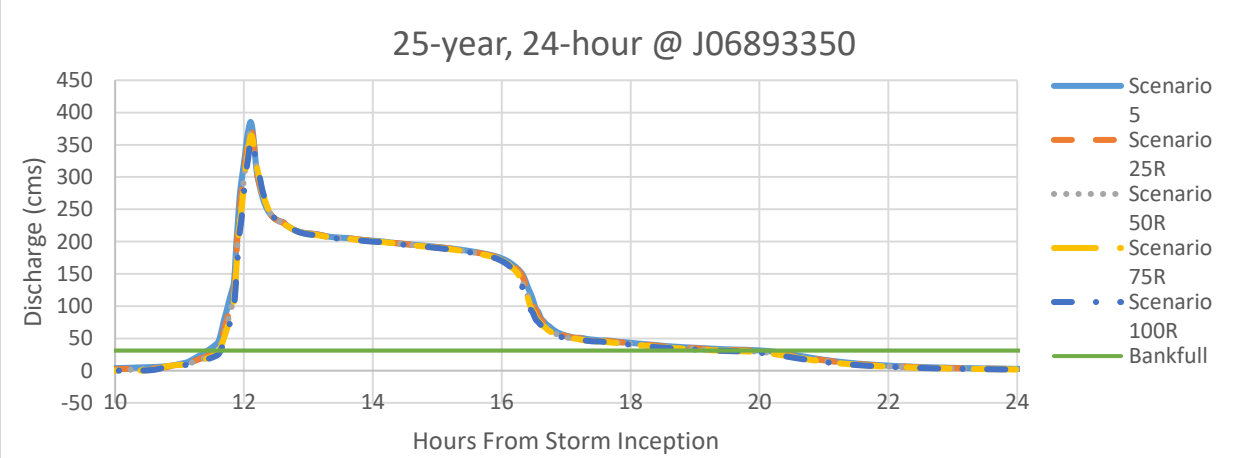

Figure C.16. Hydrograph displaying changes between baseline conditions (scenario 5) and varying levels of GI implementation for the 25-year, 24-hour storm at J06893350.

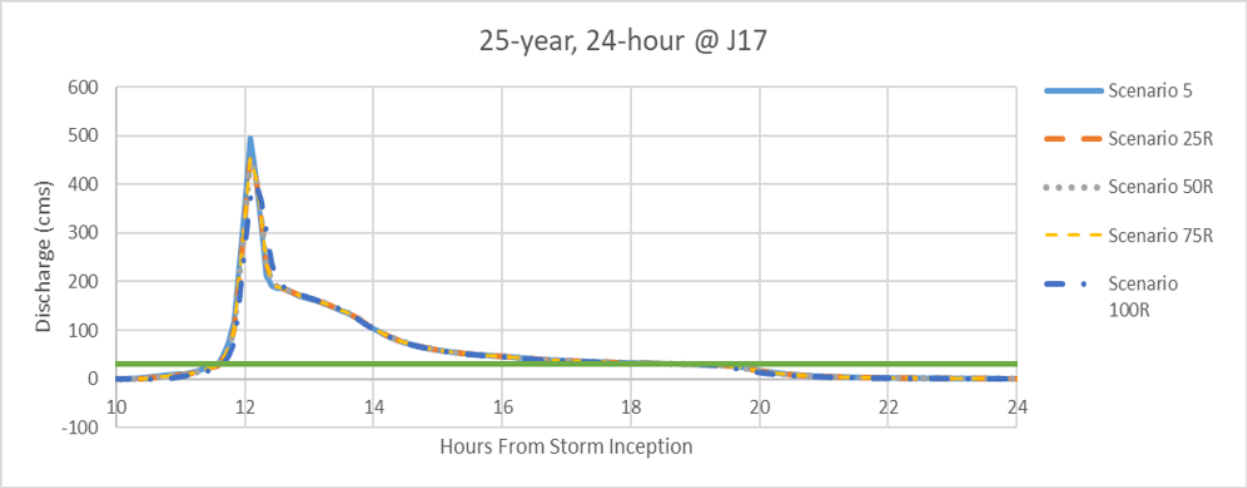

Figure C.17. Hydrograph displaying changes between baseline conditions (scenario 5) and varying levels of GI implementation for the 25-year, 24-hour storm at J17.

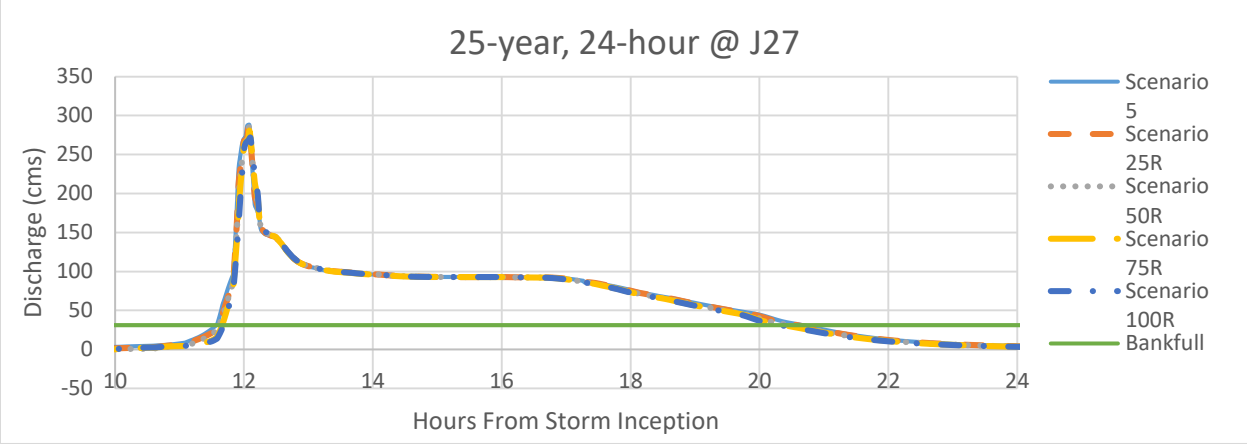

Figure C.18. Hydrograph displaying changes between baseline conditions (scenario 5) and varying levels of GI implementation for the 25-year, 24-hour storm at J27.

Table C.6. Percent reduction in peak inflow and total volume of inflow from current conditions for the 25-year, 24-hour precipitation event. Shading indicates statistically significant results.

25-year, 24-hour						
	Peak Inflow (cms)			Total Volume (m^3)		
Scenario	J17	J06893350	J27	J17	J06893350	J27
0	-1.57	-0.31	-0.03	-0.40	-0.54	-0.61
5	0.00	0.00	0.00	0.00	0.00	0.00
25	5.81	1.29	0.17	1.18	1.74	2.02
50	12.58	3.10	0.38	2.80	3.64	4.03
75	15.15	4.92	0.76	3.71	4.97	5.68
100	16.92	6.73	2.18	4.60	6.04	6.45
0R	2.15	1.47	0.28	1.95	2.07	1.83
5R	3.60	1.76	0.31	2.28	2.56	2.29
25R	8.88	2.85	0.52	3.24	4.06	3.85
50R	15.17	4.37	0.94	4.71	5.73	5.41
75R	17.85	5.85	2.64	5.55	6.91	6.75
100R	19.23	7.32	5.79	6.36	7.87	7.37

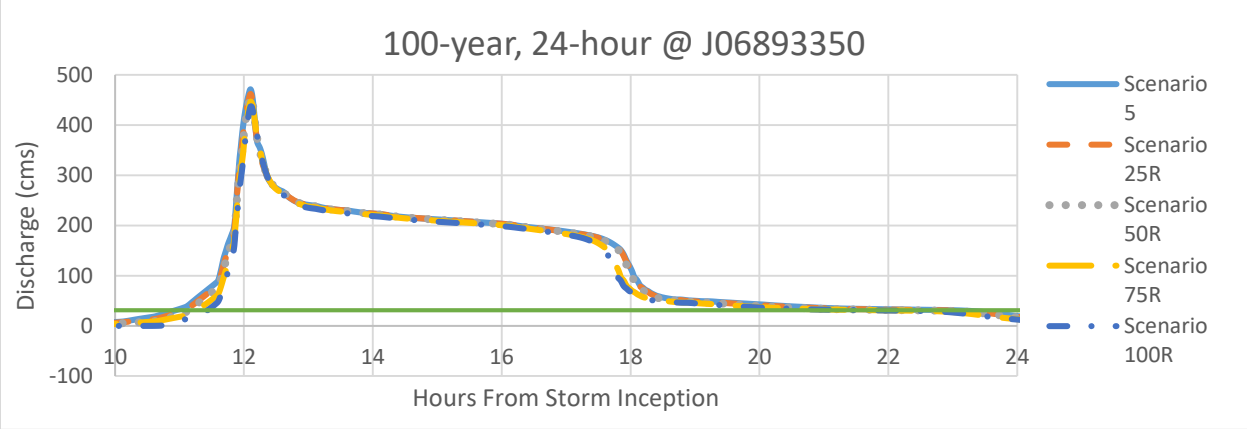

Figure C.19. Hydrograph displaying changes between baseline conditions (scenario 5) and varying levels of GI implementation for the 100-year, 24-hour storm at J06893350.

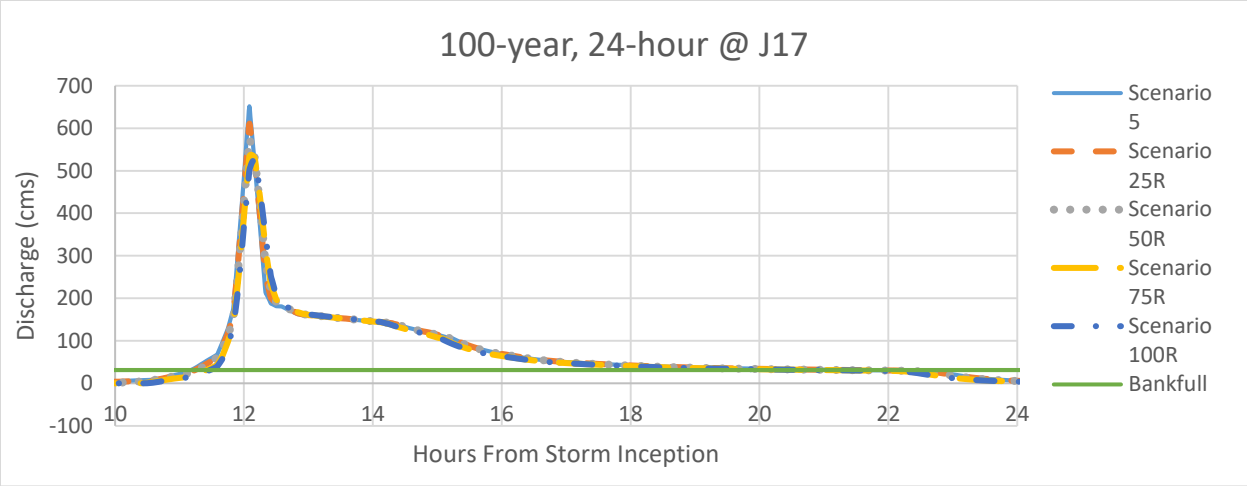

Figure C.20. Hydrograph displaying changes between baseline conditions (scenario 5) and varying levels of GI implementation for the 100-year, 24-hour storm at J17.

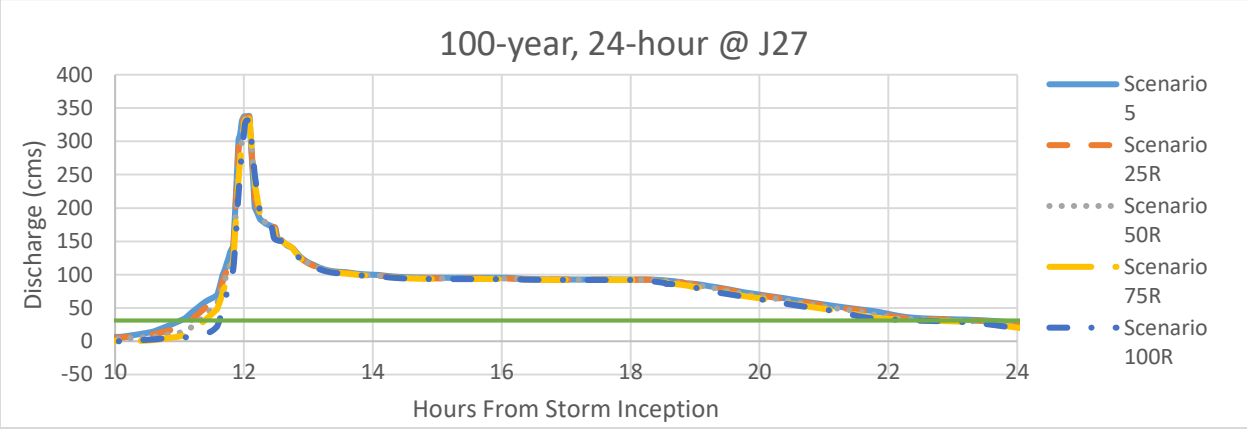

Figure C.21. Hydrograph displaying changes between baseline conditions (scenario 5) and varying levels of GI implementation for the 100-year, 24-hour storm at J27.

Table C.7. Percent reduction in peak inflow and total volume of inflow from current conditions for the 100-year, 24-hour precipitation event. Shading indicates statistically significant results.

100-year, 24-hour						
	Peak Inflow (cms)			Total Volume (m^3)		
Scenario	J17	J06893350	J27	J17	J06893350	J27
0	-1.32	-0.28	0.00	-0.28	-0.42	-0.53
5	0.00	0.00	0.00	0.00	0.00	0.00
25	5.09	1.16	0.24	1.11	1.51	2.67
50	10.86	2.84	0.47	2.06	3.42	5.19
75	16.63	5.17	1.12	6.14	7.45	9.08
100	18.13	7.43	1.39	6.94	9.98	11.28
0R	0.47	1.04	0.24	1.57	1.87	1.72
5R	1.73	1.27	0.27	1.85	2.24	2.18
25R	6.51	2.20	0.47	2.78	3.56	4.39
50R	12.04	3.54	0.71	3.65	5.19	6.59
75R	17.69	5.46	1.33	7.56	8.97	10.06
100R	19.22	7.45	1.63	8.30	11.44	12.06

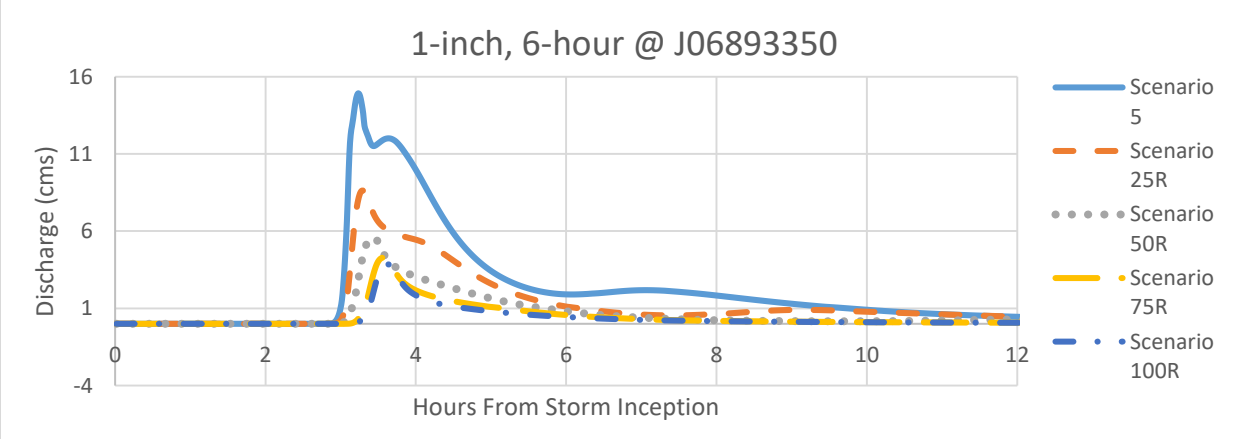

Figure C.22. Hydrograph displaying changes between baseline conditions (scenario 5) and varying levels of GI implementation for the 1-inch, 6-hour storm at J06893350.

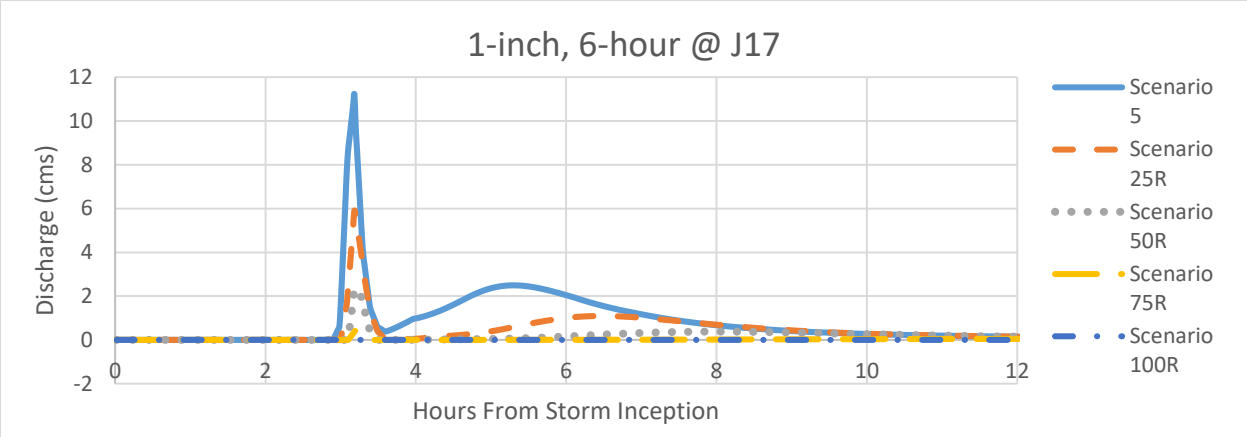

Figure C.23. Hydrograph displaying changes between baseline conditions (scenario 5) and varying levels of GI implementation for the 1-inch, 6-hour storm at J17.

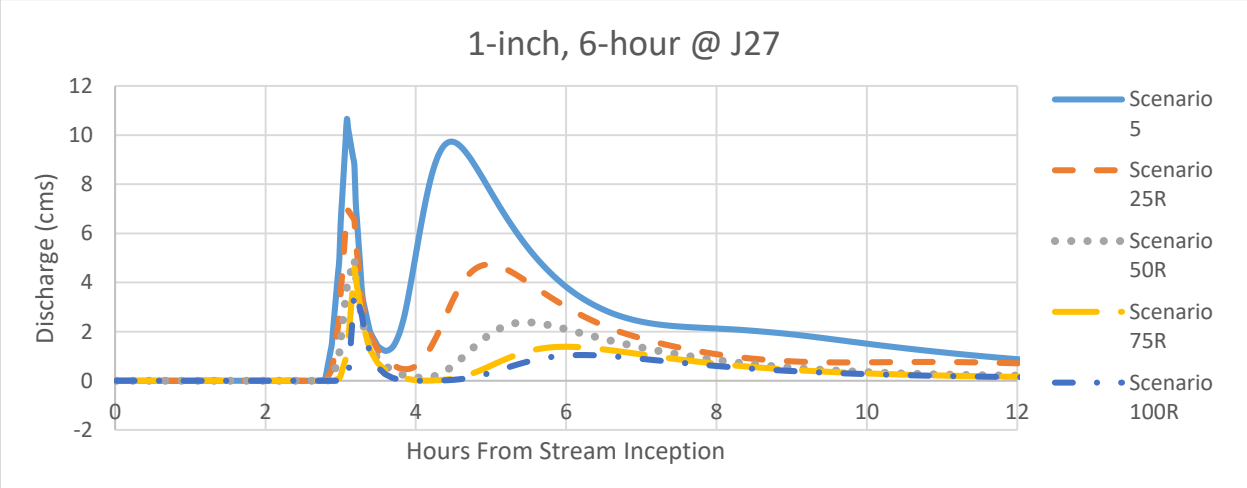

Figure C.24. Hydrograph displaying changes between baseline conditions (scenario 5) and varying levels of GI implementation for the 1-inch, 6-hour storm at J27.

Table C.8. Percent reduction in peak inflow and total volume of inflow from current conditions for the 1.37-inch, 6-hour precipitation event. Shading indicates statistically significant results.

1-inch, 6-hour						
	Peak Inflow (cms)			Total Volume (m^3)		
Scenario	J17	J06893350	J27	J17	J06893350	J27
0	-5.68	-9.31	-12.44	-9.08	-8.32	-8.59
5	0.00	0.00	0.00	0.00	0.00	0.00
25	23.25	31.85	33.11	33.44	29.85	30.61
50	56.20	56.07	55.24	67.59	58.57	59.58
75	84.70	68.30	51.85	89.37	75.54	76.34
100	99.85	72.99	56.88	99.89	81.99	82.52
0R	18.25	17.56	19.02	22.58	18.46	17.79
5R	24.65	24.47	23.99	30.03	25.51	25.02
25R	51.36	49.53	44.41	55.85	49.74	49.93
50R	80.79	67.25	60.43	78.24	70.38	70.96
75R	96.47	74.92	63.27	93.86	82.97	83.42
100R	100.00	77.32	71.07	99.92	86.43	86.88

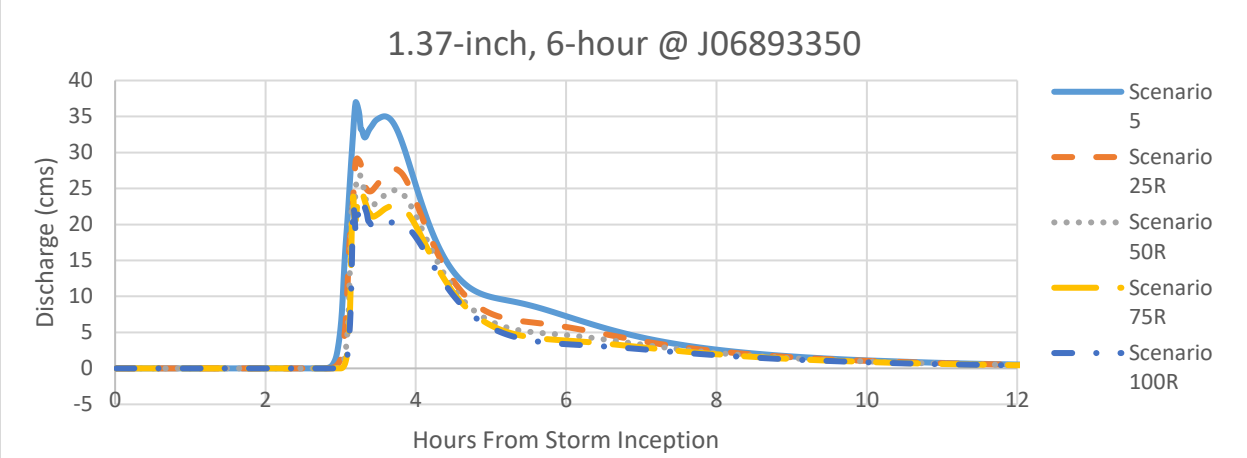

Figure C.25. Hydrograph displaying changes between baseline conditions (scenario 5) and varying levels of GI implementation for the 1.37-inch, 6-hour storm at J06893350.

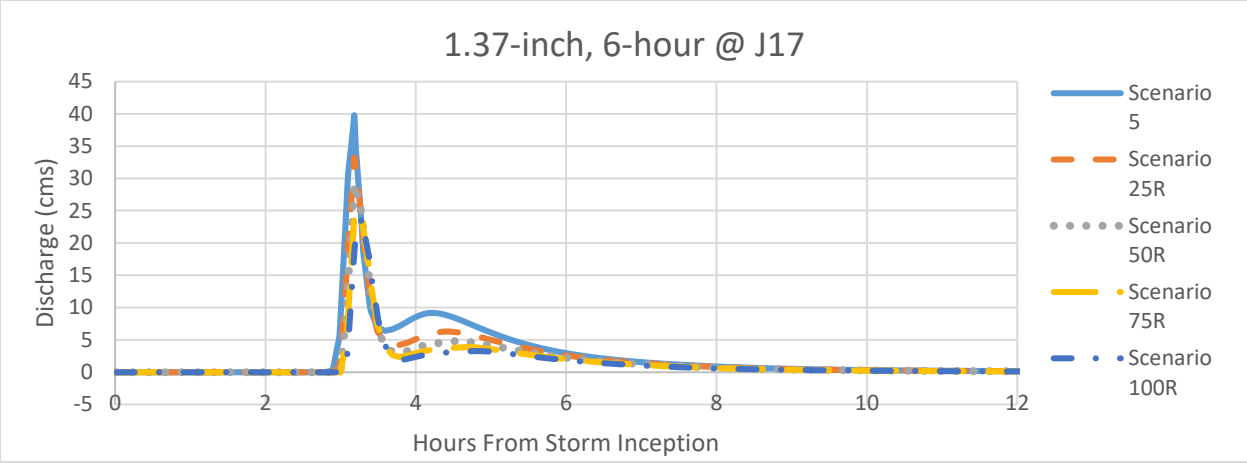

Figure C.26. Hydrograph displaying changes between baseline conditions (scenario 5) and varying levels of GI implementation for the 1.37-inch, 6-hour storm at J17.

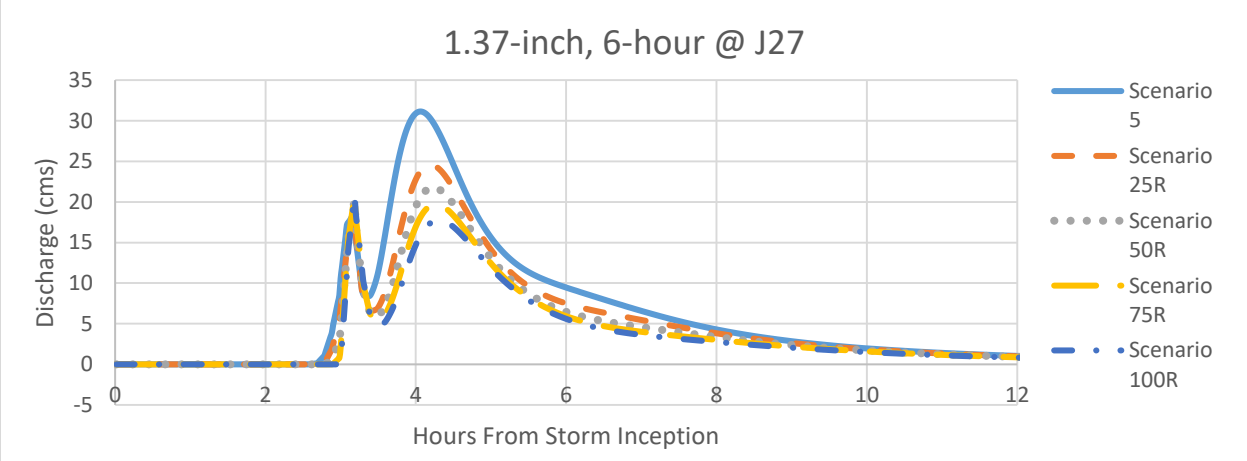

Figure C.27. Hydrograph displaying changes between baseline conditions (scenario 5) and varying levels of GI implementation for the 1.37-inch, 6-hour storm at J27.

Table C.9. Percent reduction in peak inflow and total volume of inflow from current conditions for the 1.37-inch, 6-hour precipitation event. Shading indicates statistically significant results.

1.37-inch, 6-hour						
	Peak Inflow (cms)			Total Volume (m^3)		
Scenario	J17	J06893350	J27	J17	J06893350	J27
0	-1.85	-2.65	-3.55	-3.93	-3.56	-3.58
5	0.00	0.00	0.00	0.00	0.00	0.00
25	6.62	8.35	10.49	13.69	11.97	11.63
50	15.05	16.65	20.22	25.98	22.05	21.24
75	25.12	25.87	27.35	34.35	29.13	27.85
100	34.20	31.68	32.76	40.14	33.95	32.54
0R	10.79	20.32	14.99	12.93	12.81	12.21
5R	12.74	23.46	18.40	16.34	15.91	15.30
25R	20.06	29.63	28.97	28.27	26.13	25.34
50R	30.08	35.11	37.12	38.52	34.44	33.27
75R	39.93	40.37	39.77	45.55	40.23	38.78
100R	42.51	43.58	39.51	50.67	44.77	43.25

Appendix D - Tukey Honest Significance Test Results

Table D.1 Scenario-scenario Tukey Honest Significance Test results for peak inflow at J06893350. Comparisons to the current conditions scenario are highlighted.

	diff	lwr	upr	p adj	
0R-0N	-8.1927778	-15.4227527	-0.9628029	1.31E-02	Significant
100N-0N	-22.4241444	-29.6541193	-15.19416957	3.56E-10	Significant
100R-0N	-26.1988889	-33.4288638	-18.96891401	3.56E-10	Significant
25N-0N	-6.1204444	-13.3504193	1.10953043	1.81E-01	Fail to Reject Null
25R-0N	-13.2865556	-20.5165304	-6.05658068	1.31E-06	Significant
50N-0N	-11.7578889	-18.9878638	-4.52791401	2.72E-05	Significant
50R-0N	-17.738	-24.9679749	-10.50802512	4.56E-10	Significant
5N-0N	-1.3523333	-8.5823082	5.87764155	1.00E+00	Fail to Reject Null
5R-0N	-9.3922222	-16.6221971	-2.16224734	1.97E-03	Significant
75N-0N	-17.4219333	-24.6519082	-10.19195845	5.55E-10	Significant
75R-0N	-22.1432222	-29.3731971	-14.91324734	3.56E-10	Significant
100N-0R	-14.2313667	-21.4613415	-7.00139179	1.86E-07	Significant
100R-0R	-18.0061111	-25.236086	-10.77613623	4.12E-10	Significant
25N-0R	2.0723333	-5.1576415	9.30230821	9.98E-01	Fail to Reject Null
25R-0R	-5.0937778	-12.3237527	2.1361971	4.40E-01	Fail to Reject Null
50N-0R	-3.5651111	-10.795086	3.66486377	8.83E-01	Fail to Reject Null
50R-0R	-9.5452222	-16.7751971	-2.31524734	1.52E-03	Significant
5N-0R	6.8404444	-0.3895304	14.07041932	8.13E-02	Fail to Reject Null
5R-0R	-1.1994444	-8.4294193	6.03053043	1.00E+00	Fail to Reject Null
75N-0R	-9.2291556	-16.4591304	-1.99918068	2.58E-03	Significant
75R-0R	-13.9504444	-21.1804193	-6.72046957	3.34E-07	Significant
100R-100N	-3.7747444	-11.0047193	3.45523043	8.38E-01	Fail to Reject Null
25N-100N	16.3037	9.0737251	23.53367488	2.61E-09	Significant
25R-100N	9.1375889	1.907614	16.36756377	3.00E-03	Significant
50N-100N	10.6662556	3.4362807	17.89623043	2.11E-04	Significant
50R-100N	4.6861444	-2.5438304	11.91611932	5.71E-01	Fail to Reject Null
5N-100N	21.0718111	13.8418362	28.30178599	3.56E-10	Significant
5R-100N	13.0319222	5.8019473	20.2618971	2.19E-06	Significant
75N-100N	5.0022111	-2.2277638	12.23218599	4.69E-01	Fail to Reject Null
75R-100N	0.2809222	-6.9490527	7.5108971	1.00E+00	Fail to Reject Null
25N-100R	20.0784444	12.8484696	27.30841932	3.57E-10	Significant
25R-100R	12.9123333	5.6823585	20.14230821	2.79E-06	Significant
50N-100R	14.441	7.2110251	21.67097488	1.20E-07	Significant

50R-100R	8.4608889	1.230914	15.69086377	8.76E-03	Significant
5N-100R	24.8465556	17.6165807	32.07653043	3.56E-10	Significant
5R-100R	16.8066667	9.5766918	24.03664155	1.11E-09	Significant
75N-100R	8.7769556	1.5469807	16.00693043	5.36E-03	Significant
75R-100R	4.0556667	-3.1743082	11.28564155	7.66E-01	Fail to Reject Null
25R-25N	-7.1661111	-14.396086	0.06386377	5.43E-02	Fail to Reject Null
50N-25N	-5.6374444	-12.8674193	1.59253043	2.86E-01	Fail to Reject Null
50R-25N	-11.6175556	-18.8475304	-4.38758068	3.56E-05	Significant
5N-25N	4.7681111	-2.4618638	11.99808599	5.44E-01	Fail to Reject Null
5R-25N	-3.2717778	-10.5017527	3.9581971	9.31E-01	Fail to Reject Null
75N-25N	-11.3014889	-18.5314638	-4.07151401	6.50E-05	Significant
75R-25N	-16.0227778	-23.2527527	-8.7928029	4.49E-09	Significant
50N-25R	1.5286667	-5.7013082	8.75864155	1.00E+00	Fail to Reject Null
50R-25R	-4.4514444	-11.6814193	2.77853043	6.47E-01	Fail to Reject Null
5N-25R	11.9342222	4.7042473	19.1641971	1.93E-05	Significant
5R-25R	3.8943333	-3.3356415	11.12430821	8.09E-01	Fail to Reject Null
75N-25R	-4.1353778	-11.3653527	3.0945971	7.43E-01	Fail to Reject Null
75R-25R	-8.8566667	-16.0866415	-1.62669179	4.72E-03	Significant
50R-50N	-5.9801111	-13.210086	1.24986377	2.08E-01	Fail to Reject Null
5N-50N	10.4055556	3.1755807	17.63553043	3.39E-04	Significant
5R-50N	2.3656667	-4.8643082	9.59564155	9.94E-01	Fail to Reject Null
75N-50N	-5.6640444	-12.8940193	1.56593043	2.79E-01	Fail to Reject Null
75R-50N	-10.3853333	-17.6153082	-3.15535845	3.52E-04	Significant
5N-50R	16.3856667	9.1556918	23.61564155	2.25E-09	Significant
5R-50R	8.3457778	1.1158029	15.57575266	1.04E-02	Significant
75N-50R	0.3160667	-6.9139082	7.54604155	1.00E+00	Fail to Reject Null
75R-50R	-4.4052222	-11.6351971	2.82475266	6.61E-01	Fail to Reject Null
5R-5N	-8.0398889	-15.2698638	-0.80991401	1.64E-02	Significant
75N-5N	-16.0696	-23.2995749	-8.83962512	4.10E-09	Significant
75R-5N	-20.7908889	-28.0208638	-13.56091401	3.56E-10	Significant
75N-5R	-8.0297111	-15.259686	-0.79973623	1.67E-02	Significant
75R-5R	-12.751	-19.9809749	-5.52102512	3.85E-06	Significant
75R-75N	-4.7212889	-11.9512638	2.50868599	5.59E-01	Fail to Reject Null

Table D.2. Storm-storm Tukey Honest Significance Test results for peak inflow at J06893500.

	diff	lwr	upr	p adj	
1.37in_6hr-1.37in_24hr	21.376417	1.54E+01	27.307071	3.56E-10	Significant

100yr_24hr-1.37in_24hr	446.86725	4.41E+02	452.797904	3.56E-10	Significant
10yr_24hr-1.37in_24hr	301.875583	2.96E+02	307.806238	3.56E-10	Significant
1in_24hr-1.37in_24hr	-7.063058	-1.30E+01	-1.132404	8.12E-03	Significant
1in_6hr-1.37in_24hr	-1.135	-7.07E+00	4.795654	1.00E+00	Fail to Reject Null
1yr_24hr-1.37in_24hr	144.475583	1.39E+02	150.406238	3.56E-10	Significant
25yr_24hr-1.37in_24hr	363.16725	3.57E+02	369.097904	3.56E-10	Significant
5yr_24hr-1.37in_24hr	259.158917	2.53E+02	265.089571	3.56E-10	Significant
100yr_24hr-1.37in_6hr	425.490833	4.20E+02	431.421488	3.56E-10	Significant
10yr_24hr-1.37in_6hr	280.499167	2.75E+02	286.429821	3.56E-10	Significant
1in_24hr-1.37in_6hr	-28.439475	-3.44E+01	-22.508821	3.56E-10	Significant
1in_6hr-1.37in_6hr	-22.511417	-2.84E+01	-16.580762	3.56E-10	Significant
1yr_24hr-1.37in_6hr	123.099167	1.17E+02	129.029821	3.56E-10	Significant
25yr_24hr-1.37in_6hr	341.790833	3.36E+02	347.721488	3.56E-10	Significant
5yr_24hr-1.37in_6hr	237.7825	2.32E+02	243.713154	3.56E-10	Significant
10yr_24hr-100yr_24hr	-144.991667	-1.51E+02	-139.061012	3.56E-10	Significant
1in_24hr-100yr_24hr	-453.930308	-4.60E+02	-447.999654	3.56E-10	Significant
1in_6hr-100yr_24hr	-448.00225	-4.54E+02	-442.071596	3.56E-10	Significant
1yr_24hr-100yr_24hr	-302.391667	-3.08E+02	-296.461012	3.56E-10	Significant
25yr_24hr-100yr_24hr	-83.7	-8.96E+01	-77.769346	3.56E-10	Significant
5yr_24hr-100yr_24hr	-187.708333	-1.94E+02	-181.777679	3.56E-10	Significant
1in_24hr-10yr_24hr	-308.938642	-3.15E+02	-303.007987	3.56E-10	Significant
1in_6hr-10yr_24hr	-303.010583	-3.09E+02	-297.079929	3.56E-10	Significant
1yr_24hr-10yr_24hr	-157.4	-1.63E+02	-151.469346	3.56E-10	Significant
25yr_24hr-10yr_24hr	61.291667	5.54E+01	67.222321	3.56E-10	Significant
5yr_24hr-10yr_24hr	-42.716667	-4.86E+01	-36.786012	3.56E-10	Significant
1in_6hr-1in_24hr	5.928058	-2.60E-03	11.858713	5.02E-02	Fail to Reject Null
1yr_24hr-1in_24hr	151.538642	1.46E+02	157.469296	3.56E-10	Significant
25yr_24hr-1in_24hr	370.230308	3.64E+02	376.160963	3.56E-10	Significant
5yr_24hr-1in_24hr	266.221975	2.60E+02	272.152629	3.56E-10	Significant
1yr_24hr-1in_6hr	145.610583	1.40E+02	151.541238	3.56E-10	Significant
25yr_24hr-1in_6hr	364.30225	3.58E+02	370.232904	3.56E-10	Significant
5yr_24hr-1in_6hr	260.293917	2.54E+02	266.224571	3.56E-10	Significant
25yr_24hr-1yr_24hr	218.691667	2.13E+02	224.622321	3.56E-10	Significant
5yr_24hr-1yr_24hr	114.683333	1.09E+02	120.613988	3.56E-10	Significant
5yr_24hr-25yr_24hr	-104.008333	-1.10E+02	-98.077679	3.56E-10	Significant

Table D.3. Scenario-scenario Tukey Honest Significance Test results for peak inflow at J17. Comparisons to the current conditions scenario are highlighted.

	diff	lwr	upr	p adj	
0R-0N	-11.533889	-39.6701025	16.6023247	9.65E-01	Fail to Reject Null
100N-0N	-48.330778	-76.4669914	-20.1945642	7.46E-06	Significant
100R-0N	-54.464	-82.6002136	-26.3277864	3.04E-07	Significant
25N-0N	-17.867667	-46.0038803	10.268547	6.02E-01	Fail to Reject Null
25R-0N	-27.193744	-55.3299581	0.9424692	6.79E-02	Fail to Reject Null
50N-0N	-33.528333	-61.664547	-5.3921197	6.90E-03	Significant
50R-0N	-41.718733	-69.854947	-13.5825197	1.92E-04	Significant
5N-0N	-3.744	-31.8802136	24.3922136	1.00E+00	Fail to Reject Null
5R-0N	-14.819444	-42.9556581	13.3167692	8.30E-01	Fail to Reject Null
75N-0N	-42.842477	-70.9786903	-14.706263	1.12E-04	Significant
75R-0N	-50.630798	-78.7670118	-22.4945846	2.29E-06	Significant
100N-0R	-36.796889	-64.9331025	-8.6606753	1.77E-03	Significant
100R-0R	-42.930111	-71.0663247	-14.7938975	1.08E-04	Significant
25N-0R	-6.333778	-34.4699914	21.8024358	1.00E+00	Fail to Reject Null
25R-0R	-15.659856	-43.7960692	12.4763581	7.75E-01	Fail to Reject Null
50N-0R	-21.994444	-50.1306581	6.1417692	2.82E-01	Fail to Reject Null
50R-0R	-30.184844	-58.3210581	-2.0486308	2.46E-02	Significant
5N-0R	7.789889	-20.3463247	35.9261025	9.99E-01	Fail to Reject Null
5R-0R	-3.285556	-31.4217692	24.8506581	1.00E+00	Fail to Reject Null
75N-0R	-31.308588	-59.4448014	-3.1723742	1.63E-02	Significant
75R-0R	-39.096909	-67.233123	-10.9606957	6.42E-04	Significant
100R-100N	-6.133222	-34.2694358	22.0029914	1.00E+00	Fail to Reject Null
25N-100N	30.463111	2.3268975	58.5993247	2.22E-02	Significant
25R-100N	21.137033	-6.9991803	49.273247	3.40E-01	Fail to Reject Null
50N-100N	14.802444	-13.3337692	42.9386581	8.31E-01	Fail to Reject Null
50R-100N	6.612044	-21.5241692	34.7482581	1.00E+00	Fail to Reject Null
5N-100N	44.586778	16.4505642	72.7229914	4.84E-05	Significant
5R-100N	33.511333	5.3751197	61.647547	6.95E-03	Significant
75N-100N	5.488301	-22.6479125	33.6245147	1.00E+00	Fail to Reject Null
75R-100N	-2.30002	-30.4362341	25.8361932	1.00E+00	Fail to Reject Null
25N-100R	36.596333	8.4601197	64.732547	1.93E-03	Significant
25R-100R	27.270256	-0.8659581	55.4064692	6.63E-02	Fail to Reject Null
50N-100R	20.935667	-7.200547	49.0718803	3.55E-01	Fail to Reject Null
50R-100R	12.745267	-15.390947	40.8814803	9.31E-01	Fail to Reject Null
5N-100R	50.72	22.5837864	78.8562136	2.18E-06	Significant
5R-100R	39.644556	11.5083419	67.7807692	5.01E-04	Significant
75N-100R	11.621523	-16.5146903	39.757737	9.63E-01	Fail to Reject Null

75R-100R	3.833202	-24.3030118	31.9694154	1.00E+00	Fail to Reject Null
25R-25N	-9.326078	-37.4622914	18.8101358	9.93E-01	Fail to Reject Null
50N-25N	-15.660667	-43.7968803	12.475547	7.75E-01	Fail to Reject Null
50R-25N	-23.851067	-51.9872803	4.285147	1.79E-01	Fail to Reject Null
5N-25N	14.123667	-14.012547	42.2598803	8.70E-01	Fail to Reject Null
5R-25N	3.048222	-25.0879914	31.1844358	1.00E+00	Fail to Reject Null
75N-25N	-24.97481	-53.1110236	3.1614036	1.32E-01	Fail to Reject Null
75R-25N	-32.763132	-60.8993452	-4.6269179	9.34E-03	Significant
50N-25R	-6.334589	-34.4708025	21.8016247	1.00E+00	Fail to Reject Null
50R-25R	-14.524989	-42.6612025	13.6112247	8.48E-01	Fail to Reject Null
5N-25R	23.449744	-4.6864692	51.5859581	1.99E-01	Fail to Reject Null
5R-25R	12.3743	-15.7619136	40.5105136	9.43E-01	Fail to Reject Null
75N-25R	-15.648732	-43.7849458	12.4874814	7.75E-01	Fail to Reject Null
75R-25R	-23.437054	-51.5732674	4.6991598	2.00E-01	Fail to Reject Null
50R-50N	-8.1904	-36.3266136	19.9458136	9.98E-01	Fail to Reject Null
5N-50N	29.784333	1.6481197	57.920547	2.84E-02	Significant
5R-50N	18.708889	-9.4273247	46.8451025	5.31E-01	Fail to Reject Null
75N-50N	-9.314143	-37.450357	18.8220703	9.93E-01	Fail to Reject Null
75R-50N	-17.102465	-45.2386785	11.0337487	6.65E-01	Fail to Reject Null
5N-50R	37.974733	9.8385197	66.110947	1.06E-03	Significant
5R-50R	26.899289	-1.2369247	55.0355025	7.45E-02	Fail to Reject Null
75N-50R	-1.123743	-29.259957	27.0124703	1.00E+00	Fail to Reject Null
75R-50R	-8.912065	-37.0482785	19.2241487	9.95E-01	Fail to Reject Null
5R-5N	-11.075444	-39.2116581	17.0607692	9.74E-01	Fail to Reject Null
75N-5N	-39.098477	-67.2346903	-10.962263	6.41E-04	Significant
75R-5N	-46.886798	-75.0230118	-18.7505846	1.55E-05	Significant
75N-5R	-28.023032	-56.1592458	0.1131814	5.19E-02	Fail to Reject Null
75R-5R	-35.811354	-63.9475674	-7.6751402	2.70E-03	Significant
75R-75N	-7.788322	-35.9245352	20.3478921	9.99E-01	Fail to Reject Null

Table D.4. Storm-storm Tukey Honest Significance Test results for peak inflow at J06893500.

	diff	lwr	upr	p adj	
1.37in_6hr-1.37in_24hr	25.821675	2.741905	48.901445	1.68E-02	Significant
100yr_24hr-1.37in_24hr	587.091675	564.011905	610.171445	3.56E-10	Significant
10yr_24hr-1.37in_24hr	350.191675	327.111905	373.271445	3.56E-10	Significant
1in_24hr-1.37in_24hr	-6.286723	-29.366493	16.793047	9.94E-01	Fail to Reject Null

1in_6hr-1.37in_24hr	-1.790317	-24.870086	21.289453	1.00E+00	Fail to Reject Null
1yr_24hr-1.37in_24hr	147.791675	124.711905	170.871445	3.56E-10	Significant
25yr_24hr-1.37in_24hr	442.033342	418.953572	465.113111	3.56E-10	Significant
5yr_24hr-1.37in_24hr	288.491675	265.411905	311.571445	3.56E-10	Significant
100yr_24hr-1.37in_6hr	561.27	538.19023	584.34977	3.56E-10	Significant
10yr_24hr-1.37in_6hr	324.37	301.29023	347.44977	3.56E-10	Significant
1in_24hr-1.37in_6hr	-32.108398	-55.188168	-9.028628	8.91E-04	Significant
1in_6hr-1.37in_6hr	-27.611992	-50.691761	-4.532222	7.68E-03	Significant
1yr_24hr-1.37in_6hr	121.97	98.89023	145.04977	3.56E-10	Significant
25yr_24hr-1.37in_6hr	416.211667	393.131897	439.291436	3.56E-10	Significant
5yr_24hr-1.37in_6hr	262.67	239.59023	285.74977	3.56E-10	Significant
10yr_24hr-100yr_24hr	-236.9	-259.97977	-213.82023	3.56E-10	Significant
1in_24hr-100yr_24hr	-593.378398	-616.458168	-570.298628	3.56E-10	Significant
1in_6hr-100yr_24hr	-588.881992	-611.961761	-565.802222	3.56E-10	Significant
1yr_24hr-100yr_24hr	-439.3	-462.37977	-416.22023	3.56E-10	Significant
25yr_24hr-100yr_24hr	-145.058333	-168.138103	-121.978564	3.56E-10	Significant
5yr_24hr-100yr_24hr	-298.6	-321.67977	-275.52023	3.56E-10	Significant
1in_24hr-10yr_24hr	-356.478398	-379.558168	-333.398628	3.56E-10	Significant
1in_6hr-10yr_24hr	-351.981992	-375.061761	-328.902222	3.56E-10	Significant
1yr_24hr-10yr_24hr	-202.4	-225.47977	-179.32023	3.56E-10	Significant
25yr_24hr-10yr_24hr	91.841667	68.761897	114.921436	3.56E-10	Significant
5yr_24hr-10yr_24hr	-61.7	-84.77977	-38.62023	3.72E-10	Significant
1in_6hr-1in_24hr	4.496406	-18.583364	27.576176	9.99E-01	Fail to Reject Null
1yr_24hr-1in_24hr	154.078398	130.998628	177.158168	3.56E-10	Significant
25yr_24hr-1in_24hr	448.320065	425.240295	471.399834	3.56E-10	Significant
5yr_24hr-1in_24hr	294.778398	271.698628	317.858168	3.56E-10	Significant
1yr_24hr-1in_6hr	149.581992	126.502222	172.661761	3.56E-10	Significant
25yr_24hr-1in_6hr	443.823658	420.743889	466.903428	3.56E-10	Significant
5yr_24hr-1in_6hr	290.281992	267.202222	313.361761	3.56E-10	Significant
25yr_24hr-1yr_24hr	294.241667	271.161897	317.321436	3.56E-10	Significant
5yr_24hr-1yr_24hr	140.7	117.62023	163.77977	3.56E-10	Significant
5yr_24hr-25yr_24hr	-153.541667	-176.621436	-130.461897	3.56E-10	Significant

Table D.5. Scenario-scenario Tukey Honest Significance Test results for peak inflow at J27. Comparisons to the current conditions scenario are highlighted.

	diff	lwr	upr	p adj	
0R-0N	-3.8775556	-8.4281459	0.67303484	1.74E-01	Fail to Reject Null
100N-0N	-10.1607778	-14.7113682	-5.61018738	3.55E-09	Significant
100R-0N	-13.7393789	-18.2899693	-9.1887885	3.56E-10	Significant
25N-0N	-3.5591111	-8.1097015	0.99147928	2.82E-01	Fail to Reject Null
25R-0N	-6.5965556	-11.1471459	-2.04596516	2.96E-04	Significant
50N-0N	-5.8265556	-10.3771459	-1.27596516	2.47E-03	Significant
50R-0N	-8.6654444	-13.2160348	-4.11485405	4.87E-07	Significant
5N-0N	-0.763	-5.3135904	3.78759039	1.00E+00	Fail to Reject Null
5R-0N	-4.4037778	-8.9543682	0.14681262	6.72E-02	Fail to Reject Null
75N-0N	-8.1398222	-12.6904126	-3.58923183	2.68E-06	Significant
75R-0N	-11.4621333	-16.0127237	-6.91154294	3.92E-10	Significant
100N-0R	-6.2832222	-10.8338126	-1.73263183	7.18E-04	Significant
100R-0R	-9.8618233	-14.4124137	-5.31123294	9.21E-09	Significant
25N-0R	0.3184444	-4.2321459	4.86903484	1.00E+00	Fail to Reject Null
25R-0R	-2.719	-7.2695904	1.83159039	6.88E-01	Fail to Reject Null
50N-0R	-1.949	-6.4995904	2.60159039	9.52E-01	Fail to Reject Null
50R-0R	-4.7878889	-9.3384793	-0.2372985	3.03E-02	Significant
5N-0R	3.1145556	-1.4360348	7.66514595	4.86E-01	Fail to Reject Null
5R-0R	-0.5262222	-5.0768126	4.02436817	1.00E+00	Fail to Reject Null
75N-0R	-4.2622667	-8.8128571	0.28832373	8.82E-02	Fail to Reject Null
75R-0R	-7.5845778	-12.1351682	-3.03398738	1.54E-05	Significant
100R-100N	-3.5786011	-8.1291915	0.97198928	2.74E-01	Fail to Reject Null
25N-100N	6.6016667	2.0510763	11.15225706	2.92E-04	Significant
25R-100N	3.5642222	-0.9863682	8.11481262	2.80E-01	Fail to Reject Null
50N-100N	4.3342222	-0.2163682	8.88481262	7.69E-02	Fail to Reject Null
50R-100N	1.4953333	-3.0552571	6.04592373	9.94E-01	Fail to Reject Null
5N-100N	9.3977778	4.8471874	13.94836817	4.30E-08	Significant
5R-100N	5.757	1.2064096	10.30759039	2.96E-03	Significant
75N-100N	2.0209556	-2.5296348	6.57154595	9.39E-01	Fail to Reject Null
75R-100N	-1.3013556	-5.8519459	3.24923484	9.98E-01	Fail to Reject Null
25N-100R	10.1802678	5.6296774	14.73085817	3.34E-09	Significant
25R-100R	7.1428233	2.5922329	11.69341373	5.94E-05	Significant
50N-100R	7.9128233	3.3622329	12.46341373	5.51E-06	Significant
50R-100R	5.0739344	0.5233441	9.62452484	1.59E-02	Significant
5N-100R	12.9763789	8.4257885	17.52696928	3.56E-10	Significant
5R-100R	9.3356011	4.7850107	13.8861915	5.29E-08	Significant

75N-100R	5.5995567	1.0489663	10.15014706	4.43E-03	Significant
75R-100R	2.2772456	-2.2733448	6.82783595	8.72E-01	Fail to Reject Null
25R-25N	-3.0374444	-7.5880348	1.51314595	5.25E-01	Fail to Reject Null
50N-25N	-2.2674444	-6.8180348	2.28314595	8.75E-01	Fail to Reject Null
50R-25N	-5.1063333	-9.6569237	-0.55574294	1.48E-02	Significant
5N-25N	2.7961111	-1.7544793	7.3467015	6.50E-01	Fail to Reject Null
5R-25N	-0.8446667	-5.3952571	3.70592373	1.00E+00	Fail to Reject Null
75N-25N	-4.5807111	-9.1313015	-0.03012072	4.70E-02	Significant
75R-25N	-7.9030222	-12.4536126	-3.35243183	5.68E-06	Significant
50N-25R	0.77	-3.7805904	5.32059039	1.00E+00	Fail to Reject Null
50R-25R	-2.0688889	-6.6194793	2.4817015	9.29E-01	Fail to Reject Null
5N-25R	5.8335556	1.2829652	10.38414595	2.42E-03	Significant
5R-25R	2.1927778	-2.3578126	6.74336817	8.98E-01	Fail to Reject Null
75N-25R	-1.5432667	-6.0938571	3.00732373	9.92E-01	Fail to Reject Null
75R-25R	-4.8655778	-9.4161682	-0.31498738	2.55E-02	Significant
50R-50N	-2.8388889	-7.3894793	1.7117015	6.28E-01	Fail to Reject Null
5N-50N	5.0635556	0.5129652	9.61414595	1.63E-02	Significant
5R-50N	1.4227778	-3.1278126	5.97336817	9.96E-01	Fail to Reject Null
75N-50N	-2.3132667	-6.8638571	2.23732373	8.60E-01	Fail to Reject Null
75R-50N	-5.6355778	-10.1861682	-1.08498738	4.04E-03	Significant
5N-50R	7.9024444	3.3518541	12.45303484	5.69E-06	Significant
5R-50R	4.2616667	-0.2889237	8.81225706	8.83E-02	Fail to Reject Null
75N-50R	0.5256222	-4.0249682	5.07621262	1.00E+00	Fail to Reject Null
75R-50R	-2.7966889	-7.3472793	1.7539015	6.49E-01	Fail to Reject Null
5R-5N	-3.6407778	-8.1913682	0.90981262	2.51E-01	Fail to Reject Null
75N-5N	-7.3768222	-11.9274126	-2.82623183	2.92E-05	Significant
75R-5N	-10.6991333	-15.2497237	-6.14854294	8.56E-10	Significant
75N-5R	-3.7360444	-8.2866348	0.81454595	2.17E-01	Fail to Reject Null
75R-5R	-7.0583556	-11.6089459	-2.50776516	7.66E-05	Significant
75R-75N	-3.3223111	-7.8729015	1.22827928	3.84E-01	Fail to Reject Null

Table D.6 Storm-storm Tukey Honest Significance Test results for peak inflow at J27.

	diff	lwr	upr	p adj	
1.37in_6hr-1.37in_24hr	17.694083	13.9612933	21.426873	3.56E-10	Significant
100yr_24hr-1.37in_24hr	326.832417	323.0996266	330.565207	3.56E-10	Significant
10yr_24hr-1.37in_24hr	229.807417	226.0746266	233.540207	3.56E-10	Significant

1in_24hr-1.37in_24hr	-5.609751	-9.3425409	-1.876961	2.33E-04	Significant
1in_6hr-1.37in_24hr	-1.638083	-5.3708734	2.094707	8.97E-01	Fail to Reject Null
1yr_24hr-1.37in_24hr	91.62825	87.8954599	95.36104	3.56E-10	Significant
25yr_24hr-1.37in_24hr	275.799083	272.0662933	279.531873	3.56E-10	Significant
5yr_24hr-1.37in_24hr	195.16575	191.4329599	198.89854	3.56E-10	Significant
100yr_24hr-1.37in_6hr	309.138333	305.4055433	312.871123	3.56E-10	Significant
10yr_24hr-1.37in_6hr	212.113333	208.3805433	215.846123	3.56E-10	Significant
1in_24hr-1.37in_6hr	-23.303834	-27.0366242	-19.571044	3.56E-10	Significant
1in_6hr-1.37in_6hr	-19.332167	-23.0649567	-15.599377	3.56E-10	Significant
1yr_24hr-1.37in_6hr	73.934167	70.2013766	77.666957	3.56E-10	Significant
25yr_24hr-1.37in_6hr	258.105	254.3722099	261.83779	3.56E-10	Significant
5yr_24hr-1.37in_6hr	177.471667	173.7388766	181.204457	3.56E-10	Significant
10yr_24hr-100yr_24hr	-97.025	-100.7577901	-93.29221	3.56E-10	Significant
1in_24hr-100yr_24hr	-332.442168	-336.1749576	-328.709377	3.56E-10	Significant
1in_6hr-100yr_24hr	-328.4705	-332.2032901	-324.73771	3.56E-10	Significant
1yr_24hr-100yr_24hr	-235.204167	-238.9369567	-231.471377	3.56E-10	Significant
25yr_24hr-100yr_24hr	-51.033333	-54.7661234	-47.300543	3.56E-10	Significant
5yr_24hr-100yr_24hr	-131.666667	-135.3994567	-127.933877	3.56E-10	Significant
1in_24hr-10yr_24hr	-235.417168	-239.1499576	-231.684377	3.56E-10	Significant
1in_6hr-10yr_24hr	-231.4455	-235.1782901	-227.71271	3.56E-10	Significant
1yr_24hr-10yr_24hr	-138.179167	-141.9119567	-134.446377	3.56E-10	Significant
25yr_24hr-10yr_24hr	45.991667	42.2588766	49.724457	3.56E-10	Significant

5yr_24hr-10yr_24hr	-34.641667	-38.3744567	-30.908877	3.56E-10	Significant
1in_6hr-1in_24hr	3.971668	0.2388774	7.704458	2.82E-02	Significant
1yr_24hr-1in_24hr	97.238001	93.5052108	100.970791	3.56E-10	Significant
25yr_24hr-1in_24hr	281.408834	277.6760441	285.141624	3.56E-10	Significant
5yr_24hr-1in_24hr	200.775501	197.0427108	204.508291	3.56E-10	Significant
1yr_24hr-1in_6hr	93.266333	89.5335433	96.999123	3.56E-10	Significant
25yr_24hr-1in_6hr	277.437167	273.7043766	281.169957	3.56E-10	Significant
5yr_24hr-1in_6hr	196.803833	193.0710433	200.536623	3.56E-10	Significant
25yr_24hr-1yr_24hr	184.170833	180.4380433	187.903623	3.56E-10	Significant
5yr_24hr-1yr_24hr	103.5375	99.8047099	107.27029	3.56E-10	Significant
5yr_24hr-25yr_24hr	-80.633333	-84.3661234	-76.900543	3.56E-10	Significant

Table D.7. Scenario-scenario Tukey Honest Significance Test results for total inflow volume at J06893350. Comparisons to the current conditions scenario are highlighted.

	diff	lwr	upr	p adj	
0R-0N	-76481.11	-192098.661	39136.4383	5.39E-01	Fail to Reject Null
100N-0N	-218275.33	-333892.883	-102657.7839	6.21E-07	Significant
100R-0N	-264932.33	-380549.883	-149314.7839	1.63E-09	Significant
25N-0N	-63693.33	-179310.883	51924.2161	7.86E-01	Fail to Reject Null
25R-0N	-129935.56	-245553.105	-14318.0061	1.45E-02	Significant
50N-0N	-118080	-233697.549	-2462.4506	4.09E-02	Significant
50R-0N	-174935.56	-290553.105	-59318.0061	1.28E-04	Significant
5N-0N	-13771.11	-129388.661	101846.4383	1.00E+00	Fail to Reject Null
5R-0N	-88394.44	-204011.994	27223.105	3.14E-01	Fail to Reject Null
75N-0N	-178525.56	-294143.105	-62908.0061	8.42E-05	Significant
75R-0N	-228806.56	-344424.105	-113189.0061	1.59E-07	Significant
100N-0R	-141794.22	-257411.772	-26176.6728	4.65E-03	Significant
100R-0R	-188451.22	-304068.772	-72833.6728	2.58E-05	Significant
25N-0R	12787.78	-102829.772	128405.3272	1.00E+00	Fail to Reject Null
25R-0R	-53454.44	-169071.994	62163.105	9.21E-01	Fail to Reject Null
50N-0R	-41598.89	-157216.438	74018.6605	9.87E-01	Fail to Reject Null
50R-0R	-98454.44	-214071.994	17163.105	1.74E-01	Fail to Reject Null

5N-0R	62710	-52907.549	178327.5494	8.02E-01	Fail to Reject Null
5R-0R	-11913.33	-127530.883	103704.2161	1.00E+00	Fail to Reject Null
75N-0R	-102044.44	-217661.994	13573.105	1.38E-01	Fail to Reject Null
75R-0R	-152325.44	-267942.994	-36707.895	1.57E-03	Significant
100R-100N	-46657	-162274.549	68960.5494	9.69E-01	Fail to Reject Null
25N-100N	154582	38964.451	270199.5494	1.24E-03	Significant
25R-100N	88339.78	-27277.772	203957.3272	3.15E-01	Fail to Reject Null
50N-100N	100195.33	-15422.216	215812.8827	1.56E-01	Fail to Reject Null
50R-100N	43339.78	-72277.772	158957.3272	9.82E-01	Fail to Reject Null
5N-100N	204504.22	88886.673	320121.7716	3.57E-06	Significant
5R-100N	129880.89	14263.339	245498.4383	1.46E-02	Significant
75N-100N	39749.78	-75867.772	155367.3272	9.91E-01	Fail to Reject Null
75R-100N	-10531.22	-126148.772	105086.3272	1.00E+00	Fail to Reject Null
25N-100R	201239	85621.451	316856.5494	5.38E-06	Significant
25R-100R	134996.78	19379.228	250614.3272	9.02E-03	Significant
50N-100R	146852.33	31234.784	262469.8827	2.78E-03	Significant
50R-100R	89996.78	-25620.772	205614.3272	2.88E-01	Fail to Reject Null
5N-100R	251161.22	135543.673	366778.7716	8.53E-09	Significant
5R-100R	176537.89	60920.339	292155.4383	1.06E-04	Significant
75N-100R	86406.78	-29210.772	202024.3272	3.48E-01	Fail to Reject Null
75R-100R	36125.78	-79491.772	151743.3272	9.96E-01	Fail to Reject Null
25R-25N	-66242.22	-181859.772	49375.3272	7.41E-01	Fail to Reject Null
50N-25N	-54386.67	-170004.216	61230.8827	9.12E-01	Fail to Reject Null
50R-25N	-111242.22	-226859.772	4375.3272	7.06E-02	Fail to Reject Null
5N-25N	49922.22	-65695.327	165539.7716	9.50E-01	Fail to Reject Null
5R-25N	-24701.11	-140318.661	90916.4383	1.00E+00	Fail to Reject Null
75N-25N	-114832.22	-230449.772	785.3272	5.33E-02	Fail to Reject Null
75R-25N	-165113.22	-280730.772	-49495.6728	3.92E-04	Significant
50N-25R	11855.56	-103761.994	127473.105	1.00E+00	Fail to Reject Null
50R-25R	-45000	-160617.549	70617.5494	9.76E-01	Fail to Reject Null
5N-25R	116164.44	546.895	231781.9939	4.78E-02	Significant
5R-25R	41541.11	-74076.438	157158.6605	9.87E-01	Fail to Reject Null
75N-25R	-48590	-164207.549	67027.5494	9.58E-01	Fail to Reject Null
75R-25R	-98871	-214488.549	16746.5494	1.70E-01	Fail to Reject Null
50R-50N	-56855.56	-172473.105	58761.9939	8.85E-01	Fail to Reject Null
5N-50N	104308.89	-11308.661	219926.4383	1.18E-01	Fail to Reject Null
5R-50N	29685.56	-85931.994	145303.105	9.99E-01	Fail to Reject Null

75N-50N	-60445.56	-176063.105	55171.9939	8.37E-01	Fail to Reject Null
75R-50N	-110726.56	-226344.105	4890.9939	7.34E-02	Fail to Reject Null
5N-50R	161164.44	45546.895	276781.9939	6.07E-04	Significant
5R-50R	86541.11	-29076.438	202158.6605	3.46E-01	Fail to Reject Null
75N-50R	-3590	-119207.549	112027.5494	1.00E+00	Fail to Reject Null
75R-50R	-53871	-169488.549	61746.5494	9.17E-01	Fail to Reject Null
5R-5N	-74623.33	-190240.883	40994.2161	5.77E-01	Fail to Reject Null
75N-5N	-164754.44	-280371.994	-49136.895	4.08E-04	Significant
75R-5N	-215035.44	-330652.994	-99417.895	9.41E-07	Significant
75N-5R	-90131.11	-205748.661	25486.4383	2.86E-01	Fail to Reject Null
75R-5R	-140412.11	-256029.661	-24794.5617	5.33E-03	Significant
75R-75N	-50281	-165898.549	65336.5494	9.47E-01	Fail to Reject Null

Table D.8. Storm-storm Tukey Honest Significance Test results for total inflow volume at J06893350.

	diff	lwr	upr	p adj	
1.37in_6hr-1.37in_24hr	147297.5	52457.93	242137.07	1.25E-04	Significant
100yr_24hr-1.37in_24hr	6060747.5	5965907.93	6155587.07	3.56E-10	Significant
10yr_24hr-1.37in_24hr	3207247.5	3112407.93	3302087.07	3.56E-10	Significant
1in_24hr-1.37in_24hr	-45104	-139943.57	49735.57	8.47E-01	Fail to Reject Null
1in_6hr-1.37in_24hr	-6053.333	-100892.9	88786.24	1.00E+00	Fail to Reject Null
1yr_24hr-1.37in_24hr	1082414.167	987574.6	1177253.74	3.56E-10	Significant
25yr_24hr-1.37in_24hr	4240247.5	4145407.93	4335087.07	3.56E-10	Significant
5yr_24hr-1.37in_24hr	2529247.5	2434407.93	2624087.07	3.56E-10	Significant
100yr_24hr-1.37in_6hr	5913450	5818610.43	6008289.57	3.56E-10	Significant
10yr_24hr-1.37in_6hr	3059950	2965110.43	3154789.57	3.56E-10	Significant
1in_24hr-1.37in_6hr	-192401.5	-287241.07	-97561.93	2.06E-07	Significant
1in_6hr-1.37in_6hr	-153350.833	-248190.4	-58511.26	5.55E-05	Significant
1yr_24hr-1.37in_6hr	935116.667	840277.1	1029956.24	3.56E-10	Significant
25yr_24hr-1.37in_6hr	4092950	3998110.43	4187789.57	3.56E-10	Significant
5yr_24hr-1.37in_6hr	2381950	2287110.43	2476789.57	3.56E-10	Significant
10yr_24hr-100yr_24hr	-2853500	-2948339.57	-2758660.43	3.56E-10	Significant
1in_24hr-100yr_24hr	-6105851.5	-6200691.07	-6011011.93	3.56E-10	Significant

1in_6hr-100yr_24hr	-6066800.833	-6161640.4	-5971961.26	3.56E-10	Significant
1yr_24hr-100yr_24hr	-4978333.333	-5073172.9	-4883493.76	3.56E-10	Significant
25yr_24hr-100yr_24hr	-1820500	-1915339.57	-1725660.43	3.56E-10	Significant
5yr_24hr-100yr_24hr	-3531500	-3626339.57	-3436660.43	3.56E-10	Significant
1in_24hr-10yr_24hr	-3252351.5	-3347191.07	-3157511.93	3.56E-10	Significant
1in_6hr-10yr_24hr	-3213300.833	-3308140.4	-3118461.26	3.56E-10	Significant
1yr_24hr-10yr_24hr	-2124833.333	-2219672.9	-2029993.76	3.56E-10	Significant
25yr_24hr-10yr_24hr	1033000	938160.43	1127839.57	3.56E-10	Significant
5yr_24hr-10yr_24hr	-678000	-772839.57	-583160.43	3.56E-10	Significant
1in_6hr-1in_24hr	39050.667	-55788.9	133890.24	9.26E-01	Fail to Reject Null
1yr_24hr-1in_24hr	1127518.167	1032678.6	1222357.74	3.56E-10	Significant
25yr_24hr-1in_24hr	4285351.5	4190511.93	4380191.07	3.56E-10	Significant
5yr_24hr-1in_24hr	2574351.5	2479511.93	2669191.07	3.56E-10	Significant
1yr_24hr-1in_6hr	1088467.5	993627.93	1183307.07	3.56E-10	Significant
25yr_24hr-1in_6hr	4246300.833	4151461.26	4341140.4	3.56E-10	Significant
5yr_24hr-1in_6hr	2535300.833	2440461.26	2630140.4	3.56E-10	Significant
25yr_24hr-1yr_24hr	3157833.333	3062993.76	3252672.9	3.56E-10	Significant
5yr_24hr-1yr_24hr	1446833.333	1351993.76	1541672.9	3.56E-10	Significant
5yr_24hr-25yr_24hr	-1711000	-1805839.57	-1616160.43	3.56E-10	Significant

Table D.9. Scenario-scenario Tukey Honest Significance Test results for total inflow volume at J17. Comparisons to the current conditions scenario are highlighted.

	diff	lwr	upr	p adj	
0R-0N	-39531.111	-93055.645	13993.422	3.66E-01	Fail to Reject Null
100N-0N	-98203.05	-151727.584	-44678.516	1.36E-06	Significant
100R-0N	-123856.789	-177381.322	-70332.255	1.25E-09	Significant
25N-0N	-27417.778	-80942.311	26106.756	8.54E-01	Fail to Reject Null

25R-0N	-61623	-115147.534	-8098.466	1.08E-02	Significant
50N-0N	-51221.222	-104745.756	2303.311	7.39E-02	Fail to Reject Null
50R-0N	-81512.333	-135036.867	-27987.8	1.12E-04	Significant
5N-0N	-5566.667	-59091.2	47957.867	1.00E+00	Fail to Reject Null
5R-0N	-44054.444	-97578.978	9470.089	2.14E-01	Fail to Reject Null
75N-0N	-83316.222	-136840.756	-29791.689	7.10E-05	Significant
75R-0N	-111019.989	-164544.522	-57495.455	3.75E-08	Significant
100N-0R	-58671.939	-112196.472	-5147.405	1.94E-02	Significant
100R-0R	-84325.678	-137850.211	-30801.144	5.49E-05	Significant
25N-0R	12113.333	-41411.2	65637.867	1.00E+00	Fail to Reject Null
25R-0R	-22091.889	-75616.422	31432.645	9.63E-01	Fail to Reject Null
50N-0R	-11690.111	-65214.645	41834.422	1.00E+00	Fail to Reject Null
50R-0R	-41981.222	-95505.756	11543.311	2.78E-01	Fail to Reject Null
5N-0R	33964.444	-19560.089	87488.978	6.03E-01	Fail to Reject Null
5R-0R	-4523.333	-58047.867	49001.2	1.00E+00	Fail to Reject Null
75N-0R	-43785.111	-97309.645	9739.422	2.22E-01	Fail to Reject Null
75R-0R	-71488.878	-125013.411	-17964.344	1.26E-03	Significant
100R-100N	-25653.739	-79178.272	27870.795	9.01E-01	Fail to Reject Null
25N-100N	70785.272	17260.739	124309.806	1.48E-03	Significant
25R-100N	36580.05	-16944.484	90104.584	4.88E-01	Fail to Reject Null
50N-100N	46981.828	-6542.706	100506.361	1.43E-01	Fail to Reject Null
50R-100N	16690.717	-36833.817	70215.25	9.96E-01	Fail to Reject Null
5N-100N	92636.383	39111.85	146160.917	6.19E-06	Significant
5R-100N	54148.606	624.072	107673.139	4.48E-02	Significant
75N-100N	14886.828	-38637.706	68411.361	9.99E-01	Fail to Reject Null
75R-100N	-12816.939	-66341.472	40707.595	1.00E+00	Fail to Reject Null
25N-100R	96439.011	42914.478	149963.545	2.21E-06	Significant
25R-100R	62233.789	8709.255	115758.322	9.52E-03	Significant
50N-100R	72635.567	19111.033	126160.1	9.66E-04	Significant
50R-100R	42344.456	-11180.078	95868.989	2.66E-01	Fail to Reject Null
5N-100R	118290.122	64765.589	171814.656	4.91E-09	Significant
5R-100R	79802.344	26277.811	133326.878	1.72E-04	Significant
75N-100R	40540.567	-12983.967	94065.1	3.28E-01	Fail to Reject Null
75R-100R	12836.8	-40687.734	66361.334	1.00E+00	Fail to Reject Null
25R-25N	-34205.222	-87729.756	19319.311	5.92E-01	Fail to Reject Null
50N-25N	-23803.444	-77327.978	29721.089	9.39E-01	Fail to Reject Null
50R-25N	-54094.556	-107619.089	-570.022	4.52E-02	Significant
5N-25N	21851.111	-31673.422	75375.645	9.66E-01	Fail to Reject Null
5R-25N	-16636.667	-70161.2	36887.867	9.96E-01	Fail to Reject Null

75N-25N	-55898.444	-109422.978	-2373.911	3.27E-02	Significant
75R-25N	-83602.211	-137126.745	-30077.678	6.61E-05	Significant
50N-25R	10401.778	-43122.756	63926.311	1.00E+00	Fail to Reject Null
50R-25R	-19889.333	-73413.867	33635.2	9.83E-01	Fail to Reject Null
5N-25R	56056.333	2531.8	109580.867	3.18E-02	Significant
5R-25R	17568.556	-35955.978	71093.089	9.94E-01	Fail to Reject Null
75N-25R	-21693.222	-75217.756	31831.311	9.68E-01	Fail to Reject Null
75R-25R	-49396.989	-102921.522	4127.545	9.91E-02	Fail to Reject Null
50R-50N	-30291.111	-83815.645	23233.422	7.56E-01	Fail to Reject Null
5N-50N	45654.556	-7869.978	99179.089	1.73E-01	Fail to Reject Null
5R-50N	7166.778	-46357.756	60691.311	1.00E+00	Fail to Reject Null
75N-50N	-32095	-85619.534	21429.534	6.83E-01	Fail to Reject Null
75R-50N	-59798.767	-113323.3	-6274.233	1.55E-02	Significant
5N-50R	75945.667	22421.133	129470.2	4.41E-04	Significant
5R-50R	37457.889	-16066.645	90982.422	4.51E-01	Fail to Reject Null
75N-50R	-1803.889	-55328.422	51720.645	1.00E+00	Fail to Reject Null
75R-50R	-29507.656	-83032.189	24016.878	7.85E-01	Fail to Reject Null
5R-5N	-38487.778	-92012.311	15036.756	4.08E-01	Fail to Reject Null
75N-5N	-77749.556	-131274.089	-24225.022	2.85E-04	Significant
75R-5N	-105453.322	-158977.856	-51928.789	1.81E-07	Significant
75N-5R	-39261.778	-92786.311	14262.756	3.77E-01	Fail to Reject Null
75R-5R	-66965.544	-120490.078	-13441.011	3.49E-03	Significant
75R-75N	-27703.767	-81228.3	25820.767	8.46E-01	Fail to Reject Null

Table D.10. Storm-storm Tukey Honest Significance Test results for total inflow volume at J17.

	diff	lwr	upr	p adj	
1.37in_6hr-1.37in_24hr	72989.167	29083.69	116894.64	3.08E-05	Significant
100yr_24hr-1.37in_24hr	3730033.333	3686127.86	3773938.81	3.56E-10	Significant
10yr_24hr-1.37in_24hr	1979616.667	1935711.19	2023522.14	3.56E-10	Significant
1in_24hr-1.37in_24hr	-15833.658	-59739.14	28071.82	9.65E-01	Fail to Reject Null
1in_6hr-1.37in_24hr	-2462.462	-46367.94	41443.02	1.00E+00	Fail to Reject Null
1yr_24hr-1.37in_24hr	658308.333	614402.86	702213.81	3.56E-10	Significant
25yr_24hr-1.37in_24hr	2611616.667	2567711.19	2655522.14	3.56E-10	Significant
5yr_24hr-1.37in_24hr	1563450	1519544.52	1607355.48	3.56E-10	Significant
100yr_24hr-1.37in_6hr	3657044.167	3613138.69	3700949.64	3.56E-10	Significant
10yr_24hr-1.37in_6hr	1906627.5	1862722.02	1950532.98	3.56E-10	Significant

1in_24hr-1.37in_6hr	-88822.825	-132728.3	-44917.35	2.24E-07	Significant
1in_6hr-1.37in_6hr	-75451.629	-119357.11	-31546.15	1.47E-05	Significant
1yr_24hr-1.37in_6hr	585319.167	541413.69	629224.64	3.56E-10	Significant
25yr_24hr-1.37in_6hr	2538627.5	2494722.02	2582532.98	3.56E-10	Significant
5yr_24hr-1.37in_6hr	1490460.833	1446555.36	1534366.31	3.56E-10	Significant
10yr_24hr-100yr_24hr	-1750416.667	-1794322.14	-1706511.19	3.56E-10	Significant
1in_24hr-100yr_24hr	-3745866.992	-3789772.47	-3701961.51	3.56E-10	Significant
1in_6hr-100yr_24hr	-3732495.796	-3776401.27	-3688590.32	3.56E-10	Significant
1yr_24hr-100yr_24hr	-3071725	-3115630.48	-3027819.52	3.56E-10	Significant
25yr_24hr-100yr_24hr	-1118416.667	-1162322.14	-1074511.19	3.56E-10	Significant
5yr_24hr-100yr_24hr	-2166583.333	-2210488.81	-2122677.86	3.56E-10	Significant
1in_24hr-10yr_24hr	-1995450.325	-2039355.8	-1951544.85	3.56E-10	Significant
1in_6hr-10yr_24hr	-1982079.129	-2025984.61	-1938173.65	3.56E-10	Significant
1yr_24hr-10yr_24hr	-1321308.333	-1365213.81	-1277402.86	3.56E-10	Significant
25yr_24hr-10yr_24hr	632000	588094.52	675905.48	3.56E-10	Significant
5yr_24hr-10yr_24hr	-416166.667	-460072.14	-372261.19	3.56E-10	Significant
1in_6hr-1in_24hr	13371.196	-30534.28	57276.67	9.88E-01	Fail to Reject Null
1yr_24hr-1in_24hr	674141.992	630236.51	718047.47	3.56E-10	Significant
25yr_24hr-1in_24hr	2627450.325	2583544.85	2671355.8	3.56E-10	Significant
5yr_24hr-1in_24hr	1579283.658	1535378.18	1623189.14	3.56E-10	Significant
1yr_24hr-1in_6hr	660770.796	616865.32	704676.27	3.56E-10	Significant
25yr_24hr-1in_6hr	2614079.129	2570173.65	2657984.61	3.56E-10	Significant
5yr_24hr-1in_6hr	1565912.462	1522006.98	1609817.94	3.56E-10	Significant
25yr_24hr-1yr_24hr	1953308.333	1909402.86	1997213.81	3.56E-10	Significant
5yr_24hr-1yr_24hr	905141.667	861236.19	949047.14	3.56E-10	Significant
5yr_24hr-25yr_24hr	-1048166.667	-1092072.14	-1004261.19	3.56E-10	Significant

Table D.11. Scenario-scenario Tukey Honest Significance Test results for total inflow volume at J27. Comparisons to the current conditions scenario are highlighted.

diff	lwr	upr	p adj

0R-0N	-58815.556	-136966.4118	19335.301	3.38E-01	Fail to Reject Null
100N-0N	-188491.556	-266642.4118	-110340.699	5.48E-10	Significant
100R-0N	-212899.778	-291050.634	-134748.922	3.58E-10	Significant
25N-0N	-65000	-143150.8562	13150.856	2.01E-01	Fail to Reject Null
25R-0N	-110758.889	-188909.7451	-32608.033	4.51E-04	Significant
50N-0N	-115386.667	-193537.5229	-37235.81	2.08E-04	Significant
50R-0N	-150928.889	-229079.7451	-72778.033	3.25E-07	Significant
5N-0N	-13248.889	-91399.7451	64901.967	1.00E+00	Fail to Reject Null
5R-0N	-69212.222	-147363.0785	8938.634	1.34E-01	Fail to Reject Null
75N-0N	-162593.111	-240743.9674	-84442.255	3.41E-08	Significant
75R-0N	-191085.667	-269236.5229	-112934.81	4.70E-10	Significant
100N-0R	-129676	-207826.8562	-51525.144	1.71E-05	Significant
100R-0R	-154084.222	-232235.0785	-75933.366	1.77E-07	Significant
25N-0R	-6184.444	-84335.3007	71966.412	1.00E+00	Fail to Reject Null
25R-0R	-51943.333	-130094.1896	26207.523	5.32E-01	Fail to Reject Null
50N-0R	-56571.111	-134721.9674	21579.745	3.97E-01	Fail to Reject Null
50R-0R	-92113.333	-170264.1896	-13962.477	7.98E-03	Significant
5N-0R	45566.667	-32584.1896	123717.523	7.20E-01	Fail to Reject Null
5R-0R	-10396.667	-88547.5229	67754.19	1.00E+00	Fail to Reject Null
75N-0R	-103777.556	-181928.4118	-25626.699	1.39E-03	Significant
75R-0R	-132270.111	-210420.9674	-54119.255	1.07E-05	Significant
100R-100N	-24408.222	-102559.0785	53742.634	9.96E-01	Fail to Reject Null
25N-100N	123491.556	45340.6993	201642.412	5.15E-05	Significant
25R-100N	77732.667	-418.1896	155883.523	5.26E-02	Fail to Reject Null
50N-100N	73104.889	-5045.9674	151255.745	8.91E-02	Fail to Reject Null
50R-100N	37562.667	-40588.1896	115713.523	8.99E-01	Fail to Reject Null
5N-100N	175242.667	97091.8104	253393.523	3.11E-09	Significant
5R-100N	119279.333	41128.4771	197430.19	1.07E-04	Significant
75N-100N	25898.444	-52252.4118	104049.301	9.93E-01	Fail to Reject Null
75R-100N	-2594.111	-80744.9674	75556.745	1.00E+00	Fail to Reject Null
25N-100R	147899.778	69748.9215	226050.634	5.80E-07	Significant
25R-100R	102140.889	23990.0326	180291.745	1.79E-03	Significant
50N-100R	97513.111	19362.2549	175663.967	3.63E-03	Significant
50R-100R	61970.889	-16179.9674	140121.745	2.63E-01	Fail to Reject Null
5N-100R	199650.889	121500.0326	277801.745	3.76E-10	Significant
5R-100R	143687.556	65536.6993	221838.412	1.29E-06	Significant
75N-100R	50306.667	-27844.1896	128457.523	5.81E-01	Fail to Reject Null

75R-100R	21814.111	-56336.7451	99964.967	9.99E-01	Fail to Reject Null
25R-25N	-45758.889	-123909.7451	32391.967	7.14E-01	Fail to Reject Null
50N-25N	-50386.667	-128537.5229	27764.19	5.79E-01	Fail to Reject Null
50R-25N	-85928.889	-164079.7451	-7778.033	1.87E-02	Significant
5N-25N	51751.111	-26399.7451	129901.967	5.38E-01	Fail to Reject Null
5R-25N	-4212.222	-82363.0785	73938.634	1.00E+00	Fail to Reject Null
75N-25N	-97593.111	-175743.9674	-19442.255	3.58E-03	Significant
75R-25N	-126085.667	-204236.5229	-47934.81	3.25E-05	Significant
50N-25R	-4627.778	-82778.634	73523.078	1.00E+00	Fail to Reject Null
50R-25R	-40170	-118320.8562	37980.856	8.51E-01	Fail to Reject Null
5N-25R	97510	19359.1438	175660.856	3.63E-03	Significant
5R-25R	41546.667	-36604.1896	119697.523	8.22E-01	Fail to Reject Null
75N-25R	-51834.222	-129985.0785	26316.634	5.35E-01	Fail to Reject Null
75R-25R	-80326.778	-158477.634	-2175.922	3.84E-02	Significant
50R-50N	-35542.222	-113693.0785	42608.634	9.29E-01	Fail to Reject Null
5N-50N	102137.778	23986.9215	180288.634	1.79E-03	Significant
5R-50N	46174.444	-31976.4118	124325.301	7.03E-01	Fail to Reject Null
75N-50N	-47206.444	-125357.3007	30944.412	6.73E-01	Fail to Reject Null
75R-50N	-75699	-153849.8562	2451.856	6.66E-02	Fail to Reject Null
5N-50R	137680	59529.1438	215830.856	3.96E-06	Significant
5R-50R	81716.667	3565.8104	159867.523	3.23E-02	Significant
75N-50R	-11664.222	-89815.0785	66486.634	1.00E+00	Fail to Reject Null
75R-50R	-40156.778	-118307.634	37994.078	8.52E-01	Fail to Reject Null
5R-5N	-55963.333	-134114.1896	22187.523	4.14E-01	Fail to Reject Null
75N-5N	-149344.222	-227495.0785	-71193.366	4.40E-07	Significant
75R-5N	-177836.778	-255987.634	-99685.922	1.99E-09	Significant
75N-5R	-93380.889	-171531.7451	-15230.033	6.65E-03	Significant
75R-5R	-121873.444	-200024.3007	-43722.588	6.83E-05	Significant
75R-75N	-28492.556	-106643.4118	49658.301	9.86E-01	Fail to Reject Null

Table D.12. Storm-storm Tukey Honest Significance Test results for total inflow volume at J06893350.

	diff	lwr	upr	p adj	
1.37in_6hr-1.37in_24hr	172590	108483.87	236696.13	3.68E-10	Significant
100yr_24hr-1.37in_24hr	4033423.33	3969317.2	4097529.46	3.56E-10	Significant
10yr_24hr-1.37in_24hr	2509923.33	2445817.2	2574029.46	3.56E-10	Significant
1in_24hr-1.37in_24hr	-51400.92	-115507.05	12705.21	2.23E-01	Fail to Reject Null

1in_6hr-1.37in_24hr	-7435	-71541.13	56671.13	1.00E+00	Fail to Reject Null
1yr_24hr-1.37in_24hr	1244923.33	1180817.2	1309029.46	3.56E-10	Significant
25yr_24hr-1.37in_24hr	3065173.33	3001067.2	3129279.46	3.56E-10	Significant
5yr_24hr-1.37in_24hr	2140756.67	2076650.54	2204862.8	3.56E-10	Significant
100yr_24hr-1.37in_6hr	3860833.33	3796727.2	3924939.46	3.56E-10	Significant
10yr_24hr-1.37in_6hr	2337333.33	2273227.2	2401439.46	3.56E-10	Significant
1in_24hr-1.37in_6hr	-223990.92	-288097.05	-159884.79	3.56E-10	Significant
1in_6hr-1.37in_6hr	-180025	-244131.13	-115918.87	3.58E-10	Significant
1yr_24hr-1.37in_6hr	1072333.33	1008227.2	1136439.46	3.56E-10	Significant
25yr_24hr-1.37in_6hr	2892583.33	2828477.2	2956689.46	3.56E-10	Significant
5yr_24hr-1.37in_6hr	1968166.67	1904060.54	2032272.8	3.56E-10	Significant
10yr_24hr-100yr_24hr	-1523500	-1587606.13	-1459393.87	3.56E-10	Significant
1in_24hr-100yr_24hr	-4084824.25	-4148930.38	-4020718.12	3.56E-10	Significant
1in_6hr-100yr_24hr	-4040858.33	-4104964.46	-3976752.2	3.56E-10	Significant
1yr_24hr-100yr_24hr	-2788500	-2852606.13	-2724393.87	3.56E-10	Significant
25yr_24hr-100yr_24hr	-968250	-1032356.13	-904143.87	3.56E-10	Significant
5yr_24hr-100yr_24hr	-1892666.67	-1956772.8	-1828560.54	3.56E-10	Significant
1in_24hr-10yr_24hr	-2561324.25	-2625430.38	-2497218.12	3.56E-10	Significant
1in_6hr-10yr_24hr	-2517358.33	-2581464.46	-2453252.2	3.56E-10	Significant
1yr_24hr-10yr_24hr	-1265000	-1329106.13	-1200893.87	3.56E-10	Significant
25yr_24hr-10yr_24hr	555250	491143.87	619356.13	3.56E-10	Significant
5yr_24hr-10yr_24hr	-369166.67	-433272.8	-305060.54	3.56E-10	Significant

1in_6hr-1in_24hr	43965.92	-20140.21	108072.05	4.27E-01	Fail to Reject Null
1yr_24hr-1in_24hr	1296324.25	1232218.12	1360430.38	3.56E-10	Significant
25yr_24hr-1in_24hr	3116574.25	3052468.12	3180680.38	3.56E-10	Significant
5yr_24hr-1in_24hr	2192157.58	2128051.45	2256263.71	3.56E-10	Significant
1yr_24hr-1in_6hr	1252358.33	1188252.2	1316464.46	3.56E-10	Significant
25yr_24hr-1in_6hr	3072608.33	3008502.2	3136714.46	3.56E-10	Significant
5yr_24hr-1in_6hr	2148191.67	2084085.54	2212297.8	3.56E-10	Significant
25yr_24hr-1yr_24hr	1820250	1756143.87	1884356.13	3.56E-10	Significant
5yr_24hr-1yr_24hr	895833.33	831727.2	959939.46	3.56E-10	Significant
5yr_24hr-25yr_24hr	-924416.67	-988522.8	-860310.54	3.56E-10	Significant

Appendix E - Step-by-Step Tomahawk Creek Watershed Model Creation Instructions

PCSWMM Layer	PCSWMM Parameter	Data File	ArcGIS Tool Used	Notes
Subcatchment	Name	-	-	User-defined
	Outlet	LiDAR	-	Created in the PCSWMM delineation process (e.g., pour points)
	Area	LiDAR	Verified with geometry calculator	Created in the delineation process (e.g., "shape_area")
	Slope (%)	LiDAR	Zonal Statistics to find elevation max, Map Algebra Raster to map highest elevation, Raster to Point	(Highest Point Elev – Outlet Elev)/(Length between points) -Length measured two ways: straight line, along flow path
	Flow Length	-	-	Conversation w/ Dr. H, determined to set to 30 m (max overland sheet flow length).
	Width	-	-	Calculated in excel by dividing Sub Area by 30 m (Flow Length)
	Impervious (%)	NLCD 2016 Percent Developed Imperviousness (CONUS)	Conver raster to points, Spatial Join Subcatchments to Impervious Points Layer, Join One-to-One, Set Merge rule for GridCode to mean	This gives us the average % impervious of each subcatchment
	Manning's N	NLCD 2016	Polygon to Raster, NLCD. Tabulate Intersection Tool (Zone Fields: ID, Input Class Features: NLCDPolygon, Class Field: Gridcode).	Pull results of the Tabulate Intersection into excel. This gives the percent area of each gridcode in each subcatchment. Use values in Look-Up Table for LULC to find weighted average.
	Depression Storage	NLCD 2016	Polygon to Raster, NLCD. Tabulate Intersection Tool (Zone Fields: ID, Input	Pull results of the Tabulate Intersection into excel. This gives the percent area of

			Class Features: NLCDPolygon, Class Field: Gridcode).	each gridcode in each subcatchment. Use values in Look-Up Table for LULC to find weighted average.
	Zero Imperv (%)	-	-	User-defined; PCSWMM recommends 25%. Discussion with Dr. H, determined 25%.
	Subarea Routing	-	-	User-defined. PERVIOUS
	PCT Routed			User-defined. Set at 5%
	Suction Head	Soil	Tabulate Intersection Tool to get muname on subcatchment basis. The Web Soil Survey has the corresponding texture type for each soil series.	Use James et al 2010 Soil data table in Dr. Kelsey McDonough's 2018 dissertation for values corresponding to each soil texture. Perform weighted-average in excel. Area not given a soil class (ie water) was not included in area weighting.
	Conductivity	Soil		
	Initial Deficit	Soil		
Junctions	Name	-	-	User-defined
	Location	-	-	User-defined
	Invert Elev.	DEM		Use DEM to set rim elevation.
	Rim Elev. (Ground)	DEM		Subtract the upstream channel depth from the rim elevation of the junction.
	Initial Depth	-	-	User-defined; set to 0.
	Surcharge Depth	-	-	User-defined; set to 0. From PCSWMM Manual- "Additional depth of water beyond the maximum depth that is allowed before the junction floods (feet or meters)."
	Ponded Area	-	-	User-defined; set equal to 50. Make sure that you have "Allow Ponding" enabled in the settings.
Outfalls	Name	-	-	User-defined
	Location	-	-	User-defined
	Invert Elevation	DEM		For surface hydrology, I set this equation to the surface

				elevation of the area where the outlet was.
	Tide Gate			Set to NO.
	Type			Set to FREE.
Storages	Name	-	-	User-defined
	Location	-	-	User-defined
	Invert Elevation	DEM		For surface hydrology, I set this equation to the surface elevation of the area where the outlet was.
	Initial Depth			User-defined; I typically assumed 0.
	Storage Curve	Aerial imagery / DEM	"Measure" tool (in generic toolbar) / Interpolate Line or Polygon tool with Profile Graph in 3D Analyst toolbar	See comment.
Conduits	Name	-	-	User-defined
	Inlet Node	-	-	User-defined
	Outlet Node	-	-	User-defined
	Length	DEM	Measure length tool in GIS	
	Roughness	Aerial imagery	-	Use aerial imagery to observe channel conditions. Values from Soil and Water Conservation Engineering 7th Edition, Huffman et al., Appendix B- Table B.1 Channel: 0.03 (earth bottom, rubble sides) Overbanks: 0.1 (very weedy reaches of natural streams)
*set=0	Inlet Offset			User-defined: 0.
*set=0	Outlet Offset			User-defined: 0.
	Initial Flow			User-defined: 0.
	Cross-Section	Aerial imagery / DEM	-	Use transect creator tool in PCSWMM to create transects at 200 m interval. View transects for each conduit and select the best one. Ignore all others.

Note: The PCSWMM area weighting tool can also be used to determine the parameters determined from the 2016 NLCD or soil texture.

Appendix F - Subcatchment Parameters for Tomahawk Creek Watershed Current Conditions (Scenario 5)

Name	X-Coordinate	Y-Coordinate	Outlet	Area (ha)	Width (m)	Flow Length (m)	Slope (%)	Imperv. (%)	N Imperv	N Perv	Dstore Imperv (mm)	Dstore Perv (mm)	Zero Imperv (%)	Subarea Routing	Percent Routed (%)	Suction Head (mm)	Conductivity (mm/hr)	Initial Deficit (frac.)
5	35820	43092	5B	238.546	79515	30	2.03	41	0.011	0.045	1.194	2.709	25	PERVIOUS	5	206.54	4.52	0.47
6	35646	43085	6B	226.801	75600	30	1.96	56	0.011	0.038	1.199	2.643	25	PERVIOUS	5	199.51	4.89	0.47
7	35492	43084	JA22	115.708	38569	30	2.61	62	0.012	0.035	1.259	2.563	25	PERVIOUS	5	167.47	6.57	0.49
8	35414	43080	7	97.5393	32513	30	2.44	42	0.011	0.046	1.214	2.722	25	PERVIOUS	5	166.88	6.6	0.49
9	35914	43083	9B	200.003	66667	30	3.58	31	0.011	0.054	1.18	2.836	25	PERVIOUS	5	222.3	3.69	0.46
14	35586	43074	14B	148.092	49364	30	3.12	46	0.011	0.04	1.215	2.666	25	PERVIOUS	5	203.67	4.67	0.47
15	35687	43072	15B	97.8414	32613	30	3.96	32	0.011	0.05	1.202	2.772	25	PERVIOUS	5	202.84	4.71	0.47
17	35866	43074	17B	290.107	96702	30	1.75	29	0.012	0.045	1.224	2.69	25	PERVIOUS	5	216.85	3.95	0.46
18	35233	43067	21	267.437	89145	30	2.1	31	0.012	0.041	1.218	2.671	25	PERVIOUS	5	191.83	5.29	0.47
21	35345	43063	43	223.542	74514	30	0.68	37	0.011	0.05	1.215	2.756	25	PERVIOUS	5	208.88	4.39	0.46
22	35455	43067	22B	201.054	67018	30	3.03	49	0.012	0.039	1.224	2.636	25	PERVIOUS	5	181.42	5.84	0.48
23	35573	43057	23B	39.6011	13200	30	2.84	30	0.012	0.034	1.27	2.54	25	PERVIOUS	5	219.34	3.84	0.46
24	35802	43063	24B	285.734	95244	30	3.08	28	0.011	0.047	1.18	2.755	25	PERVIOUS	5	210.28	4.32	0.46
31	35645	43059	31B	309.729	10324	30	2.37	42	0.011	0.041	1.198	2.685	25	PERVIOUS	5	200.79	4.82	0.47

	35007	43053		132.187	44062									PERVIOUS				
32	3.164	32.511	45	9	.63	30	0.97	34	0.009	0.08	0.956	3.325	25		5	210.68	4.3	0.46
	35638	43046	38	96.6	32219					0.03				PERVIOUS				
38	4.385	94.598	B	595	.83	30	0.99	35	0.012	8	1.22	2.63	25		5	168.69	6.51	0.49
	35239	43048	40	330.	11030					0.06				PERVIOUS				
40	6.984	94.128	B	922	7.3	30	0.82	34	0.01	8	1.087	3.087	25		5	198.16	4.96	0.47
	35099	43048	41	193.700	64566					0.05				PERVIOUS				
41	2.687	89.386	B	5	.83	30	1.66	34	0.011	5	1.118	2.921	25		5	211.78	4.24	0.46
	35420	43048	43	223.264	74421					0.04				PERVIOUS				
43	0.536	59.207	B	4	.47	30	1.98	43	0.011	9	1.184	2.792	25		5	190.74	5.35	0.47
	35533	43048	44	161.705	53901					0.04				PERVIOUS				
44	1.311	43.069	B	3	.77	30	2.93	51	0.011	5	1.155	2.772	25		5	180.36	5.89	0.48
	35015	43041	45	104.048	34682					0.08				PERVIOUS				
45	3.137	88.422	B	3	.77	30	2.25	25	0.008	3	0.851	3.524	25		5	203.28	4.69	0.47
	35500	43039		98.9	32982					0.04				PERVIOUS				
46	6.982	29.167	44	485	.83	30	3.7	46	0.011	2	1.16	2.756	25		5	184.02	5.7	0.48
	34789	43036	48	310.415	10347									PERVIOUS				
48	2.927	96.546	B	3	1.8	30	1.3	34	0.011	0.04	1.212	2.667	25		5	184.13	5.7	0.48
	34893	43038	50	265.	88600					0.08				PERVIOUS				
50	0.083	03.95	B	801	.33	30	1.54	25	0.008	2	0.807	3.577	25		5	193.61	5.2	0.47
	35294	43032	51	407.	13581					0.04				PERVIOUS				
51	7.708	43.885	B	449	6.3	30	2.07	33	0.011	6	1.174	2.773	25		5	209.48	4.36	0.46
	34989	43028	53	264.925	88308					0.09				PERVIOUS				
53	0.426	98.87	B	5	.5	30	1.3	13	0.006	1	0.667	3.774	25		5	198.19	4.96	0.47
	35190	43024	56	195.	65256					0.05				PERVIOUS				
56	6.598	16.409	B	77	.67	30	2.13	24	0.01	1	1.083	2.926	25		5	204.17	4.64	0.47
	35113	43018		235.721	78573					0.06				PERVIOUS				
57	6.42	20.603	56	1	.7	30	1.53	15	0.009	4	0.901	3.213	25		5	172.07	6.33	0.48
	35908	43093	J2	8.23						0.25				PERVIOUS				
5B	6.192	38.529	7	8	2746	30	2.03	6	0.004	8	0.429	5.556	25		5	166.878	6.604	0.49
	35736	43076	JB	2.37	792.3					0.03				PERVIOUS				
6B	6.57	42.952	23	7	33	30	1.96	22	0.012	7	1.251	2.592	25		5	166.878	6.604	6.604
	35857	43088	J2	12.0	4033.					0.29				PERVIOUS				
9B	9.402	26.595	6	992	067	30	3.58	6	0.003	7	0.318	6.244	25		5	166.878	6.604	6.604
14	35608	43071	J2	18.5	6169.					0.13				PERVIOUS				
B	6.465	11.01	2	076	2	30	3.12	13	0.007	7	0.736	4.18	25		5	166.878	6.604	6.604
15	35699	43070	J2	13.2						0.25				PERVIOUS				
B	9.063	81.281	3	24	4408	30	3.96	7	0.005	1	0.485	5.557	25		5	166.878	6.604	6.604
17	35802	43078	J2	12.5	4173.					0.24				PERVIOUS				
B	9.103	77.669	5	201	366	30	1.75	6	0.004	1	0.464	5.524	25		5	166.878	6.604	6.604
22	35538	43057	J1	3.74	1247.					0.03				PERVIOUS				
B	2.511	91.223	9	16	2	30	3.03	19	0.012	4	1.27	2.54	25		5	166.878	6.604	6.604

23	35571	43061	J2	6.85	2283.					0.03				PERVIO				
B	8.313	09.07	0	19	967	30	2.84	10	0.012	4	1.27	2.54	25	US	5	166.878	6.604	6.604
24	35751	43075	J2	3.48	1161.					0.25				PERVIO				
B	8.345	18.69	4	41	367	30	3.08	5	0.004	8	0.38	5.791	25	US	5	166.878	6.604	6.604
31	35640	43060	J2	18.1	6048.					0.03				PERVIO				
B	9.455	86.679	1	462	733	30	2.37	20	0.012	4	1.27	2.54	25	US	5	166.878	6.604	6.604
38	35672	43053	JA	0.31	105.3					0.03				PERVIO				
B	2.112	07.105	21	6	33	30	0.99	34	0.012	4	1.27	2.54	25	US	5	166.878	6.604	6.604
40	35254	43045	J1	46.6	15563					0.21				PERVIO				
B	8.274	18.772	6	909	.63	30	0.82	7	0.005	7	0.569	5.144	25	US	5	166.878	6.604	6.604
41	35094	43045	J1	9.74	3248.					0.26				PERVIO				
B	1.553	54.529	5	55	5	30	1.66	1	0.002	2	0.188	5.914	25	US	5	166.878	6.604	6.604
43	35416	43048	J1	13.4	4482.									PERVIO				
B	4.789	12.111	7	472	4	30	1.98	10	0.005	0.22	0.486	5.285	25	US	5	166.878	6.604	6.604
44	35489	43054	J1	8.21	2737.					0.13				PERVIO				
B	6.493	87.446	8	21	367	30	2.93	21	0.008	4	0.852	4.009	25	US	5	166.878	6.604	6.604
45	35016	43042	J1	10.8	3606.									PERVIO				
B	7.742	52.522	4	206	866	30	2.25	5	0.004	0.25	0.42	5.65	25	US	5	166.878	6.604	6.604
48	34856	43038	J1	0.50	168.3					0.21				PERVIO				
B	5.426	17.556	0	51	67	30	1.3	0	0	6	0.008	5.88	25	US	5	166.878	6.604	6.604
50	34897	43038	J1		2563.					0.13				PERVIO				
B	5.543	39.327	2	7.69	333	30	1.54	7	0.003	7	0.355	4.688	25	US	5	166.878	6.604	6.604
51	35288	43034	JA	20.2	6765.					0.09				PERVIO				
B	3.296	83.121	16	976	867	30	2.07	21	0.01	5	1.048	3.391	25	US	5	166.878	6.604	6.604
53	34958	43039	J1	5.50	1836.					0.30				PERVIO				
B	0.516	76.505	3	85	167	30	1.3	3	0.002	5	0.212	6.451	25	US	5	166.878	6.604	6.604
56	35209	43029	JB	0.29						0.03				PERVIO				
B	0.305	06.826	16	1	97	30	2.13	37	0.012	4	1.27	2.54	25	US	5	166.878	6.604	6.604

Appendix G - Subcatchment Parameters for Tomahawk Creek Watershed with Deciduous Forest Riparian Buffer (Scenario 5R)

Name	X-Coordinate	Y-Coordinate	Outlet	Area (ha)	Width (m)	Flow Length (m)	Slope (%)	Imperv. (%)	N Imperv	N Perv	Dstore Imperv (mm)	Dstore Perv (mm)	Zero Imperv (%)	Subarea Routing	Percent Routed (%)	Suction Head (mm)	Conductivity (mm/hr)	Initial Deficit (frac.)
5	35820 6.208	43092 15.869	5B	238. 5463	79515 .43	30	2.03	41	0.011	0.04 5	1.194	2.709	25	PERVIO US	5	206.54	4.52	0.47
6	35646 0.063	43085 79.211	6B	226. 8011	75600 .37	30	1.96	56	0.011	0.03 8	1.199	2.643	25	PERVIO US	5	199.51	4.89	0.47
7	35492 2.027	43084 44.205	JA2 2	115. 7078	38569 .27	30	2.61	62	0.012	0.03 5	1.259	2.563	25	PERVIO US	5	167.47	6.57	0.49
8	35414 3.512	43080 44.391	7	97.5 393	32513 .1	30	2.44	42	0.011	0.04 6	1.214	2.722	25	PERVIO US	5	166.88	6.6	0.49
9	35914 5.908	43083 18.188	9B	200. 003	66667 .67	30	3.58	31	0.011	0.05 4	1.18	2.836	25	PERVIO US	5	222.3	3.69	0.46
14	35586 6.625	43074 55.362	14B	148. 0925	49364 .17	30	3.12	46	0.011	0.04	1.215	2.666	25	PERVIO US	5	203.67	4.67	0.47
15	35687 5.491	43072 37.643	15B	97.8 414	32613 .8	30	3.96	32	0.011	0.05	1.202	2.772	25	PERVIO US	5	202.84	4.71	0.47
17	35866 7.948	43074 31.239	17B	290. 1072	96702 .4	30	1.75	29	0.012	0.04 5	1.224	2.69	25	PERVIO US	5	216.85	3.95	0.46
18	35233 3.723	43067 63.322	21	267. 4367	89145 .57	30	2.1	31	0.012	0.04 1	1.218	2.671	25	PERVIO US	5	191.83	5.29	0.47
21	35345 7.349	43063 88.806	43	223. 5426	74514 .2	30	0.68	37	0.011	0.05	1.215	2.756	25	PERVIO US	5	208.88	4.39	0.46
22	35455 2.154	43067 94.339	22B	201. 0545	67018 .17	30	3.03	49	0.012	0.03 9	1.224	2.636	25	PERVIO US	5	181.42	5.84	0.48
23	35573 5.862	43057 89.215	23B	39.6 011	13200 .37	30	2.84	30	0.012	0.03 4	1.27	2.54	25	PERVIO US	5	219.34	3.84	0.46
24	35802 2.96	43063 03.845	24B	285. 7342	95244 .73	30	3.08	28	0.011	0.04 7	1.18	2.755	25	PERVIO US	5	210.28	4.32	0.46
31	35645 4.08	43059 36.102	31B	309. 7295	10324 3.2	30	2.37	42	0.011	0.04 1	1.198	2.685	25	PERVIO US	5	200.79	4.82	0.47
32	35007 3.164	43053 32.511	45	132. 1879	44062 .63	30	0.97	34	0.009	0.08	0.956	3.325	25	PERVIO US	5	210.68	4.3	0.46
38	35638 4.385	43046 94.598	38B	96.6 595	32219 .83	30	0.99	35	0.012	0.03 8	1.22	2.63	25	PERVIO US	5	168.69	6.51	0.49
40	35239 6.984	43048 94.128	40B	330. 922	11030 7.3	30	0.82	34	0.01	0.06 8	1.087	3.087	25	PERVIO US	5	198.16	4.96	0.47
41	35099 2.687	43048 89.386	41B	193. 7005	64566 .83	30	1.66	34	0.011	0.05 5	1.118	2.921	25	PERVIO US	5	211.78	4.24	0.46
43	35420 0.536	43048 59.207	43B	223. 2644	74421 .47	30	1.98	43	0.011	0.04 9	1.184	2.792	25	PERVIO US	5	190.74	5.35	0.47

	35533	43048		161.	53901					0.04				PERVIO				
44	1.311	43.069	44B	7053	.77	30	2.93	51	0.011	5	1.155	2.772	25	US	5	180.36	5.89	0.48
	35015	43041		104.	34682					0.08				PERVIO				
45	3.137	88.422	45B	0483	.77	30	2.25	25	0.008	3	0.851	3.524	25	US	5	203.28	4.69	0.47
	35500	43039		98.9	32982					0.04				PERVIO				
46	6.982	29.167	44	485	.83	30	3.7	46	0.011	2	1.16	2.756	25	US	5	184.02	5.7	0.48
	34789	43036		310.	10347									PERVIO				
48	2.927	96.546	48B	4153	1.8	30	1.3	34	0.011	0.04	1.212	2.667	25	US	5	184.13	5.7	0.48
	34893	43038		265.	88600					0.08				PERVIO				
50	0.083	03.95	50B	801	.33	30	1.54	25	0.008	2	0.807	3.577	25	US	5	193.61	5.2	0.47
	35294	43032		407.	13581					0.04				PERVIO				
51	7.708	43.885	51B	449	6.3	30	2.07	33	0.011	6	1.174	2.773	25	US	5	209.48	4.36	0.46
	34989	43028		264.	88308					0.09				PERVIO				
53	0.426	98.87	53B	9255	.5	30	1.3	13	0.006	1	0.667	3.774	25	US	5	198.19	4.96	0.47
	35190	43024		195.	65256					0.05				PERVIO				
56	6.598	16.409	56B	77	.67	30	2.13	24	0.01	1	1.083	2.926	25	US	5	204.17	4.64	0.47
	35113	43018		235.	78573					0.06				PERVIO				
57	6.42	20.603	56	7211	.7	30	1.53	15	0.009	4	0.901	3.213	25	US	5	172.07	6.33	0.48
	35908	43093		8.23						0.38				PERVIO		166.87		
5B	6.192	38.529	J27	8	2746	30	2.03	0	0	2	0	7.271	25	US	5	8	6.604	0.49
	35736	43076	JB2	2.37	792.3									PERVIO		166.87		
6B	6.57	42.952	3	7	33	30	1.96	0	0	0.4	0	7.62	25	US	5	8	6.604	6.604
	35857	43088		12.0	4033.									PERVIO		166.87		
9B	9.402	26.595	J26	992	067	30	3.58	0	0	0.4	0	7.62	25	US	5	8	6.604	6.604
14	35608	43071		18.5	6169.					0.39				PERVIO		166.87		
B	6.465	11.01	J22	076	2	30	3.12	0	0	8	0	7.581	25	US	5	8	6.604	6.604
15	35699	43070		13.2						0.39				PERVIO		166.87		
B	9.063	81.281	J23	24	4408	30	3.96	0	0	4	0	7.525	25	US	5	8	6.604	6.604
17	35802	43078		12.5	4173.									PERVIO		166.87		
B	9.103	77.669	J25	201	366	30	1.75	0	0	0.4	0	7.62	25	US	5	8	6.604	6.604
22	35538	43057		3.74	1247.									PERVIO		166.87		
B	2.511	91.223	J19	16	2	30	3.03	0	0	0.4	0	7.62	25	US	5	8	6.604	6.604
23	35571	43061		6.85	2283.									PERVIO		166.87		
B	8.313	09.07	J20	19	967	30	2.84	0	0	0.4	0	7.62	25	US	5	8	6.604	6.604
24	35751	43075		3.48	1161.									PERVIO		166.87		
B	8.345	18.69	J24	41	367	30	3.08	0	0	0.4	0	7.62	25	US	5	8	6.604	6.604
31	35640	43060		18.1	6048.									PERVIO		166.87		
B	9.455	86.679	J21	462	733	30	2.37	0	0	0.4	0	7.62	25	US	5	8	6.604	6.604
38	35672	43053	JA2	0.31	105.3									PERVIO		166.87		
B	2.112	07.105	1	6	33	30	0.99	0	0	0.4	0	7.62	25	US	5	8	6.604	6.604
40	35254	43045		46.6	15563					0.39				PERVIO		166.87		
B	8.274	18.772	J16	909	.63	30	0.82	0	0	7	0	7.58	25	US	5	8	6.604	6.604
41	35094	43045		9.74	3248.					0.38				PERVIO		166.87		
B	1.553	54.529	J15	55	5	30	1.66	0	0	1	0	7.322	25	US	5	8	6.604	6.604
43	35416	43048		13.4	4482.					0.39				PERVIO		166.87		
B	4.789	12.111	J17	472	4	30	1.98	0	0	7	0	7.575	25	US	5	8	6.604	6.604
44	35489	43054		8.21	2737.					0.39				PERVIO		166.87		
B	6.493	87.446	J18	21	367	30	2.93	0	0	8	0	7.587	25	US	5	8	6.604	6.604
45	35016	43042		10.8	3606.					0.39				PERVIO		166.87		
B	7.742	52.522	J14	206	866	30	2.25	0	0	7	0	7.577	25	US	5	8	6.604	6.604

48	34856	43038		0.50	168.3								PERVIO		166.87			
B	5.426	17.556	J10	51	67	30	1.3	0	0	0.4	0	7.62	25	US	5	8	6.604	6.604
50	34897	43038			2563.									PERVIO		166.87		
B	5.543	39.327	J12	7.69	333	30	1.54	0	0	0.4	0	7.62	25	US	5	8	6.604	6.604
51	35288	43034	JA1	20.2	6765.					0.39				PERVIO		166.87		
B	3.296	83.121	6	976	867	30	2.07	0	0	9	0	7.606	25	US	5	8	6.604	6.604
53	34958	43039		5.50	1836.									PERVIO		166.87		
B	0.516	76.505	J13	85	167	30	1.3	0	0	0.4	0	7.62	25	US	5	8	6.604	6.604
56	35209	43029	JB1	0.29										PERVIO		166.87		
B	0.305	06.826	6	1	97	30	2.13	0	0	0.4	0	7.62	25	US	5	8	6.604	6.604

Appendix H - Subcatchment Parameters for Blue River Watershed Current Conditions

(Scenario 5)

Name	X-Coordinate	Y-Coordinate	Outlet	Area (ha)	Width (m)	Flow Length (m)	Slope (%)	Imperv. (%)	N Imperv	N Perv	Dstore Imperv (mm)	Dstore Perv (mm)	Zero Imperv (%)	Subarea Routing	Percent Routed (%)	Suction Head (mm)	Conductivity (mm/hr)	Initial Deficit (frac.)
	36769	43288		1303	14385					0.03				PERVIO		171.84		
1	3	13	J2	.293	13	9.06	8.453	45.319	0.012	4	1.27	2.54	100	US	5	4	6.493	0.368
	37100	43304		84.4	93161		11.27			0.03				PERVIO				
2	0	13	B1	041	.26	9.06	4	60.185	0.012	5	1.257	2.566	100	US	5	197.19	5.08	0.34
	37063	43284		713.	78722		10.37			0.07				PERVIO		189.41		
3	4.2	09	B3	2215	0.2	9.06	3	44.545	0.01	2	1.1	3.108	100	US	5	7	9.9	0.345
	37171	43260		584.	64538		12.36			0.11				PERVIO				
4	8	62	6	7226	9.2	9.06	8	25.948	0.008	9	0.867	3.79	100	US	5	218.4	4.496	0.316
	37011	43254		555.	61348					0.07				PERVIO		199.57		
6	7	67	B6	8167	4.2	9.06	9.582	37.157	0.009	2	0.996	3.219	100	US	5	3	21.991	0.323
	36347	43241		527.	58229					0.03				PERVIO		182.07		
7	1.6	09	B7	5598	5.6	9.06	7.586	53.522	0.012	4	1.27	2.54	100	US	5	8	5.923	0.357
	36506	43231		933.	10305					0.03				PERVIO		188.84		
8	7.9	37	B8	6898	63	9.06	9.39	44.172	0.012	4	1.27	2.54	100	US	5	3	5.545	0.349
	37030	43231		1220	13469		10.46			0.09				PERVIO		208.93		
9	7.7	89	B9	.358	74	9.06	8	31.201	0.009	5	0.999	3.429	100	US	5	2	4.425	0.327
	36130	43225		903.	99731		10.72			0.03				PERVIO		183.38		
10	2	47	B10	5664	3.9	9.06	2	47.358	0.012	4	1.27	2.54	100	US	5	3	5.85	0.355
	37338	43221		689.	76158					0.10				PERVIO		205.36		
11	6.6	97	B11	9921	0.7	9.06	9.395	25.698	0.009	1	0.964	3.472	100	US	5	7	4.624	0.331
	36721	43224		365.	40337									PERVIO		189.43		
12	5.3	13	B12	454	0.9	9.06	9.792	37.942	0.011	0.06	1.149	2.908	100	US	5	2	5.513	0.349
	35749	43206		1202	13272					0.03				PERVIO		170.58		
13	1.8	98	B13	.459	18	9.06	6.15	32.663	0.012	4	1.27	2.54	100	US	5	8	6.563	0.369
	36416	43191		1366	15085					0.03				PERVIO		181.06		
15	4	00	B15	.709	09	9.06	7.028	34.043	0.012	4	1.27	2.54	100	US	5	9	5.979	0.358
	36881	43207		820.	90539		10.72			0.12				PERVIO		210.07		
16	4.2	09	B16	2888	6	9.06	1	21.989	0.009	7	0.91	3.835	100	US	5	4	6.943	0.324
	37365	43205		708.	78175					0.04				PERVIO		179.90		
17	1.8	03	B17	2729	8.2	9.06	7.461	25.273	0.011	7	1.213	2.731	100	US	5	9	6.044	0.359
	35838	43181		1919	21188					0.03				PERVIO				
18	3.8	35	B18	.646	14	9.06	6.72	24.152	0.012	4	1.27	2.54	100	US	5	169.93	6.6	0.37
	36930	43161		851.	94034		12.55			0.16				PERVIO		226.44		
22	5.8	39	B22	9527	5.1	9.06	9	11.561	0.007	8	0.785	4.408	100	US	5	5	3.948	0.307
	36592	43159		792.	87483		10.93							PERVIO		196.04		
23	2.8	48	B23	6017	6.3	9.06	4	22.915	0.009	0.1	0.975	3.499	100	US	5	4	16.658	0.331

	35947	43158		1137	12553					0.03				PERVIO		170.51				
24	2.7	14	B24	.37	75	9.06	6.002	24.898	0.012	4	1.27	2.54	100	US	5	4	6.567	0.369		
	36372	43147		1086	11986					0.07				PERVIO		199.88				
25	6.4	24	B25	.018	96	9.06	8.842	33.423	0.01	3	1.096	3.111	100	US	5	9	14.335	0.329		
	35536	43143		602.	66471					0.03				PERVIO		193.63				
26	5.4	05	B26	2284	1.3	9.06	6.234	39.167	0.012	4	1.27	2.54	100	US	5	2	5.278	0.344		
	36121	43138		645.	71219					0.04				PERVIO		185.17				
27	2.6	91	B27	2492	5.6	9.06	8.342	27.108	0.012	3	1.238	2.66	100	US	5	4	5.75	0.353		
	36804	43138		626.	69172					0.11				PERVIO		226.99				
28	0.2	84	23	7035	5.7	9.06	9.671	24.978	0.007	7	0.703	3.777	100	US	5	3	3.418	0.307		
	35723	43128		869.	96025					0.04				PERVIO		193.71				
29	1	59	B29	9946	9	9.06	6.537	27.414	0.012	1	1.24	2.643	100	US	5	4	5.274	0.344		
	35416	43129		568.	62724					0.03				PERVIO		194.16				
30	2.5	85	B30	2826	3.5	9.06	6.402	33.525	0.012	4	1.27	2.54	100	US	5	2	5.249	0.343		
	35284	43122		810.	89443					0.03				PERVIO						
31	0.1	00	B31	3586	5.5	9.06	6.867	35.551	0.012	6	1.261	2.571	100	US	5	195.81	5.157	0.342		
	36768	43111		1469	16221					0.08				PERVIO						
32	1.6	01	B25	.683	67	9.06	9.324	29.673	0.01	5	1.061	3.26	100	US	5	226.2	3.462	0.308		
	34921	43114		999.	11033					0.03				PERVIO		189.97				
33	0.1	68	B33	5948	06	9.06	6.189	43.975	0.012	6	1.26	2.576	100	US	5	4	5.482	0.348		
	35124	43115		531.	58669					0.04				PERVIO		193.06				
34	8.3	70	B34	5446	3.8	9.06	6.833	42.967	0.012	5	1.22	2.695	100	US	5	1	5.31	0.345		
	36458	43118		505.	55760		12.48							PERVIO		222.23				
36	5.4	13	B36	1897	4.5	9.06	7	16.883	0.008	0.15	0.796	4.19	100	US	5	4	3.683	0.313		
	35516	43100		549.	60634					0.03				PERVIO		202.18				
37	3.5	57	B37	3451	1.2	9.06	6.745	42.902	0.012	6	1.262	2.574	100	US	5	9	4.801	0.335		
	36414	43096		1005	11101									PERVIO		226.70				
38	4.9	58	B38	.794	48	9.06	9.137	15.855	0.008	0.13	0.854	3.885	100	US	5	5	3.434	0.308		
	35197	43090		678.	74854									PERVIO						
39	7.9	29	B39	1839	7.4	9.06	7.276	32.843	0.012	0.04	1.239	2.631	100	US	5	204.28	4.685	0.332		
	34936	43073		1237	13658					0.05				PERVIO		198.66				
41	0.2	12	B41	.459	49	9.06	6.961	26.224	0.011	7	1.121	2.923	100	US	5	3	4.998	0.338		
	36169	43076		699.	77198					0.07				PERVIO		218.94				
42	6.4	74	B42	4186	5.2	9.06	8.381	22.909	0.01	8	1.083	3.161	100	US	5	8	3.867	0.316		
	35514	43078		383.	42289									PERVIO		185.64				
43	4.9	87	B43	1384	0.1	9.06	6.25	45.233	0.012	0.04	1.226	2.647	100	US	5	3	5.724	0.353		
	36562	43076		817.	90204					0.20				PERVIO		237.61				
44	9	13	B44	2488	0.6	9.06	9.867	14.8	0.005	1	0.521	4.835	100	US	5	5	2.826	0.296		
	35567	43055		931.	10278					0.04				PERVIO		190.51				
45	1	32	B45	214	30	9.06	6.551	38.875	0.011	3	1.173	2.735	100	US	5	2	5.452	0.347		
	34649	43067		990.	10928					0.04				PERVIO		198.01				
47	7.6	72	B47	1656	98	9.06	5.835	45.727	0.011	1	1.212	2.673	100	US	5	7	5.034	0.339		
	36483	43053		722.	79800					0.19				PERVIO		227.08				
48	6.3	72	B48	9933	5.8	9.06	8.534	10.576	0.004	1	0.423	5.006	100	US	5	8	3.413	0.307		
	36267	43048		843.	93072					0.16				PERVIO		229.96				
49	6.5	53	B49	236	4.1	9.06	8.62	12.201	0.005	2	0.549	4.556	100	US	5	5	3.252	0.304		
	36075	43047		608.	67188					0.09				PERVIO		207.03				
50	8	45	B50	7311	8.6	9.06	6.469	26.773	0.008	9	0.835	3.655	100	US	5	2	4.531	0.329		
	35002	43041		1666	18394					0.07				PERVIO						
51	5.9	41	B51	.534	41	9.06	5.66	24.377	0.009	9	0.931	3.339	100	US	5	198.91	4.984	0.338		

	34471	43023		827.	91293					0.03				PERVIO		209.09				
53	6	89	B53	1215	7.7	9.06	4.978	37.217	0.012	9	1.222	2.65	100	US	5	1	4.416	0.327		
	34634	43032		504.	55649					0.03				PERVIO		186.74				
54	6.9	48	B54	1844	4.9	9.06	5.248	31.288	0.012	6	1.243	2.598	100	US	5	4	5.662	0.352		
	35801	43034		602.	66473									PERVIO		208.43				
55	9.4	67	B55	2513	6.5	9.06	6.338	21.402	0.01	0.06	1.032	3.07	100	US	5	6	4.453	0.328		
	35628	43016		1592	17581					0.05				PERVIO		216.19				
57	0.9	38	B57	.847	09	9.06	6.365	27.918	0.01	5	1.072	2.95	100	US	5	9	4.02	0.319		
	34712	43009		706.	78002									PERVIO		189.15				
60	2.1	55	J88	7009	3.1	9.06	5.168	24.294	0.009	0.06	0.934	3.079	100	US	5	4	5.528	0.349		
	35032	42994		1579	17429					0.10				PERVIO		199.17				
61	9.4	33	B61	.142	82	9.06	5.343	9.956	0.005	7	0.495	4.137	100	US	5	3	4.969	0.338		
	36234	42991		1494	16497		12.94			0.15				PERVIO		230.00				
63	2.1	57	B63	.718	99	9.06	8	6.324	0.004	1	0.41	4.542	100	US	5	9	3.25	0.304		
	35423	42987		617.	68187					0.10				PERVIO		223.69				
64	4.5	01	B64	7784	4.6	9.06	7.512	14.04	0.006	8	0.624	3.987	100	US	5	3	3.602	0.311		
	35662	42984		1134	12527					0.15				PERVIO		237.51				
65	9.5	03	B65	.958	13	9.06	8.419	10.919	0.004	2	0.472	4.529	100	US	5	1	2.832	0.296		
	34589	42986		1208	13341									PERVIO		206.40				
66	1.4	48	J88	.714	21	9.06	4.652	5.971	0.003	0.13	0.35	4.473	100	US	5	4	4.566	0.33		
	35256	42978		541.	59756					0.13				PERVIO		230.21				
67	2.8	91	B67	3943	5.4	9.06	7.52	5.125	0.003	7	0.287	4.607	100	US	5	9	3.238	0.304		
	36119	42953		1403	15496		10.85			0.17				PERVIO		233.04				
68	6.7	13	B68	.95	13	9.06	3	2.391	0.002	9	0.172	5.127	100	US	5	4	3.081	0.301		
	35903	42956		650.	71849					0.19				PERVIO		228.67				
69	8.3	75	B69	9544	2.7	9.06	6.858	1.984	0.002	6	0.162	5.348	100	US	5	2	3.325	0.305		
	35683	42934		1772	19565					0.14				PERVIO		210.58				
70	5.1	73	B69	.596	08	9.06	6.11	5.782	0.003	9	0.37	4.67	100	US	5	9	4.333	0.325		
	34351	42954		1120	12362					0.14				PERVIO		178.77				
71	8.2	02	B72	.004	07	9.06	3.98	2.444	0.001	4	0.135	4.851	100	US	5	1	6.107	0.36		
	34675	42955		1473	16260					0.13				PERVIO		190.01				
72	1.1	92	B72	.214	64	9.06	4.512	2.118	0.001	4	0.156	4.744	100	US	5	2	5.48	0.348		
	35385	42951		1098	12128					0.16				PERVIO		230.35				
73	5.1	24	B73	.881	93	9.06	7.268	6.792	0.004	4	0.4	4.808	100	US	5	8	3.23	0.304		
	35279	42922		1815	20043					0.13				PERVIO						
74	9.4	50	B74	.983	96	9.06	5.041	4.46	0.003	8	0.265	4.66	100	US	5	203.74	4.715	0.333		
	35036	42935		1055	11647					0.12				PERVIO		218.44				
75	9.2	73	B75	.234	17	9.06	5.25	3.288	0.002	7	0.197	4.648	100	US	5	8	3.895	0.317		
	34802	42934		810.	89452					0.15				PERVIO		202.46				
76	4.1	64	B72	4392	4.5	9.06	4.649	1.909	0.001	4	0.142	5.01	100	US	5	8	4.786	0.334		
	36969	43258			35871					0.05				PERVIO		129.55				
B6	5.7	55	J4	32.5	.97	9.06	9.582	31.1	0.01	7	1.055	2.981	100	US	5	9	44.597	0.383		
	36361	43222		9.01	9946.					0.03				PERVIO		195.82				
B7	8.1	26	J8	15	468	9.06	7.586	48.408	0.012	4	1.27	2.54	100	US	5	9	5.156	0.342		
	36520	43224		24.3	26884					0.03				PERVIO		172.05				
B8	7.5	23	J21	573	.44	9.06	9.39	47.276	0.012	4	1.27	2.54	100	US	5	6	6.481	0.368		
B1	37241	43216		11.7	12965					0.07				PERVIO		248.17				
1	6.9	23	J10	465	.23	9.06	9.395	27.039	0.01	8	1.067	3.126	100	US	5	3	2.237	0.284		
B1	36761	43220	J11	28.6	31641					0.09				PERVIO						
2	2.4	02	8	672	.5	9.06	9.792	27.454	0.008	6	0.83	3.156	100	US	5	169.93	6.6	0.37		

B1	36001	43204		5.91	6527.					0.03				PERVIO					
3	3.3	31	J16	41	704	9.06	6.15	12.506	0.012	4	1.27	2.54	100	US	5	169.93	6.6	0.37	
B1	36639	43220		0.09	99.44					0.03				PERVIO					
5	4.5	51	J21	01	8	9.06	7.028	16.107	0.012	4	1.27	2.54	100	US	5	169.93	6.6	0.37	
B1	36811	43205		23.1	25536		10.72			0.27				PERVIO		152.73			
6	2.1	44	J12	357	.09	9.06	1	12.376	0.003	9	0.355	5.945	100	US	5	3	22.786	0.376	
B1	37277	43211		0.24	274.5					0.36				PERVIO					
7	7.7	45	J18	87	03	9.06	7.461	2.766	0.001	6	0.117	7.152	100	US	5	270	1.02	0.26	
B1	35996	43201		0.35	394.0					0.03				PERVIO					
8	3.1	48	J23	7	4	9.06	6.72	10	0.012	4	1.27	2.54	100	US	5	169.93	6.6	0.37	
B1	36812	43187		27.5	30463		10.97			0.33				PERVIO		170.25			
9	8.9	08	J25	996	.13	9.06	7	1.87	0.001	3	0.071	6.519	100	US	5	1	6.582	0.37	
B2	36652	43154		21.1	23358		10.93			0.20				PERVIO					
3	7.9	26	J32	631	.83	9.06	4	8.353	0.003	8	0.37	5.08	100	US	5	81.205	91.882	0.398	
B2	36015	43148		0.37	414.3					0.03				PERVIO					
4	0.2	44	J36	54	49	9.06	6.002	10	0.012	4	1.27	2.54	100	US	5	169.93	6.6	0.37	
B2	36162	43136	J11	38.8	42900					0.12				PERVIO		175.22			
7	5.6	20	0	676	.22	9.06	8.342	25.166	0.009	1	0.966	3.747	100	US	5	1	6.305	0.364	
B3	35477	43113		15.1	16673					0.03				PERVIO					
0	7.7	59	J43	065	.84	9.06	6.402	21.423	0.012	4	1.27	2.54	100	US	5	169.93	6.6	0.37	
B3	35343	43109		21.6	23845					0.14				PERVIO					
1	5.9	14	J47	037	.14	9.06	6.867	20.678	0.008	8	0.861	4.113	100	US	5	169.93	6.6	0.37	
B3	35042	43109		0.25	283.1					0.10				PERVIO					
3	3.3	11	J49	65	13	9.06	6.189	9.018	0.01	5	1.023	3.528	100	US	5	169.93	6.6	0.37	
B3	36422	43119	J11	42.3	46750		12.48			0.25				PERVIO					
6	9.3	99	9	557	.22	9.06	7	4.628	0.002	9	0.261	5.54	100	US	5	175.7	6.278	0.364	
B3	35591	43116		5.82	6426.					0.11				PERVIO		170.20			
7	2.9	50	J55	22	269	9.06	6.745	11.655	0.009	6	0.987	3.671	100	US	5	9	6.584	0.37	
B3	36379	43094		32.2	35616					0.35				PERVIO		176.40			
8	5.5	08	J53	687	.67	9.06	9.137	0.225	0	8	0.028	7.166	100	US	5	2	6.239	0.363	
B4	36320	43071		14.0	15524					0.35				PERVIO		173.45			
2	6.5	19	J61	656	.95	9.06	8.381	0.924	0.001	9	0.117	7.039	100	US	5	5	6.403	0.366	
B4	36366	43078		11.5	12749					0.38				PERVIO		170.97			
4	4.5	07	J57	507	.12	9.06	9.867	0	0	2	0	7.305	100	US	5	1	6.542	0.369	
B4	34669	43060		33.1	36631					0.18				PERVIO		180.50			
7	4.2	11	J63	882	.57	9.06	5.835	14.26	0.007	8	0.702	4.66	100	US	5	9	6.01	0.358	
B4	36319	43065		0.11	129.2									PERVIO					
8	7.4	12	J69	71	49	9.06	8.534	0	0	0.4	0	7.62	100	US	5	169.93	6.6	0.37	
B4	36277	43053		33.2	36651					0.34				PERVIO		172.42			
9	9.1	94	J69	063	.54	9.06	8.62	2.587	0.001	7	0.126	6.937	100	US	5	1	6.461	0.367	
B5	35366	43045		0.29	328.3					0.12				PERVIO					
1	3.9	41	J77	75	66	9.06	5.66	17.533	0.005	6	0.576	4.304	100	US	5	169.93	6.6	0.37	
B5	36095	43029		6.45	7121.					0.36				PERVIO					
2	0.5	19	J81	24	854	9.06	7.189	1.111	0.001	5	0.122	7.133	100	US	5	173.81	6.384	0.366	
B5	34578	43048		0.21	242.4					0.03				PERVIO		207.11			
3	9.5	03	J75	97	94	9.06	4.978	10	0.012	4	1.27	2.54	100	US	5	3	4.527	0.329	
B5	34580	43047		0.20	221.4					0.14				PERVIO					
4	8.1	64	J75	06	13	9.06	5.248	6.855	0.008	9	0.871	4.138	100	US	5	169.93	6.6	0.37	
B5	35991	43022		0.08										PERVIO					
5	0.1	01	J79	27	91.28	9.06	6.338	0	0	0.4	0	7.62	100	US	5	169.93	6.6	0.37	

B5	35365	43045		0.10	115.4					0.20				PERVIO					
6	3.6	02	J77	46	52	9.06	6.535	15.506	0.006	5	0.656	4.942	100	US	5	169.93	6.6	0.37	
B5	35992	43021		0.11	122.0									PERVIO					
7	9.7	86	J79	06	75	9.06	6.365	0	0	0.4	0	7.62	100	US	5	169.93	6.6	0.37	
B6	35003	42988		44.8	49486									PERVIO		178.18			
1	4.3	67	J92	351	.86	9.06	5.343	1.196	0.001	0.25	0.105	6.039	100	US	5	6	6.14	0.361	
B6	36058	43014		0.39	433.4		12.94			0.38				PERVIO					
3	6.5	32	J90	27	44	9.06	8	0	0	7	0	7.477	100	US	5	169.93	6.6	0.37	
B6	35955	42955		0.29	320.1		10.85							PERVIO		199.00			
8	7.2	65	J99	01	99	9.06	3	0	0	0.4	0	7.62	100	US	5	6	4.979	0.338	
B7	35150	42953	J10	6.35	7013.					0.36				PERVIO		172.08			
4	5	05	9	42	466	9.06	5.041	0	0	6	0	7.261	100	US	5	9	6.48	0.368	
B7	35041	42951	J10	19.1	21102									PERVIO		188.38			
5	3.3	22	5	19	.65	9.06	5.25	0	0	0.31	0	6.765	100	US	5	7	5.571	0.35	
B3	35170	43105	J11	32.7	36193					0.21				PERVIO		171.78			
4	7.6	73	2	915	.71	9.06	6.837	14.998	0.006	3	0.612	5.058	100	US	5	7	6.496	0.368	
	35799	43083		1726	19058					0.04				PERVIO		211.61			
81	8.3	92	B81	.656	01	9.06	7.401	35.625	0.011	8	1.193	2.754	100	US	5	3	4.276	0.324	
B2	35683	43112		15.1	16677					0.31				PERVIO		177.82			
9	8.9	69	J45	095	.15	9.06	6.545	4.684	0.002	3	0.221	6.342	100	US	5	1	6.16	0.361	
B3	35207	43091	J11	36.0	39764					0.16				PERVIO		170.41			
9	2.3	99	2	262	.02	9.06	7.276	10.718	0.007	8	0.75	4.45	100	US	5	3	6.573	0.369	
	36068	43112		1450	16013					0.04				PERVIO		206.02			
35	9.4	62	B35	.829	57	9.06	8.032	27.26	0.011	8	1.205	2.741	100	US	5	5	4.587	0.33	
B2	36523	43137	J11	26.9	29769					0.21				PERVIO					
5	8.7	98	3	716	.98	9.06	8.847	7.923	0.003	3	0.322	5.01	100	US	5	88.461	91.446	0.39	
	36614	43178		350.	38660					0.07				PERVIO		181.32			
83	4.5	47	B83	2684	9.7	9.06	8.744	26.782	0.011	6	1.114	3.125	100	US	5	6	5.965	0.357	
	36950	43174		391.	43249		12.02			0.15				PERVIO		232.12			
20	9.4	86	B20	8416	6.3	9.06	2	12.647	0.008	3	0.809	4.18	100	US	5	2	3.132	0.302	
	36948	43189		995.	10989		10.97			0.11				PERVIO					
21	9.8	17	B19	6401	40	9.06	7	22.725	0.009	7	0.925	3.702	100	US	5	211.44	4.285	0.324	
	37053	43305	J12	12.2	13479					0.03				PERVIO					
B1	4.7	15	0	12	.03	9.06	8.504	46.005	0.012	4	1.27	2.54	100	US	5	169.93	6.6	0.37	
	37074	43285		44.3	48997		10.37							PERVIO					
B3	1.3	88	J2	917	.46	9.06	8	57.319	0.011	0.04	1.21	2.679	100	US	5	49.02	120.4	0.41	
B5	36043	43019	J11	22.1	24477					0.22				PERVIO					
8	6.3	83	4	77	.93	9.06	5.53	3.527	0.003	6	0.284	5.487	100	US	5	169.93	6.6	0.37	
	35915	42993		488.	53932					0.14				PERVIO		226.85			
62	6.9	69	B62	6266	2.9	9.06	9.106	7.979	0.004	7	0.467	4.552	100	US	5	3	3.426	0.307	
B6	35287	42977	J11	33.3	36801					0.29				PERVIO		178.39			
7	3.8	17	5	419	.21	9.06	7.52	1.259	0.001	1	0.077	6.425	100	US	5	4	6.128	0.361	
B7	35316	42958	J11	38.0	42010									PERVIO		189.17			
3	8.8	85	5	612	.15	9.06	7.27	1.176	0.001	0.33	0.073	6.82	100	US	5	9	5.527	0.349	
B7	34718	42951	J10	65.7	72582					0.20				PERVIO		182.52			
2	5.8	87	3	595	.23	9.06	4.51	3.377	0.003	6	0.369	5.238	100	US	5	6	5.898	0.356	
	36017	43015		157.	17423					0.11				PERVIO		193.88			
58	1.8	40	B58	8552	3.1	9.06	5.427	5.875	0.004	8	0.375	4.32	100	US	5	5	5.264	0.344	
	36265	43019		691.	76304					0.16				PERVIO		242.61			
59	6	61	B59	3164	2.4	9.06	8.757	4.616	0.002	6	0.242	4.919	100	US	5	7	2.547	0.29	

B6	35711	42984	J11	58.9	65073					0.32				PERVIO		180.92			
5	2.6	06	6	57	.95	9.06	8.427	0.604	0	7	0.05	6.709	100	US	5	7	5.987	0.358	
B6	35937	43001		45.0	49688					0.18				PERVIO					
2	7.5	91	J90	176	.3	9.06	8.773	7.693	0.005	1	0.526	4.822	100	US	5	175.28	6.302	0.364	
	35973	43040		367.	40519					0.08				PERVIO		212.94			
52	7.4	30	B52	1045	2.6	9.06	7.189	22.235	0.008	2	0.898	3.406	100	US	5	8	4.201	0.323	
B5	36163	43037		24.3	26889									PERVIO					
0	5.1	03	J73	618	.4	9.06	6.473	3.562	0.001	0.32	0.148	6.642	100	US	5	170.17	6.587	0.37	
B8	36795	43172		6.24	6889.		11.56			0.24				PERVIO					
3	4.2	53	J29	21	735	9.06	9	5.884	0.005	8	0.482	5.486	100	US	5	169.93	6.6	0.37	
B2	36751	43167		20.2	22340		11.56			0.34				PERVIO		147.28			
2	3	60	J34	405	.51	9.06	9	5.034	0.002	2	0.18	6.83	100	US	5	6	27.912	0.377	
	36245	43207		569.	62831					0.03				PERVIO		188.95			
96	7.7	09	B96	2556	7.5	9.06	6.932	33.07	0.012	4	1.27	2.54	100	US	5	1	5.539	0.349	
B1	36119	43217	J88	34.2	37823		10.69			0.03				PERVIO		171.98			
0	9.2	44	78	679	.29	9.06	4	35.015	0.012	4	1.27	2.54	100	US	5	4	6.485	0.368	
	36924	43238		17.3	19117		10.14			0.04				PERVIO					
B5	3.8	58	J6	201	.11	9.06	2	39.079	0.011	4	1.172	2.735	100	US	5	169.93	6.6	0.37	
B6	35873	42966		31.3	34593									PERVIO		193.10			
9	6.9	70	J99	421	.93	9.06	6.857	1.333	0.001	0.35	0.096	6.916	100	US	5	4	5.308	0.345	
B6	35464	42972		17.8	19692					0.29				PERVIO		180.65			
4	6.8	12	J94	414	.5	9.06	7.512	2.261	0.002	8	0.164	6.308	100	US	5	5	6.002	0.358	
	37012	43227	J11	49.5	54730		10.14			0.21				PERVIO					
B9	8	61	1	861	.8	9.06	2	12.321	0.005	5	0.484	5.282	100	US	5	179.73	6.054	0.359	
B3	36128	43113	J11	55.1	60883					0.12				PERVIO		173.68			
5	3.5	60	0	602	.22	9.06	8.05	20.073	0.008	4	0.825	3.86	100	US	5	1	6.391	0.366	
B4	35644	43066		5.30	5851.					0.10				PERVIO		172.75			
3	4.6	61	J65	19	987	9.06	6.25	7.494	0.006	7	0.668	3.93	100	US	5	1	6.443	0.367	
	35322	43061		680.	75131					0.04				PERVIO					
46	2.9	77	B46	6951	9.1	9.06	6.432	33.478	0.011	5	1.213	2.707	100	US	5	196.31	5.129	0.341	
B4	35549	43059		24.1	26639					0.06				PERVIO		176.05			
5	1.2	39	J67	352	.29	9.06	6.551	16.621	0.011	3	1.134	2.985	100	US	5	6	6.258	0.363	
	35234	43027		937.	10348					0.05				PERVIO					
56	7.5	53	B56	6065	86	9.06	6.535	22.912	0.01	3	1.067	2.946	100	US	5	200.96	4.87	0.336	
B4	35416	43048		13.2	14618					0.20				PERVIO					
6	5.2	20	J71	442	.32	9.06	6.432	11.504	0.005	1	0.563	4.983	100	US	5	169.93	6.6	0.37	
B4	34927	43075		50.0	55250					0.24				PERVIO		173.53			
1	8.2	50	J59	569	.44	9.06	6.961	10.487	0.004	9	0.468	5.496	100	US	5	8	6.399	0.366	
B2	36777	43177		13.9	15426		11.97			0.38				PERVIO					
0	8.8	45	J27	761	.16	9.06	6	1.08	0.001	4	0.054	7.399	100	US	5	169.93	6.6	0.37	
B2	35551	43117		5.24	5793.					0.03				PERVIO		180.19			
6	1.3	17	J41	9	598	9.06	6.24	29.534	0.012	4	1.27	2.54	100	US	5	4	6.028	0.359	
B8	35824	43090	J11	79.6	87956					0.22				PERVIO		178.69			
1	4.4	50	7	883	.18	9.06	7.416	10.244	0.005	8	0.551	5.239	100	US	5	7	6.111	0.36	
B9	36290	43223		4.91	5422.		10.69			0.03				PERVIO		170.26			
6	2.7	61	J14	32	958	9.06	4	56.654	0.012	4	1.27	2.54	100	US	5	3	6.581	0.37	
	36810	43251		862.	95216					0.04				PERVIO					
5	4.1	14	B5	6652	9.1	9.06	9.264	43.433	0.012	4	1.223	2.686	100	US	5	196.97	5.092	0.34	
B5	36057	43025		8.27	9128.					0.27				PERVIO					
9	1.8	54	J84	02	256	9.06	8.693	2.223	0.003	5	0.281	6.052	100	US	5	169.93	6.6	0.37	

Appendix I - Subcatchment Parameters for Blue River Watershed Model with Riparian Buffers (Scenario 5R)

Name	X-Coordinate	Y-Coordinate	Outlet	Area (ha)	Width (m)	Flow Length (m)	Slope (%)	Imperv. (%)	N Imperv	N Perv	Dstore Imperv (mm)	Dstore Perv (mm)	Zero Imperv (%)	Subarea Routing	Percent Routed (%)	Suction Head (mm)	Conductivity (mm/hr)	Initial Deficit (frac.)
1	367693	4328813	J2	130 3.293	143851 3	9.06	8.453	45.319	0.012	0.034	1.27	2.54	150.476	PERVIOUS	5	168.931	6.493	0.485
2	371000	4330413	B1	84.4041	93161.26	9.06	11.274	60.185	0.012	0.035	1.257	2.566	150.476	PERVIOUS	5	195.83	5.075	0.471
3	370634.2	4328409	B3	713.2215	787220.2	9.06	10.373	44.545	0.01	0.072	1.1	3.108	150.476	PERVIOUS	5	188.028	9.895	0.47
4	371718	4326062	6	584.722 6	645389.2	9.06	12.368	25.948	0.008	0.119	0.867	3.79	150.476	PERVIOUS	5	218.4	4.486	0.459
6	370117	4325467	B6	555.816 7	613484.2	9.06	9.582	37.157	0.009	0.072	0.996	3.219	150.476	PERVIOUS	5	200.097	21.982	0.449
7	363471.6	4324109	B7	527.559 8	582295.6	9.06	7.586	53.522	0.012	0.034	1.27	2.54	150.476	PERVIOUS	5	179.793	5.92	0.479
8	365067.9	4323137	B8	933.689 8	103056 3	9.06	9.39	44.172	0.012	0.034	1.27	2.54	150.476	PERVIOUS	5	186.972	5.542	0.476
9	370307.7	4323189	B9	122 0.358	134697 4	9.06	10.468	31.201	0.009	0.095	0.999	3.429	150.476	PERVIOUS	5	208.291	4.417	0.465
10	361302	4322547	B10	903.566 4	997313.9	9.06	10.722	47.358	0.012	0.034	1.27	2.54	150.476	PERVIOUS	5	181.172	5.847	0.479
11	373386.6	4322197	B11	689.992 1	761580.7	9.06	9.395	25.698	0.009	0.101	0.964	3.472	150.476	PERVIOUS	5	204.507	4.617	0.467
12	367215.3	4322413	B12	365.454 2	403370.9	9.06	9.792	37.942	0.011	0.06	1.149	2.908	150.476	PERVIOUS	5	187.596	5.509	0.475
13	357491.8	4320698	B13	120 2.459	132721 8	9.06	6.15	32.663	0.012	0.034	1.27	2.54	150.476	PERVIOUS	5	167.599	6.563	0.486
15	364164	4319100	B15	136 6.709	150850 9	9.06	7.028	34.043	0.012	0.034	1.27	2.54	150.476	PERVIOUS	5	178.721	5.977	0.48

	36881	43207	B1	820.288			10.72			0.12			150.476	PERVIOUS		209.767		
16	4.2	09	6	8	905396	9.06	1	21.989	0.009	7	0.91	3.835	6	US	5	7	6.934	0.461
	37365	43205	B1	708.272	781758					0.04			150.476	PERVIOUS		177.491		
17	1.8	03	7	9	.2	9.06	7.461	25.273	0.011	7	1.213	2.731	6	US	5	1	6.042	0.481
	35838	43181	B1	191	211881					0.03			150.476	PERVIOUS				
18	3.8	35	8	9.646	4	9.06	6.72	24.152	0.012	4	1.27	2.54	6	US	5	166.9	6.6	0.486
	36930	43161	B2	851.952	940345		12.55			0.16			150.476	PERVIOUS		226.875		
22	5.8	39	2	7	.1	9.06	9	11.561	0.007	8	0.785	4.408	6	US	5	5	3.939	0.455
	36592	43159	B2	792.601	874836		10.93						150.476	PERVIOUS		195.788		
23	2.8	48	3	7	.3	9.06	4	22.915	0.009	0.1	0.975	3.499	6	US	5	8	16.65	0.457
	35947	43158	B2	113	125537					0.03			150.476	PERVIOUS		167.519		
24	2.7	14	4	7.37	5	9.06	6.002	24.898	0.012	4	1.27	2.54	6	US	5	9	6.567	0.486
	36372	43147	B2	108	119869					0.07			150.476	PERVIOUS		199.653		
25	6.4	24	5	6.018	6	9.06	8.842	33.423	0.01	3	1.096	3.111	6	US	5	3	14.327	0.458
	35536	43143	B2	602.228	664711					0.03			150.476	PERVIOUS		192.049		
26	5.4	05	6	4	.3	9.06	6.234	39.167	0.012	4	1.27	2.54	6	US	5	9	5.274	0.473
	36121	43138	B2	645.249	712195					0.04			150.476	PERVIOUS		183.078		
27	2.6	91	7	2	.6	9.06	8.342	27.108	0.012	3	1.238	2.66	6	US	5	8	5.747	0.478
	36804	43138		626.703	691725					0.11			150.476	PERVIOUS		227.458		
28	0.2	84	23	5	.7	9.06	9.671	24.978	0.007	7	0.703	3.777	6	US	5	8	3.407	0.455
	35723	43128	B2	869.994						0.04			150.476	PERVIOUS		192.135		
29	1	59	9	6	960259	9.06	6.537	27.414	0.012	1	1.24	2.643	6	US	5	5	5.269	0.473
	35416	43129	B3	568.282	627243					0.03			150.476	PERVIOUS		192.616		
30	2.5	85	0	6	.5	9.06	6.402	33.525	0.012	4	1.27	2.54	6	US	5	6	5.244	0.473
	35284	43122	B3	810.358	894435					0.03			150.476	PERVIOUS		194.365		
31	0.1	00	1	6	.5	9.06	6.867	35.551	0.012	6	1.261	2.571	6	US	5	5	5.152	0.472
	36768	43111	B2	146	162216					0.08			150.476	PERVIOUS		226.617		
32	1.6	01	5	9.683	7	9.06	9.324	29.673	0.01	5	1.061	3.26	6	US	5	7	3.451	0.456
	34921	43114	B3	999.594	110330					0.03			150.476	PERVIOUS		188.171		
33	0.1	68	3	8	6	9.06	6.189	43.975	0.012	6	1.26	2.576	6	US	5	1	5.478	0.475
	35124	43115	B3	531.544	586693					0.04			150.476	PERVIOUS		191.444		
34	8.3	70	4	6	.8	9.06	6.833	42.967	0.012	5	1.22	2.695	6	US	5	4	5.306	0.474
	36458	43118	B3	505.189	557604		12.48			0.15			150.476	PERVIOUS		222.408		
36	5.4	13	6	7	.5	9.06	7	16.883	0.008		0.796	4.19	6	US	5		3.673	0.458

37	35516 3.5	43100 57	B3 7	549. 345 1	606341 .2	9.06	6.745	42.902	0.012	0.03 6	1.262	2.574	150.47 6	PERVIO US	5	201.13 6	4.795	0.469
38	36414 4.9	43096 58	B3 8	100 5.79 4	111014 8	9.06	9.137	15.855	0.008	0.13	0.854	3.885	150.47 6	PERVIO US	5	227.15 3	3.423	0.455
39	35197 7.9	43090 29	B3 9	678. 183 9	748547 .4	9.06	7.276	32.843	0.012	0.04	1.239	2.631	150.47 6	PERVIO US	5	203.35	4.678	0.467
41	34936 0.2	43073 12	B4 1	123 7.45 9	136584 9	9.06	6.961	26.224	0.011	0.05 7	1.121	2.923	150.47 6	PERVIO US	5	197.39 1	4.992	0.47
42	36169 6.4	43076 74	B4 2	699. 418 6	771985 .2	9.06	8.381	22.909	0.01	0.07 8	1.083	3.161	150.47 6	PERVIO US	5	218.92 1	3.857	0.46
43	35514 4.9	43078 87	B4 3	383. 138 4	422890 .1	9.06	6.25	45.233	0.012	0.04	1.226	2.647	150.47 6	PERVIO US	5	183.57 6	5.721	0.478
44	36562 9	43076 13	B4 4	817. 248 8	902040 .6	9.06	9.867	14.8	0.005	0.20 1	0.521	4.835	150.47 6	PERVIO US	5	238.73 1	2.812	0.449
45	35567 1	43055 32	B4 5	931. 214 0	102783 0	9.06	6.551	38.875	0.011	0.04 3	1.173	2.735	150.47 6	PERVIO US	5	188.73 3	5.449	0.475
47	34649 7.6	43067 72	B4 7	990. 165 6	109289 8	9.06	5.835	45.727	0.011	0.04 1	1.212	2.673	150.47 6	PERVIO US	5	196.70 8	5.028	0.471
48	36483 6.3	43053 72	B4 8	722. 993 3	798005 .8	9.06	8.534	10.576	0.004	0.19 1	0.423	5.006	150.47 6	PERVIO US	5	227.55 9	3.401	0.455
49	36267 6.5	43048 53	B4 9	843. 236 1	930724 .1	9.06	8.62	12.201	0.005	0.16 2	0.549	4.556	150.47 6	PERVIO US	5	230.61 2	3.24	0.454
50	36075 8	43047 45	B5 0	608. 731 1	671888 .6	9.06	6.469	26.773	0.008	0.09 9	0.835	3.655	150.47 6	PERVIO US	5	206.27 1	4.524	0.466
51	35002 5.9	43041 41	B5 1	166 6.53 4	183944 1	9.06	5.66	24.377	0.009	0.07 9	0.931	3.339	150.47 6	PERVIO US	5	197.65 5	4.978	0.47
53	34471 6	43023 89	B5 3	827. 121 5	912937 .7	9.06	4.978	37.217	0.012	0.03 9	1.222	2.65	150.47 6	PERVIO US	5	208.46	4.409	0.465
54	34634 6.9	43032 48	B5 4	504. 184 4	556494 .9	9.06	5.248	31.288	0.012	0.03 6	1.243	2.598	150.47 6	PERVIO US	5	184.74 4	5.659	0.477
55	35801 9.4	43034 67	B5 5	602. 251 3	664736 .5	9.06	6.338	21.402	0.01	0.06	1.032	3.07	150.47 6	PERVIO US	5	207.76 5	4.445	0.465
57	35628 0.9	43016 38	B5 7	159 2.84 7	175810 9	9.06	6.365	27.918	0.01	0.05 5	1.072	2.95	150.47 6	PERVIO US	5	216.00 3	4.011	0.461

	34712	43009	J8	706.700	780023								150.476	PERVIOUS	5	187.302		
60	2.1	55	8	9	.1	9.06	5.168	24.294	0.009	0.06	0.934	3.079					5.524	0.476
	35032	42994	B6	157	174298					0.10			150.476	PERVIOUS	5	197.935		
61	9.4	33	1	9.142	2	9.06	5.343	9.956	0.005	7	0.495	4.137					4.964	0.47
	36234	42991	B6	149	164979		12.94			0.15			150.476	PERVIOUS				
63	2.1	57	3	4.718	9	9.06	8	6.324	0.004	1	0.41	4.542			5	230.66	3.238	0.454
	35423	42987	B6	617.	681874					0.10			150.476	PERVIOUS		223.93		
64	4.5	01	4	7784	.6	9.06	7.512	14.04	0.006	8	0.624	3.987			5	7	3.592	0.457
	35662	42984	B6	113	125271					0.15			150.476	PERVIOUS		238.477		
65	9.5	03	5	4.958	3	9.06	8.419	10.919	0.004	2	0.472	4.529			5		2.826	0.45
	34589	42986	J8	120	133412								150.476	PERVIOUS		205.608		
66	1.4	48	8	8.714	1	9.06	4.652	5.971	0.003	0.13	0.35	4.473			5		4.559	0.466
	35256	42978	B6	541.	597565					0.13			150.476	PERVIOUS		230.882		
67	2.8	91	7	3943	.4	9.06	7.52	5.125	0.003	7	0.287	4.607			5		3.226	0.453
	36119	42953	B6	140	154961		10.85			0.17			150.476	PERVIOUS				
68	6.7	13	8	3.953	3	9.06	3	2.391	0.002	9	0.172	5.127			5	233.88	3.068	0.452
	35903	42956	B6	650.	718492					0.19			150.476	PERVIOUS				
69	8.3	75	9	9544	.7	9.06	6.858	1.984	0.002	6	0.162	5.348			5	229.24	3.313	0.454
	35683	42934	B6	177	195650					0.14			150.476	PERVIOUS		210.049		
70	5.1	73	9	2.596	8	9.06	6.11	5.782	0.003	9	0.37	4.67			5		4.325	0.464
	34351	42954	B7	112	123620					0.14			150.476	PERVIOUS		176.283		
71	8.2	02	2	0.004	7	9.06	3.98	2.444	0.001	4	0.135	4.851			5		6.105	0.481
	34675	42955	B7	147	162606					0.13			150.476	PERVIOUS		188.212		
72	1.1	92	2	3.214	4	9.06	4.512	2.118	0.001	4	0.156	4.744			5		5.476	0.475
	35385	42951	B7	109	121289					0.16			150.476	PERVIOUS		231.029		
73	5.1	24	3	8.881	3	9.06	7.268	6.792	0.004	4	0.4	4.808			5		3.218	0.453
	35279	42922	B7	181	200439					0.13			150.476	PERVIOUS		202.781		
74	9.4	50	4	5.983	6	9.06	5.041	4.46	0.003	8	0.265	4.66			5		4.708	0.468
	35036	42935	B7	105	116471					0.12			150.476	PERVIOUS				
75	9.2	73	5	5.234	7	9.06	5.25	3.288	0.002	7	0.197	4.648			5	218.39	3.885	0.46
	34802	42934	B7	810.	894524					0.15			150.476	PERVIOUS		201.431		
76	4.1	64	2	4392	.5	9.06	4.649	1.909	0.001	4	0.142	5.01			5		4.779	0.468
	36969	43258			35871.					0.39			150.476	PERVIOUS		127.701		
B6	5.7	55	J4	32.5	97	9.06	9.582	0	0	9	0	7.62			5		44.597	0.463

	36361	43222		9.01	9946.4							150.47	PERVIO		194.38				
B7	8.1	26	J8	15	68	9.06	7.586	0	0	0.4	0	7.62	6	US	5	6	5.151	0.472	
	36520	43224	J2	24.3	26884.							150.47	PERVIO		169.15				
B8	7.5	23	1	573	44	9.06	9.39	0	0	0.4	0	7.62	6	US	5	6	6.481	0.485	
B1	37241	43216	J1	11.7	12965.					0.38			150.47	PERVIO		249.93			
1	6.9	23	0	465	23	9.06	9.395	0	0	6	0	7.395	6	US	5	6	2.221	0.444	
B1	36761	43220	J1	28.6	31641.					0.34			150.47	PERVIO					
2	2.4	02	18	672	5	9.06	9.792	0	0	4	0	6.558	6	US	5	166.9	6.6	0.486	
B1	36001	43204	J1	5.91	6527.7								150.47	PERVIO					
3	3.3	31	6	41	04	9.06	6.15	0	0	0.4	0	7.62	6	US	5	166.9	6.6	0.486	
B1	36639	43220	J2	0.09									150.47	PERVIO					
5	4.5	51	1	01	99.448	9.06	7.028	0	0	0.4	0	7.62	6	US	5	166.9	6.6	0.486	
B1	36811	43205	J1	23.1	25536.		10.72			0.39			150.47	PERVIO		150.20			
6	2.1	44	2	357	09	9.06	1	0	0	2	0	7.464	6	US	5	2	22.786	0.476	
B1	37277	43211	J1	0.24	274.50								150.47	PERVIO					
7	7.7	45	8	87	3	9.06	7.461	0	0	0.4	0	7.62	6	US	5	273.1	1	0.432	
B1	35996	43201	J2	0.35									150.47	PERVIO					
8	3.1	48	3	7	394.04	9.06	6.72	0	0	0.4	0	7.62	6	US	5	166.9	6.6	0.486	
B1	36812	43187	J2	27.5	30463.		10.97						150.47	PERVIO		167.23			
9	8.9	08	5	996	13	9.06	7	0	0	0.36	0	6.863	6	US	5	3	6.582	0.486	
B2	36652	43154	J3	21.1	23358.		10.93			0.38			150.47	PERVIO					
3	7.9	26	2	631	83	9.06	4	0	0	4	0	7.318	6	US	5	80.931	91.881	0.433	
B2	36015	43148	J3	0.37	414.34								150.47	PERVIO					
4	0.2	44	6	54	9	9.06	6.002	0	0	0.4	0	7.62	6	US	5	166.9	6.6	0.486	
B2	36162	43136	J1	38.8	42900.					0.39			150.47	PERVIO		172.51			
7	5.6	20	10	676	22	9.06	8.342	0	0	9	0	7.611	6	US	5	5	6.304	0.483	
B3	35477	43113	J4	15.1	16673.								150.47	PERVIO		167.20			
0	7.7	59	3	065	84	9.06	6.402	0	0	0.4	0	7.62	6	US	5	1	6.584	0.486	
B3	35343	43109	J4	21.6	23845.					0.39			150.47	PERVIO					
1	5.9	14	7	037	14	9.06	6.867	0	0	6	0	7.557	6	US	5	166.9	6.6	0.486	
B3	35042	43109	J4	0.25	283.11								150.47	PERVIO					
3	3.3	11	9	65	3	9.06	6.189	0	0	0.4	0	7.62	6	US	5	166.9	6.6	0.486	
B3	36422	43119	J1	42.3	46750.		12.48			0.34			150.47	PERVIO		172.99			
6	9.3	99	19	557	22	9.06	7	0	0	5	0	6.729	6	US	5	6	6.279	0.483	
B3	35591	43116	J5	5.82	6426.2								150.47	PERVIO		167.19			
7	2.9	50	5	22	69	9.06	6.745	0	0	0.4	0	7.62	6	US	5	4	6.585	0.486	
B3	36379	43094	J5	32.2	35616.					0.36			150.47	PERVIO		173.76			
8	5.5	08	3	687	67	9.06	9.137	0	0	6	0	7.279	6	US	5	8	6.238	0.483	
B4	36320	43071	J6	14.0	15524.					0.39			150.47	PERVIO		170.64			
2	6.5	19	1	656	95	9.06	8.381	0	0	4	0	7.522	6	US	5	1	6.403	0.484	
B4	36366	43078	J5	11.5	12749.					0.38			150.47	PERVIO		168.00			
4	4.5	07	7	507	12	9.06	9.867	0	0	2	0	7.305	6	US	5	5	6.542	0.485	
B4	34669	43060	J6	33.1	36631.								150.47	PERVIO		178.12			
7	4.2	11	3	882	57	9.06	5.835	0	0	0.39	0	7.467	6	US	5	7	6.008	0.48	
B4	36319	43065	J6	0.11	129.24								150.47	PERVIO					
8	7.4	12	9	71	9	9.06	8.534	0	0	0.4	0	7.62	6	US	5	166.9	6.6	0.486	
B4	36277	43053	J6	33.2	36651.					0.39			150.47	PERVIO		169.53			
9	9.1	94	9	063	54	9.06	8.62	0	0	7	0	7.568	6	US	5	9	6.461	0.485	
B5	35366	43045	J7	0.29	328.36								150.47	PERVIO					
1	3.9	41	7	75	6	9.06	5.66	0	0	0.4	0	7.62	6	US	5	166.9	6.6	0.486	

B5	36095	43029	J8	6.45	7121.8								150.47	PERVIO		170.81			
2	0.5	19	1	24	54	9.06	7.189	0	0	0.4	0	7.62	6	US	5	2	6.394	0.484	
B5	34578	43048	J7	0.21	242.49								150.47	PERVIO		206.36			
3	9.5	03	5	97	4	9.06	4.978	0	0	0.4	0	7.62	6	US	5	1	4.519	0.466	
B5	34580	43047	J7	0.20	221.41								150.47	PERVIO					
4	8.1	64	5	06	3	9.06	5.248	0	0	0.4	0	7.62	6	US	5	166.9	6.6	0.486	
B5	35991	43022	J7	0.08									150.47	PERVIO					
5	0.1	01	9	27	91.28	9.06	6.338	0	0	0.4	0	7.62	6	US	5	166.9	6.6	0.486	
B5	35365	43045	J7	0.10	115.45								150.47	PERVIO					
6	3.6	02	7	46	2	9.06	6.535	0	0	0.4	0	7.62	6	US	5	166.9	6.6	0.486	
B5	35992	43021	J7	0.11	122.07								150.47	PERVIO					
7	9.7	86	9	06	5	9.06	6.365	0	0	0.4	0	7.62	6	US	5	166.9	6.6	0.486	
B6	35003	42988	J9	44.8	49486.					0.39			150.47	PERVIO		175.66			
1	4.3	67	2	351	86	9.06	5.343	0	0	7	0	7.567	6	US	5	1	6.138	0.482	
B6	36058	43014	J9	0.39	433.44		12.94						150.47	PERVIO					
3	6.5	32	0	27	4	9.06	8	0	0	0.4	0	7.62	6	US	5	166.9	6.6	0.486	
B6	35955	42955	J9	0.29	320.19		10.85						150.47	PERVIO		197.75			
8	7.2	65	9	01	9	9.06	3	0	0	0.4	0	7.62	6	US	5	7	4.973	0.47	
B7	35150	42953	J1	6.35	7013.4					0.39			150.47	PERVIO		169.19			
4	5	05	09	42	66	9.06	5.041	0	0	4	0	7.521	6	US	5	1	6.479	0.485	
B7	35041	42951	J1	19.1	21102.					0.39			150.47	PERVIO		186.48			
5	3.3	22	05	19	65	9.06	5.25	0	0	8	0	7.594	6	US	5	7	5.567	0.476	
B3	35170	43105	J1	32.7	36193.					0.39				PERVIO		168.93			
4	7.6	73	12	915	71	9.06	6.837	0	0	8	0	7.591	100	US	5	5	6.493	0.485	
			J1	172															
	35799	43083	85	6.65	190580					0.04				PERVIO		211.01			
81	8.3	92	0	6	1	9.06	7.401	35.625	0.011	8	1.193	2.754	100	US	5	6	4.274	0.464	
B2	35683	43112	J4	15.1	16677.					0.38				PERVIO		175.18			
9	8.9	69	5	095	15	9.06	6.545	0	0	1	0	7.269	100	US	5	4	6.163	0.482	
B3	35207	43091	J1	36.0	39764.					0.39				PERVIO		167.49			
9	2.3	99	12	262	02	9.06	7.276	0	0	9	0	7.604	100	US	5	2	6.569	0.486	
				145															
	36068	43112	B3	0.82	160135					0.04				PERVIO		205.34			
35	9.4	62	5	9	7	9.06	8.032	27.26	0.011	8	1.205	2.741	100	US	5	9	4.573	0.466	
B2	36523	43137	J1	26.9	29769.					0.35				PERVIO					
5	8.7	98	13	716	98	9.06	8.847	0	0	4	0	6.755	100	US	5	88.619	91.453	0.429	
				350.															
	36614	43178	B8	268	386609					0.07				PERVIO		179.06			
83	4.5	47	3	4	.7	9.06	8.744	26.782	0.011	6	1.114	3.125	100	US	5	2	5.959	0.48	
				391.															
	36950	43174	B2	841	432496		12.02			0.15				PERVIO		232.80			
20	9.4	86	0	6	.3	9.06	2	12.647	0.008	3	0.809	4.18	100	US	5	5	3.124	0.452	
				995.															
	36948	43189	B1	640	109894		10.97			0.11				PERVIO		210.96			
21	9.8	17	9	1	0	9.06	7	22.725	0.009	7	0.925	3.702	100	US	5	9	4.276	0.464	
	37053	43305	J1	12.2	13479.									PERVIO		167.42			
B1	4.7	15	20	12	03	9.06	8.504	0	0	0.4	0	7.62	100	US	5	7	6.572	0.486	
	37074	43285		44.3	48997.		10.37			0.39				PERVIO					
B3	1.3	88	J2	917	46	9.06	8	0	0	8	0	7.62	100	US	5	49.5	120.4	0.417	

B58	36043 6.3	43019 83	J114	22.1 77	24477. 93	9.06	5.53	0	0	0.4	0	7.62	100	PERVIOUS	5	167.093	6.59	0.486
62	35915 6.9	42993 69	B62	626	539322 .9	9.06	9.106	7.979	0.004	0.147	0.467	4.552	100	PERVIOUS	5	227.249	3.417	0.455
B67	35287 3.8	42977 17	J1515	33.3 419	36801. 21	9.06	7.52	0	0	0.396	0	7.548	100	PERVIOUS	5	176.406	6.099	0.481
B73	35316 8.8	42958 85	J1515	38.0 612	42010. 15	9.06	7.27	0	0	0.392	0	7.497	100	PERVIOUS	5	187.318	5.523	0.476
B72	34718 5.8	42951 87	J103	65.7 595	72582. 23	9.06	4.51	0	0	0.395	0	7.536	100	PERVIOUS	5	180.284	5.895	0.479
58	36017 1.8	43015 40	B582	855 2	157. 174233 .1	9.06	5.427	5.875	0.004	0.118	0.375	4.32	100	PERVIOUS	5	192.213	5.265	0.473
59	36265 6	43019 61	B594	316 4	691. 763042 .4	9.06	8.757	4.616	0.002	0.166	0.242	4.919	100	PERVIOUS	5	239.803	2.756	0.449
B65	35711 2.6	42984 06	J1616	58.9 57	65073. 95	9.06	8.427	0	0	0.381	0	7.311	100	PERVIOUS	5	180.152	5.902	0.479
B62	35937 7.5	43001 91	J90	45.0 176	49688. 3	9.06	8.773	0	0	0.396	0	7.545	100	PERVIOUS	5	240.021	2.744	0.449
52	35973 7.4	43040 30	B552	104 5	367. 405192 .6	9.06	7.189	22.235	0.008	0.082	0.898	3.406	100	PERVIOUS	5	212.554	4.193	0.463
B50	36163 5.1	43037 03	J73	24.3 618	26889. 4	9.06	6.473	0	0	0.399	0	7.597	100	PERVIOUS	5	167.256	6.582	0.486
B83	36795 4.2	43172 53	J29	6.24 21	6889.7 35	9.06	11.56 9	0	0	0.387	0	7.414	100	PERVIOUS	5	151.757	22.815	0.475
B22	36751 3	43167 60	J34	20.2 405	22340. 51	9.06	11.56 9	0	0	0.398	0	7.592	100	PERVIOUS	5	151.757	22.815	0.475
96	36245 7.7	43207 09	B96	569. 255 6	628317 .5	9.06	6.932	33.07	0.012	0.034	1.27	2.54	100	PERVIOUS	5	187.087	5.536	0.476
B10	36119 9.2	43217 44	J887	34.2 679	37823. 29	9.06	10.69 4	0	0	0.4	0	7.62	100	PERVIOUS	5	168.876	6.495	0.485
B53	36924 3.8	43238 58	J6	17.3 201	19117. 11	9.06	10.14 2	0	0	0.4	0	7.62	100	PERVIOUS	5	174.613	6.193	0.482
B69	35873 6.9	42966 70	J99	31.3 421	34593. 93	9.06	6.857	0	0	0.387	0	7.387	100	PERVIOUS	5	191.515	5.302	0.473
B64	35464 6.8	42972 12	J731	17.8 414	19692. 5	9.06	7.512	0	0	0.382	0	7.328	100	PERVIOUS	5	177.936	6.018	0.481
B9	37012 8	43227 61	J111	49.5 861	54730. 8	9.06	10.14 2	0	0	0.385	0	7.542	100	PERVIOUS	5	174.613	6.193	0.482
B35	36128 3.5	43113 60	J110	55.1 602	60883. 22	9.06	8.05	0	0	0.379	0	7.322	100	PERVIOUS	5	170.775	6.396	0.484
B43	35644 4.6	43066 61	J65	5.30 19	5851.9 87	9.06	6.25	0	0	0.389	0	7.439	100	PERVIOUS	5	169.895	6.442	0.484

	35322	43061	B4	680. 695	751319					0.04				PERVIO		194.90			
46	2.9	77	6	1	.1	9.06	6.432	33.478	0.011	5	1.213	2.707	100	US	5	7	5.123	0.472	
B4	35549	43059	J6	24.1	26639.									PERVIO		173.40			
5	1.2	39	7	352	29	9.06	6.551	0	0	0.4	0	7.62	100	US	5	1	6.257	0.483	
	35234	43027	B5	937. 606	103488					0.05				PERVIO		199.83			
56	7.5	53	6	5	6	9.06	6.535	22.912	0.01	3	1.067	2.946	100	US	5	2	4.863	0.469	
B4	35416	43048	J7	13.2	14618.					0.39				PERVIO					
6	5.2	20	1	442	32	9.06	6.432	0	0	4	0	7.523	100	US	5	166.9	6.6	0.486	
B4	34927	43075	J5	50.0	55250.					0.38				PERVIO		170.76			
1	8.2	50	9	569	44	9.06	6.961	0	0	4	0	7.368	100	US	5	4	6.396	0.484	
B2	36777	43177	J2	13.9	15426.		11.97							PERVIO		166.91			
0	8.8	45	7	761	16	9.06	6	0	0	0.4	0	7.617	100	US	5	4	6.599	0.486	
B2	35551	43117	J4	5.24	5793.5									PERVIO		177.51			
6	1.3	17	1	9	98	9.06	6.24	0	0	0.4	0	7.62	100	US	5	1	6.041	0.481	
B8	35824	43090	J1	79.6	87956.					0.39				PERVIO		176.41			
1	4.4	50	17	883	18	9.06	7.416	0	0	1	0	7.484	100	US	5	8	6.098	0.481	
B9	36290	43223	J1	4.91	5422.9		10.69							PERVIO		168.87			
6	2.7	61	4	32	58	9.06	4	0	0	0.4	0	7.62	100	US	5	6	6.495	0.485	
	36810	43251		862. 665	952169					0.04				PERVIO		195.59			
5	4.1	14	B5	2	.1	9.06	9.264	43.433	0.012	4	1.223	2.686	100	US	5	6	5.087	0.471	
B5	36057	43025	J8	8.27	9128.2					0.39				PERVIO		167.06			
9	1.8	54	4	02	56	9.06	8.693	0	0	7	0	7.571	100	US	5	1	6.592	0.486	